ORGANIC TRANSFORMATIONS IN MICROEMULSION MEDIA

A Thesis submitted to the University of North Bengal

For the Award of

Doctor of Philosophy

in

Chemistry

BY

Barnali Kar

GUIDE

Dr. Sajal Das

Assistant Professor
Department of Chemistry
University of North Bengal

CO-GUIDE

Prof. Swapan Kumar Saha (Retd.)

Emeritus Fellow (UGC)
Department of Chemistry
University of North Bengal

March - 2017

DEDICATED

TO

MY PARENTS

DECLARATION

I declare that the thesis entitled "**Organic Transformations in Microemulsion Media**" has been prepared by me under the guidance of Dr. Sajal Das (Guide), Assistant Professor of Chemistry, University of North Bengal and Prof. Swapan Kumar Saha (Retd.), UGC Emeritus Fellow (Co-Guide), University of North Bengal. No part of this thesis has formed the basis for the award of any degree or fellowship previously.

Barnali Kar

BARNALI KAR

Department of Chemistry
University of North Bengal
Darjeeling-734013
West Bengal
India

DATE: 05-03-2017

UNIVERSITY OF NORTH BENGAL
DEPARTMENT OF CHEMISTRY

P.O. NORTH BENGAL UNIVERSITY, RAJA RAMMOHUNPUR, DIST. DARJEELING, WEST BENGAL, INDIA, PIN - 734 013.
PHONE : (0353) 2776 381, FAX : (0353) 2699 001

Ref. No. ..... *Dated* .....*20*.....

CERTIFICATE

I certify that Mrs. Barnali Kar has prepared the thesis entitled "**ORGANIC TRANSFORMATIONS IN MICROEMULSION MEDIA",** for the award of Ph.D. degree of the University of North Bengal, under the guidance of Prof. Swapan Kumar Saha (Retd.), UGC-Emeritus Fellow (Co-Guide) and myself (Guide). She has carried out the work at the Department of Chemistry, University of North Bengal. No part of this thesis has formed the basis for the award of any degree or fellowship previously.

Sajal

Assistant Professor
Department of Chemistry
University of North Bengal
Darjeeling - 734013, India

Dr. Sajal Das
Assistant Professor
Department of Chemistry
University of North Bengal
Darjeeling-734013
West Bengal
India

DATE: 05-03-2017

UNIVERSITY OF NORTH BENGAL
DEPARTMENT OF CHEMISTRY

P.O. NORTH BENGAL UNIVERSITY, RAJA RAMMOHUNPUR, DIST. DARJEELING, WEST BENGAL, INDIA, PIN - 734 013.
PHONE : (0353) 2776 381, FAX : (0353) 2699 001

Ref. No. ..... *Dated* .....20.....

CERTIFICATE

I certify that Mrs. Barnali Kar has prepared the thesis entitled "**ORGANIC TRANSFORMATIONS IN MICROEMULSION MEDIA**", for the award of Ph.D. degree of the University of North Bengal, under the guidance of Dr. Sajal Das (Guide) and myself (Co-Guide). She has carried out the work at the Department of Chemistry, University of North Bengal. No part of this thesis has formed the basis for the award of any degree or fellowship previously.

Prof. Swapan Kumar Saha (Retd.)
Emeritus Fellow (UGC)
Department of Chemistry
University of North Bengal
Darjeeling-734013
West Bengal
India

Emeritus Fellow
Department of Chemistry
University of North Bengal
Darjeeling - 734013, India

DATE: 05.07.2017

ACKNOWLEDGEMENTS

At the outset, I would like to thank my supervisor Dr. Sajal Das, Department of Chemistry, University of North Bengal, Darjeeling and cosupervisor Professor Swapan K. Saha, Department of Chemistry, University of North Bengal, Darjeeling sincerely for giving me the opportunity to carry out my PhD thesis under their supervision, throughout the entire course of study.

I would like to thank UGC, DST and CSIR, Govt. of India for Financial supports. I express my full gratitude to Prof. M.N. Roy, Head, and all respected teachers, office staff and research scholars of the Department of Chemistry, University of North Bengal, Darjeeling for their assistance and support during my research work.

I express my sincere gratitude to Prof. Basudeb Basu, Prof. Pranab Ghosh, Department of Chemistry, NBU, for their constant motivation.

My special thanks to Dr. Soumik Bardhan, Research Associate, Department of Biotechnology, Indian Institute of Technology, Madras for his support during my research work.

I am grateful to Prof. Bidyut Kumar Paul, Surface and Colloid Science Laboratory, Geological Studies Unit, Indian Statistical Institute, Kolkata and

Dr. Kausik Kundu, Post-doctoral Fellow, Department of Inorganic and Physical Chemistry,Indian Institute of Science for extending their helping hands whenever needed.

My thanks are also expressed to my laboratory friends Prasanjit, Bhaskar da, Madhurima di, Gulmi etc. for the lively and cooperative environment we had together.

I should thank my beloved husband, Ankush Maitra for his constant support throughout my work, without his help my work would not have been possible.

The single largest contribution is properly shaping me what I am today comes from the faith, hope and pride of parents, Sri Tapan Kumar Kar and Smt. Sangita Kar. Words are inadequate for expressing such feelings.

Thank You.

Barnali Kar

Barnali Kar

ABSTRACT

Microemulsions have been emerged as an alternative and promising aqueous-organic reaction medium in overcoming some environmental or practical issues presented by traditional organic solvents in recent years. The discrete droplets in an immiscible continuous (carrier) phase are analogous to the traditional chemist's flask, with the added advantages of reduced reagent consumption, rapid mixing, automated handling, and continuous processing. Incredible selectivities and activities can be achieved by using this droplet-based microfluidic model as reaction media. The reaction rate can also be altered by changing the parameters. The microheterogeneous nature of microemulsions induces drastic changes in the reagent concentrations, and this can be specifically used for tuning the reaction rates. The amphiphilic organic molecules can accumulate and orient at the oil–water interface, inducing regiospecificity in organic reactions. This dissertation depicts the understanding of different physicochemical characterisation parameters and interactions during the progress of the organic reactions for designing microemulsions as suitable reaction media for organic synthesis. An in-depth characterization of microenvironment of w/o microemulsion, starting from simple titrimetric method to sophisticated instrumentations has been employed to locate the plausible reaction site in such solvent. This dissertation is divided into for chapters.

The **Chapter–I** describes the general introduction of microemulsions, their structural characteristics and its application as an effective organic reaction medium. This chapter also elaborates how the magical properties of microemulsion can be tuned for carrying out the reactions in such solvent.

The **Chapter–II** focuses on the evaluation of the interfacial composition and the thermodynamics of transfer of 1-pentanol (Pn) from the continuous oil phase to the interface of w/o nonionic microemulsion [Tween-20/Pn/cyclohexane(Cy)/water] in absence and presence of an ionic liquid (IL) (1-butyl-3-propylbenzimidazolium bromide) under different physicochemical conditions [viz. variation in concentration of IL (0.0→0.20 mol dm^{-3}) and temperature (293→323K] at a fixed molar ratio of water to surfactant (ω) by the Schulman's method of cosurfactant titration at the oil/water interface. The overall transfer process has been found to be spontaneous, exothermic and organized in absence or presence of IL, but shown to be influenced by [IL]. The microstructure and state of water organization inside the pool of these systems have been characterized by different experimental techniques, e.g.,

conductivity, DLS and FTIR in absence or presence of IL. In addition, C-C cross coupling reaction (Heck reaction) has been employed to explore the properties of the IL (additive) in confined environment of the microemulsion vis-à-vis its interaction with the constituents of the interface. The progress of reaction has been monitored using above techniques. The reaction was ended up with the highest yield (75%) in presence of 0.05 mol dm^{-3} of IL, wherein the microemulsion forms spontaneously with highest stability.

The **Chapter–III** designed a fresh modus operandi for additive and ligand free transition metal-catalyzed C-C homo/cross-coupling reactions of arylboronic acid in a novel template of reverse micellar (RMs) gallows. Three RMs based on different charge types with variation in sizes and types of polar head groups and hydrophobic moieties of surfactants [such as, anionic (AOT), cationic (DDAB), and non-ionic (TX 100)] in cyclohexane have been chosen as reaction templates. The reaction proceeds rapidly in these media and completes within 10 minutes at ambient condition. Performance of the reaction in terms of yield of the desired product in RMs, has been correlated with different physicochemical parameters of these RMs as obtained from conductance, DLS and FTIR measurements.

In the **Chapter–IV**, the formulation and characterization of a high-temperature stable quaternary IL-in-oil microemulsions comprising of IL ([EpBzim]Br), CTAB, 1-On and Dc has been illustrated with a detailed description of the interfacial composition and energetic parameters for the transfer of 1-On from bulk oil phase to the interface as a function of system composition and temperatures. Additionally, nitration reaction of some aromatic compound has been performed in the IL/O microemulsion. The reaction ends up with the highest regioselectivity of para isomer. The confinement of IL imparts the regioselectivity on the nitrated product.

The **Chapter-V** reports a model C–C cross coupling Heck reaction between n-butyl acrylate and 4-iodo-toluene both in micelles and water/oil microemulsion systems as reaction media using a similar set of surfactants, [cetyltrimethylammonium bromide (CTAB) and polyoxyethylene (20)cetyl ether (C16E20)], in their single and mixed states. Multitechnique approaches are employed to understand the mutual interactions between surfactant(s) and other constituents in pure and mixed states at air–water as well as oil–water interfaces.

PREFACE

Microemulsions are macroscopically homogeneous mixtures of oil, water, surfactant and/or cosurfactant, whereas in the microscopic level it consists of individual domains of oil and water separated by a monolayer of surfactant and/or cosurfactant. The microheterogeneity of such dispersion with unique physicochemical properties viz. spontaneous formation, clear appearance, thermodynamical stability, ultra-low interfacial tension, low viscosity, large interfacial area, high solubilization capacity for both hydrophilic and lipophilic compounds induce drastic changes in the reagent concentrations, and this can be specifically used for tuning the reaction rates.

Generating discrete droplets in an immiscible continuous (carrier) phase allows reactions to be compartmentalized into femtolitre to nanolitre volumes. In essence, each droplet reactor is analogous to the traditional chemist's flask, with the added advantages of reduced reagent consumption, rapid mixing, automated handling, and continuous processing. Building on advances in continuous flow chemistry, droplet-based micro fluidics has been used to conduct a variety of organic reactions. This platform provides opportunities for handling precious reagents that are not possible with conventional synthetic techniques and has been used to screen reaction conditions using microgram amounts of starting material.

Moreover, microemulsion can induce regioselectivity in organic reactions changing the product composition compared with the products obtained in a microhomogeneous solution. The induced regioselectivity is believed to be due to the interface acting as a template for reactants having one more polar and one less polar end.

In view of these, this dissertation depicts the formation, characterizations and mainly the prospective applications of microemulsions as reaction media in 'synthetic organic chemistry and the most possible reaction location/site in such microheterogeneous media. Hence, such a highly exciting field can be expected to flourish greatly in the coming years to meet the high standards demanded by the organic synthetic chemist.

TABLE OF CONTENTS

LIST OF TABLES

LIST OF SCHEMES

Chapter II

Chapter III

Chapter IV

LIST OF FIGURES

Chapter IV

Chapter V

LIST OF PUBLICATION AND POSTER

Thesis Publication:

1.“Physicochemical studies of water-in-oil nonionic microemulsion in presence of benzimidazole-based ionic liquid and probing of microenvironment using model C-C cross coupling (Heck) reaction**” Barnali Kar**, Soumik Bardhan, Kaushik Kundu, Swapan Kumar Saha, Bidyut Kumar Paul, Sajal Das, RSC Advances, 2014, 4, 21000-21009.

2.“A fast and additive free C-C homo/cross-coupling reaction in reverse micellar gallows: A brief understanding on role of surfactant, water content and base on the yield of product and possible reaction site therein**” Barnali Kar,** Soumik Bardhan, Prasanjit Ghosh, Bhaskar Ganguly, Kaushik Kundu, Sonali Sarkar, Bidyut Kumar Paul, Chemistry Select, 2017, 2, 1079-1088

3.“Synergistic Interaction of Surfactant Blends in Aqueous Medium Reciprocates in Non-polar Medium with Improved Efficacy as Nanoreactor” Soumik Bardhan, Kaushik Kundu, **Barnali Kar**, Gulmi Chakraborty, Dibbendu Ghosh, Debayan Sarkar, Sajal Das, Sanjib Senapati, Swapan Kumar Saha, Bidyut Kumar Paul, RSC Advances, 2016,6, 55104-55116

4.“Formation of High-Temperature Stable Benzimidazolium Ionic Liquid-in-Oil Microemulsion and Regioselective Nitration Reaction Therein**” Barnali Kar**, Soumik Bardhan, Kaushik Kundu, Prasanjit Ghosh, Bidyut Kumar Paul, Sajal Das, (Communicated)

Non-Thesis Publication:

1.“Microemulsion Mediated Organic Synthesis and the Possible Reaction Site” Prasanjit Ghosh, **Barnali Kar**, Soumik Bardhan, Kaushik Kundu, Swapan kumar Saha, Bidyut Kumar Paul, Sajal das, J. Surface Sci. Technol. 2016, 32, 8–16.

2.“The Mixing Behaviour of Anionic and Nonionic Surfactant Blends in Aqueous Environment Correlates in Fatty Acid Ester Medium” Kaushik Kundu**,** Arindam Das, Soumik Bardhan, Gulmi Chakraborty, Dibbendu Ghosh, **Barnali Kar**, Swapan K. Saha, Sanjib Senapati, Rajib Kumar Mitra, Bidyut K. Paul, Colloids and Surfaces A, 2016, 504, 331-342.

3. "Microemulsion (mEs) mediated rapid synthesis of Imidazo[1,2-a]pyridine and its late-stage functionalization" Prasanjit Ghosh, Bhaskar Ganguly, **Barnali Kar**, Sajal Das (Communicated)

4. "Microstructural Transition from Aqueous to Acetonitrile-based Non-aqueous Reverse Micelle: An Experimental and Theoretical Investigations" Madhurima Paul Chowdhury, Kaushik Kundu, Soumik Bardhan, **Barnali Kar**, Gulmi Chakraborty, Swapan Kumar Saha (Communicated)

Poster Presentation:

1. "Formation, thermodynamic properties and microstructures of water-in-oil nonionic microemulsion in presence of benzimidazole-based ionic liquid and probing of microenvironment via model C-C cross coupling (Heck) reaction" **Barnali Kar**, Soumik Bardhan, Kaushik Kundu, Swapan Kumar Saha, Bidyut K. Paul, Sajal Das, 5^{TH} Asian Conference on Colloid and Interface Science, 2013, Department of Chemistry, University of North Bengal, Darjeeling.

2."A fast and additive free Suzuki self/cross-coupling reaction in confined environment of reverse micellar gallows" **Barnali Kar**, Soumik Bardhan, Bhaskar Ganguly, Sajal Das, National Symposium on RTPC-2015, 2015, Department of Chemistry, NIT Sikkim.

3."Organic Reactions in Reverse Micelle" Barnali Kar, Soumik Bardhan, Bhaskar Ganguly, Prasanjit Ghosh, Sajal Das, 19^{TH} CRSI National Symposium in Chemistry, 2016, Department of Chemistry, University of North Bengal, Darjeeling.

LIST OF APPENDICES

Appendix A

Physicochemical studies of water-in-oil nonionic microemulsion in presence of benzimidazole-based ionic liquid and probing of microenvironment using model C-C cross coupling (Heck) reaction

[A] Basics of the dilution method and thermodynamics of the transfer of cosurfactant from oil to the interface

For a quaternary water-in-oil microemulsion system composed of water/ surfactant/cosurfactant /oil, the solubilization of water is governed by the distribution of cosurfactant molecules between oil and the interface at a fixed temperature. A small amount of cosurfactant may remain solubilized in the aqueous phase depending on its lipophilicity. A threshold amount of cosurfactant is required to stabilize a water-in-oil dispersion at a fixed molar ratio of water to surfactant (ω). As a result, an appropriate distribution constant (K_d) is attained, and governs cosurfactant molecules distributed between the interfacial region (consisting of surfactant molecules) and the oleic phase at a fixed temperature. The stable w/o microemulsion gets disrupted when excess oil is added and the system splits up into two distinct phases. Again, a threshold amount of cosurfactant is necessary to restore the w/o microemulsion equilibrium. This process is repeatedly followed in the dilution experiment. The concentrations of cosurfactant at the interface and in the bulk oil phase were estimated to get the distribution constant (K_d) by the dilution experiments in the light of the physicochemical rationale elaborated by Zheng et al.[1], Moulik et al.[2,3], Paul et al.[4-6], and Abuin et al.[7] The total number of moles of the cosurfactant, n_a present in the stable microemulsion is given by the relation,

$$n_a \quad n_a^i + n_a^w + n_a^o \qquad \text{(S1)}$$

where, n_a^i, n_a^w, $n_a^o$are the number of moles of cosurfactant in the interfacial, water and oil phases respectively. Since the solubility of cosurfactant in the oil is constant at a given temperature, the constant k_o can be written as

$$k_o \quad \frac{n_a^o}{n_o} \qquad \text{(S2)}$$

where n_o is the total number of moles of oil in the system. Combining Equations S1 and S2 we get

$$n_a \quad n_a^i + n_a^w + k_o n_o \qquad \text{(S3)}$$

Since the moles of cosurfactant in the interface and in the dispersed phase (water) depend on the surfactant concentration, Equation S3 may be converted into a more convenient form by dividing throughout by total number of moles of surfactant, n_s to give

$$\frac{n_a}{n_s} \quad \frac{n_a^i + n_a^w}{n_s} + k_o \frac{n_o}{n_s} \qquad \text{(S4)}$$

In our experiment, negligible water solubility of cosurfactant (Pn) leads to $n_a^w \approx 0$.[5] Thus, above equation becomes,

$$\frac{n_a}{n_s} \quad \frac{n_a^i}{n_s} + k_o \frac{n_o}{n_s} \qquad \text{(S5)}$$

A plot of n_a/n_s against n_o/n_s should yield the values of the slope (S) and the intercept (I). Slope (S) is actually k_o and n_a^o can be determined from Equation S2. On the other hand, n_a^i can be calculated from the intercept (I), which is equal to n_a^i/n_s.

The partition of Pn between the continuous oil phase and the interface of the droplet can be expressed in terms of the distribution constant (K_d). K_d can be calculated from the ratio of mole fraction of Pn in the interfacial composition (X_a^i) to the mole fraction of Pn in the bulk oil phase (X_a^o),

$$K_d \quad \frac{X_a^i}{X_a^o} \quad \frac{n_a^i/\left(n_a^i+n_s\right)}{n_a^o/\left(n_a^o+n_o\right)} \quad \frac{n_a^i\left(n_a^o+n_o\right)}{n_a^o\left(n_a^i+n_s\right)} \tag{S6}$$

Dividing numerator and denominator by $n_a^i n_a^o$, and putting the values of the slope (S) and the intercept (I) from Equation S5, we get

$$K_d \quad \frac{\left(1+n_o/n_a^o\right)}{\left(1+n_s/n_a^i\right)} \quad \frac{\left(1+1/S\right)}{\left(1+1/I\right)} \quad \frac{I(1+S)}{S(1+I)} \tag{S7}$$

The standard Gibbs free energy change of transfer ($\Delta G^0_{o\text{-}i}$) of Pn from the continuous oil phase to the interfacial region, between the water and oil, is obtained from the relation

$$\Delta G^0_{o-i} \quad -RT\ln K_d \quad -RT\ln\frac{X_a^i}{X_a^o} \quad -RT\ln\frac{I(1+S)}{S(1+I)} \tag{S8}$$

The Gibbs-Helmholtz equation[8] was used to get the standard enthalpy of the said transfer process of alkanol from oil to interface ($\Delta H^0_{o\rightarrow i}$). Thus,

$$[\partial(\Delta G^0_{o\text{-}i}/T)/\partial T]_p = -\Delta H^0_{o\text{-}i}/T^2 \tag{S9}$$

Using chain rule of differentiation on the left hand side of equation (S9),

$$[\partial(\Delta G^0_{o\text{-}i}/T)/\partial T]_p = [\partial(\Delta G^0_{o\text{-}i}/T)/\partial(1/T)]_p\,[d(1/T)/dT] = [\partial(\Delta G^0_{o\text{-}i}/T)/\partial(1/T)]_p\,(-1/T^2) \tag{S10}$$

Substituting this value into eqn. S(9) we get,

$$[\partial(\Delta G^0_{o\text{-}i}/T)/\partial(1/T)]_p\,(-1/T^2) = -\Delta H^0_{o\text{-}i}/T^2 \tag{S11}$$

Hence[8], $\Delta H^0_{o\text{-}i} = [\partial(\Delta G^0_{o\text{-}i}/T)/\partial(1/T)]_p$ (S12)

Herein, the $\Delta G^0_{o\text{-}i}/T$ vs. 1/T plots is nonlinear in nature in each case. Therefore, the points in $\Delta G^0_{o\text{-}i}/T$ vs. 1/T plots have been fitted in a 2^0 polynomial equation as follows,

$$\Delta G^0_{o\text{-}i}/T = A + B\,(1/T) + C\,(1/T)^2 \tag{S13}$$

Where, A, B and C are the polynomial coefficients.

The first derivation of equation (S13) produced the enthalpy ($\Delta H^0_{o\rightarrow i}$), [2,3]

$$\Delta H^0_{o\text{-}i} = B + 2C^2\,(1/T) \tag{S14}$$

Conseqently, the corresponding entropy change ($\Delta S^0_{o\text{-}i}$) can be found by the following relation,

$$\Delta S^0_{o\text{-}i} = (\Delta H^0_{o\text{-}i} - \Delta G^0_{o\text{-}i})/T \tag{S15}$$

The evaluation of standard specific heat capacity change of transfer process, $(-\Delta C^0_P)_{o\text{-}i}$, follows from the relation,

$$[(\Delta C^0_p)]_{o\text{-}i} = [\partial \Delta H^0_{o\text{-}i}/\partial T]_p \quad \text{(S16)}$$

The standard state herein considered is the hypothetical ideal state of the unit mole fraction.

[B] Interfacial composition of water (or, IL)/Tween-20/Pn/Cy microemulsion in absence and presence of IL

The dilution method was employed for a nonionic surfactant, Tween-20-based w/o microemulsion system stabilized in Pn (cosurfactant) and Cy (oil) with varying IL content (= 0.0, 0.05, 0.10, 0.15 and 0.20 mol dm^{-3}) at a fixed ω (= 30) and temperatures (293K→323K). From the data collected, graphs were constructed by plotting n_a/n_s against n_o/n_s according to Eq. (S5). Representative plots are illustrated in Figure S1. The plots were strikingly linear (average correlation of coefficients was 0.9965). From the Figure S1, the values of n_a^o and n_a^i were obtained from slopes (S) and intercepts (I), respectively and subsequently all the thermodynamic parameters [K_d, $\Delta G^0_{o\rightarrow i}$, $\Delta H^0_{o\rightarrow i}$, $\Delta S^0_{o\rightarrow i}$ and $(\Delta C^0_p)_{o\rightarrow i}$] were evaluated acording to Eqs. (S1-S16).[2-6] The values of above physicochemical parameters are presented in Table S1.

In order to underline the influence of IL content on the interfacial composition of Tween-20-based w/o microemulsion systems stabilized in Pn and Cy under various physicochemical conditions (mentioned earlier), n_a^i/n_s values [i.e. compositional variations of amphiphiles (both Tween-20 and Pn) at the interface] are plotted against [IL] (0.0→0.20 mol dm^{-3}) and respective plots are depicted in Figure 1 (inset A). It has been observed from Figure 1 (inset A) that n_a^i values gradually increase with increase in [IL] at all temperatures with some exceptions at low and high temperatures (293 and 323K). The increase in n_a^i values may be attributed to the salting out of the polar head group of Tween-20 in the aqueous phase (i.e., nano water pool), resulting in enhanced interfacial packing of Tween-20 and Pn. Small and polarizable anion (Br^-) of 1-butyl-3-propyl benzimidazolium bromide tends to promote the water structure and dehydrate the ether oxygen of polyoxyethylene type nonionic surfactant (Tween-20 having 20 POE chains). Consequently, hydrophilicity of the surfactant (due to salting-out effect) decreases.[9] Recently, it was reported that POE chains of Tween-20 produce electrostatic interaction with imidazolium cation, and thereby, stimulate the rigidity of IL/oil interface.[10,11] Further, delocalization of the charge as well as the charge shielding due to the presence of both benzene and imidazolium ring in IL contribute the factor that influences the effective binding of Pn with IL and Tween-20 at the droplet surface. With increasing [IL], delocalization of charge will be more. Hence, requirement of Tween-20 molecules decreases at the interface, and consequently, Pn population (n_a^i) increases.[12] All these phenomena are responsible for observed increase in Pn population (n_a^i) at the interface with increase in [IL]. Similar results were also observed by Wang et al.[13] for [bmim][BF_4]/Brij-35/1-butanol/toluene microemulsion with different m_{IL}/m_{H2O} values at different temperatures. On the other hand, n_a^i increases with increase in temperature in absence and presence of IL with some exceptions at higher [IL]. It can be explained on the basis of the interactions between the active constituents at the interfacial layer of the microemulsion (for example, hydrogen bonding interaction between IL-water, dipole-dipole or dipole-induced dipole interaction between Pn-Tween-20, and ion-dipole interaction between IL-Pn and IL-Tween-20) (Scheme 1). With increase in temperature, all these interactions are diminished. Consequently, more Pn is accommodated at the interfacial layer, which imparts stability of the microemulsions.[14] Similar behavior was also observed for both [C_{12}mim]Br/1-pentanol/octane/[bmim][BF_4] systems[13] and CTAB/alkanol/toluene/ [bmim][BF_4] systems.[15] No systematic trend as a function of IL content has been observed for n_a^o values (Table S1) at the studied temperature range.

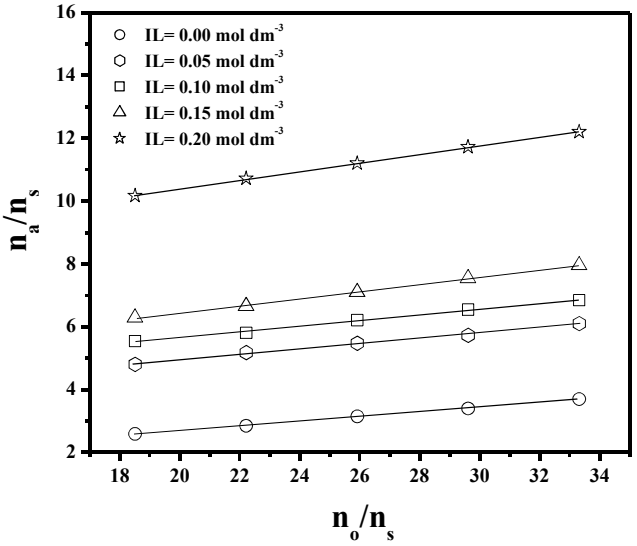

Figure-A.S1. Plots of n_a/n_s vs. n_o/n_s according to Eq. (S4) for water/Tween-20/ pentanol /cyclohexane microemulsion system with different [IL] at $\omega = 30$ at constant temperature of 303K.

Table-A.S1: Interfacial and bulk compositions of 1-pentanol, distribution constant (K_d) and thermodynamic parameters of its transfer from cyclohexane to the interface for w/o microemulsion containing 3.6 ml oil, 1 mmol of surfactant at constant ω (= 30) with varying [IL].

IL (mol dm^{-3})	T(K)	$10^4 n_a^i$ (mol)	$10^3 n_a^o$ (mol)	K_d	$-\Delta G^0_{o\rightarrow i}$ (kJ mol^{-1})	$\Delta H^0_{o\rightarrow i}$ (kJ mol^{-1})	$\Delta S^0_{o\rightarrow i}$ (JK^{-1} mol^{-1})	$[\Delta C_p{}^0]_{o\rightarrow i}$ (kJ mol^{-1} K^{-1})
0.0	293	5.55	1.98	4.94	3.89	-32.58	-97.92	0.74
	303	5.82	1.23	7.81	5.18	-25.43	-66.83	
	313	9.34	1.25	9.35	5.82	-18.04	-39.03	
	323	9.99	1.00	11.79	6.63	-10.41	-11.69	
0.05	293	14.42	1.33	10.04	5.62	-11.70	-20.74	0.06
	303	16.18	1.41	9.76	5.74	-11.10	-17.69	
	313	16.46	1.00	13.57	6.79	-10.48	-11.80	
	323	17.10	1.07	13.94	6.86	-9.85	-9.25	
0.10	293	17.57	1.66	8.57	5.23	-14.15	-30.46	0.55
	303	18.95	1.57	9.21	5.59	-8.79	-10.56	
	313	18.03	1.07	13.01	6.68	-3.25	-10.97	
	323	18.12	1.15	12.7	6.70	2.48	28.42	
0.15	293	15.72	1.65	8.42	5.19	-4.07	3.82	-0.37
	303	20.8	1.90	7.88	5.20	-7.64	-8.07	
	313	22.28	1.23	11.85	6.43	-11.34	-15.69	
	323	17.75	1.15	12.09	6.69	-15.16	-26.21	
0.20	293	17.20	1.83	7.82	5.01	-0.4	15.73	-0.43
	303	39.55	2.16	7.72	5.15	-4.58	1.88	
	313	28.48	1.48	10.41	6.10	-8.89	-8.91	
	323	19.50	1.25	11.42	6.54	-13.34	-21.05	

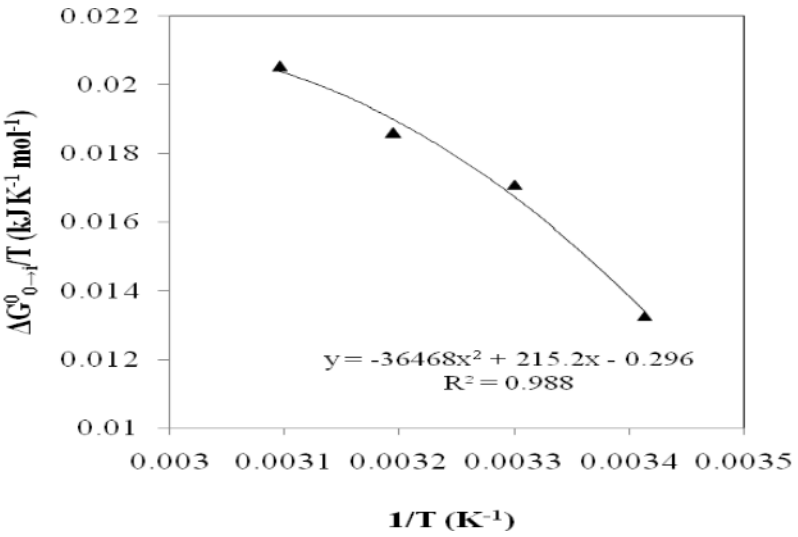

Figure-A.S2. Plots of nonlinear dependence of ($\Delta G^0_{o\rightarrow i}/T$) on (1/T) in terms of a two degree polynomial equation for water/Tween-20/pentanol/cyclohexane microemulsion system in absence of IL at ω = 30 with varied temperature (293K→323K).

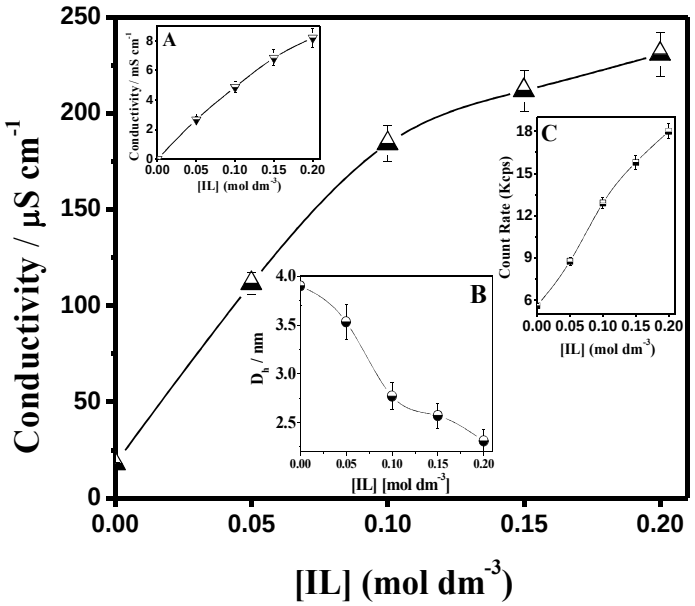

Figure-A.S3. A representative plot for the variation of conductance as a function of IL content for water/Tween-20 /pentanol/cyclohexane microemulsion system at ω (= 30) and 303K. Inset A: Result of blank experiment (same concentration of IL in water). Inset B and C: Hydrodynamic diameter (D_h) (B) and Count Rate (C) of the microemulsion droplets for the same w/o systems with increasing IL content at identical condition.

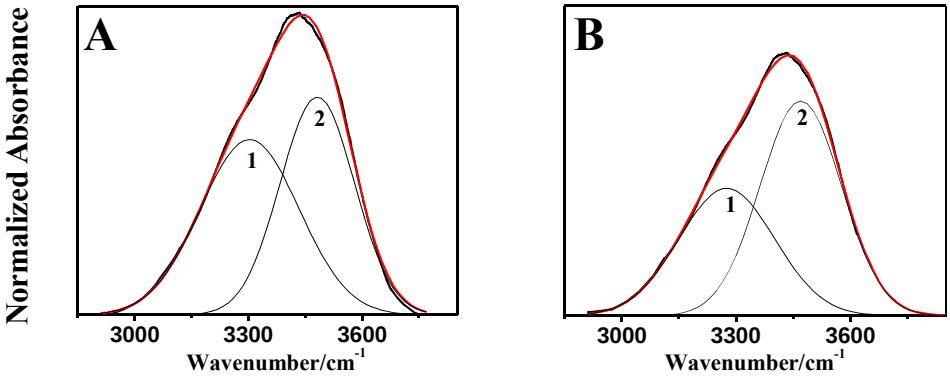

Figure-A.S4: Representative FTIR spectra of O-H band for water/Tween-20/pentanol/cyclohexane microemulsion system at constant ω (= 30) and fixed temperature (303K). (A) In absence of IL and (B) in presence of [IL] = 0.20 mol dm^{-3}. Specification: Experimental spectra (black curve), overall fitted curve (red) and deconvoluted curves (1: bulk water; 2: bound water).

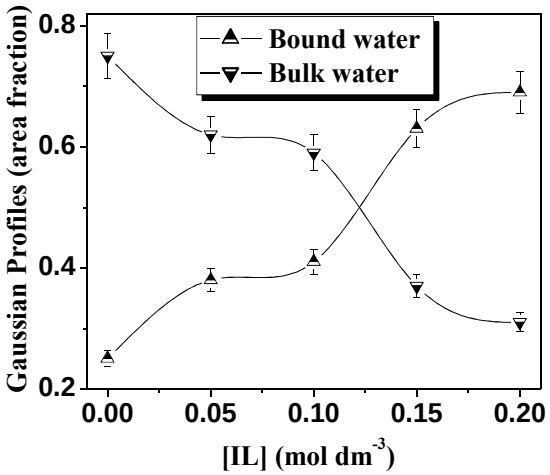

Figure-A.S5. The variation of Gaussian profiles (area fraction) of the normalized spectra of different water species in water/Tween-20/pentanol/cyclohexane as a function of IL content.

Table-A.S2. Heck coupling reaction in water (IL)/Tween-20/Pn/Cy microemulsion medium in presence of different bases at constant ω (= 30) and temperature (323K) ([IL] = 0.05 mol dm^{-3}).

Entry	Base used	Time	Yield (%)
1	K_2CO_3	1 hr.	30
2	NEt_3	1 hr.	75
3	TMEDA	1 hr.	40

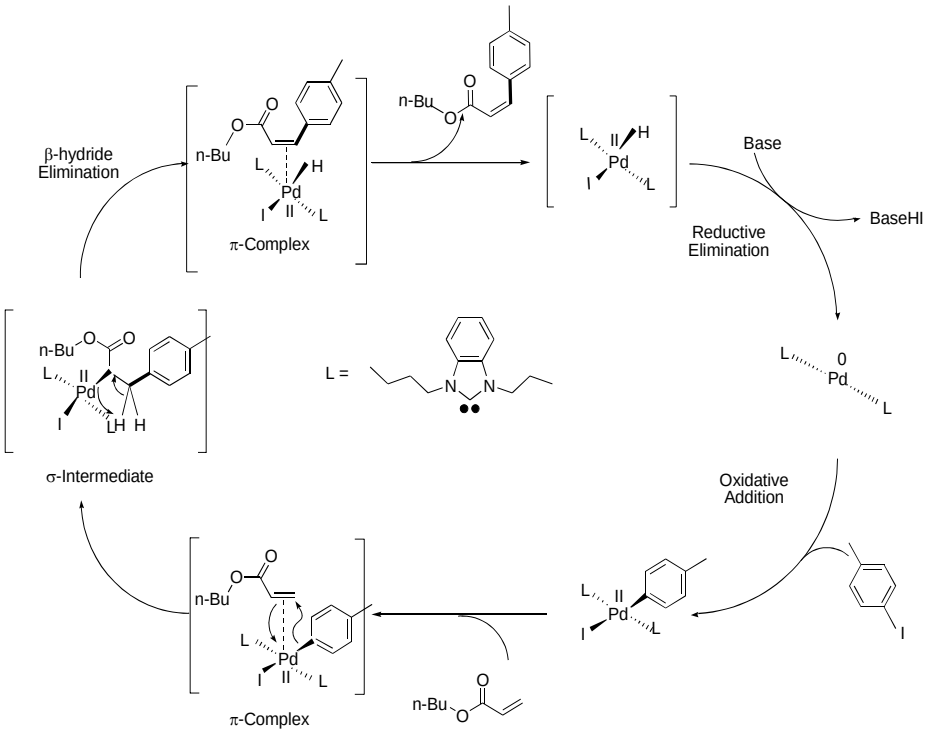

Scheme-A.S1. Mechanism of Heck reaction

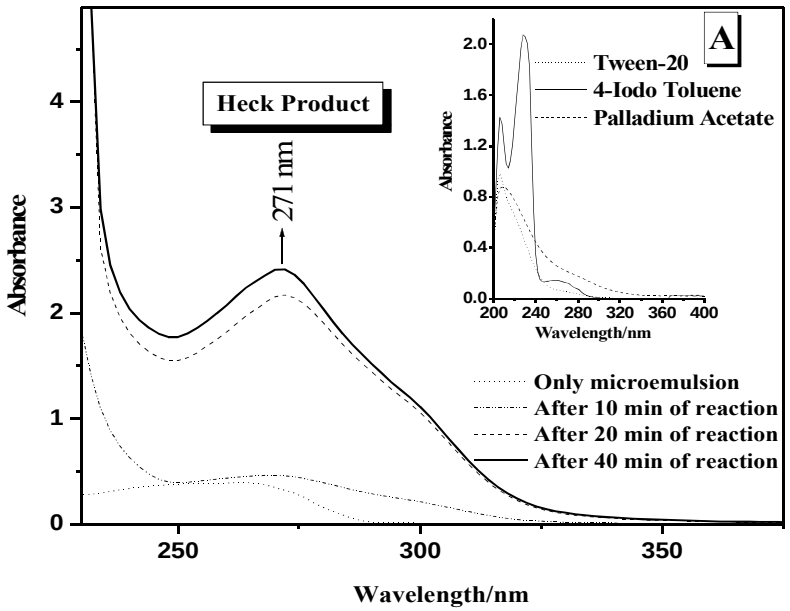

Figure-A.S6. UV-Vis spectra of the water/Tween-20/Pn/Cy microemulsion system with the progress of reaction in presence of IL (= 0.05 mol dm^{-3}). Inset A: UV-Vis spectra of individual component.

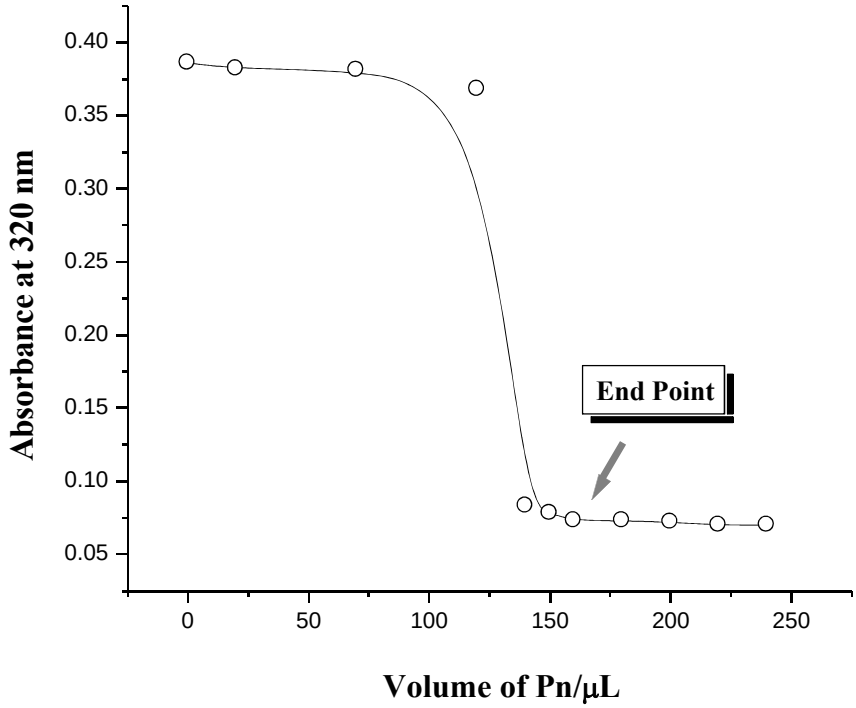

Figure-A.S7. Plots of sample absorbance (measured at 320 nm) vs. volume of pentanol (Pn) for water/Tween-20/pentanol/cyclohexane microemulsion system at ω = 30 and constant temperature of 303K .

[C] Spectral analysis (^{1}H-NMR and ^{13}C-NMR)

1-Butyl-3-propylbenzimidazolium Bromide:

^{1}H-NMR ($CDCl_3$, 300 MHz) δ 1.01-0.92 (m, 6H),1.42-1.32 (m, 2H),2.02-1.87 (m, 4H),4.40-4.33 (m, 4H),7.61 (s, 1H),7.64 (s, 1H), 10.30 (s, 1H); ^{13}C-NMR ($CDCl_3$, 75 MHz) δ 11.5, 14.2, 20.2, 24.5, 32.9, 50.5, 52.1, 123.3, 123.4, 137.3.

4-methyl butyl cinnamate:

^{1}H- NMR ($CDCl_3$, 300MHz) δ0.96 (t, 3H, *J* = 7.2 Hz), 1.44 (m, 2H), 1.68 (m, 2H), 2.36 (s, 3H), 4.20 (t, 2H, *J* = 6.6 Hz), 6.39 (d, 1H, *J* = 16.2 Hz), 7.18 (d, 2H, *J* = 7.8 Hz), 7.42 (d, 2H, *J* = 7.8 Hz), 7.66 (d, 2H, *J* = 16.2 Hz); ^{13}C-NMR ($CDCl_3$, 75 MHz) δ13.8, 19.2, 21.4, 30.8, 64.3, 117.2, 128.1, 129.6, 131.8, 140.6, 144.6, 167.3.

References:

1. O. Zheng, J-X. Zhao and X.-M. Fu, *Langmuir,* 2006**, 22**, 3528-3532.

2. D. Mitra, I. Chakraborty, S.C. Bhattacharya, S.P. Moulik, S. Roy, D. Das and P.K. Das, *J. Phys.Chem. B,* 2006, **110**, 11314-11326.

3. K. Maiti, I. Chakraborty, S.C. Bhattacharya, A.K. Panda and S.P. Moulik, *J. Phys.Chem. B,* 2007, **111**, 14175-14185.

4. B.K. Paul and D.D. Nandy, *J. Colloid Interface Sci.,* 2007, **316**, 751-761.

5. K. Kundu, G. Guin and B. K. Paul, *J. Colloid Interface Sci.,* 2012, **385**, 96-110.

6. K. Kundu and B. K. Paul, *Colloid Polym. Sci.,* 2013, **291**, 613-632.

7. E. Abuin, E. Lissi and K. Olivares, *J. Colloid Interface Sci*., 2004, **276**, 208-211.

8. Atkins' Physical Chemistry, P. Atkins, J. D. Paula, Oxford University Press, 2004, pp126.

9. R. K. Mitra and B. K. Paul, *J. Colloid and Interface Sci.,* 2005, **291**, 550-559.
10. S. Paul and A. K. Panda, *Colloids and Surfaces A: Physicochem. Eng. Aspects,* 2013, **419**, 113–124.

11. Y. Gao, L. Hilfert, A. Voigt and K. Sundmacher, *J. Phys. Chem. B,* 2008, **112**, 3711-3719.

12. S. Bardhan, K. Kundu, B. K. Paul and S. K. Saha, *Colloid Surfaces A,* 2013, **433**, 219-229. 13. F. Wang, Z. Zhang, D. Li, J. Yang, C. Chu and L. Xu, *J. Chem. Eng. Data*, 2011, **56**, 3328–3335.

14. J. Chai, L. Xu, W. Liu and M. Zhu, *J. Chem. Eng. Data,* 2012, **57**, 2394-2400.

15. Z. Zhang, F. Wang, D. Li and J. Yang, *J. Disp. Sci. Technol.*, 2012, **33**, 141-14

Appendix B

A fast and additive free C-C homo/cross-coupling reaction in reverse micellar gallows: A brief understanding on role of surfactant, water content and base on the yield of product and possible reaction site therein

Table-B.S1. Basic Data of the electrical conductivity of AOT RMs at regular interval during homocoupling reaction at fixed ω (= 15) and temperature (303K).

Time	Conductivity/μS cm^{-1}
Blank RM	0.15
Just adding $Pd(OAc)_2$	0.18
5 min	0.16
Just adding reagent	0.19
2 min	0.19
4 min	0.22
6 min	0.24
8 min	0.26
10 min	0.279

Table-B.S2. Basic data of DLS measurement of AOT RMs at regular interval during homocoupling reaction at fixed ω (= 15) and temperature (303K).

Time	D_h/nm
Blank RM	8.64 (±0.26)
Add reagent	13.35 (±0.40)
2 min	14.26 (±0.47)
4 min	15.90 (±0.43)
6 min	17.30 (±0.51)
8 min	19.33 (±0.59)
10 min	19.55 (±0.57)

Appendix C

Formation of High-Temperature Stable Benzimidazolium Ionic Liquid-in-Oil Microemulsion and Regioselective Nitration Reaction Therein

1-Ethyl-3-Propyl Benzimidazolium Bromide

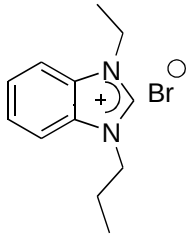

^{1}H NMR ($CDCl_3$, 300 MHz) δ 0.96 (t, J = 7.2 Hz, 3H), 1.65 (t, J = 7.2 Hz, 3H), 4.54 (q, J = 7.2 Hz, 2H), 4.64 (q, J = 7.2 Hz, 2H), 7.29-7.63 (m, 2H), 7.71-7.79 (m, 2H). ^{13}C NMR ($CDCl_3$, 75 MHz) δ

***p*-nitro anisole**

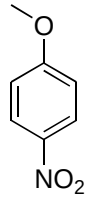

Yellow solid, MP = 52-54°C, ^{1}H NMR ($CDCl_3$, 300 MHz) δ 3.90 (s, 3H), 6.93-6.99 (m, 2H), 8.17-8.23 (m, 2H), ^{13}C NMR ($CDCl_3$, 75 MHz) δ 56.0, 114.0, 125.9, 141.5, 164.6.

***p*-nitro phenol**

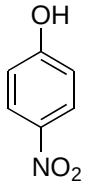

Yellow needles solid, MP = 113-115°C, ^{1}H NMR ($CDCl_3$, 300 MHz) δ 6.86-6.91 (m, 2H), 8.03-8.08 (m, 2H), 11.01 (s, 1H), ^{13}C NMR ($CDCl_3$, 75 MHz) δ 116.1, 126.5, 140.0, 164.3.

***p*-nitro aniline**

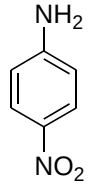

Yellow needles solid, MP = 146-149°C, ^{1}H NMR ($CDCl_3$, 300 MHz) δ 6.59-6.68 (m, 4H), 7.92-7.96 (m, 2H), ^{13}C NMR ($CDCl_3$, 75 MHz) δ 112.8, 113.1, 126.8, 136.1, 156.1.

Appendix D

Synergistic Interaction of Surfactant Blends in Aqueous Medium Reciprocates in Non-polar Medium with Improved Efficacy as Nanoreactor

Analytical data for Heck Product (4-methyl butyl cinnamate):

^{1}H- NMR ($CDCl_3$, 300MHz) δ 0.96 (t, 3H, *J* = 7.2 Hz), 1.44 (m, 2H), 1.68 (m, 2H), 2.36 (s, 3H), 4.20 (t, 2H, *J* = 6.6 Hz), 6.39 (d, 1H, *J* = 16.2 Hz), 7.18 (d, 2H, *J* = 7.8 Hz), 7.42 (d, 2H, *J* = 7.8 Hz), 7.66 (d, 2H, *J* = 16.2 Hz); ^{13}C-NMR ($CDCl_3$, 75 MHz) δ 13.8, 19.2, 21.5, 30.8, 64.4, 117.2, 128.0, 129.6, 131.7, 140.6, 144.6, 167.3.

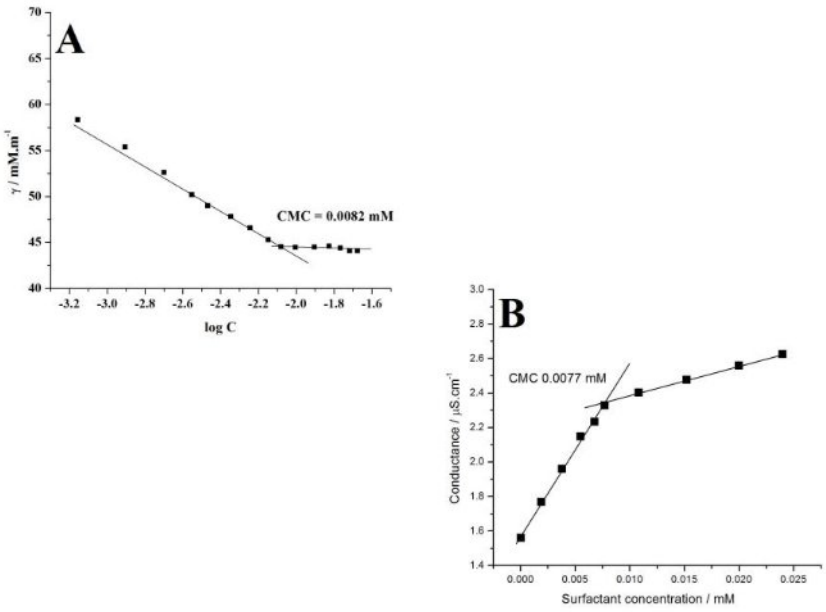

Figure-D.S1. Tensiometric (A) and conductometric (B) determination of critical micellar concentration (CMC) for single $C_{16}E_{20}$ surfactant system at a fixed temperature (303K).

Table-D.S1. Micellar parameters: experimental CMC values obtained from surface tension and conductivity techniques at 303K, literature CMC (CMC_{lit}) and ideal CMC (CMC_{ideal}) of binary mixture of cationic CTAB with non-ionic $C_{16}E_{20}$.

Micellar System	**CMC_{exp} (mM)**		**CMC_{lit} (mM)**	**CMC_{ideal} (mM)**
	Surface Tension	**Conductance**		
CTAB	0.9301	-	0.92[a], 0.871[b]	-
$C_{16}E_{20}$	0.0077	-	0.0080[c]	-
CTAB/$C_{16}E_{20}$ (1:1)	0.0105	0.0109	-	0.0150

[a,c]Ref,[1] [b]Ref.[2]

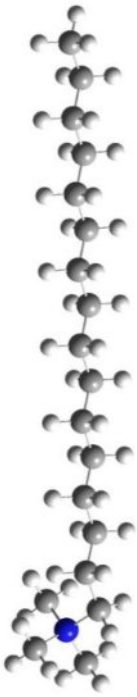

Figure-D.S2A. Optimized geometry at the B3LYP/6-31G level for isolated CTAB. Color code for atoms: blue, nitrogen; dark gray, carbon; and light gray, hydrogen.

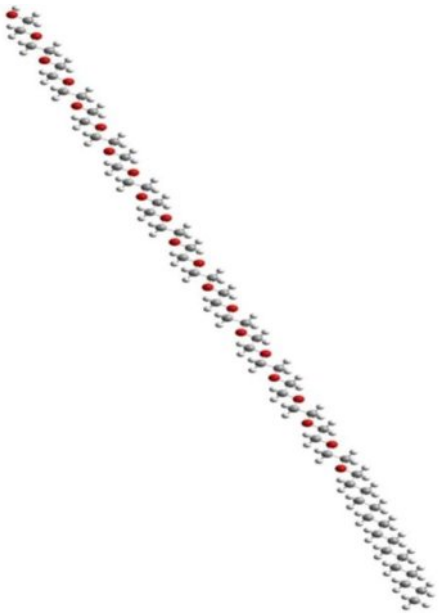

Figure-D.S2B. Optimized geometry at the B3LYP/6-31G level for isolated $C_{16}E_{20}$. Color code for atoms: red, oxygen; dark gray, carbon; and light gray, hydrogen.

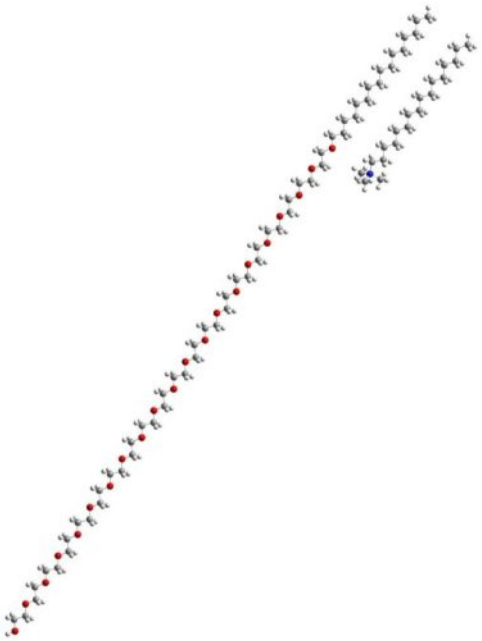

Figure-D.S2C. Optimized geometry at the B3LYP/6-31G level for CTAB/$C_{16}E_{20}$. Color code for atoms: blue, nitrogen; red, oxygen; dark gray, carbon; and light gray, hydrogen.

Table-D.S2. Optimization of C-C cross coupling Heck reaction in micelles and w/o mixed microemulsion media at 303K.[a]

Entry	Solvent	Water content (ω)	Yield (%)[d]
1.	Water	-	07
2.	CTAB[b]	-	57
3.	$C_{16}E_{20}$[b]	-	44
4.	CTAB/ $C_{16}E_{20}$[b]	-	66
5.	Heptane (Hp)	-	37
6.	Decane (Dc)	-	15
7.	Hp/1-pentanol (Pn) (1:2, wt%)	-	40
8.	Dc/Pn (1:2, wt%)	-	19
9.	Water/CTAB/ $C_{16}E_{20}$/Pn/Hp[c]	10	79
10.	Water/CTAB/ $C_{16}E_{20}$/Pn/Hp[c]	20	70

11.	Water/CTAB/ $C_{16}E_{20}$/Pn/Hp[c]	30	59
12.	Water/CTAB/ $C_{16}E_{20}$/Pn/Hp[c]	40	56
13.	Water/CTAB/ $C_{16}E_{20}$/Pn/Hp[c]	50	54
14.	Water/CTAB/ $C_{16}E_{20}$/Pn/Dc[c]	10	68
15.	Water/CTAB/ $C_{16}E_{20}$/Pn/Dc[c]	20	57
16.	Water/CTAB/ $C_{16}E_{20}$/Pn/Dc[c]	30	45
17.	Water/CTAB/ $C_{16}E_{20}$/Pn/Dc[c]	40	44
18.	Water/CTAB/ $C_{16}E_{20}$/Pn/Dc[c]	50	41

[a] Reaction condition: 4-iodo toluene (0.5 mmol), n-butyl acrylate (0.6 mmol), Triethylamine (1.0 mmol), $Pd(OAC)_2$ (0.02 mmol, 4 mol%), temperature; 303K, [b] Micellar system, [CTAB]= 0.9301 mM, [$C_{16}E_{20}$] = 0.0077 mM, [CTAB]:[$C_{16}E_{20}$] (1:1) = 0.0105 mM, [c] w/o mixed microemulsion; [water/CTAB/$C_{16}E_{20}$/Pn/oil, [CTAB]:[$C_{16}E_{20}$] (1:1); S:CS = 1:2 wt.%], [d] HPLC yield of the Heck product.

Table-D.S3. Interfacial composition and thermodynamicparameters of CTAB/$C_{16}E_{20}$/1-pentanol/*n*-heptane (or *n*-decane)/water microemulsion at 303K with varying water content (ω).

Ω	**10**	**20**	**30**	**40**	**50**
10^4 n_a^i/mol	15.30 (10.12)[c]	9.90 (7.42)	7.39 (5.92)	6.60 (5.45)	5.69 (4.68)
$10^4 n_a^0$/mol	10.29 (23.29)	20.59 (26.73)	28.50 (31.75)	33.34 (37.67)	42.48 (49.96)
K_d	20.65 (13.25)	10.46 (8.77)	5.24 (5.03)	4.07 (3.86)	3.54 (3.26)
$-\Delta G_t^0$/KJ mol^{-1}	7.62 (6.50)	5.91 (5.47)	4.17 (4.07)	3.53 (3.40)	3.18 (2.98)

[a]All the mixed microemulsion systems are formed using constant amount of mixed surfactant (0.5 mmol) and oil (14.0 mmol).

[b] The average errors in K_d and ΔG_t^0 were within ±5 and ±3%, respectively.

[c] The values in parentheses indicate parameters for n-decane (Dc) stabilized system.

Evaluation of interfacial and bulk composition of cosurfactant from thermodynamic point of view by the dilution method

W/o microemulsion consists of dispersion of water droplets in Hp or Dc continuum wherein the mixed surfactants (CTAB and $C_{16}E_{20}$ at equimolar composition) were considered to populate at the oil/water interface in partial association with the cosurfactant (Pn), which remained distributed between the

interface and the bulk oil, because of its negligible solubility in water.[3] Thus, at a fixed [surfactant(s)], a critical concentration of Pn is required for the stabilization of the mixed microemulsions. Addition of extra oil (Hp or Dc) extracts Pn from the interface to destabilize the system, which can be stabilized by the addition of extra cosurfactant in the system. This is the fundamental basis of oil dilution experiment (the dilution method). The following equations are helpful to rationalize the distribution vis-à-vis transfer process of Pn from the continuous oil phase to the interfacial region:

$$k_o = {n_a^0}/{n_o} \tag{S1}$$

$$\frac{n_a}{n_s} = \frac{n_a^i}{n_s} + k_o \frac{n_o}{n_s} \tag{S2}$$

$$K_d = {X_a^i}/{X_a^o} = \frac{{n_a^i}/{n_a^i + n_s}}{{n_a^o}/{n_a^o + n_o}} = \frac{n_a^i(n_a^o + n_o)}{n_a^o(n_a^i + n_s)} \tag{S3}$$

$$\Delta G_t^0 = -RT\ln K_d = -RT\ln \frac{X_a^i}{X_a^o} = -RT\ln \frac{I(1+S)}{S(1+I)} \tag{S4}$$

where, n_a, (n_a^i) and Gibbs free energy ($-\Delta G^0_t$), n_a^o, n_o, n_s denote the total number of moles of cosurfactant, its number at the interface, in the oil phase, the total number of moles of oil and the total number of moles of surfactant, respectively. A plot of n_a/n_s against n_o/n_s (Fig. S3) according to Eq. (S2) yields the values of the slope (*S*) and the intercept (*I*). Slope (*S*) is actually k_o and n_a^o can be determined from Eq. (S1). On the other hand, n_a^i can be calculated from the intercept (*I*), which is equal to n_a^i/n_s. The partition of cosurfactant between the continuous oil phase and the interface of the droplet can be expressed in terms of the distribution constant, which is represented by K_d. X_a^i and X_a^o are the mole fraction of alkanol in the interfacial layer and in the oil, respectively. ΔG^0_t represents standard Gibbs free energy change of transfer of cosurfactant from oil to the interface.

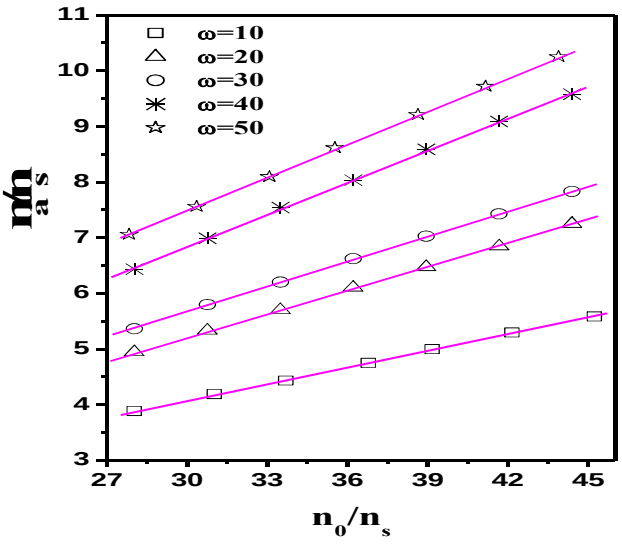

Figure-D.S3. Plot of n_a/n_s against n_o/n_s for systems comprising equimolar (1:1) mixed surfactant (CTAB and $C_{16}E_{20}$) (0.5mmol) and n-decane (14.0 mmol) stabilized by 1-Pn with different ω (10→50) at a constant temperature (303K).

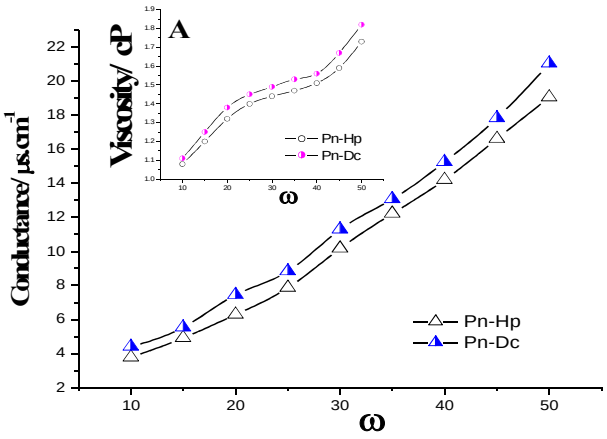

Figure-D.S4. Dependence of conductance value on water content (ω) for CTAB/$C_{16}E_{20}$ (1:1)/Pn/Hp (Dc)/water microemulsions at 303K. **Inset A**: Dependence of viscosity on water content (ω) for the same systems of similar composition at 303K.

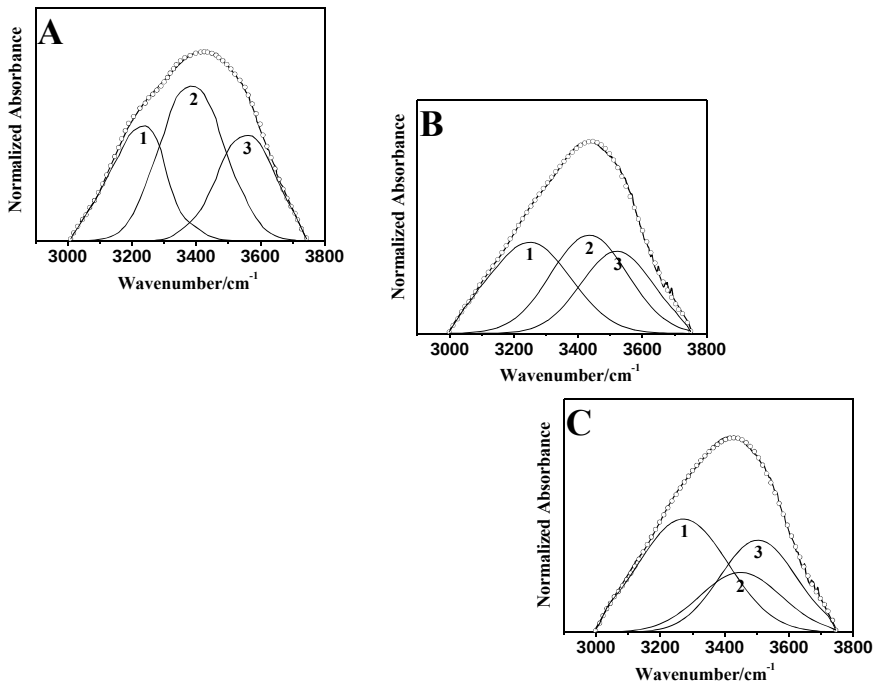

Figure-D.S5. Representative FTIR spectra of O-H band for w/o mixed surfactant microemulsions, CTAB/$C_{16}E_{20}$/Pn/Hp/water at equimolar composition (1:1) as a function water content (ω) at fixed **surfactant and cosurfactant mass ratio (1:2)**and temperature (303K) [A: ω = 10; B: ω =30; and, C: ω= 50 (Specification: experimental spectra, overall fitted curve (open circle) and deconvoluted curves (*1: free water; 2: bound water; 3: trapped water*)].

Reference:

1] S.K.Mehta, S. Chaudhary, *Colloids Surf. B* 2011, **83,** 139-147.
2] T.Chakraborty, S. Ghosh, S.P.Moulik, *J. Phys. Chem. B* 2005, **109,** 14813-14823.
3] S.P.Moulik, L.G.Digout, W.M.Aylward, R. Palepu, *Langmuir*, 2000, **16,** 3101-3106.

CHAPTER I

Brief Review on Microemulsion as Reaction Media

I.A.Introduction

The consciousness over the massive use of organic solvents having some undesirable characteristics as high boiling points, high inflammability, toxicity in synthetic chemistry leads much effort to carry out the reactions in water which is an environmentally benign solvent. But, the potential inconvenience with the application of water is the incompatibility of organic molecules with water. To solve this problem, many attempts have been made, e.g., the application of the "on water" process,[1-4] the application of hydrophilic cosolvents,[1,5] the use of phase-transfer catalysis,[6] pH regulation of the reaction mixture,[1,7] the use of super-heated water[8,9] or the application of ultrasound or microwave irradiation.[9] Another interesting way is to study the chemical reactions in microemulsions as excellent solvents both for hydrophobic organic compounds and for inorganic salts.[10]

The introduction of microemulsion in the scientific literature is normally ascribed to Schulman. He and his co-workers produced a considerable fraction of the early work regarding their preparation and properties.[11-15] In 1943, Hoar and Schulman[11] found that a ternary system consisting of sodium stearate-cetane-water became transparent as a straight chain alcohol (*n*-hexyl alcohol) was added. In 1959, Schulman and Stoechnius[15] introduced the term "microemulsion" to describe this four-component system. The straight chain alcohol was called "cosurfactant". In 1985, Shah *et al.*[16] further gave a complete definition: *i.e.*, microemulsion is a thermodynamically steady isotropic dispersion of two immiscible liquids consisting of micro-domains of one or both liquids, which are stabilized by the interfacial film of surface-active molecules.

The breakthroughs in microemulsions studies have occurred in the past decade. Now-a-days, mEs are generally considered as monodispersed spherically droplets (10-100nm in diameter) of water-in-oil (w/o) or oil-in-water (o/w) type (Scheme I.1) depending on the nature of surfactants and composition of mEs. The w/o microemulsions are grossly differs from reverse micelles (RMs) in terms of water content in the pool. If the water content exceeds the solvation requirement of the amphiphilic head groups, the term "reverse micelle" is replaced by "w/o microemulsion".[17] The microheterogeneity or compartmentalization of such dispersion with unique physicochemical properties viz. spontaneous formation, clear

appearance, thermodynamic stability, low viscosity, ultra-low interfacial tension, large interfacial area and high solubilization capacity for both hydrophilic and lipophilic compounds, make them useful in biological and technological applications, Such as oil recovery to pharmaceutics, food technology, photochemical reaction, enzymatic catalysis, nano-particle synthesis, organic and bio-organic reactions etc.[18-24]The first studies were carried out in the exploration of microemulsions as media for organic reactions by Fendler et al.[25] and Menger et al.[26] Microemulsions are nowadays grasped as a highly versatile reaction media, which currently find many applications. Two introductory review articles by Sanchez-Ferrer and Garcia-Carmona[27] and by Holmberg[28] should be cited from the extensive literature. In the first review, reverse micelles are compared with reverse vesicles, which were uniquely described for the first time in 1991.[29] Recently, Ghosh et al. has explored a review article in which plausible reaction location in microemulsion has been discussed.[30]

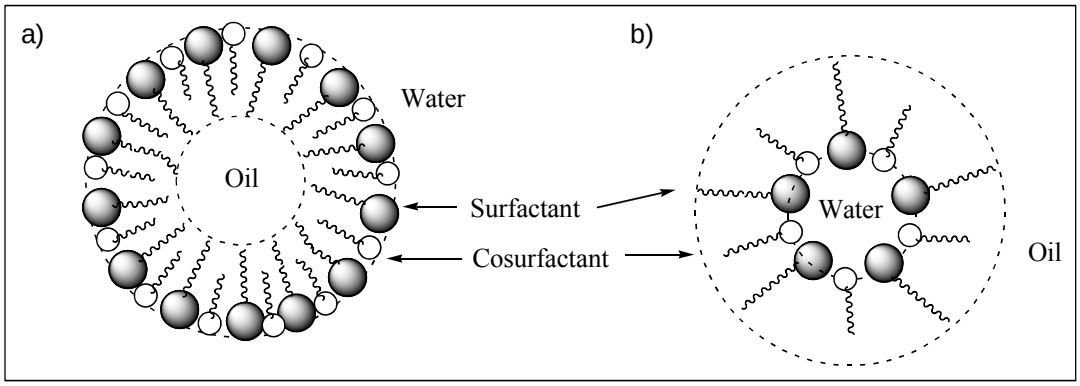

Scheme-I.1 The two types of microemulsion: a) Direct microemulsion b) Inverse microemulsion

I.B.Characterization of microemulsions

The organic reactions in microemulsion medium have been facilitated by the effect of the microsructure of such complexed fluid. The reaction parameters can also be altered by changing the microenvironment, such as the droplet size, the interfacial area etc. In this way, rapid attention has been paid to focus on the characterisation of composition and physical properties of the different pseudo-phases of the microemulsions. Due to their complexity, namely different types of structures and components involved in these systems, as well as the limitations associated with each technique, the characterization of microemulsions is rather a difficult task. Multiple complementary techniques are required in order to understand and also to manipulate microemulsion behavior. Some of these techniques, starting from phase

behavior to Electron microscopy are presented, in brief, to identify and characterize microemulsions in the following section.[17]

I.B.1.Phase behavior of microemulsions

Phase studies are inevitable for the basic understanding of general phase behavior and kinetics of the structural changes of a system.[31, 32] Phase diagrams for microemulsions are quite complex since there are at least three components; water, oil and surfactant. A map of the locations of different phases in composition space is known as a "phase diagram" of microemulsions.[17] A pictorial representation of "phase diagram" (as a model) considering different phases in composition (of water, surfactant and oil mixtures) has been depicted in Figure-I.1.

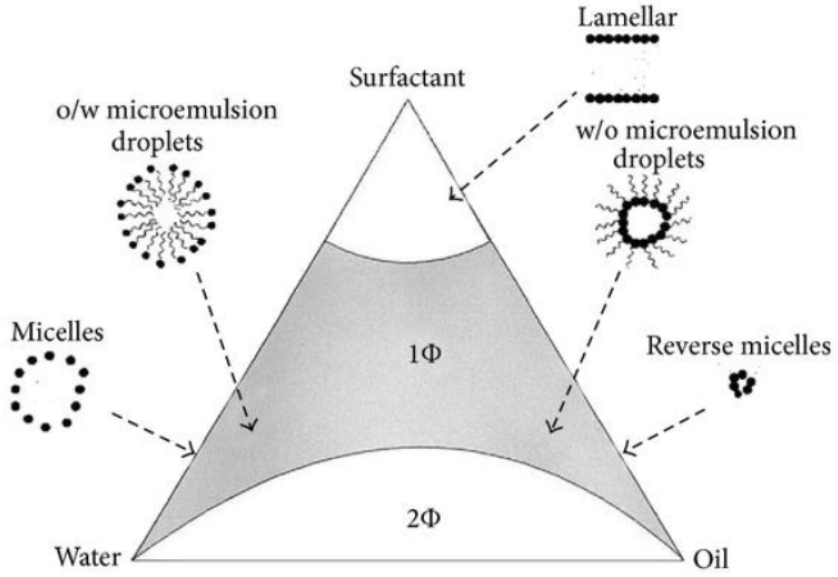

Figure-I.1. Pictorial representation of "phase diagram" of water, surfactant and oil mixtures.

The phase behavior of microemulsions depends on chemical structures of oils and surfactants, temperature, pressure and additives such as salt and polymers etc. Phase diagram provide information on the boundaries of the different phases as a function of composition variables, temperatures, and, more important, structural organization can be inferred. Phase behaviour studies also allow comparison of the efficiency of different surfactants for a given application.[10] In the phase behaviour studies, simple measurement and equipments are required. The boundaries of one-phase region can be assessed easily by visual observation of samples of known composition.

I.B.2.The Schulman's cosurfactant titration at the oil/water interface (Dilution method)

It is considered that in the formation of water-in-oil (w/o) microemulsion using a blend of surfactant/cosurfactant (amphiphiles), all the surfactant molecules reside at the interface and the cosurfactant molecules are distributed between the bulk oil and the interface depending upon their solubility in water. At fixed water to surfactant composition, a threshold amount of cosurfactant is required for the formation of stable microemulsion, and the size of the dispersed droplets in the dispersion is controlled by the cosurfactant composition. Although direct determination of cosurfactant distribution between the interfacial plane and the bulk oil is difficult, [33] reports are available in literature using techniques, like SANS, SAXS and DLS,[34, 35] conductivity,[36] interfacial tension.[37] To understand chemical reactivity of a single or mixed species either inside the water pool or at the interface of a quaternary w/o microemulsion, the in depth knowledge on (i) interfacial composition such as relative population of surfactant and cosurfactant at the oil/water interface, (ii) the distribution of cosurfactant among the interface and bulk oil phase vis-à-vis the thermodynamics of this transfer process of cosurfactant, (iii) the number and the size of the droplets and (iv) the physicochemical characteristics of the entrapped water, are essential. These parameters are strongly influenced by the type and alkyl chain length of oil and the amphiphiles (surfactant or cosurfactant).[36] All these parameters [except (iv), which can be determined from Fourier transform infrared spectroscopy and FTIR measurements],[38] can be evaluated (without using sophisticated instruments) from the dilution method which is a pioneering work of Bowcott and Schulman.[13] This simple but elegant method is accomplished by adding oil at a constant water and surfactant ratio to destabilize an otherwise stable w/o microemulsion and then restabilizing it by adding a requisite amount of cosurfactant (alcohol). For these reasons, the dilution method (which is commonly represents the Schulman's cosurfactant titration of the oil/water interface) has been widely used by a number of workers to estimate the parameters involved in the transfer of alcohol from the bulk oil to the interface.[39-43] The method provides an understanding of the interfacial compositions of surfactant and cosurfactant as well as distribution of the cosurfactant between the interface and oil, and can quantatively account for the thermodynamic stability of microemulsion. The mathematical model based on the dilution method and the evaluation of corresponding parameters has been discussed in details in subsequent chapters.

I.B.3.Electrical conductivity

Electrical conductivity is a structure-sensitive property. Nevertheless, the results obtained from conductivity study do not provide a straightforward picture of the microstructure of microemulsions, but transition from water continuous to oil continuous microemulsion can easily be obtained from such measurements, since water continuous formulation (o/w microemulsion) usually shows higher conductance than the oil-continuous formulations (w/o microemulsion).[44] The low conductance in dilute w/o microemulsion has been explained on the basis of charge fluctuation model.[45,46] Further, for the w/o microemulsion systems, transition from discrete droplet structure to connected droplet or bicontinuous structure can be envisaged from sharp increase in conductance value (100-1000 times increase) with increasing volume fraction of the polar solvent or temperature. Such phenomenon is called "conductance percolation".

I.B.4.Viscosity measurement

Microemulsions have varied flow behaviors, for example, lamellar (Newtonian) and non-lamellar (non-Newtonian). Low viscous microemulsions show Newtonian behavior. The Winsor-III and the bicontinuous types are usually non-Newtonian in nature and they can show plasticity.[47] The viscous properties of microemulsions depend on the type, shape and number density of aggregates present, as well as the interactions between these aggregates. The phenomenon of percolation in microemulsion is associated with droplet clustering and fusion, i.e. internal structure changes and hence, it is reflected in viscosity.

I.B.5.Light scattering techniques

Among the light scattering techniques, dynamic light scattering (DLS), also known as photon correlation spectroscopy, can be used to analyze droplet size of microemulsion via determination of hydrodynamic radius from measurements of the diffusion constants of diluted dispersed phase (droplets) undergoing Brownian motion.[44] This technique provides the determination of z-average diffusion coefficients (D). If interparticle interaction is assumed to be absent in a system, the hydrodynamic radius of particles (droplets) (d_h) can be obtained from the Stokes-Einstein equation:

$$D = k_B T/6\pi\eta\, d_h$$

where, k_B is Boltzmann constant, T is absolute temperature, η is the viscosity of the medium. The DLS technique is useful to characterize size and size distribution of microemulsion droplets, as it monitors the collective diffusive motion in such systems, provided simple diffusion is the sole mechanism responsible for the variation of the scattered intensity.[48,49] Polydispersity index (PDI) is another important parameter for evaluation of measurement from DLS experiment. The ratio SE/d_h, where SE is the standard error in d_h, is called PDI.[50] For a mono-dispersed sample, the PDI value is taken to be less than 0.08; whereas the value ranges from 0.08-0.7 is considered as a mid-range polydispersity.[51] Several authors have significantly contributed to the understanding of different interactions in the microemulsion droplet core by measuring the droplet size.[48, 51, 52]

The interaction between droplets can be investigated by employing Static Light Scattering (SLS) technique, where the intensity of scattered light is generally measured at various angles for different concentrations of microemulsion droplets. At sufficiently low concentrations, the Rayleigh approximation is used provided the particles are small enough.[53]

I.B.6.Neutron and X-ray scattering techniques

In small angle neutron scattering (SANS), neutrons from a reactor source are scattered by the atomic nuclei of the sample. An advantage of the use of neutrons is that neutrons are non-destructive compare to X-rays, and hence, radiation damage rarely occurs in a neutron based experiment. SANS provides relevant information about structure of microemulsions.[54-56] Normal hydrogen and deuterium have significantly different scattering lengths. Thus scattering contrast between heavy water and hydrocarbon is very high. By varying the contrast and even matching the contrast between different components of a mixture, selective portions can be highlighted. By matching the scattering length densities of water and oil, structure of both droplet-type and bicontinuous microemulsions can be established.[57,58] Radiation wavelength of X-rays (1-10 Å) is smaller than the typical structural length scale in microemulsion. Thus, small angle scattering with X-rays can be very useful to determine the size and shapes of microemulsion droplets from the magnitude and angular dependence of the scattered intensity.[52, 59, 60] Using synchrotron radiation sources, information about a wide range of systems can be obtained with this technique, including those systems in which the surfactant molecules are poor X-ray scatterers.[61]

I.B.7.Spectroscopic probing techniques

Several spectroscopic techniques have been used to study different aspects of structures and properties of microemulsions. The absorption and steady-state emission spectroscopy of probe molecules solubilized in a microemulsion system can probe the polarity of the microemulsion at their solvation location.[62] Chemiluminescence techniques have also been employed to study transitions between polar and non-polar environments in microemulsion systems. Time-resolved emission spectroscopy provides the information about the dynamics and rotation relaxation of solvent in microemulsions.[62-64] In particular, fluorescence lifetime measurement is a highly sensitive method where the lifetime of a fluorophore can alter in response to changes in the conformational state of the probe molecules or in response to the interaction with local environment in microemulsion systems.[65] The steady-state anisotropy or polarized fluorescence study provides a simple means of monitoring the processes, in which the microstructure of the microemulsion is affected in some way.[65]

In addition, fluorescence correlation spectroscopy (FCS), which may be considered as a miniaturization of DLS, measures the tiny spontaneous fluctuations in fluorescence intensity of molecules in a very small volume (spot), and quantifies it by temporarily auto-correlating the recorded intensity signal to obtain the variation in local concentration of fluorescent species and hence, their diffusion coefficient.[66] This technique is an excellent tool for measuring molecular diffusion and size of microemulsion droplets under extremely dilute conditions. In recent experiments, FCS technique has been shown to be applicable to microemulsion systems, where for the w/o AOT system from the diffusion times hydrodynamic radii were determined which compared well to the values obtained in parallel by SANS.[67]

I.B.8.Nuclear Magnetic Resonance (NMR)

This experimental technique provides important information about the microstructure of microemulsions. Proton magnetic resonance has proven to be a useful technique for identifying the structure of water solubilized in reverse micelles. Addition of water to reverse micelles does not significantly affect the chemical shift of other protons, except H_2O. The water proton magnetic resonance exhibits a single peak, indicating the rapid exchange between water protons at various states.[68, 69] The observed chemical shift results from the weighted average of different water species.

I.B.9.Fourier Transform Infrared Spectroscopy (FTIR) measurements

The knowledge about hydration of surfactants in w/o microemulsions or reverse micelles is helpful for understanding of the dynamics of different physicochemical processes operative within the confined environment (i.e, local interactions in the vicinity of water molecules in w/o microemulsion). Further, it is also helpful and prospective for applications in biological and chemical reactions occurring in w/o microemulsions or reverse micelles.[70] In order to get a clear understanding of various interactions in the droplet core, including the type of H-bonding which is operative within the water pool, an excellent and non-invasive technique viz., Fourier transform infrared spectroscopy **(**FTIR) has been introduced. Several authors significantly contributed to the understanding of the water dynamics in single and mixed surfactant derived w/o microemulsion systems by studying the state of water using FTIR method.[38,39,68] The characteristics of the water molecules confined inside the water pool depend strongly on both water content and the nature or type of the surfactant head group.[71]

I.B.10.Electron Microscopy

Transmission Electron Microscopy (TEM) is the most important technique for the study of microstructures of microemulsions because it directly produces images at high resolution and it can capture any co-existent structure and micro-structural transitions.[72]

There are two variations of the TEM technique for fluid samples.[73]

1. The cryo-TEM analyses in which samples are directly visualized after fast freeze and freeze fructose in the cold microscope.

2. The Freeze Fracture TEM technique in which a replica of the specimen is images under RT conditions

I.C.Effect of the Microenvironment on Reaction

Microemulsions can accelerate the reaction because of their special structural features which can be tuned by proper selection of ingredients in the formulation. The reaction rate is often influenced by the charge at the interface and this charge depends on the surfactant used.[10] The surfactant monolayer attracts reagents of opposite charge situated in the water domain, thus increasing its concentration in the interfacial zone, wherein the reaction occurs. Microemulsion can also induce regioselectivity in organic reactions changing the product

composition compared with the products obtained in a microhomogeneous solution. The induced regioselectivity is believed to be due to the interface acting as a template for reactants having one more polar and one less polar end.[74] Such a compartmentalization and concentration of the reagents may lead to a rate enhancement.

The dynamic character of these nano-reactors is one of the most important features for chemical reactions carried out in these media.[75] Dynamic means the continuous motion or movement of a particle not static ones and this is also true in case of microemulsion. The dynamical nature favors contact between the reactant molecules. In motion, several particles collide with each other and exchange of materials can takes place. As microemulsion domains are mainly constituted by spherical droplets. All droplet-droplet collision does not effective for the material interchange. The collision between the nanodroplets containing different reactant molecules, the reactant can be transferred and both reactants can be located inside the same droplet. As the reaction takes place, more droplets could contain products and reactants simultaneously.

Again, the character of the oil used in the microemulsion formulation may also influence the reaction at the interface. Luis García-Río et al. investigated a chemical reaction by hydrolysis of anisoyl chloride.[76] A water-in-oil microemulsion was formulated with an anionic surfactant and a range of organic solvents were explored as oil component. It was found that the hydrolysis reaction proceeded faster with alicyclic hydrocarbons than with cyclic hydrocarbons and smaller alicyclic hydrocarbons gave faster reaction than the longer homologues. Moreover, changing the droplet size one could allow to tune the ratio of unbounded to bounded molecules in nanodroplets and hence its solvation properties. This confinement can enable the reactivity to be controlled. Microemulsion can also influence both reaction kinetics and equilibria.[10, 77, 78] It has been shown that mEs media can enhance or retard the chemical reaction [79-83] depending on the nature of the surfactant, the nature of the oil phase, and the size of the water pool present in the medium. Hence, Microemulsions are very versatile solvent systems, which also play an outstanding role as reaction media.

I.D.Examples of Reactions in Microemulsion

I.D.1.Transition Metal Catalysed C-C Coupling Reaction

Coupling reactions are widely used routes for the formation of carbon-carbon bonds and carbon–heteroatom bonds in particular for the synthesis of biaryl compounds.

I.D.1.1. Homocoupling as well as Suzuki Coupling Reaction

The Suzuki cross-coupling reaction is one of the most widely used reactions for the synthesis of polymers, liquid crystals, agrochemicals, and pharmaceuticals. An enhancement of palladium-catalyzed Suzuki cross-coupling reactions between substrates possessing long-chain alkyl or oxyalkyl substituents in toluene or dimethoxyethane/water mixtures by the addition of sodium dodecylsulfate (SDS) and n-butyl alcohol as co-surfactants is shown by Vashchenko et al. [84]

In 2008, Jiang et al. have presented ligand-free Suzuki reactions catalyzed by Pd/C can be efficiently performed in TX100 microemulsions (Scheme I.2.). A number of aryl halides, including aryl iodides, bromides, and chlorides, were with arylboronic acids smoothly and efficiently to produce good to excellent yields.[85]

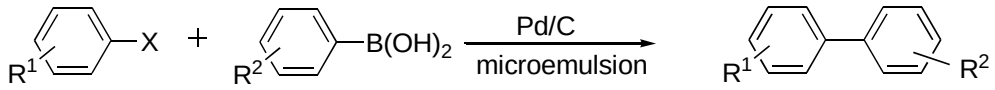

Scheme-I.2. Ligand-free Suzuki reaction catalysed by Pd/C in microemulsion.

I.D.1.2. Heck Reaction

The Heck reaction is one of the most important methods in synthetic organic chemistry for the formation of C–C bonds.[86] Jiang et al. reported heptane/TX 10/butanol/water/propylene glycol microemulsion containing in situ formed palladium nanoparticles, a very efficient catalyst system for the ligand-free Heck reaction (Scheme I.3).[87]The results indicated that the aqueous phase concentration, the base concentration, and the temperature played key roles in the conversion of the reaction. Iodobenzene was converted to the corresponding *trans*-stilbene quantitatively within 90–150 min.

Another report presented by Zhang et al. is Ligand free Heck reaction in the water-in-Ionic Liquid microemulsion [H_2O/TX-100/1-butyl-3-methylimidazolium hexafluoro phosphate ([BMIM]PF_6)][88] in which the Pd nanoparticles were prepared *in situ.* Surfactant TX-100 served as the reductant and the stabilizer of the nanoparticles. The TEM images presented that the monodispersed Pd nanoparticles have a mean particle size of 3 nm.

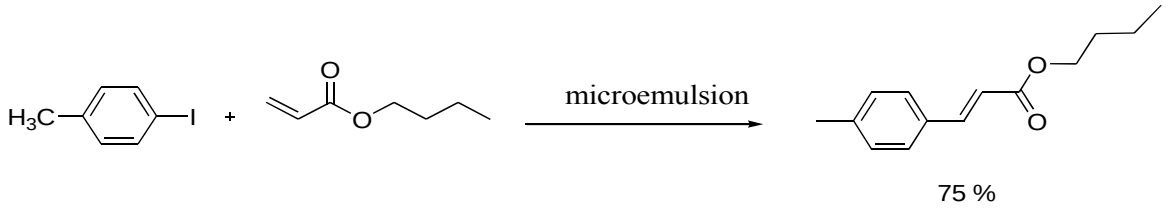

Scheme-I.3. The Heck Reaction in microemulsion media

I.D.1.3. Chiral Synthesis

Gayet et al. employs a ternary system $BnPyrNTf_2$/TX100/toluene as nanoreactors to perform a Matsuda-Heck reaction between p-methoxyphenyl diazonium salt and 2,3-dihydrofurane in the presence of a palladium catalyst at 27^0C. The reaction results the two two regioisomers A and B and their corresponding stereoisomers (Scheme I.4).[89]

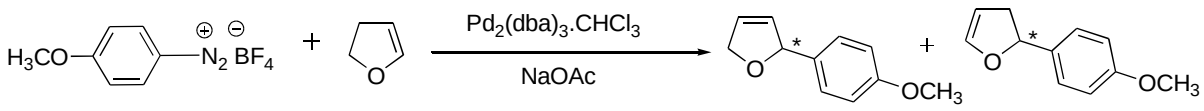

Scheme-I.4. Matsuda-Heck reaction between a p-methoxyphenyl diazonium salt and 2,3-dihydrofurane using a palladium catalyst.

I.D.1.4. Sonogashira Reaction

In absence of ligand, copper or amine, Pd/C catalyzed Sonogashira reactions of aryl iodides and bromides with phenylacetylene were performed well in TX10 microemulsions at 70°C by Jiang et al. (Scheme-I.5) Aryl iodides and activated aryl bromides were converted to the corresponding diaryl-substituted alkynes quantitatively within 30–150 min and the reactivity in the microemulsion was higher than that in biphasic system.[90] The "heterogeneously" catalyzed Sonogashira coupling reaction was due to "dissolved Pd-species".

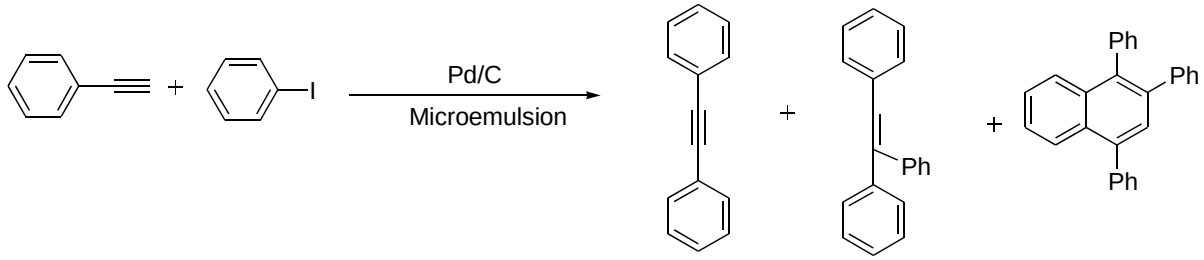

Scheme-I.5. Sonogashira coupling reaction of iodobenzene with phenylacetylene in TX10 microemulsion

Again, a rapid copper- and ligand-free Sonogashira reaction was performed in an oil-in-water microemulsion (Scheme-I.6) by Jiang et al. Palladium nanoparticles can be in situ formed in the microemulsion, heptane-in-water, without other reductants.[91] Excellent yield of the Sonogashira reaction catalyzed by 0.5 mol% palladium could be achieved at 80°C within 2 min. It has been observed that the ligand-free Sonogashira reaction resulted good yield in microemulsion compared to micelle. The effect of surfactants, alcohols, reaction temperature was also investigated. The reaction in CTAB microemulsion had higher reactivity than that in TX100 microemulsion.

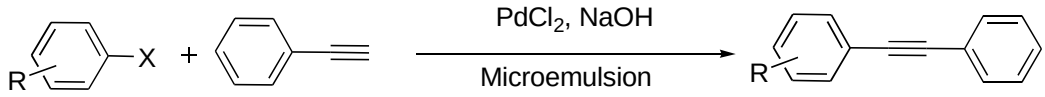

Scheme-I.6. Sonogashira reaction catalysed by $PdCl_2$ and NaOH in microemulsion**.**

I.D.2. Catalytic Hydrogenation

Brusco et al. have studied structural dimensions of two different microemulsions and correlated with the catalytic hydrogenation of dimethyl itaconate (DMI) performed in such media: (a) [Triton X-100–1-pentanol]–cyclohexane–water and (b) Igepal CA-520–cyclohexane–water (Scheme-I.7). [92] Dynamic light scattering (DLS) and small angle neutron scattering (SANS) measurements were used to determine the characteristic sizes of the Igepal and Triton microemulsions, respectively, showing a linear dependence between the initial hydrogenation rate of DMI and the radius of the micelles. The initial hydrogenation rate of DMI in bulk water is exceeded in both microemulsions. Indications of deformation of the originally spherical Triton X-100 reverse micelles upon addition of the water-soluble catalyst complex Rh–TPPTS were found.

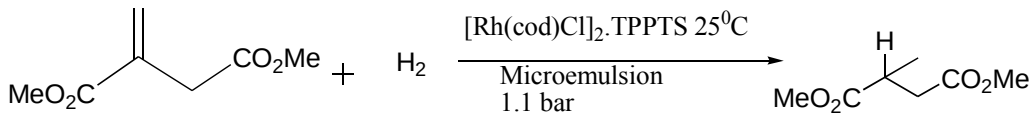

Scheme-I.7. Hydrogenation of dimethyl itaconate formal reaction.

I.D.3. Cycloaddition

Diels-Alder (DA) reactions provide a powerful synthetic tool in organic chemistry and constitute the key step in the preparation of a large number of six-membered rings. The Diels-Alder reaction between *N*-ethylmaleimide and cyclopentadiene in water/AOT/isooctane microemulsions, where AOT denotes sodium bis(2-ethylhexyl)sulfosuccinate, was first studied by Engberts et al. (Scheme-I.8).[93] The rate of the reaction was found to be higher than that obtained in pure isooctane, irrespective of the particular microemulsion composition used. On the basis of these results, the reaction takes place simultaneously in the continuous medium and at the microemulsion interface. The favourable arrangement of the reactants at the interface results in more than 95% of the reaction occurring in this microenvironment. The kinetic analysis revealed the rate constant at the microemulsion interface to change with the water content.

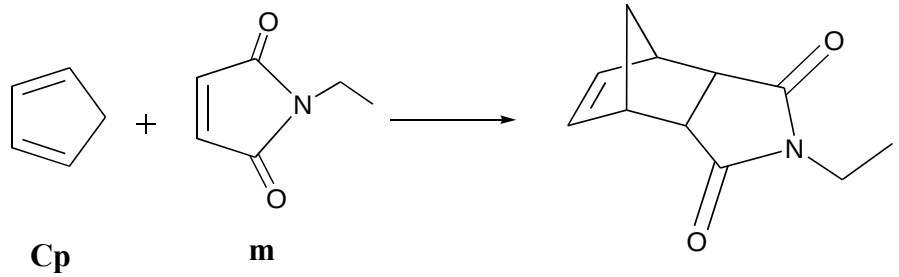

Cp **m**

Scheme-I.8. The Diels Alder Reaction between *N*-ethylmaleimide and cyclopentadiene

Further, they have studied the 1, 3-dipolar cycloaddition of benzonitrile oxide to *N*-ethylmaleimide in AOT/isooctane/ water microemulsions at 25.0 °C and found the reaction rate to be roughly 150 and 35 times greater than that in isooctane and pure water, respectively (Scheme-I.9). The accelerating effect of the microemulsion is the combined result of an increase in the local concentrations of the reactants through incorporation into the interface and of the intrinsic rate of the process through electrostatic interactions with the headgroups in the surfactant (Scheme-I.10).[94]

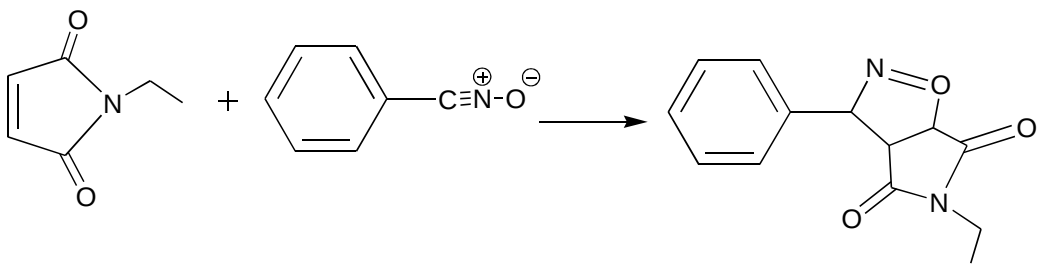

Scheme-I.9. The Diels Alder Reaction between N-ethylmaleimide and benzonitrile oxide

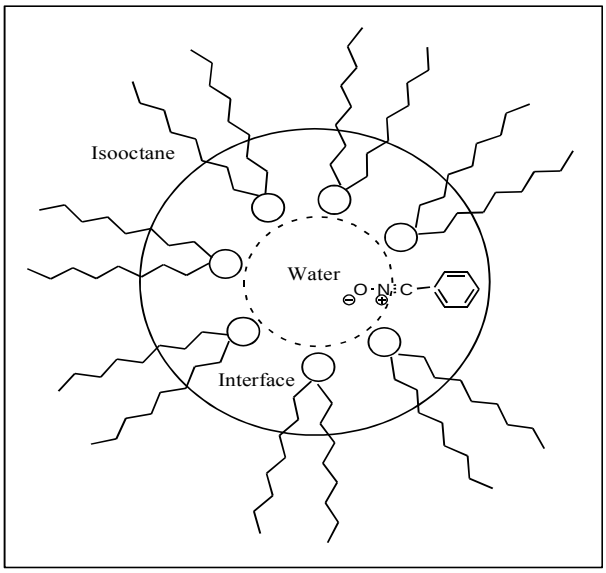

Scheme-I.10. Dipolar benzonitrile oxide, in the innermost region of the microemulsion interface

In 2012, Lu et al. have studied Diels-Alder Reaction (DAR) between N-ethylmaleimide and 2,3-dimethyl-1,3-butadiene in microemulsions with ionic liquid (IL) (IL-H_2O/AOT/isooctane) (Scheme-I.11). [95]The effect of solvent, IL and temperature on the DAR rate was investigated and interpreted. The experimental results showed that the reaction rate in the microemulsion with IL was enhanced and it was faster than that in pure isooctane and in generic AOT microemulsion.

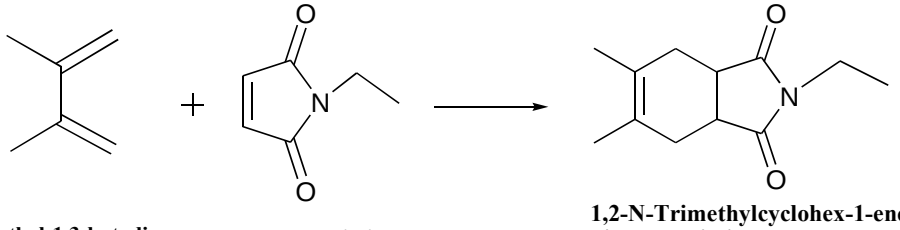

2,3-Dimethyl-1,3-butadiene **N-Ethylmaleimide** **1,2-N-Trimethylcyclohex-1-ene-4,5-dicarboxylimide**

Scheme-I.11. The Diels alder Reaction in IL-microemulsion

I.D.4. Oxidation

Blach et al. have described a recyclable and environmentally friendly process for the oxidation of cyclohexene by hydrogen peroxide in microemulsions, water/ Benzalkonium chlorides (BenzCl)/cyclohexene (Scheme-I.12).[96] Microemulsion provides homogeneous

media for close contact between the reagents in the hydrogen peroxide phase, leading to a better reactivity without the need for strong stirring or very high temperatures.

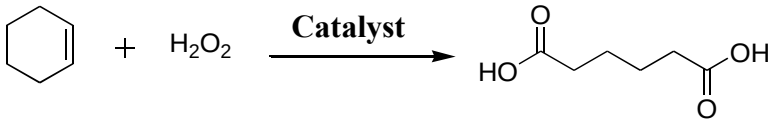

Scheme-I.12. Oxidation of cyclohexane with hydrogen peroxide

I.D.5. Solvolysis

In 2006, Garcia-Rio et al. have demonstrated butylaminolysis of 4-nitrophenyl caprate (NPC) in AOT/chlorobenzene/water microemulsions.[97] It is shown that the reaction, i.e., nucleophilic attack of butylamine on the ester occurred both at the interface and in the continuous medium simultaneously.

In a review, García-Río et al. shows Solvolysis of substituted benzoyl chlorides in AOT based microemulsion (Scheme-I.13).[98]

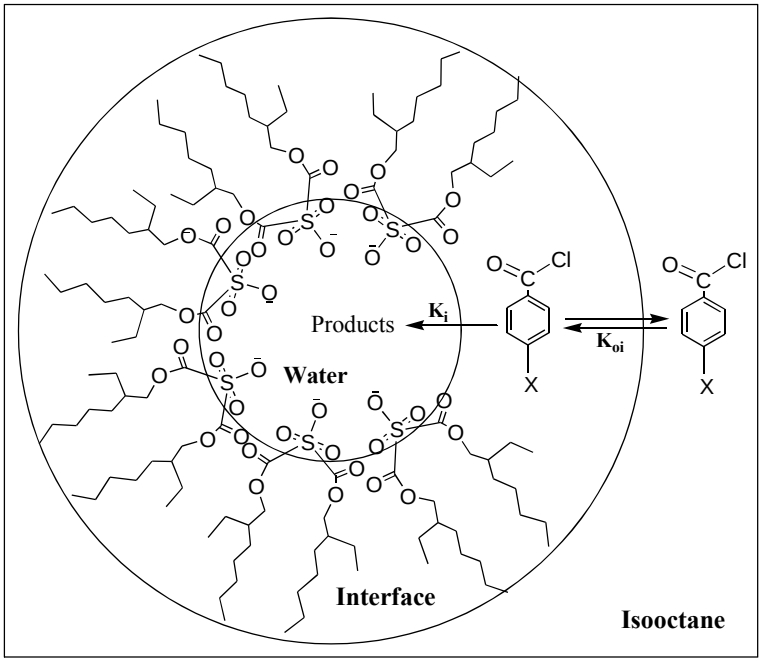

Scheme-I.13. Solvolysis of substituted benzoyl chloride

I.D.6. Condensation Reaction

J.J. Shrikhande et al.[99] have demonstrated the condensation between benzaldehyde and acetone in a cationic surfactant based o/w microemulsion prepared from the combination of n-butanol as co-surfactant, n-hexane as oil and cetyltrimethylammonium bromide (CTAB) as the cationic surfactant(Scheme-I.14). Various parameters influencing the formation of microemulsions, e.g., oil content, surfactant content, oil and co-surfactant ratio were varied and their corresponding effects on the solubilisation of reactants and rate of a condensation reaction were studied. A direct correlation between the droplet size of the microemulsion and rate of the reaction is observed.

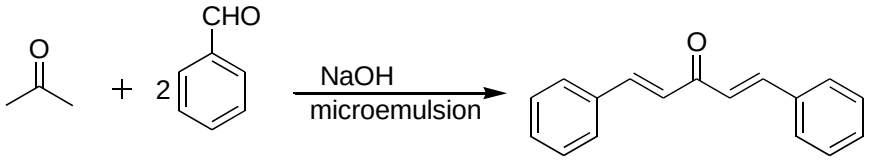

Scheme-I.14. The condensation Reaction in o/w microemulsion

Further a proline catalysed aldol reaction between acetone and p-nitrobenzaldehyde has been studied by P. R. Arivalagan et al. (Scheme-I.15). [100] L-Proline and their derivatives are among the most important class of organic catalysts. Three prolinamide surfactants are designed and synthesized herein. Although the surfactants carried identical catalytic groups (Scheme-I.16), their headgroups contained different functionalities that affected their ability to self-assemble under reverse micelle conditions (DMSO-in-Benzene) and hydrogen-bond with the reactants. The surfactant with a zwitterionic headgroup (catalyst 3) capable of strong aggregation was found to have the highest activity.

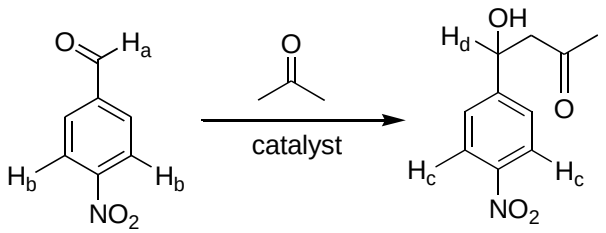

Scheme-I.15. Aldol Condensation in acetone and p-nitrobenzaldehyde

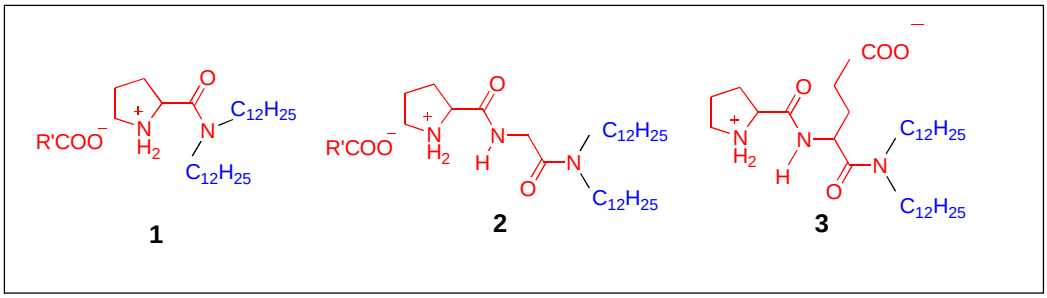

Scheme-I.16. Structures of prolinamide surfactants.

I.D.7. Nitration

M. Hojo reported Nitration of phenol in reversed micelle systems, $CHCl_3$/CTAC/H_2O with dilute nitric acid at 35°C to obtain 2- and 4-nitrophenols, where CTAC represents cetyltrimethylammonium chloride. In CTAC and AOT reversed micelle ($CHCl_3$ or heptane/AOT) medium, 4-methylphenol was converted to 2-nitro-4-methylphenol, where AOT stands for sodium bis (2-ethylhexyl) sulfosuccinate.[101]

Highly regiospecific mononitration of phenol by the reagent $NaNO_3$ and dilute sulfuric acid was carried out in a TX100 oil-in-water microemulsion by Jiang et al. [102] (Scheme-I.17). Effects of acid type, surfactant concentration, water content, and alcohol have been investigated.

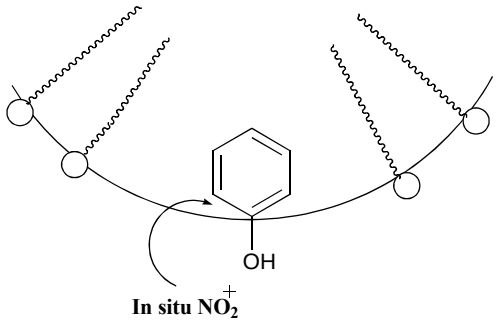

Scheme-I.17. Nitration of Phenol in O/W microemulsion with dilute Hydrochloric acid and sodium nitrate

I.D.8. Miscellaneous

Mehta et al. have reported a novel synthetic route for preparing organoselenium compounds [4-chloro-2-(naphthalen-2-ylselanyl) pyrimidine] in mixed AOT/lecithin surfactants based reverse isooctane microemulsion (Scheme-I.18).[103]

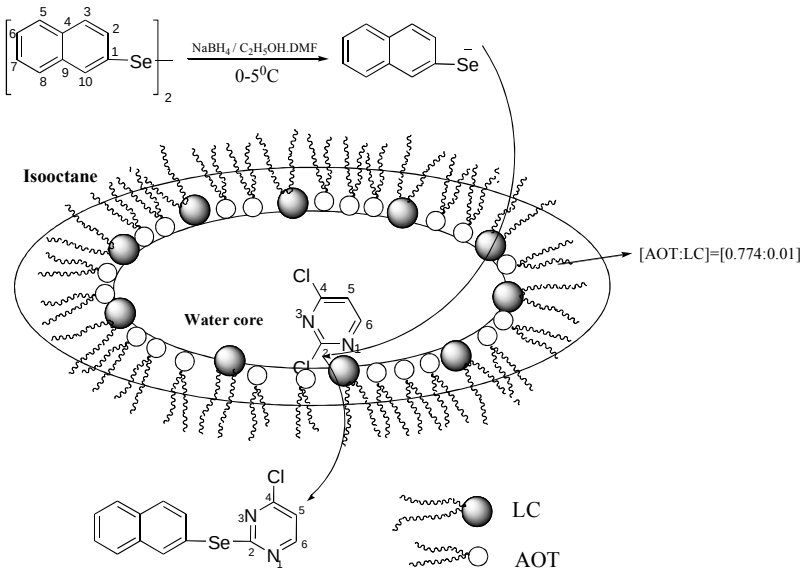

Scheme-I.18. Probable Mechanism for the Synthesis of 4-Chloro-2-(naphthalene-2-ylselanyl) Pyrimidine

I.E. Microemulsion as Biomimetric Model

It is very complicated to get information about the biomolecular behaviours in locally confined spaces due to the complexities of the biological systems. Reverse micelles (RMs) can perform as a cell membrane-mimetic medium as it provide local hydrophilic moiety in an organic phase resembling to biological membranes of the amphiphilic phospholipids.[104] Again, the radial dimensions of RMs are similar to the confined aqueous compartments in cells and tissues. [105] The dynamics of confined water in the vicinity of biomacromolecules are believed to be responsible for many biological functions, such as molecular recognition and enzymatic catalysis.[106] It can also be used in the field of biochemistry for storing bioactive chemical reagents. Hence, surfactant-based reverse micellar interior is excellent biophysical models to study the confinement effect.[107]

In 2008, A. Singha et al.[108] have exhibited a significant improvement in biological hydrogen production achieved by the use of coupled bacterial cells in reverse micellar systems. Two coupled systems (a) Rhodopseudomonas palustris CGA009/Citrobacter Y19, and (b) Rhodobacter sphaeroides 2.4.1/Citrobacter Y19 bacteria have been immobilized separately in aqueous pool of the reverse micelles fabricated by various surfactants such as sodium lauryl sulphate (SDS), sodium bis-2-ethylhexyl-sulfosuccinate (AOT), cetylbenzyldimethyl-ammonium chloride (CBAC) and apolar organic solvents (benzene and isooctane). More than two fold increase in hydrogen production was obtained by the use of Hup_ mutants instead of

wild-type photosynthetic bacteria together with Citrobacter Y19. Addition of sodium dithionite, a reducing agent to AOT/H_2O/ isooctane reverse micellar system with the coupled systems of wild-type photosynthetic bacteria and fermentative bacterium Y19 effected similar increase in hydrogen production rate as it is obtained by the use of mutants. CBAC/H_2O/isooctane reverse micellar system is used for hydrogen production and is as promising as AOT/H_2O/isooctane reverse micellar system. All reverse micellar systems of coupled bacterial cultures furnished encouraging hydrogen production compared to uncoupled bacterial culture. Multi-fold improvement in hydrogen production could be achieved by the use of coupled systems of the photosynthetic bacteria (wild-type or mutated) and the fermentative bacteria entrapped in various reverse micellar systems. Hence, Compartmentalization of the bacterial cells and the enzymes in the reverse micellar systems made the systems very efficient.

Further, S. Pramanik reported the detailed studies of the tetraplex formation in RM to elucidate how these confinements affect the biological function.[107] In this study, they investigated the formation of tetraplex structure from the equimolar mixture of the human telomeric oligonucleotides d[AGGG(TTAGGG)$_3$] (22AG) and d[(CCCTAA)$_3$CCCT] (22CT) in bis(2-ethylhexyl)sulfosuccinate (AOT) reverse micelles. The study provides an insight into the formation of G-quadruplexes and i-motif structures under conditions that mimic the interior of the cell. The experimental findings revealed that the Watson–Crick double helix is the predominant form of human telomeric repeat motif (TTAGGG):(CCCTAA) in the dilute solution. However, in AOT RM, which mimics the in-cell confined space; a significant fraction of the equimolar mixture of these complementary strands adopts non-canonical tetraplex structure. It was also demonstrated that the duplex–tetraplex conversion of human telomeric DNA depends on the water pool size i.e. the degree of confinement. Accordingly, fundamental biological functions might be regulated by the degrees of confinement.

I.F. References

References are given in BIBLIOGRAPHY under Chapter I (pp. 101-105).

CHAPTER-II

Physicochemical studies of water-in-oil nonionic microemulsion in presence of benzimidazole-based ionic liquid and probing of microenvironment using model C-C cross coupling (Heck) reaction

II.A. Introduction

Ionic liquids (ILs) are organic salts/solvents being constituted of distinct cations and anions, having low vapor pressure, high thermal and chemical stability. They are non-flammable and of good catalytic and solvation.[1] The importance and application of ILs are reflected by the contribution of different myriads of researchers.[2] A number of physicochemical investigations of imidazolium-based ILs have been reported.[3] On the other hand, the example of benzimidazole-based ILs is relatively new and scarcely reported in literature.[4] Benzimidazole is an important motif which is found both in naturally occurring and biologically active compounds. It is an important pharmacophore as well.[5]

In the field of colloid and interface science, the investigation of surfactant molecular assemblies in room temperature ionic liquid (RTIL) is of great interest because the former systems can solubilize substances being essentially insoluble in the latter and thus, solubilizing power of surfactant assemblies may widen the application of RTILs. From this point of view, the elucidation of self-assembling phenomena of surfactant molecules in ILs and its applications have become a interesting area of research.[6] Furthermore, IL based microemulsion are used as reaction media in various organic transformations, viz. aminolysis of esters,[7] Diels-Alder reaction,[8] Matsuda-Heck reaction[9] etc. Water-in-oil (w/o) microemulsions or reverse micelles (RMs) are macroscopically homogeneous mixtures of oil, water, surfactant and/or cosurfactant, whereas in the microscopic level it consists of individual domains of oil and water separated by a monolayer of surfactant and/or cosurfactant. The stability, flexibility and microhetrogeneity of microemulsions make them convenient for biological and technological applications.[10] The microstructure of microemulsions critically depends on the system composition, temperature, and additives.[10] Very recently, we have reported the characteristics roles of surfactant (s), cosurfactant and

oils for the formation and stabilization of w/o microemulsions in absence or presence of additive by employing the Schulman's method of cosurfactant titration of the oil/water interface (or, the dilution method).[11-13] Wang et.al.[14] employed the dilution method for the first time to investigate the physicochemical parameters of [bmim][BF_4]/ Brij-35/1-butanol/toluene-based IL/O microemulsion.

In view of these studies, we contemplate to undertake the study of the formation of a water-in-oil (w/o) nonionic surfactant microemulsion, water/Tween-20/Pn/Cy with special reference to its characteristics features of the oil/water interface under different physicochemical conditions in absence or presence of IL, 1-butyl-3-propylbenzimidazolium bromide ([bpBzim]Br) as an additive. Thermodynamics of formation, microstructure, transport properties and dynamics of H-bonding of this system, water-IL/Tween-20/Pn/Cy w/o microemulsion, have been investigated by employing the dilution method, conductivity, DLS, FTIR. Further, an in-depth characterization of the microenvironment of the system in absence or presence of IL has been made by performing a model C-C cross coupling reaction (Heck reaction). The famed name reaction, Heck, is one of the fine studied responses in the meadow of organic synthesis.[15] Report on study of Heck reaction in IL-microemulsion is available in literature.[16] The yield of Heck coupled product depends on the type of surfactant used as well as the nature of confinement of these systems. [9,16] An attempt has been made to monitor the effective physicochemical changes in microemulsion, leading to microenvironmental changes during the course of reaction. Finally, a correlation of the results in terms of the evaluated physicochemical parameters vis-à-vis microstructural features during Heck reaction has been drawn and provides a new horizon to understand the most plausible location/site as well as to determine the actual reaction parameter required for effective reaction in the studied micro-heterogeneous system. To the best of our knowledge, such a comprehensive study on w/o microemulsion in presence of benzimidazole- based IL has not been reported earlier.

II.B. Results and discussions

II.B.1. The Schulman's cosurfactant titration at the oil/water interface (The dilution method)

In order to underline the influence of IL and its content on the interfacial composition of Tween-20-based w/o microemulsion stabilized in Pn and Cy under various physicochemical conditions (i.e., at different temperatures and fixed molar ratio of water to surfactant, ω), n_a^i/n_s values [i.e. compositional variations of amphiphiles (both Tween-20 and Pn) at the interface] are plotted against [IL] (0.0→0.20 mol dm^{-3}) and respective plots are depicted in Figure-II.1 (inset A). The mathematical evaluation and the results of interfacial composition have been discussed elaborately indicating all possible interactions among the constituents in the microenvironment of this compartmentalized system (depicted in Scheme-II.1) and are presented in Appendix A (Sec. A and B) and Figure-A.S1.

II.B.1.1.Thermodynamics of transfer of Pn (oil→interface) (in absence or presence of IL)

In this section, analysis of the transfer of Pn from oil phase to the interface (Pn_{oil}→$Pn_{interface}$) of water (IL)/Tween-20/Pn/Cy microemulsion system by employing the dilution method is presented from thermodynamic point of view, which is rarely reported.[14,17] The details of the estimation have been given in Appendix A (Sec. A, Eqs. S1-S16).

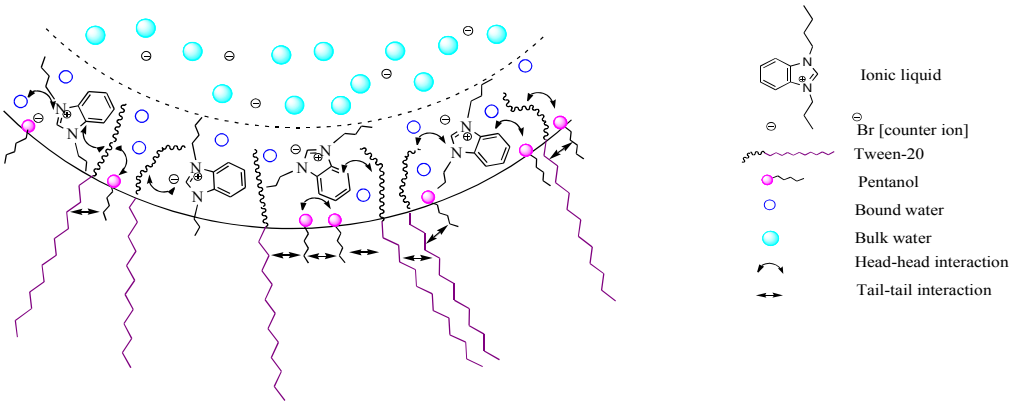

Scheme-II.1. Schematic Representation showing possible interactions in microenvironment

II.B.1.2. Effect of [IL] and temperature on $\Delta G^0_{o\rightarrow i}$

$\Delta G^0_{o\rightarrow i}$ values are negative in absence or presence of IL, and hence, spontaneous formation of w/o microemulsions is suggested. Both similar and dissimilar values in this energetic parameter at comparable physicochemical conditions are reported.[14,17-19] Both K_d and $\Delta G^0_{o\rightarrow i}$ show maxima in presence of 0.05 mol dm^{-3} of IL at each temperature (Figure-II.1 and inset B).

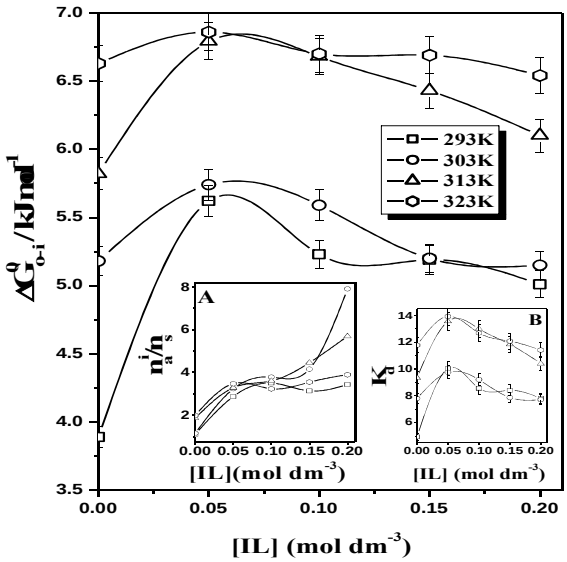

Figure-II.1. Plots of $\Delta G^0_{o\rightarrow i}$ as a function of [IL] for water/Tween-20/Pn/Cy microemulsion system at ω (= 30) with varying temperatures. Inset A: Plots of interfacial composition (n_a^i/n_s) as a function of [IL] for water/Tween-20/ Pn/Cy microemulsion system at ω (= 30) with varying temperatures. Inset B : Same plots for K_d

Though, the variations of K_d and $\Delta G^0_{o\rightarrow i}$ values between 0.05 mol dm^{-3} and 0.10 mol dm^{-3} may be small at higher temperatures (viz. 313 and 323 K), but both the values are still higher at 0.05 mol dm^{-3} compare to other concentrations of IL (Figure-II.1 and inset B, Table-A.S1) . This indicates that the transfer process of Pn from the oil phase to the interface is much favoured at 0.05 mol dm^{-3} of IL irrespective of temperature. Further, a low line secondary maximum in K_d or $\Delta G^0_{o->i}$ values appears at 0.15 mol dm^{-3} of [IL] (Figure-II.1, including the error bars). A plausible explanation for this type of trend can be explained in view of the physicochemical (molecular) interactions

among the constituents involved in the transfer process of Pn (oil→interface).[11,12,14,17] In this system, the interaction between nonionic surfactant (Tween-20) and alkanol (Pn) is of dipole-dipole or dipole-induced dipole or London dispersion type, because of the presence of uncharged or neutral hydroxyl groups (Pn) and POE chains (Tween-20), whereas, the interaction between $[bpBzim]^+$ and Pn is possibly of ion-dipole type. Ion-dipole interaction is much stronger compared to dipole-dipole or dipole-induced dipole or London dispersion interactions.[20] Therefore, the association between Pn and Tween-20 becomes more favorable in presence of 0.05 mol dm^{-3} of [bpBzim][Br]. Consequently, the transfer process of Pn from the oil phase to the interface is much favoured at 0.05 mol dm^{-3} of [IL] irrespective of temperature. But at higher IL concentration (i.e., 0.10→0.20 mol dm^{-3}), the addition of IL diminishes the interfacial area per polar head group of surfactant molecules by screening the steric repulsion between nonionic surfactants (herein, Tween-20), and this makes the interfacial layer more rigid and favors a greater curvature of the interface.[14,17] As a result, the attractive interaction among the droplets decreases and subsequently, the transfer process of Pn (oil→interface) is also diminished. However, the appearance of a low line secondary maximum at [IL] equals to 0.15 mol dm^{-3} is likely to be originated from the non-ideality of the systems. Usually, different types of forces (viz. London dispersion forces, dipole-dipole forces, dipole-dipole induced forces etc.) act on real mixtures, making it difficult to predict the properties of such solutions. Non-ideal mixtures are identified by determining the strength and types (specifics) of the intermolecular forces (viz. intermolecular forces between the similar molecules and intermolecular forces between the dissimilar molecules) in that particular system.[21]However, non-ideal behavior is not uncommon in multicomponent derived microemulsion systems.[22-26]

Further, it has been observed that K_d or $\Delta G^0_{o\rightarrow i}$ gradually increases with the increase in temperature (Figure-II.1 and inset B) and this suggests that the transfer of Pn (oil→interface) is much favored at higher temperatures. The higher absolute values of $\Delta G^0_{o\rightarrow i}$ at higher temperatures indicate a comparatively stronger interaction between Tween-20 and Pn at the interface, which corroborates well with the interfacial composition (Figure-II.1, inset A). This trend corroborates well with the reports of Zhang et al.[18] and Wang et al.[14] for [bmim][BF_4]/CTAB/alkanol/toluene and [bmim][BF_4]/Brij-35/1-butanol/toluene w/o microemulsion systems, respectively. However, the overall scenario indicates towards formation of a more spontaneous w/o

microemulsion accompanied with 0.05 mol dm^{-3} of IL, as evident from K_d and $\Delta G^0_{o\rightarrow i}$ values at each temperature (Table-A.S1, Figure-II.1 and inset B).

Further, a significant difference in K_d or $\Delta G^0_{o\rightarrow i}$ values has been observed for 303K and 313K (Figure-II.1 and inset B). It may be due to the influence of temperature on the constituents (in particular to Tween-20 consisting of POE chains as polar head groups and IL as organic electrolyte, [bpBzim][Br]) and hence, two different mechanisms might be operative for the formation of microemulsions at lower temperature region (i.e., 293 and 303 K) as well as at higher temperature region (i.e., 313 and 323 K). The ordered structure formed from IL molecules around hydrophilic moiety (POE chains) of Tween-20, produced by ionic interaction instead of hydrogen bonding interaction, is considered to be an origin for the surfactant self-assembly[27]as represented in Scheme-II.1. It is obvious that Tween-20 molecules assemble to form reverse micelles in order to avoid the entropy loss due to ordered arrangement of IL molecules at low temperature region. On the other hand, at higher temperature region, the IL molecules participating in the ionic interaction with POE chains of Tween-20 may be less ordered (more disordered) due to their enhanced dehydration.[27,28] Hence, it is imperative that the enthalpy loss for the release of solvated IL molecules would be overcome by the enthalpy gain for the contact of POE chains at higher temperature region. The reversal of entropy and enthalpy parameters might be occurred during transition from low temperature region (293 and 303 K) to high temperature region (313 and 323 K). This is why, a significant difference in $\Delta G^0_{o\rightarrow i}$ values has been observed for two sets of temperatures.

II.B.1.3. Effect of [IL] and temperature on $\Delta H^0_{o\rightarrow i}$ and $\Delta S^0_{o\rightarrow i}$

Due to nonlinear dependence of ($\Delta G^0_{o\rightarrow i}$/T) on (1/T) (the result fits a two degree polynomial equation (Figure-A.S2)), at each composition of surfactant (at [IL] = 0.0 → 0.20 mol dm^{-3}), four values of the standard enthalpy change, $\Delta H^0_{o\rightarrow i}$ and the standard entropy change ($\Delta S^0_{o\rightarrow i}$) of the Pn transfer process (oil→interface) at four different temperatures have been evaluated according to Eqs. (S12) and (S15) and are presented Table-A.S1 and Figure-II.2. For pure Tween-20 system (i.e., in absence of IL), the overall transfer process is exothermic at all experimental temperatures with negative entropy change (more ordered) in Cy (Table-A.S1 and Figure-II.2). So, Pn causes release of heat during the transfer process. Consequently, the negative entropy

change may be due to more organization of the interface and its surroundings. Therefore, it may be argued that in the presence of Pn and Tween-20, the interface to some extent becomes ordered. Similar observation was also reported by Bardhan et al.[12] for water/Brij-35/Pn/IPM microemulsion systems. However, De et al.[29] and Kundu et al.[11]reported an opposite behavior (i.e., positive enthalpy and entropy changes) for Tween-20/Bu or Pn/Hp/water and Brij-58 or Brij-78/Pn/Hp or Dc/water microemulsion systems, respectively. Hence, difference in trends of $\Delta H^0_{o\rightarrow i}$ and $\Delta S^0_{o\rightarrow i}$ may be attributed to the differences in hydrophobic configuration and/or size of the polar head group of the nonionic surfactants vis-à-vis type of oil.

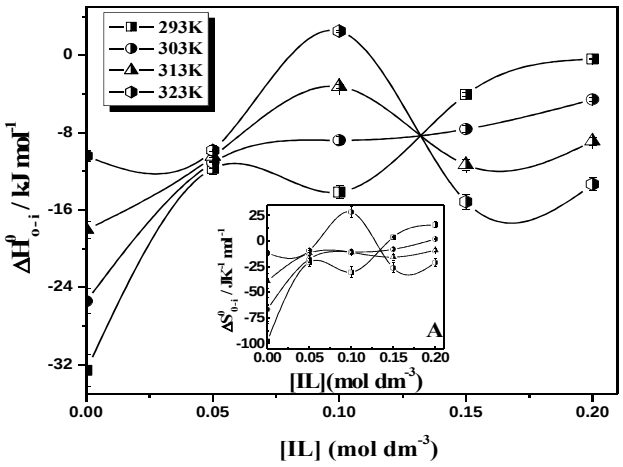

Figure-II.2. Plots of $\Delta H^0_{o\rightarrow i}$ as a function of [IL] for water/Tween-20/Pn/Cy microemulsion system at ω (= 30) with varying temperatures. Inset A: Same plot for $\Delta S^0_{o\rightarrow i}$.

Further, it can be observed from Table-A.S1 and Figure-II.2 that, the overall transfer process is exothermic at all the experimental temperatures with negative entropy change (order) in Tween-20/Pn system in the presence of IL ([IL] = 0.05→0.20 mol dm-3). Such a negative enthalpy or entropy change was observed by Mukherjee et al.[19] for triisobutyl (methyl) phosphoniumtosylate/IPM/trihexyl (tetradecyl) phosphoniumbis 2,4,4-(trimethylpentyl) phosphinate : isopropanol or butanol systems. It is quite likely that the negative contribution towards $\Delta H^0_{o\rightarrow i}$ is identified with the transfer of the surfactant tail from water to liquid hydrocarbon state in the interfacial layer and for restoring the hydrogen bonding structure of the water around the surfactant head group.[30] Further, it can be argued for negative entropy, - $\Delta S^0_{o\rightarrow i}$ as

follows: During formation of nano-droplets in w/o microemulsions, the penetration of water into the oil (Cy)/Tween-20/Pn (amphiphiles) continuum forming cavity and subsequently, organization of the amphiphiles at the droplet interface results in an increase in overall order with negative entropy of the multicomponent system.[31] Further, - $\Delta S^0_{o\rightarrow i}$ suggests that both entropy as well as enthalpy are involved in the transfer process.[32] Consequently, IL dependent microemulsion compositions with larger - $\Delta H^0_{o\rightarrow i}$ values (more exothermic) results in larger -$\Delta S^0_{o\rightarrow i}$ values (ordered) i.e., greater interaction between the constituents at the interface, leading to more ordered interface due to transfer of Pn (oil→interface).[33]

The variation of $\Delta H^0_{o\rightarrow i}$ and $\Delta S^0_{o\rightarrow i}$ values with temperatures from Table S1 and Figure 2 indicates that the presence of IL influences the degree of exothermicity with orderliness of the transfer process (oil→interface). Interestingly, the transfer process approaches towards less exothermic as well as less ordered with increase in temperature up to 0.10 mol dm^{-3} of IL, and thereafter, the degree of exothermicity and orderliness reverses in the vicinity of 0.136 mol dm^{-3}. Subsequently, the process is more exothermic as well as more ordered with increase in temperature at [IL] equals to 0.15 and 0.20 mol dm^{-3} (Figure-II.2). This trend can be explained in the following way: The addition of IL to Tween-20 based microemulsions might have at least two effects. First, the partial reduction of the hydration of water around the polar head group of the non-associated surfactant molecule occurs with increase in temperature. As a result, a decrease in the energy needed for breaking down of this structure during the process of microemulsion formation and also to a decrease in the exothermic contribution i.e., decrease in the value of $\Delta H^0_{o\rightarrow i}$. The second consequence of the presence of higher IL concentrations appears to be related to the influence of counter ion binding on the structure of the microemulsions.[34] The reduction in disorder may be attributed to the effect of the liberation of surfactant hydration water molecules on microemulsification to be less important than the loss of freedom when monomers join each other to form reverse micelles.[35]

Also, $\Delta S^0_{o\rightarrow i}$ values have been found to increase with temperatures up to 0.10 mol dm^{-3} of IL and thereafter, reversal of trend has been observed in the vicinity of 0.136 mol dm^{-3}, as in case of $\Delta H^0_{o\rightarrow i}$ (Figure-II.2, inset A). This result is indeed interesting. It is quite likely that molecular interactions, arising from the tendency of the water molecules to regain their normal tetrahedral structure, and the attractive dispersion forces between hydrocarbon chains act cooperatively to remove the hydrocarbon

chains from the water cages, leading to the disorder of water and subsequently, increase in the entropy values.[36,37] On the other hand, the decrease in entropy may be due to the breakdown of the normal hydrogen-bonded structure of water accompanied by the formation of water with different structures.[36,37] The presence of higher concentration of hydrophilic species (herein, IL) promotes an ordering of water molecules in the vicinity of the hydrophilic head group of Tween.[36] However, no significant change in both thermodynamic parameters (i.e., $\Delta H^0_{o\rightarrow i}$ and $\Delta S^0_{o\rightarrow i}$) with temperature has been observed at certain IL concentration (i.e., at 0.05 and ~0.136 mol dm^{-3}), leading to the formation of isoenthalpic and isoentropic microemulsion systems (Figure-II.2 and inset A). Similar observation was also reported earlier for mixed surfactant microemulsion systems comprising of cationic or anionic-nonionic.[11,12,38]

II.B.1.4. Effect of [IL] on $(\Delta C^0_p)_{o\rightarrow i}$

Since $\Delta H^0_{o\rightarrow i}$ has become a function of temperature, the $(\Delta C^0_p)_{o\rightarrow i}$ values have also been evaluated for these systems (in absence or presence of IL) from the slope (= $\delta\Delta H^0_{o\rightarrow i}/\delta T$) of the plots of $\Delta H^0_{o\rightarrow i}$ vs. T (not illustrated) according to Eq. (S11).[12] All these values are presented in Table-A.S1. It can be observed from Table-A.S1 that, at [IL] = 0.0→0.10 mol dm^{-3}, $(\Delta C^0_p)_{o\rightarrow i} > 0$; whereas $(\Delta C^0_p)_{o\rightarrow i} < 0$ at [IL] = 0.15 and 0.20 mol dm^{-3}. Negative values are usually observed for the self-association of amphiphiles and can be attributed to the removal of large areas of non-polar surface from contact with water on the formation of reverse micelles.[39] However, $(\Delta C^0_p)_{o\rightarrow i}$ tends to almost zero at [IL] = 0.05 and ~0.136 mol dm^{-3}, which corroborates well with profile of $\Delta H^0_{o\rightarrow i}$ vs. [IL] at different temperatures (Figure-II.2). This indicates the formation of temperature-insensitive microemulsions at [IL] of 0.05 and ~0.136 mol dm^{-3}. Similar observation [i.e., reversal of trend of $(\Delta C^0_p)_{o\rightarrow i}$ with concentration of methanol] was reported earlier by Perez-Casas et al.[40] for water/AOT/methanol/decane reverse micelles. Kunz et al.[41] reported that formation of temperature-insensitive microemulsions are important for some practical purposes (e.g. for formulation of product).

II.B.2. Electrical Conductivity and Dynamic light scattering measurement

The electrical conductivity, size and size distribution of w/o microemulsion systems have been measured by conductometric and DLS, respectively for water/Tween-

20/Pn/Cy microemulsion system with the variation of [IL] (= 0.0 mol dm-^{3} → 0.20 mol dm^{-3}) at a constant ω (= 30) and fixed temperature (303K). The results are depicted in Figure-A.S3. It can be observed from Figure-A.S3 that the electrical conductivity gradually increases with increase in [IL] in microemulsion. This trend may be attributed to high conducting nature of IL, as the blank experiment (similar concentration of IL in water) shows the identical trend with the variation of [IL] (Figure-A.S3, inset A). It can be observed that the conductance values in water-IL media range from 0.0016 to 8.2 mS cm^{-1}, whereas low values (17.84 - 231.0 μS cm^{-1}) are obtained for IL in microemulsions at similar concentrations. The low value in microemulsion system can be justified as follows. In the present system, electrostatic interaction between imidazolium cation of IL and electronegative oxygen atoms of POE units of Tween-20 is quite likely to occur along with water-IL hydrogen bonding interaction (Scheme-II.1). However, the later part, i.e., water-IL hydrogen bonding interaction is present in bulk IL or water-IL media. The electrostatic interaction makes the palisade layer comprising Tween-20/Pn/IL more rigid[42] and subsequently, decreases the conductance values. Hence, it can be concluded that the physicochemical properties of water molecules localized in the interior of the microemulsions are different from those of water-IL media.

Further, hydrodynamic diameter (D_h) of microemulsion droplet decreases from 3.90 nm to 2.31 nm with increase in [IL] (0.0 mol dm^{-3}→ 0.20 mol dm^{-3}) wherein about 3 fold increase of the droplet count rate has been observed under the prevailing condition (Figure-A.S3, inset B and C).The droplet count rate is directly proportional to the droplet number of the microemulsion system. Hence, the addition of IL shrinks the droplet size and thereby increases in droplet number. It was reported earlier that the curvature of the oil/water interface of a microemulsion can be adjusted by adding IL (a class of organic electrolyte)[43] or NaCl (inorganic electrolyte)[44] at different concentrations. The addition of electrolyte gives rise to a decrease in the repulsive interaction between the head groups of the nonionic surfactant, Tween-20, which further increases the packing parameter of surfactant molecules (P = v/al, where 'v' and 'l' are the volume and the length of hydrophobic chain, respectively and 'a' the area of polar head group of the surfactant) and decreases the droplet diameter. In addition, the presence of IL within the water pool weakens the hydrogen-bonding between water and POE chains of Tween-20 and thereby reduces hydration of POE chains, which results in the formation of smaller droplets due to decrease in swelling

of POE chains[45] In other words, when IL is solubilized in microemulsions, it decreases the average area occupied by each head group of surfactant (Tween-20), and subsequently, enhances the packing density and rigidity of the surfactant monolayer of the droplet, which may reduce the size of the droplets.[46] Typical values of polydispersity index (PDI) obtained here are in the range between 0.1–0.2, which indicates the monodispersity of the sample.[12,13,38]

II.B.3. FTIR spectroscopy

Reports on the properties of the encapsulated water in a range of size and type of w/o microemulsions by studying the states of water organization using FT-IR measurement, are available in literature.[13,37,41,47] The characteristics of the water molecules in confined environment of w/o microemulsion depend strongly on water content or the droplet size and the nature of the interface as well.[47,48]As discussed in previous section that the values of hydrodynamic diameter of droplet (D_h) varies from 3.90 nm to 2.31 nm as a function of [IL] (0.0mol dm^{-3}→ 0.20 mol dm^{-3}) at fixed ω (= 30) and temperature (= 303K) from DLS measurements. Further, the values of hydrodynamic diameter of droplet (D_h) are well comparable with microemulsion systems, wherein existence of different types/states of water species reported in confined environment using FTIR measurement.[47,49] However, the influence of Pn (cosurfactant) on the O-H stretching vibration of the confined water needs to be underlined for the present system. To eliminate the effect of Pn on the O-H vibration of water, the spectra of Pn at same concentration is subtracted from the spectral intensity of O-H stretching band and the differential spectra have been analyzed. Different types of hydrogen bonded water molecules exist in reverse micelles which can broadly be classified into two major classes, namely, bound and bulk-like water molecules.[13,37,41,50] The differential spectra obtained in the present study have been deconvoluted into two peaks at ~3500 and ~3300 cm^{-1}, corresponding to the O-H stretching frequency of the bound and bulk-like water molecules, respectively (Figure-A.S4) and a representative result of deconvolution (relative abundance of different water species) is depicted in Figure-A.S5 . It reveals from Figure-A.S5 that the bound water proportion is the least in absence of IL. Whereas, the proportion of bound water increases with increase in [IL] in microemulsion. These results indicate a significant role of IL in determining the proportion of different water species (bound and bulk) in the confined environment of w/o microemulsion. However, this result is not very

surprising if one considers possibility of interaction between IL and water molecules. With the increase in IL content, more bulk water molecules hydrate IL molecules and subsequently, increase the proportion of bound water molecules in microemulsion core.[42] Further, it is evident from DLS measurements that the droplet size decreases with the increase in IL content. It is reported that as the droplet size decreases, the bound water proportion increases in the microemulsion and vice versa.[47,50] Hence, DLS and FTIR results corroborate each other.

II.C. Study of C-C cross coupling (Heck) reaction in microemulsion

A model Heck reaction (Scheme-II.2) has been performed in the well characterized system (presented herein), to explore the properties of IL (additive) within the restricted geometry provided by microemulsions and the nature of interaction of the IL with the constituents of the interface and the subsequent changes of microenvironment during the reaction and the detection of most probable reaction site and yield of the Heck reaction. The progress of reaction was monitored by employing various instrumental techniques such as, conductance, FTIR, UV-Visible spectroscopy.

II.C.1. Standardization of Heck coupling reaction

The reaction has been performed in presence of different bases (inorganic and organic) to optimize the reaction at 323 K. It has been found that water soluble bases (potassium carbonate and tetramethyl ethelene diamine) produce almost comparable yield (30 % and 40%, respectively) of the desired product, whereas highest yield (75%) has been achieved using sparingly water soluble base, viz, triethyl amine (TEA) (Table-A.S2). Hence, the subsequent study on the Heck reaction in microemulsion media at varying [IL] (0.0 mol dm^{-3} → 0.2 mol dm^{-3}) was performed in the presence of TEA as base and the standard mechanism of Heck coupling reaction is presented in Scheme-A.S1.

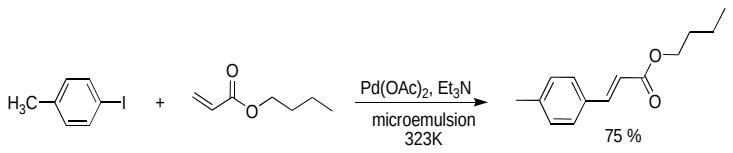

Scheme-II.2. Study of Heck reaction in microemulsion

In order to underline the effect of encapsulation or compartmentalization (provides with microemulsion), the Heck reaction has also been performed in bulk IL (water-IL media) containing [IL] similar to that of available in microemulsions and the results are presented in Table-II.1. The study showed (Table-II.1) that the yield of the desired product in water-IL media was very low in comparison with the microemulsion systems. The strong effect of confined environment of microemulsion, therefore, seems to play a vital role in studying this reaction.[9] However, yields of the final product in microemulsion is not a direct function of IL concentration (Table-II.1). The reaction has also been critically monitored in the case of two different temperature-insensitive formulations at [IL] = 0.05 and 0.136 mol dm^{-3} (discussed in previous section, "Effect of [IL] on $(\Delta C^0_p)_{o\rightarrow i}$", Figure-II.2). The yield of the final product has been found to be highest at lower range of [IL] (i.e., at 0.05 mol dm^{-3}), at which highest spontaneity of Pn transfer process and temperature-insensitivity were exhibited (Figure-II.1 and 2). But at higher range of [IL] (i.e., at ~0.136 mol dm^{-3}),the yield is least, where another temperature-insensitive formulation is obtained. Hence, it can be suggested that temperature insensitive composition is not the sole factor, rather than the highest spontaneity of Pn transfer (oil→interface) leads to highest yield of the product.

Table-II.1. Heck coupling reaction in both water and in microemulsion media (water/Tween-20/Pn/Cy) as a function of [IL] in presence of TEA at a fixed ω (= 30) and 323K.

Ionic liquid mol dm^{-3})	Yield (%) in water-IL	Yield (%) in microemulsion
0.00	07.0	17
0.05	04.5	75
0.10	06.8	25
0.136	08.3	13
0.15	10.0	59
0.20	12.0	22

II.C.2. Conductance Study

Electrical conductance of w/o microemulsion system has been measured at regular interval during the course of reaction both in absence or presence of IL and the results are displayed in Figure-II.3. In both cases the trend of conductance curve is almost identical with smaller values in absence of IL. In absence of IL, the addition of palladium acetate [$Pd(OAc)_2$] results in a small increase in conductance due to the presence of charge carrier (viz. $Pd(OAc)_2$) and followed by decrease in conductivity, which may be due to the formation of the aqua palladium complex in the mixture.[51]

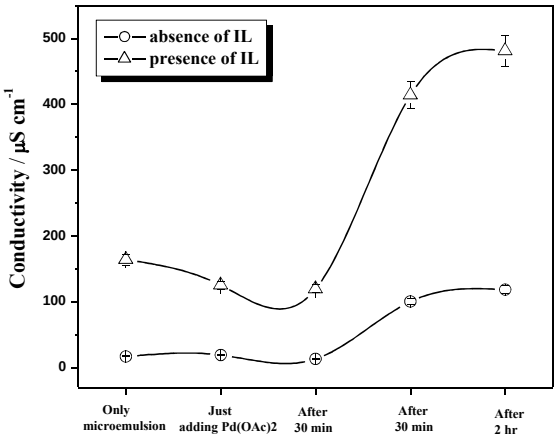

Figure-II.3. The conductivity of microemulsion in absence and presence of IL (= 0.05 mol dm^{-3}) at regular interval during Heck reaction at 323K.

On the contrary, in presence of IL, the addition of $Pd(OAc)_2$ decreases the conductivity indicating the formation of palladium complex (Pd-NHC) with IL, the precursor of N-heterocyclic carbene (NHC).[52] However, the process of Pd-NHC complexation is much faster in comparison with the palladium-aqua complexation which subsides the conducting properties of $Pd(OAc)_2$. However, a sharp increase in conductivity has been observed in both cases after addition of reagents (4-iodotoluene, triethylamine and butylacrylate) implying the progress of Heck reaction.

II.C.3. FTIR measurement

The observation FTIR studies during reaction (Figure-II.4) are very much supportive with the conductivity experiment. Addition of palladium acetate reduces the population of bound water indicates the formation of Pd-NHC complex which decreases the interaction with water molecules and the optimal decrease of bound

water implying the end point of complexation. Thereafter, a regular enhancement in population of bound water molecules have been observed with the addition of reagents (4-iodotoluene, triethylamine and butylacrylate) indicating the formation of the Heck coupled and the other possible side products (such as, halogen acid and corresponding amine salt). This trend is continued until the completion of reaction.

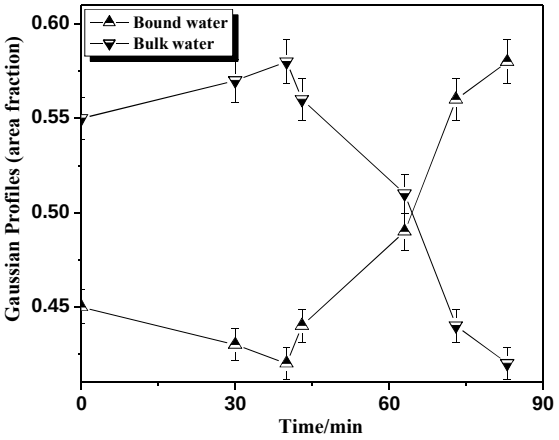

Figure-II.4. The variation of Gaussian profiles (area fraction) of the normalized spectra of different water species (bound water, bulk water) of IL containing (0.05 mol dm^{-3}) w/o microemulsion system with the reaction time.

II.C.4. UV-Visible spectroscopy

Comparing the UV-Visible spectra of individual components and the spectra recorded during the course of reaction at regular interval of time, a single absorption peak at 271 nm has been observed after 10 minutes of the reaction (Figure-A.S6). The λ_{max} of the product is reported to be 274 nm.[53] The little decrease in λ_{max} of the product from that of the literature value may be due to H-bonding between ester group of the product and medium of the reaction. The absorption became more intense after 40 minutes of reaction. The increase in intensity of the spectral band increases with the progress of reaction indicating increase in concentration of the product with the progress of time.

II.D. Comprehension of the Results

The Heck reaction was carried out in w/o microemulsion with varying amount of IL (0.0 → 0.20 mol dm^{-3}) and the corresponding results are presented in Table-II.1. The optimal concentration of IL required for effective Heck reaction is 0.05 mol dm^{-3} in the present system. Further, it is evident from the dilution method that the spontaneity of formation with maximization in stability of the microemulsion system can be achieved with 0.05 mol dm^{-3} of IL (Table-A.S1 and Figure-II.1). It is obvious that IL with 0.05 mol dm^{-3} facilitates the Pn transfer process (oil→interface) due to favorable organization of the constituents at the interface, and thereby, results in achieving more stability, which leads to better performance of the Heck reaction in microemulsion medium. The decrease in the conductance with the addition of palladium acetate [$Pd(OAc)_2$] indicates the formation of palladium complex (Pd-NHC) with IL (Figure-II.3). FTIR study also supported the formation of Pd-NHC complex which reduces the number of IL molecules inside the water pool and thereby decreases the bound water population (Figure-II.4). The ratio between bound and bulk water populations indicates that no interaction persists between water and newly formed Pd-NHC complex. However, it can be concluded that the availability of Pd-NHC complex inside the water pool is least. In bulk IL i.e, water-IL media, the possibility of Pd-NHC complex formation is negligible, because of the instability of N-heterocyclic carbenes in water, and subsequently, reducing the rate of the forward reaction. It can be inferred from the low yield of the desired product in water-IL media indicates that formation of stable Pd-NHC complex during the performance of Heck reaction in compartmentalized systems plays a pivotal role, which leads to higher yields compare to corresponding bulk [IL] (Table-II.1). In addition, use of water soluble bases (viz., K_2CO_3 and TMEDA) which are quite likely to be located in the water pool of microemulsion, results in low yield of the desire product. Whereas TEA preferentially soluble in Pn, as reveals from solubility analysis, ends up with best results (75% yield of the product) (entry 2, Table-A.S2). A plausible explanation emerges from the increase in population of Pn at the interfacial region vis-à-vis its interaction with TEA, which rationalizes the availability of all constituents involved in this reaction. It can be inferred that apart from the molecular interactions of the constituents involved in formation of microemulsion as template (discussed in Appendix A (Sec. B)), two types of interactions are likely to occur at the oil/water interface or in the palisade

layer of the microemulsion at one hand. On the other hand, bound water in the confined environment. For example, (i) dipole-dipole interaction between Pn and TEA, which enhances the availability of TEA at the interfacial region with increasing population of Pn at the interface, and (ii) water binds to TEA to form a surrounding OH^- base in the following fashion [Eq.(1)].[54]

$$(C_2H_5)_3\dot{N} + H_2O \longrightarrow (C_2H_5)_3N.H_2O \longrightarrow (C_2H_5)_3\overset{+}{N}H + OH$$

Hence, small amounts of the OH^- are likely to be entered the palisade layer of microemulsion and subsequently, basic environment develops in the peripheral region of the interface, which is essentially required for Heck reaction (Scheme-II.2 and Scheme-A.S1) and a good yield of the product is achieved. However, the correlation between [IL] and reaction yield is not straightforward. After getting the utmost yield of 75% at [IL] (= 0.05 mol dm^{-3}), the reaction yield decreases to 25% at [IL] (= 0.10 mol dm^{-3}) and shows further increase (59%) at [IL] (= 0.15 mol dm^{-3}). As stated earlier, a low line secondary maxima in K_d and $\Delta G^0_{o->i}$ values appear at 0.15 mol dm^{-3} of [IL] after achieving the highest values at 0.05 mol dm^{-3} of [IL] (Figure-II.1) and the second highest yield of Heck product has been found at the same IL concentration (=0.15 mol dm^{-3}) (Table-II.1). K_d and $\Delta G^0_{o\rightarrow i}$ values actually signify the spontaneity of Pn transfer process from bulk to interface. Hence, it is probable that accumulation of Pn at the interface governs the availability of TEA and OH^- in the vicinity of the interface as well as tunes the interfacial characteristics with different degrees by interaction with IL (of different contents) which influences the yield of desired Heck product. Gayet et al.[9] reported that the IL content affects the yields of Matsuda-Heck reaction in reverse microemulsions. All these observations together sensing that the most plausible location or site of the Heck reaction in the studied microheterogeneous system is the interfacial region. However, the present report is not comprehensive from the view point of the direct correlation between the content of IL and the reaction yield (herein, the Heck couple product). However, this is trivial as because a maximum in both K_d and $\Delta G^0_{o->i}$ values was obtained at 0.05 mol dm^{-3} and we concern on the maximum values of physicochemical parameters (K_d and $\Delta G^0_{o->i}$) with that of highest yield in Heck product at same concentration of [IL]. Several factors, such as, changes in molecular interactions between the constituents at the interface,

microstructure, polarity due to the presence of phenyl group in IL with the variation in [IL], might be responsible for overall yield of the final product. Further studies in this direction by employing SANS, 1H NMR along with two-dimensional rotating frame nuclear Overhauser effect (NOE) experiments (ROESY) are warranted.

II.E. Experimental

II.E.1. Materials and methods

Polyoxyethylenesorbitanmonolaurate (Tween-20, ≥ 99%), palladium acetate [$Pd(OAc)_2$, ≥ 99.98%] and 4-iodo-toluene ($CH_3C_6H_4I$, ≥ 99%) werepurchased from Sigma Aldrich, USA. 1-Pentanol (Pn, ≥ 99%) and cyclohexane (Cy, ≥ 98%) were the products of Fluka, Switzerland. Triethyl amine (TEA, ≥ 99.5%) and n-butyl acrylate were purchased from Merck, Germany. All these chemicals were used without further purification. The IL, 1-butyl-3-propylbenzimidazolium bromide ([bpBzim]Br) was synthesized in accordance our reported method.[4] Doubly distilled water of conductivity less than 3 μS cm-1was used in the experiments.

The dilution experiment was performed to investigate the interfacial composition of Tween-20 based microemulsion in different physicochemical conditions, as described earlier[11-14,17] using spectrophotometric technique[55] to measure the change in sample turbidity produced by Pn addition (Figure-A.S7). The detail of the spectrophotometric technique was provided in our previous report.[12] Basics of the dilution method and thermodynamics of the transfer of cosurfactant from oil to the interface has been dealt in Appendix A (Sec. A).

Conductivity measurements were performed using Mettler Toledo (Switzerland) Conductivity Bridge. The instrument was calibrated with standard KCl solution. The uncertainty in conductance measurement was within ±1%.

DLS measurements were carried out using Zetasizer Nano ZS90 (ZEN3690, Malvern Instruments Ltd, U.K.). He-Ne laser of 632.8 nm wavelength was used and the measurements were made at a scattering angle of 90^0. Details of the measurement have been provided in our previous report.[12,13]

FTIR absorption spectra were recorded in the range of 400-4000 $cm^{-1}$with a Shimadzu 83000 spectrometer (Japan) using a CaF_2-IR crystal window (Sigma-Aldrich) equipped with Press lock holder with 100 number scans and spectral resolution of 4 cm^{-1}. Deconvolution of spectra has been made using Origin software.

3 ml microemulsion (water/Tween-20/Pn/Cy) containing IL (0- 0.20 mol dm-3)at ω (= 30) and 4.48 mg (0.02 mmol, 4 mol %) Pd(OAc)2 were taken in a 25 ml round bottom flask and the mixture was placed in a preheated oil bath at 323 K for 30 minutes with constant stirring. Thereafter, 109 mg (0.5 mmol) of 4-iodotoluene, 76.8 mg (0.6 mmol) of n-butylacrylate and 101.12 mg (1 mmol) of triethylamine (TEA) were introduced into it and the resulting mixture was heated at 323K for 45 minutes. The resulting multicomponent solution shows no instability towards temperature or otherwise. The progress of the reaction was monitored by silica gel thin layer chromatography (TLC). In addition, conductance, FTIR, and UV-Vis spectroscopy were employed to characterize the microenvironment of microemulsion with the progress of reaction. Yield of Heck coupled product was determined by HPLC. Finally, the product was characterized by ^{1}H-NMR and ^{13}C-NMR (Appendix A, Sec. 2). Similar experiment was performed in water-IL media (bulk IL) at the corresponding [IL] as used in microemulsion system.

II.F. Summary

Present study is focused on the characterization of a quaternary water-in-oil microemulsions comprising of Tween-20, Pn and Cy in absence and presence of IL, 1-butyl-3-propylbenzimidazolium bromide ([bpBzim]Br) with a detailed description of the interfacial composition as a function of transfer of Pn from bulk oil phase to the interface on the system composition. Synergism in distribution constant (K_d) and -$\Delta G^0_{o\rightarrow i}$ have been observed in the vicinity of 0.05 mol dm^{-3} of IL at each temperature (293, 303, 313 and 323K). This indicates that the transfer process of Pn from oil phase to the interface is more favoured at 0.05 mol dm^{-3}of IL irrespective of temperature. The standard enthalpy change ($\Delta H^0_{o\rightarrow i}$) and the standard entropy change ($\Delta S^0_{o\rightarrow i}$) of the transfer process have been found to be negative [i.e., exothermic process with less disordered (organized)] in absence or presence of IL at all the experimental temperatures. Further, temperature-insensitive microemulsion has been formed at [IL] of 0.05 and ~0.136 mol dm^{-3}. FTIR study reveals an increase in the proportion of bound water molecules with increasing [IL]. This shows the significant role of IL in determining the states of different water species (bound and bulk) in the confined environment of w/o microemulsion.

Additionally, an in-depth characterization of microenvironment of w/o microemulsion in presence of IL has been made during the performance of the model C-C cross

coupling (Heck) reaction. The reaction ends up with the highest yield in presence of 0.05 mol dm^{-3} of IL, wherein Pn transfer process reported to be most spontaneous as evident from the physicochemical and thermodynamic parameters obtained by the dilution method. All findings of the present investigation, starting from simple titrimetric method to sophisticated instrumentations, lead to the conclusion that the most plausible reaction location/site is the interfacial region of w/o microemulsion, where the population of all active ingredients of both template and the Heck reaction are impart stability to the system. The confinement of IL (as additive) improved the reactivity of Heck reaction, which can be used in various domains, such as biocatalysts or nanomaterial synthesis.[9] The understanding of physicochemical parameters and interactions during the progress of the organic reaction in w/o microemulsion has implications for designing of suitable reaction media for organic synthesis.

II.G. References

References are given in BIBLIOGRAPHY under Chapter-II (pp. 105-108).

CHAPTER-III

A fast and additive free C-C homo/cross-coupling reaction in reverse micellar gallows: A brief understanding on role of surfactant, water content and base on the yield of the product and possible reaction site therein

III.A. Introduction

Biaryls are important structural motifs, available in various natural products, ligands, drug molecules and functional materials. Various distinct classes of therapeutic molecules are containing biaryl framework.[1] Biaryls are also known to have potential as antitumor, [2] and antihypertensive agents.[3] Several synthetic methods have been developed so far for the construction of biaryl skeletons through C–C coupling reactions. The field of C-C homo/cross coupling reactions is dominated by palladium catalyst. [4-11] Use of additive is very common in palladium catalyzed homocoupling reaction of arylboronic acid. In addition to the palladium (Pd) catalysis, some gold (Au)[12,13] copper (Cu)[14] and manganese [Mn(III)][15] catalyzed homocoupling reactions of arylboronic acids have also been reported. But the common problems associated with these methods are high temperature and long reaction time.[12] In view of these, search to find out a suitable medium for studying these types of reactions is warranted.

Reverse micelles (RMs) can execute as an excellent biomimetic model since it provide local hydrophilic moiety in an organic phase resembling to biological membranes of the amphiphilic phospholipids. The water pool of the RM provides a compartmentalized environment with properties considered to be similar to those found at polar/non-polar interfaces in vivo.[16] In the confined region, free movement of water molecules is restricted and the three-dimensional hydrogen-bonded network is disrupted.[17]The dynamics of confined water in the vicinity of biomacromolecules are believed to be responsible for many biological functions, such as molecular recognition and enzymatic catalysis.[18] In view of these, RMs are reported to be used as microreactors to study a variety of organic reactions[19-22] and yield of the product(s) depend on the type of surfactant used, also on the nature of confinement in RMs.[19-21] Thus, the task specific RMs can, therefore, be formulated by judicious selection of the ingredients. Very recently, we have reported the Pd-NHC catalyzed Heck reaction in

ionic liquid based w/o non-ionic microemulsions/RMs.[22] Highest yield of the coupled product was obtained where microemulsion formed spontaneously with maximum stability. Sometimes, surfactant monolayer also plays vital role in controlling the reaction dynamics in confined environment by attracting reagents at the interfacial region which was considered as the reaction site.[19-22] Hence, a wide scope prevails to study organic reactions in RMs comprising surfactants with different charge types [*viz*. anionic, AOT, (sodium 1,4-bis(2-ethylhexyl)sulfosuccinate, Na(DEHSS)), cationic, DDAB (didodecyldimethylammonium bromide) and non-ionic TX-100 (t-octylphenoxypolyethoxy ethanol) with variation in configuration of polar head groups and hydrophobic moieties (Scheme-III.1) under varied physicochemical conditions. Cyclohexane (Cy) has been chosen as bulk phase for convenient extraction of the final products.

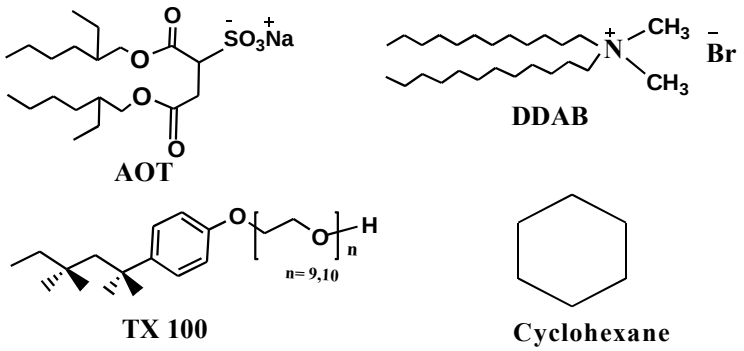

Scheme-III.1. Molecular structure of AOT, DDAB, TX-100 and cyclohexane

This report has been emphasized on the construction of C-C bond with special reference to the transition metal catalyzed additive free C-C homo/cross-coupling reaction of arylboronic acid (herein, phenylboronic acid was selected as a model compound) in these reverse micellar gallows at ambient condition. At the outset, all these RMs (stabilized by surfactants of different molecular structures and physicochemical properties etc. mentioned earlier) have been characterized by employing conductance, DLS and FTIR techniques in order to provide an outline on the performance of the reaction as well as a comparative output of the final product in terms of the yield. Further, a series of studies were undertaken to perform above mentioned reaction in the medium which produces highest yield (herein, AOT/Cy RM) to find out a most suitable base (which is essential for this type of reaction) and also, variation of the yield as a function of water content (ω) under optimized condition. A rationale on the progress of the reaction(s) in constrained environment of AOT RM and the possible reaction site, have also been assessed by employing conductance, DLS and FTIR techniques. Finally, it was contemplated to explore the construction of unsymmetrical biaryl *via* Suzuki-Miyaura

cross-coupling reaction of aryl halides with phenylboronic acid (28 different entries) in AOT RM using same protocol. The yield of coupled products have been discussed in view of variation in electron withdrawing group in arylhalides (Cl^-, Br^- and I^-) and bond strength between C-halides.

II.B. Results and Discussion

Before going to discuss about the construction of C-C bond and design of different organic motif through the transition metal catalyzed additive free C-C homo/cross-coupling reaction in reverse micellar media at ambient condition, first we emphasize on the microstructural and microenvironmental characteristics of the templates viz. anionic, cationic and non-ionic surfactant based reverse micelles (RMs).

II.B.1. Formation and Characterization of anionic, cationic and non-ionic RMs

The anionic surfactant, AOT, cationic, DDAB and nonionic TX-100 are well-known emulsifiers and envisioned for the formulation of RMs in cyclohexane by exploiting the same.[7-12] All the measurements were performed at a fixed surfactant concentration, [S_T] of 0.5 mol dm^{-3} at 303K.

II.B.1.1.Conductivity measurement

Electrical conductivity is a structure sensitive property of water-in–oil (w/o) microemulsion/RMs. The existence of microstructural regimes, namely spherical droplets and aggregated clusters, can be predicted from the nature of the plots.[23] Figure-III.1. (A, B and C) shows the variation of electrical conductivity as a function of water content (ω) for AOT/Cy, DDAB/Cy and TX-100/Cy RMs, respectively at 303K.

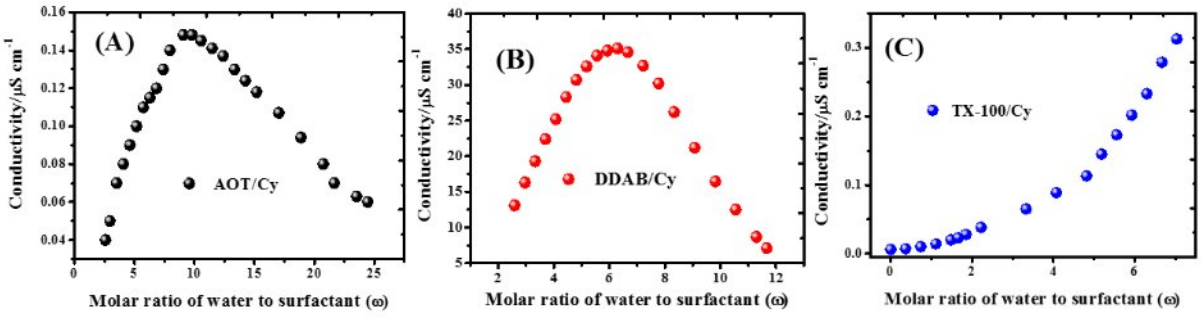

Figure-III.1. The variation of electrical conductivity a function of water content (ω) for AOT (A), DDAB (B) and TX-100 (C) RMs, respectively in cyclohexane (Cy) at 303K.

It can be seen in Figure-III.1. A, the conductivity of AOT/Cy RM increases upon increasing ω at the initial stage. After reaching a maximum (at ω= 10), it decreases until phase separation. The low-conductance behavior and also, a maximum in conductivity in this medium can be explained as follows:[24,25] At low water content, the solubilized water molecules, which are mainly encapsulated in nanosized domains, are preferably involved in ion hydration and associate to Na^+ and head groups tightly. Some of these Na^+ ions bind to the surfactant reside in close proximity of the oil/water interface or palisade layer and hence, they are immobilized, which makes the aqueous environment quite rigid. The surfactant aggregates approach and fuse to form a short-lived dimer and subsequently, they separate to form two new isolated droplets. During this process, the counter ions randomly redistribute and give rise to separately charged droplets, which migrate in the oil-rich medium under an electrical field and result in the low conductance.[26, 27]The appearance of maximum in conductivity is an outcome of several antagonistic effects that influence the conductance behaviors of the system. The added water tends to form water pools in the cores of nanodroplets as the water content exceeds the demand for hydrating surfactant headgroups and counter ions. With increase in water solubilization, the hydrated counter ions exchange and redistribute readily during the process of droplet collision and transient fusion, which contributes to the increase in conductivity.[27] An analogous variation in conductance i.e. appearance of bell-shaped curve with a maximum in conductivity (at ω= 6), has been observed for DDAB/Cy RM as a function of ω, as shown in Figure-III.1.B and can be attributed to charge fluctuation.[28] The conductivity of DDAB RMs show higher values than that of AOT based RM and the maxima in conductance occur at lower water content (ω) (Figure-III.1.A and B). Different types of (i) polar head groups and counter ions of AOT ($DEHSS^-/Na^+$) and DDAB ((DDA^+/Br^-), (ii) size of polar head groups (55 A^{02} for AOT/ 68 A^{02} for DDAB) and (iii) penetration of their polar head groups inside the water pool and constitution of the interface *vis-a-vis* its flexibility or rigidity might be effective for above variation in conductance.[29, 30] However, TX-100/Cy RM shows gradual increase in conductivity with increase in ω. However, no maximum in conductivity was observed even at high water content (in the presence of 0.9 % NaCl) till phase separation,[31] as illustrated in Figure-III.1. C. This reflects a regular buildup of an infinite network containing connected or fused droplets in TX-100 RMs.

III.B.1.2. Dynamic light scattering measurement

A DLS experiment allows the droplet size determination of the RMs, and is also, competent to identify populations with distinct size distributions, and therefore, reveals the presence/formation of aggregates.[32] In view of this, the size and size distributions of RM droplets are measured by DLS technique. Figure-III.2 (A, B) depicts the variation of droplet size and droplet count rate for AOT, DDAB and TX-100 based RMs in cyclohexane as a function of water content (ω) at a fixed temperature (303K). The hydrodynamic diameter (D_h) of RM droplet increases with increase in water content (ω) for all the RMs whereas decrease of the droplet count rate has been observed under the prevailing condition, keeping other parameters constant [Figure-III.2 (A, B)]. Bardhan et al. reported that the droplet count rate is directly proportional to the droplet number of the RMs.[33, 34] Hence, it clearly indicates the swelling behaviour of RMs and aggregation of smaller droplets into large one and thereby, increases the droplet size and decreases the droplet number with the addition of water. Further, the results clearly indicated that D_h follows the order: $RM_{AOT} < RM_{DDAB} < RM_{TX\text{-}100}$ at comparable ω (up to 7.0) whilst droplet count rate shows reverse trend [Figure-III.2 (A, B)].

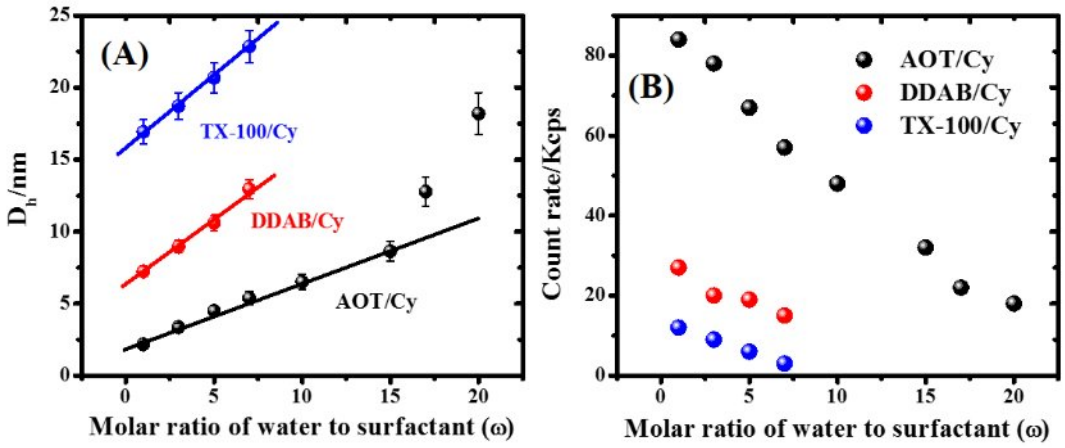

Figure-III.2. The variation of droplet size (A) and droplet count rate and (B) for AOT, DDAB and TX-100-Cy blended RMs as a function of water content (ω) at a fixed temperature (303K).

The droplet size of RMs depends, among many other variables, on the surfactant packing parameter (P).[23] Such phenomena could be attributed to the variation in an effective packing parameter of surfactant, v/al_c, in which v and l_c are the volume and the length of the

hydrocarbon chain, respectively, and *a* is the head group area of surfactant.[27, 35, 36] It is noteworthy that the polar head group area (*a*) of the nonionic surfactant (herein, TX-100) is larger than that of cationic (DDAB) and/or anionic (AOT) surfactant as nonionic surfactant possesses long polyoxyethylene chain (9/10-POE chains) as polar head thereby decrease the value of effective packing parameter (P).[37,38] It gives rise to an increase in radius of the droplets in nonionic RMs (herein, TX-100).[27, 33] It can be inferred that variation in D_h of these RMs depends on type and size of polar head groups and hydrophobic moieties of surfactant (AOT, DDAB and TX-100), which influence the formation of reverse aggregates (Figure-III.2 A). Moreover, the linear variation of droplet size as function of ω indicates that the droplets do not interact each other and are probably spherical. The deviation from linearity as evident for AOT RMs at higher ω value (> 10) is due to several factors. Of these, the most relevant one being enhanced droplet-droplet interaction and shape of the RMs.[39]

III.B.1.3. FTIR spectroscopy

Reports on the properties of the encapsulated water in a range of size and charge type of RMs by studying the states of water organization using FT-IR measurement, are available in literature. [22, 34, 40-43] We have measured mid infrared region (MIR) FTIR spectra for different RMs in cyclohexane as a function of water content (ω) and the temperature (303K). We focus our attention to the 3000−3800 cm^{-1} frequency window as this is a fingerprint region for the symmetric and asymmetric vibrational stretch of O−H bonds in water.[44-46] It is well known that the nanoscopic confinement and droplet size have a strong impact on water hydrogen bond network dynamics regardless of the nature of the interface in RMs. Different types of hydrogen bonded water molecules exist in RMs which can broadly be classified into two major classes, namely, bound and bulk-like water molecules.[40-43] Hence, FTIR spectra of O-H band of water for AOT, DDAB and TX-100 derived RMs have been analyzed and deconvoluted into two peaks at ~3450 and ~3250 cm^{-1}, corresponding to the O-H stretching frequency of the bound and bulk-like water molecules, respectively. A representative result of deconvolution (relative abundance of different water species) is depicted in Figure-III.3 (A, B and C).[40-43]

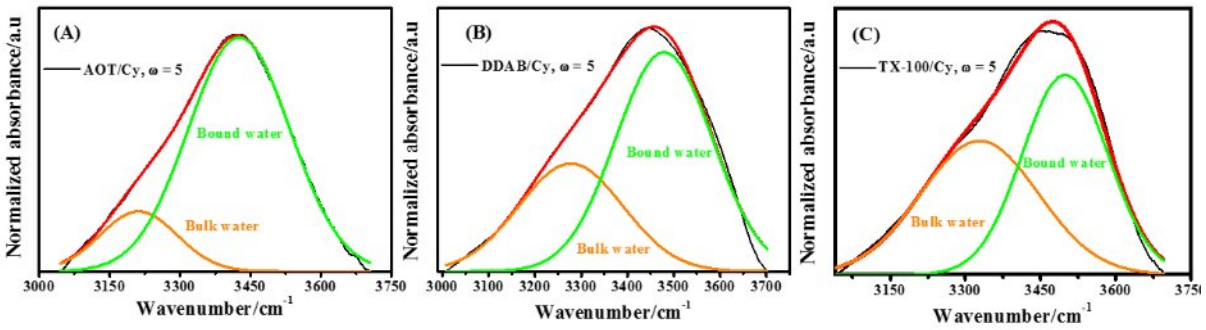

Figure-III.3. Representative normalized (normalized to intensity of 1.0) FTIR spectra of O-H band for AOT (A), DDAB (B) and TX-100 (C)- Cy blended RMs at a fixed water content (ω=5) and temperature (303K). Specification: Experimental spectra (black curve), overall fitted line (red) and deconvoluted curves (bulk water (orange), bound water (green).

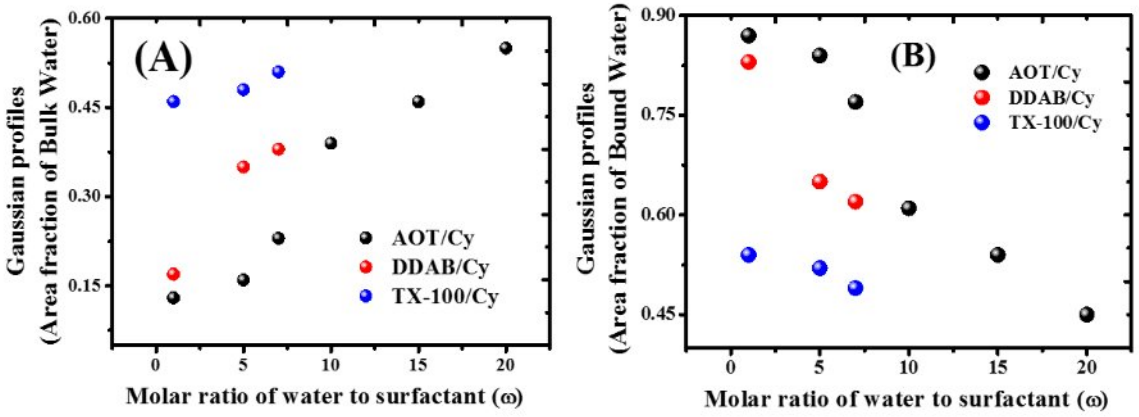

Figure-III.4. The relative abundance [Gaussian profiles (area fraction)] of different water species (bulk (A) and bound (Bound)) in AOT, DDAB and TX-100–Cy blended RMs as a function of ω.

The relative abundance [Gaussian profiles (area fraction)] of different water species in these systems as a function of ω is presented in Figure-III.4. It reveals that the relative abundance of bulk water increases and that of bound water decreases with increasing water content vis-à-vis droplet size (D_h) for all the RMs. Actually, once water is added to a RM forming system, a portion of the water goes to the interface and hydrates the head groups of surfactants till they become fully hydrated at a certain ω. Further addition of water goes primarily to the inner core, leading to a continuous increase in the fraction of unbounded free bulk like water with increase in ω.[47] Interestingly, it reveals from Figure-III.3 and 4 that the bound water proportion is the least in TX-100 formed RMs. Whereas, the proportion of bound water increases in presence ionic surfactant (AOT or DDAB) derived RMs and

follows the order: $RM_{TX\text{-}100} < RM_{DDAB} < RM_{AOT}$. These results indicate a significant role of surfactant charged types and polar head group in determining the proportion of different water species (bound and bulk) in the confined environment of RMs. Uncharged head group nonionic surfactant (herein, POE chain of TX-100) interacts less strongly with the water molecules as does the ionic surfactant head groups (DDAB and AOT), thereby decreasing the population of bound type water molecules in TX-100 formed RMs.[48] Further, the surface area per AOT head group is larger, leading to its interactions with more water molecules and increased water penetration at the interface of AOT RMs leading to water-ester interactions by intermolecular H-bonding vis-à-vis highest bound water population.[49] It is noteworthy that lowest D_h of AOT RMs also subsidizes the highest bound water population as decreasing droplet size increases the bound water proportion in RMs and vice versa.[22, 33, 34]

III.B.2. Standardization of Homocoupling reaction

In preceding paragraphs, AOT, DDAB and TX-100 RMs in cyclohexane show considerable difference in physicochemical characteristics which depend on the charge types, configuration of polar head groups and hydrophobic moieties of surfactant under varied conditions, as evident from conductivity, DLS and FTIR measurements. In view of all these aspects an attempt has been made to compare the effect of different types of RMs on the reaction yield and also, to find out the best combination of RM medium and the base required for effective C-C homocoupling reaction of arylboronic acid which is albeit a major part of presentation of this section. Herein, phenylboronic acid was selected as a model compound for homocoupling reaction.

Triton X-100 RMs in cyclohexane can solubilize maximum amount of water only up to ω (molar ratio of water to surfactant) equals to 7 at a fixed surfactant concentration, $[S_T]$ of 0.5 mol dm^{-3}. Hence, identical hydration level and $[S_T]$ of other two surfactants (viz. AOT and DDAB) has been chosen to underline the comparative efficacy and the corresponding results are summarized in Table-III.1.

Table-III.1. Optimization of reaction condition for homocoupling reaction in RMs[a]

Entry	Solvent	ω	Base	Yield(%)[d]
1	Cy[b]	——	K_2CO_3	50
2	H_2O[b]	——	K_2CO_3	62
3	Water/TX-100/Cy[c]	7	K_2CO_3	64
4	Water/DDAB/Cy[c]	7	K_2CO_3	75
5	Water/AOT/Cy[c]	7	K_2CO_3	81
6	Water/AOT/Cy[c]	5	K_2CO_3	73
7	Water/AOT/Cy[c]	10	K_2CO_3	88
8	Water//AOTCy[c]	15	K_2CO_3	91
9	Water/AOT/Cy[c]	20	K_2CO_3	82
10	Water/AOT/Cy[c]	15	Na_2CO_3	86
11	Water/AOT/Cy[c]	15	Cs_2CO_3	96
12	Water/AOT/Cy[c]	15	K_3PO_4	93
13	Water/AOT/Cy[c]	15	——	86
14[e]	Water/AOT/Cy[c]	15	Cs_2CO_3	<10

[a]Reaction Condition: Phenylboronic acid (1 mmol), base (2 mmol), $Pd(OAc)_2$ (2 mol%), Solvent (3 ml); [b]Reaction was continued for overnight; [c]Water/surfactant/oil, RM contains 1 mmol surfactant and 2 ml oil in each case; [d]Isolated Yield; [e]$Cu(OTf)_2$ was used as catalyst.

Both nonionic TX 100 and cationic DDAB based RMs responded well and resulted in good yield (64% and 75%, respectively) of desired homo-coupled product (Table-III.1; entry 3, 4). However, highest yield (81%) was obtained in presence of anionic AOT under identical condition. In addition, the yields of the product are also measured in the constituents of these formulations as media (Table-III.1; entries 1, 2). Both water and cyclohexane results in low yield compared to RM, Hence, it may be concluded that AOT, DDAB and TX-100 surfactants are quite competent to tune the architecture of RMs starting from the interfacial film to the confined environment (water pool) in a different way due to their inherent characteristics and subsequently, effect the reaction yield at comparable physicochemical condition.[34, 50]

For example, DDAB is essentially insoluble in pure oil, and the small amount water required to form reverse micelle is believed to solvate the head groups and counterion, and beyond which phase separation occurs. Further, because of its poor solubility in water and oil too, it is reported that DDAB molecules are predominantly adsorbed at the oil/water interface and results in less flexible (rigid) so that penetration of the bulkier headgroups (cationic, DDA^+) into the water pool makes difficult. (Scheme-III.1).[51,52] On the other hand, AOT has received much larger attention to form RM due to its ability to solubilize large amounts of water in a variety of nonpolar solvents over a wide range of concentrations. Its special structural characteristics (Scheme-III.1) reveal formation of a more flexible interface so that a comparable less dimension of polar headgroups (anionic, $DEHSS^-$) can protrude towards water pool more easily.[53] Whereas, TX 100 contains polyoxyethylene (POE) group as a hydrophobic part (polar head group), which may be larger than the hydrophobic part of the molecule. Because of the presence of long POE group, polar interior of reverse micellar aggregates thus formed, has shown much different nature from formed with ionic surfactants.[54, 55] Interestingly, the results reveal that AOT is best suited for present study. The low conductivity, small droplet size and high population of bound water species of AOT RMs might be operational for the hike in reaction yield therein. In addition, a plausible explanation in view of the foregoing discussions on difference in characteristic features of microenvironment of the water pool of three RMs can be drawn that

stronger electrostatic interaction between catalyst [$Pd(OAc)_2$] and anionic head group of AOT prevails inside the pool, which corroborates stronger catalytic support to enhance the yield. Whereas, DDAB and TX- 100 do not subscribe any additional support due to difference in microenvironments and microstructures of these RMs emerges from bulkier cationic polar head group (DDA^+) and bulkier POE group (as dipole).

Henceforth, the optimization with respect to other reaction parameters (viz. droplet size, base etc.) has been resolved using AOT based RMs in subsequent sections. The schematic diagram for the homocoupling reaction in AOT based RMs is depicted in Scheme-III.2, which reveals compartmentalization of hydrophilic and lipophilic reactants in water pool and palisade layer of surfactant, respectively separated by the oil/water interface. Size of the aggregated droplets, characterized by ω, affects the local aqueous environments of RMs.[16] Changes in the droplet size of RMs are another proposition to tune the population of amphiphiles at the droplet surface under identical [S_T]. In order to compare the effect of encapsulation or compartmentalization of the constituents/reactants in the present reaction with variation of ω (=5→20) vis-à-vis droplet size (D_h =4.49→ 18.20), we have performed model reaction in water/AOT/cyclohexane RMs and the results are presented in Table-III.1 (Entry-6,7,8,9). It is evident from Table-III.1 that the yield of the desired product increases with ω up to 15 and thereafter, it decreases. More precisely, the highest yield of the desired product (91%) has been observed at ω=15 indicating the finest level of size (D_h =8.64) which facilitates the coupling reaction therein. Hence, it reveals that the different degrees of confinement as a function of ω in water pool can enable to control the reactivity in RMs.[19]

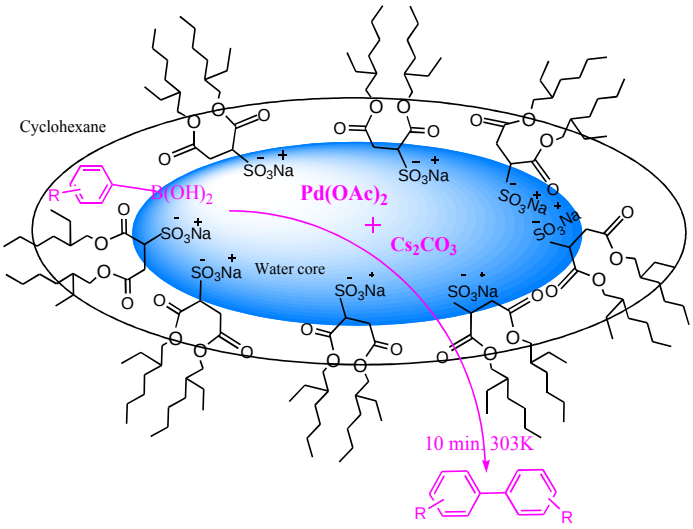

Scheme-III.2: Homocoupling of arylboronic acid in RMs

Among the different bases as enlisted in Table-III.1, highest yield (96%) of the product (Table-III.1; entry-8) was obtained in the presence of Cs_2CO_3 and its superiority to all bases validated under the reaction condition. After optimizing all parameter, we have tested one reaction in presence of $Cu(OTf)_2$, and corresponding result is given in Table-III.1, entry 14. It is cleared from the results that $Pd(OAc)_2$ is better catalyst in comparison to the $Cu(OTf)_2$ for the homocoupling reaction of arylboronic acids.

III.B.3. Growth of reaction in RMs gallows and plausible reaction site therein

From preceding sections, it reveals that AOT/Cy RM has been found to be an effective reaction medium for C-C coupling reactions. The model homocoupling reaction has been performed in this medium and followed by evaluation of different physicochemical properties during proceedings of the reaction to monitor the growth of reaction and accordingly, most plausible reaction location in AOT RM has been deciphered in the following sections.

III.B.3.1.Conductivity measurement

Electrical conductivity of RM has been measured at regular interval during progress of the reaction under optimized condition and the results are presented in Figure-III.5 (A, Table-B.S1). At onset, increase in conductivity upon addition of catalyst $Pd(OAc)_2$ is

obvious but subsequent decrease in conductivity reflecting the formation of non-conducting aqua-palladium complex.[22,56] A sharp increase in conductivity has observed after addition of other reagents and this trend is continued until the completion of reaction. In homocoupling reaction, the product biaryls are formed along with highly conducting side-products [$B(OH)_4^-Cs^+$, $CsHCO_3$] which are responsible for hike in conductivity during reaction.[57] Hence, it can be reasonable to assume that the reaction probably occurring within the droplets of AOT RM.

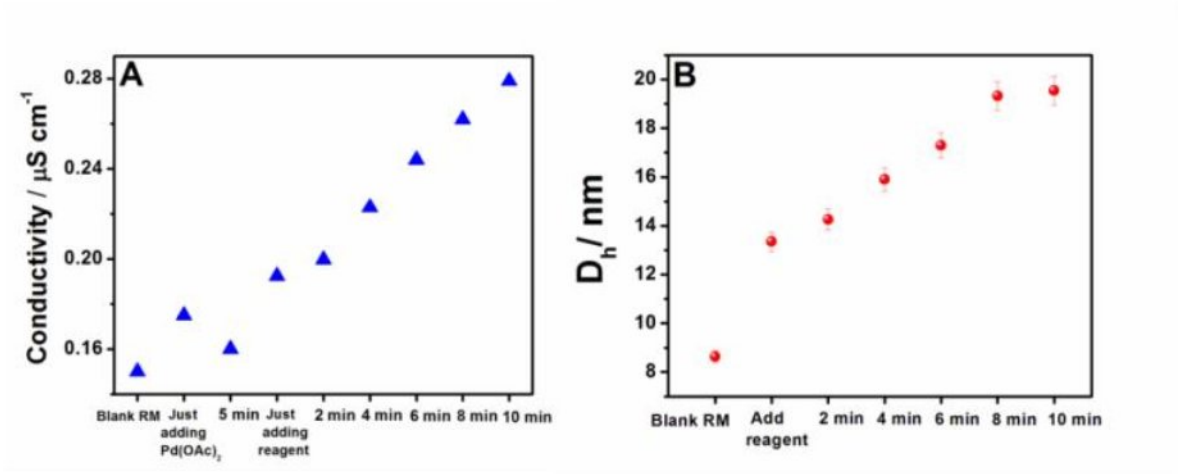

Figure-III.5. (A) The conductivity and (B) the hydrodynamic diameter (D_h) of RMs during course of the reaction.

III.B.3.2.Dynamic light scattering (DLS) measurement

Results of DLS measurement of droplet sizes (D_h) of AOT RMs during course of reaction are presented in Fiure-III.5.B. A sudden increase in D_h (from 8.64 to 13.35 nm) has been observed after addition of reagents, and this trend continues until it reaches to optimal label which actually indicates the end point of reaction. Water soluble reagents [*viz*. catalyst, base mentioned in Table-III.1] get easily solubilized inside the water pool whereas phenylboronic acid, being a sparingly water soluble reagent which possess both hydrophilic and hydrophobic components is expected to be located at the vicinity of oil/water interface of RMs. As a consequence, hydrophilic part of the molecule extends towards water pool due to hydrogen bonding and hydrophobic part obviously incorporates into hydrocarbon domain in the vicinity of the interface/palisade layer.[20, 22] Nevertheless, accumulation of reagents inside water droplets and the presence of phenylboronic acid in the palisade layer of RMs together are responsible for enlargement of droplet size. The regular increase in droplet size during reaction might be due to the formation of the products (both desired and side) and optimal

droplet size reflecting the end of reaction. All these observations together sensing that the reaction takes place inside the water droplets.

III.B.3.3.FTIR measurement

As discussed earlier, the different types of hydrogen bonded water molecules exist in RMs, can broadly be classified into two major classes, namely, bound and bulk-like water molecules [34, 40-43, 58-61] with a characteristic O-H stretching frequency in IR spectroscopy at ~3450 and ~3250 cm^{-1}, respectively (Figure-III.6 and Inset A). Interestingly, the progress of the reaction monitored by FTIR reveals that the addition of palladium acetate initially reduces the population of bound water due to the formation

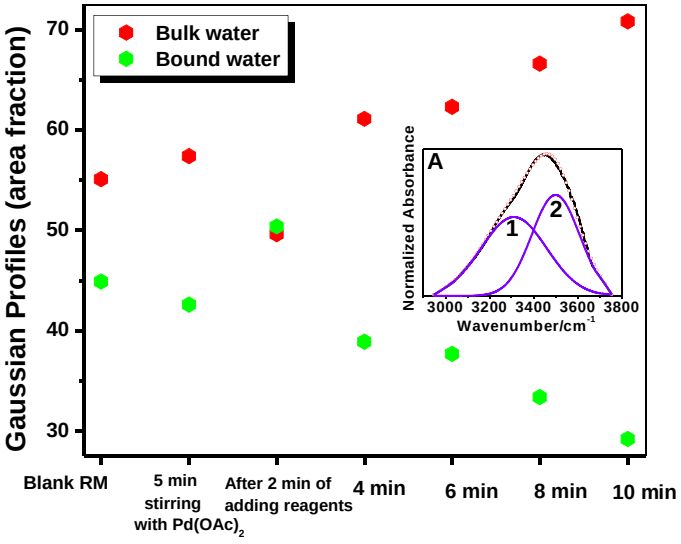

Figure-III.6. The Gaussian Profiles of FTIR study of AOT RMs at regular interval during homocoupling reaction at fixed ω (= 15) and 303 K. Inset A. Representative normalized (normalized to intensity of 1.0) FTIR spectra of O-H band for blank AOT RMs at constant ω (= 15) and 303K. Specification: Experimental spectra (black curve), overall fitted points (red) and deconvoluted curves (1: bulk water; 2: bound water).

of aqua-palladium complex, which decreases the interaction of bound water with polar head groups of AOT. Subsequently, the addition of phenylboronic acid initially enhances the population of bound water as it form H-bond with confined water molecules. Hence, it can be inferred that the molecules of phenylboronic acid essentially reside in the vicinity of the oil/water interface. Thereafter, the bound water population regularly decreases till the completion of reaction. This observation indicated by the formation of biaryls results in

decrease in population of phenylboronic acid at the oil/water interface. Further, the decrease in bound water population may be due to the effect of limiting the interaction between the polar head groups ($DEHSS^-$) of AOT and water.[61] Hence, it can be concluded from overall observations that the reaction takes place in droplets of RMs with special reference to the bound layer of water molecules.

III.B.4.Generalization of AOT RM as reaction media

With this optimized condition presented, an attempt has been made further to establish the versatility of our present protocol. A variety of arylboronic acids were examined under the optimal reaction condition in AOT RMs and the corresponding results/products are summarized in Table-III. 2.

Table-III.2. Homocoupling of different arylboronic acids[a]

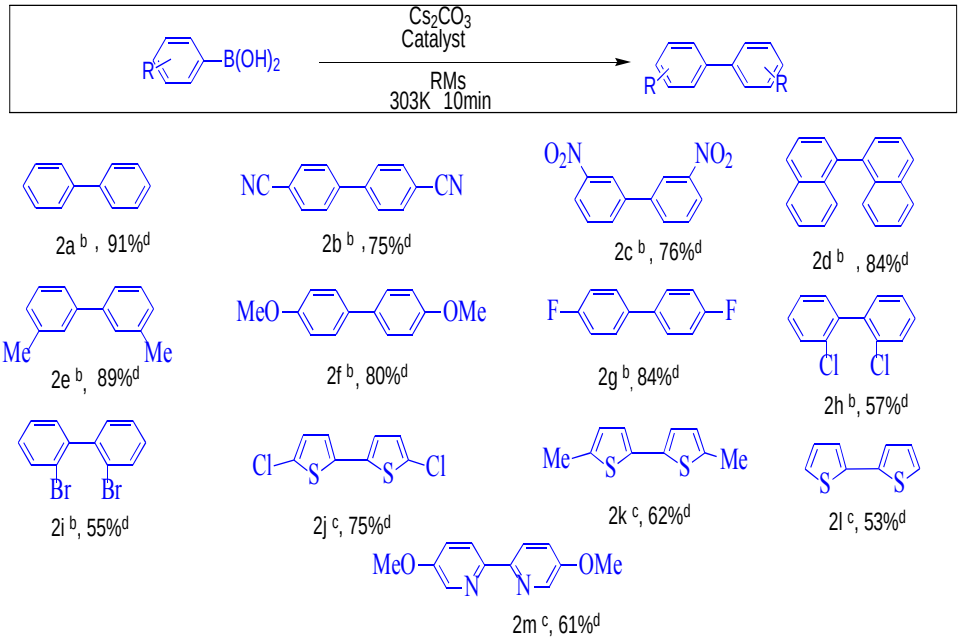

[a]Reaction condition: Arylboronic acid (1mmol); base (2 mmol); catalyst (2 mol%); RMs (3 ml); [b]$Pd(OAc)_2$ used as catalyst; [c]$Cu(OTf)_2$ used as catalyst; [d]Isolated yield after column chromatography.

The reaction progressed smoothly and functional groups were well tolerated under the reaction condition. It is clear from the results that arylboronic acids bearing electron withdrawing groups, (*e.g.,* -Br, -Cl, -F, -CN and $-NO_2$), participate in reactions smoothly and results in good yield of the desired homo-coupled products (Table-III.2; 2b,2c,2g-2i). Arylboronic acids bearing electron-donating groups, (e.g.,-Me and –OMe) furnished the desired products with high yields of 89% and 80%, respectively (Table-III.2; 2e,2f) upon

isolation. *Para* and *meta* substituted arylboronic acids afforded good yields whereas, the dimerisation of *ortho* substituted phenylboronic acids produced the corresponding product with low yields (Table-III.2; 2h,2i), which may be attributed to the steric effect of the substituents present in *ortho* position. Under the same reaction condition, 84% of binaphthyl product was isolated from the naphthylboronic acid (Table-III.2; 2d).

After successful completion of homo-coupling reaction of arylboronic acid, we turned to apply same protocol in case of heteroarylboronic acids. Homo-coupling of heteroarylboronic acid under optimized condition persistently resulted in low yield of the desired product. It might be due to the strong affinity of hetero atom to palladium and accordingly, poisons of the catalyst.[62] We then, modified our protocol and introduced $Cu(OTf)_2$ as catalyst instead of $Pd(OAc)_2$. Under this modified condition, heteroarylboronic acid proficiently responded in homo-coupling reaction and resulted in good yield of the desired product (Table-III.2; 2j-2m).

III.B.4.1.Suzuki cross coupling reaction of aryl halides with phenylboronic acid

In this section, scope of the protocol under investigation was further explored for the construction of unsymmetrical biaryl *via* Suzuki-Miyaura cross-coupling reaction. Accordingly, we have performed a few cross-coupling reactions and results are presented in Table-III.3. Interestingly, the cross-coupling reaction under optimized condition facilitated over homo-coupling reaction and resulted in unsymmetrical biaryl in good to moderate yield. Aryl iodides are ended up with the good yield of cross-coupled product in comparison to arylbromides (Table-III.3).Whereas arylchlorides are not responding in reaction under the optimized condition even after 24 hrs (3l, 3m, 3n).

A slight decrease in product yield for aryl bromides has been observed, and may be due to the higher bond strength of C-Br in comparison with C-I.[63] The presence of electron withdrawing group in arylhalide (Table-III.3, entry 3d, 3g) enhances the yield of the coupled product. The cross-coupled product 1-(3-chlorophenyl)benzene (3j) has been isolated in good yield upon reaction between 1-chloro-3-iodobenzene and phenylboronic acid on selective basis. When 1,3-dibromobenzne treated with phenylboronic acid (2 equivalent) under optimized condition, a decent yield (62%) of 1,3-diphenylbenzene (3k) has been observed.

Table-III.3. Suzuki-Miyaura cross coupling of different Aryl halides with Phenylboronic acid[a]

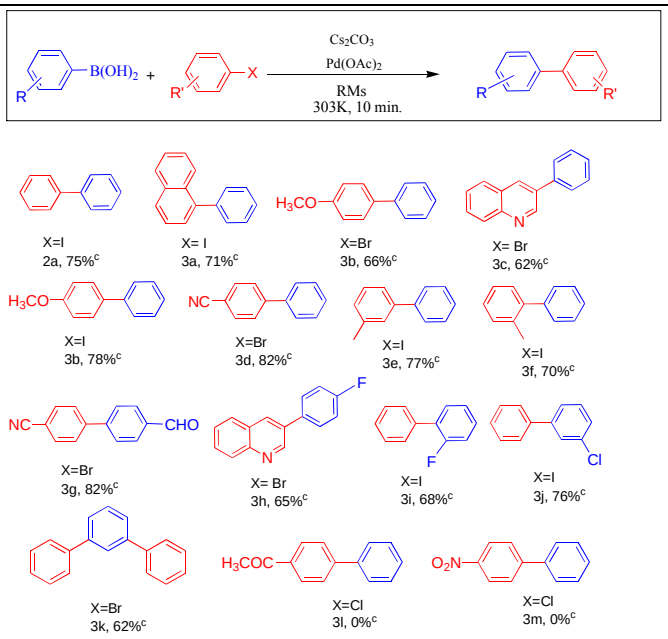

[a]Reaction condition: Arylboronic acid (1mmol); aryl halide (1mmol); base (2 mmol); catalyst (2 mol%); RMs (3 ml); [c]Isolated yield after column chromatography.

III.C. Experimental

III.C.1.Materials and Methods

Dioctyl sulfosuccinate sodium salt (AOT, ≥ 98%, commercial name of the sodium salt of bis(2-ethylhexyl)sulfosuccinate [Na(DEHSS)]), didodecyldimethylammonium bromide (DDAB, ≥ 98%), t-octylphenoxypolyethoxyethanol, palladium acetate [Pd(OAc)2, ≥ 99.98%] arylboronic acids, cesium carbonate, potassium carbonate, palladium acetate, and copper triflate were purchased from Sigma Aldrich, USA. cyclohexane (Cy, ≥ 98%) was the product of Fluka, Switzerland. All these chemicals were used without further purification. Doubly distilled water of conductivity less than 3 μS cm^{-1} was used in the experiments.

Conductivity measurements were performed using Mettler Toledo (Switzerland) Conductivity Bridge. The instrument was calibrated with standard KCl solution. The uncertainty in conductance measurement was within ±1%.

DLS measurements were carried out using Zetasizer Nano ZS90 (ZEN3690, Malvern Instruments Ltd, U.K.). He-Ne laser of 632.8 nm wavelength was used and

the measurements were made at a scattering angle of 90^0. FTIR absorption spectra were recorded in the range of 400-4000 cm^{-1} with a Shimadzu 83000 spectrometer (Japan) using a CaF_2-IR crystal window (Sigma-Aldrich) equipped with Press lock holder with 100 number scans and spectral resolution of 4 cm^{-1}. Deconvolution of spectra has been made using Origin software.

NMR spectra were recorded on 300 MHz spectrometer at 298 K and calibrations were done on the basis of solvent residual peak. Products were isolated using column chromatography on silica gel (60-120 mesh) and a mixture of petroleum ether (60^0-80^0C)/ethyl acetate was used as an eluent. Reaction progress was monitored by silica gel TLC.

III.C.2. General procedure for C-C homo/cross coupling reactions

A 10 ml reaction vial was charged with arylboronic acids (1 mmol), base (2 mmol), catalyst [2 mol%, $Pd(OAc)_2$ for arylboronic acids and $Cu(OTf)_2$ for heteroarylboronic acids]/aryl halide (1 mmol) [only for cross-coupling reaction] and RM (3 mL; $[S_T]$ of 0.5 mol dm^{-3} at 303K). The mixture was stirred at room temperature for 10 minutes. Then the reaction mixture was diluted with water and extracted with dichloromethane (3 x 10 mL). Combined organic layer was dried over anhydrous Na_2SO_4 and concentrated under reduced pressure. The crude residue was purified by silica gel column chromatography using the mixture of petroleum ether and ethyl acetate as eluent.

III.C.3. Spectral analysis

Biphenyl (2a)[64] **:** White solid; mp 68-71°C; 1H NMR ($CDCl_3$, 300 MHz); δ: 7.30–7.35 (m, 2 H), 7.39–7.45 (m, 4 H), 7.56–7.59 (m, 4 H); ^{13}C NMR (75 MHz, $CDCl_3$): δ 127.26, 127.34, 128.85, 141.31.

4,4´-Dicyanobiphenyl (2b)[4] **:** White solid; mp 233-235^{0}C; 1H NMR ($CDCl_3$, 300 MHz) δ : 7.68 (dd, J = 4.8 Hz, 6.6 Hz, 4H), 7.77 (dd, J = 4.8 Hz, 6.6 Hz, 4H); 13C NMR (CDCl3, 75 MHz)δ : 143.4, 132.8, 127.8, 118.3, 112.3.

3,3´-Dinitrobiphenyl (2c)[14] **:***Yellow solid; mp 200-202^{0}C; 1H NMR (CDCl3, 300 MHz) δ : 7.71 (t, J = 7.1Hz, 2H), 7.97 (d, J = 7.5Hz, 2H), 8.31 (d, J = 7.6Hz, 2H), 8.50 (t, J = 1.8Hz, 2H); ^{13}C NMR (CDCl3, 75 MHz) δ: 122.1,123.3,130.3,133.0,140.3,148.8.*

1,1´-Binaphthyl (2d)[15]**:***White solid; mp 141-142^{0}C; 1H NMR ($CDCl_3$, 300 MHz) δ : 7.22-7.29 (m, 2H), 7.40-7.49 (m, 6H), 7.57 (t, J = 7.5Hz, 2H), 7.93 (d, J = 8.4Hz, 4H); 13C NMR ($CDCl_3$, 75 MHz)δ:125.4, 125.8, 126.0, 126.5, 127.8, 127.9, 128.1, 132.8, 133.5, 138.4.*

3,3´-Dimethylbiphenyl (2e)[64]**:***Colourless liquid; bp 286^{0}C; 1H NMR (CDCl3, 300 MHz) δ : 2.46 (s, 6H), 7.19 (d, J = 6.6Hz, 2H), 7.36 (t, J = 7.8Hz, 2H), 7.43 (d, J = 7.2Hz, 4H); 13C NMR (CDCl3, 75MHz) δ: 21.2,123.9, 127.5, 127.6, 128.2, 137.9, 140.9*

4,4´-Dimethoxybiphenyl (2f)[64]**:** *White solid; mp 178-179^{0}C; 1H NMR ($CDCl_3$, 300 MHz) δ : 3.84 (s, 6H), 6.95 (dd, J = 4.8Hz, 6.9 Hz, 4H), 7.47 (dd, J = 4.8Hz, 6.9Hz, 4H); ^{13}C NMR ($CDCl_3$, 75 MHz) δ: 55.36, 114.1, 127.7, 133.4, 158.6.*

4,4´-Difluorobiphenyl (2g)[4]**:***White solid; mp 89-90^{0}C; ^{1}H NMR ($CDCl_3$, 300 MHz) δ : 7.09-7.15 (m, 4H), 7.46-7.51 (m, 4H); ^{13}C NMR ($CDCl_3$, 75 MHz) δ: 115.7(d, J= 21 Hz), 128.6(d, J = 8 Hz), 136.4(d, J = 4 Hz), 162.4 (d, J= 245 Hz).*

2,2´-Dichlorobiphenyl (2h)[15]**:***White solid; mp 60-62^{0}C; ^{1}H NMR ($CDCl_3$, 300 MHz) δ : 7.26-7.37 (m, 6H), 7.47-7.51 (m, 2H); ^{13}C NMR ($CDCl_3$, 75 MHz) δ: 126.4, 129.1, 129.3, 131.0, 133.4, 138.2.*

2,2´-Dibromobiphenyl (2i)[65]**:** *White solid; mp 79-81^{0}C; ^{1}H NMR ($CDCl_3$, 300 MHz) δ : 7.23-7.29 (m, 4H), 7.32-7.40 (m, 2H), 7,67 (d, J = 8.1Hz, 2H); ^{13}C NMR ($CDCl_3$, 75 MHz) δ: 123.5, 127.1, 129.4, 131.0, 132.6, 142.0.*

5,5´-Dichloro-2,2´-bithiophene (2j)[66]**:** *White solid; mp 107^{0}C; ^{1}H NMR ($CDCl_3$, 300 MHz) δ : 6.82 (d, J = 3.9 Hz, 2H), 6.85 (d, J = 3.6 Hz, 2H); ^{13}C NMR ($CDCl_3$, 75 MHz) δ: 122.9, 126.7, 129.1, 134.9.*

5,5´-Dimethyl-2,2´-bithiophene(2k)[67]**:** Yellow solid; mp 65-67^{0}C; ^{1}H NMR ($CDCl_3$, 300 MHz) δ : 2.46 (s, 6H), 6.63 (dd, *J* = 2.4Hz, 3.6Hz, 2H), 6.87 (d, *J* = 3.6Hz, 2H); ^{13}C NMR ($CDCl_3$, 75 MHz) δ: 15.3, 122.8, 125.7, 135.5, 138.4.

2,2´-dithiophene (2l)[64]**:** White solid; mp 33-34 °C; ^{1}H NMR ($CDCl_3$, 300 MHz,): δ 7.00-7.03 (m, 2 H), 7.18 (dd, *J* = 3.6 Hz, *J* = 1.2 Hz, 2 H), 7.22 (dd, *J* = 5.1 Hz, *J* = 0.9 Hz, 2 H); ^{13}C NMR (75 MHz, $CDCl_3$): δ 123.77, 124.36, 127.78, 137.40.

6,6´-Dimethoxy-3,3´-dipyridyl (2m)[68]**:** White solid; mp 105°C; ^{1}H NMR ($CDCl_3$, 300 MHz) δ : 3.98 (s, 6H), 6.84 (d, *J* = 8.4Hz, 2H), 7.73 (dd, *J* = 6Hz, 8.7Hz, 2H), 8.32 (d, *J* = 2.4Hz, 2H); ^{13}C NMR ($CDCl_3$, 75 MHz) δ: 53.7, 111.1, 126.9, 137.2, 144.3, 163.5.

1-Phenylnaphthalene (3a)[69]**:** Colorless liquid; ^{1}H NMR ($CDCl_3$, 300 MHz) δ: 7.39-7.54 (m, 9H), 7.84-7.91 (m, 3H); ^{13}C NMR ($CDCl_3$, 75 MHz) δ: 125.3, 125.7, 126.01, 126.03, 126.9, 127.2, 127.6, 128.2, 130, 131.6, 133.8, 140.2, 140.7, 145.6.

4-methoxybiphenyl (3b)[69]**:** White solid; mp 86^{0}C ^{1}H NMR ($CDCl_3$, 300 MHz) δ: 3.86 (s, 3H), 6.99 (dd, *J* = 2.1Hz, 6.9Hz, 2H), 7.27-7.34 (m, 1H), 7.40-7.45 (m, 2H), 7.53-7.58 (m,

4H); ^{13}C NMR ($CDCl_3$, 75 MHz) δ: 54.3, 113.2, 125.6, 125.7, 127.1, 127.7, 132.7, 139.8, 158.1.

3-Phenylquinoline (3c)[69]**:** Faint yellowish oil; ^{1}H NMR ($CDCl_3$, 300 MHz) δ: 7.25 (s, 1H), 7.41-7.61 (m, 3H), 7.69-7.76 (m, 3H), 7.89 (d, *J* = 7.8Hz, 1H), 8.16 (d, *J* = 8.4Hz, 1H), 8.32 (d, *J* = 2.1Hz, 1H), 9.22 (bs,1H); ^{13}C NMR ($CDCl_3$, 75MHz) δ: 127.1, 127.4, 128.0, 128.1, 129.0, 129.2, 129.5, 133.4, 133,9, 137.8.

4-cyanobiphenyl (3d)[70]**:** White solid; ^{1}H NMR ($CDCl_3$, 300MHz) δ: 7.64-7.71 (m, 4H), 7.55-7.59 (m, 2H), 7.38-7.50 (m, 3H); ^{13}C NMR ($CDCl_3$, 75 MHz) δ: 145.66, 139.16, 132. 62, 129.16, 128.71, 127.75, 127.25, 118.99, 110.91.

3-methylbiphenyl (3e)[71]**:** Isolated as a colorless liquid; ^{1}H NMR (300MHz, $CDCl_3$) δ: 7.69 (d, *J* = 8.7Hz, 2H),7.52 (m, 4H),7.43(m,2H), 7.26 (d, *J* = 7.2Hz,1H), 2.59 (s, 3H); ^{13}C NMR (75MHz, $CDCl_3$) δ: 141.5, 141.3, 138.4,128.9, 128.80,128.78,128.2,128.1,127.3,124.4, 21.6.

2-methylbiphenyl (3f)[8]**:** Colorless oil; ^{1}H NMR (300 MHz, $CDCl_3$) δ: 7.46-7.57 (m, 5H), 7.38-7.45 (m, 4H), 2.42 (s, 1H); ^{13}C NMR (75 MHz, $CDCl_3$) δ: 142.1, 141.4, 135.5, 130.5, 129.9, 129.3, 128.2, 127.4, 126.9, 125.9, 20.6.

4-Cyano-4'-formylbiphenyl (3g)[8]**:** Isolated as a white solid; ^{1}H NMR ($CDCl_3$, 300MHz) δ: 10.02 (s, 1H), 7.99 (d, *J* = 7.8 Hz, 2H), 7.72-7.79 (m, 6H); ^{13}C NMR (75 MHz, $CDCl_3$) δ: 191.7, 144.9, 144.1, 136.1, 132.8, 130.5, 128.1, 127.9, 118.6, 112.1.

3-(4-Fluro-phenyl)-quinoline (3h)[8]**:** Isolated as a white solid; ^{1}H NMR ($CDCl_3$, 300MHz) δ: 9.16 (d, *J* = 2.1Hz, 1H), 8.33 (d, *J* = 2.1Hz, 1H), 8.21 (d, *J*=8.4Hz,1H), 7.71-7.80 (m,1H), 7.60-7.71 (m, 4H), 7.23-7.28 (m,2H) ^{13}C NMR (75 MHz, $CDCl_3$) δ: 164.7,161.4,149.0(J_{CF} = 3.3Hz), 146.5, 134.1, 133.7 (J_{CF} = 7.4 Hz), 133.4, 133.0, 129.9, 129.5, 129.1 (J_{CF} = 8 Hz), 128.7, 128.0 (J_{CF} = 3.9 Hz), 127.2 (J_{CF} = 26.70 Hz), 116.3 (J_{CF} = 21.5 Hz).

2-fluorobiphenyl (3i)[72]**:** Isolated as a white solid; Isolated as white solid; ^{1}H NMR (300 MHz, $CDCl_3$) δ: 7.15-7.57 (m, 9H); ^{13}C NMR (75 MHz, $CDCl_3$) δ: 159.8 (J_{CF} = 246 Hz, CF), 135.8 (C_6H_5), 130.8 (J_{CF} = 3.6 Hz, CH), 129.2 (C_6H_5), 129.0 (J_{CF} = 3Hz, CH), 128.9 (C_6H_5), 128.7 (C_6H_5), 128.4 (C_6H_5), 127.4 (J_{CF} = 36 Hz, C_6H_5F), 124.3 (J_{CF}= 3.6 Hz, CH), 116.1 (J_{CF} = 22.5 Hz, CH).

3-chlorobiphenyl (3j)[73]**:** Isolated as colorless oil; ^{1}H NMR (300 MHz, $CDCl_3$) δ: 7.59-7.65 (m, 3H), 7.35-7.53 (m, 6H); ^{13}C NMR (75MHz, $CDCl_3$) δ: 143.1, 139.8, 134.7, 130.1, 129.0, 128.0, 127.4, 127.3, 127.2, 125.4.

1,3-Diphenylbenzene (3k)[8]**:** Isolated as white solid; ^{1}H NMR (300 MHz, $CDCl_3$) δ: 7.81 (m,1H), 7.65 (dd, *J* = 8.4Hz,1.5Hz, 4H), 7.55-7.61 (m, 2H), 7.54 (t, 1H), 7.46-7.49 (m, 3H),

7.44 (t, 1H), 7.35-7.40 (m, 2H); ^{13}C NMR (75 MHz, $CDCl_3$) δ: 141.8, 141.2, 129.2, 128.8, 127.4, 127.3,126.2, 126.1.

III.D.Summary

This report summarizes anionic, water/AOT/Cy RM as an efficient reaction medium for additive and ligand-free transition metal catalysed C-C homo/cross coupling reactions with a broad range of substrates compares to cationic (DDAB) and non-ionic (TX 100) RMs in cyclohexane under comparable physicochemical conditions. The reaction proceeds rapidly and completes within 10 mins at ambient condition. Performance of the reaction has been correlated with different physicochemical parameters of these self-organized media using conductance, DLS and FTIR techniques. A plausible explanation is suggested in favor of AOT/Cy RM to be an effective reaction medium in terms of yield of the final product. Subsequently, a series of studies were undertaken to find out a most suitable base and the influence of water content (ω) of this medium under optimized condition for effective C-C homocoupling reaction of arylboronic acid (herein, phenylboronic acid was selected as a model compound) which constitute a major part of this report. K_2CO_3 (91%) and Cs_2CO_3 (96%) have been found to be least and most effective base, respectively in terms of yield. Droplet size [in other words (ω)] influences the yield in studied ω range (5→20) and shows a maximum at ω equals to 15. The progress of the reaction in constrained environment of RM and the possible reaction site have also been assessed by employing conductance, DLS and FTIR techniques. The droplet core in nano-cage of RM, especially the bound water layer of RM gallows has been emphasized as the probable reaction site. Finally, it was explored for the construction of symmetrical and unsymmetrical biaryl *via* C-C bond forming homo/cross-coupling reaction (28 different entries) in AOT RM using same protocol. The yield of coupled products have been discussed in view of variation in electron withdrawing group in arylhalides (Cl^-, Br^- and I^-) and bond strength between C-halide. Investigations of other organic reactions in such promising micellar and RM media comprising single and mixed surfactant(s) are currently underway in our laboratory.

III.E.References

References are given in BIBLIOGRAPHY under Chapter-III (pp. 108-111).

CHAPTER-IV

Formation of High-Temperature Stable Benzimidazolium Ionic Liquid-in-Oil Microemulsion and Regioselective Nitration Reaction Therein

IV.A.Introduction

Microemulsions are thermodynamically stable 'nano-dispersions' of water in oil (or oil in water) stabilized by a surfactant film, frequently in combination with a cosurfactant.[1] There has been considerable interest in the use of microemulsions as media for organic synthesis in recent years. Not only can such a formulation be a way to overcome compatibility problems, the capability of microemulsions to compartmentalize and concentrate reactants can also lead to considerable rate enhancement compared to one-phase systems. A third aspect of interest for preparative organic synthesis is that the large oil-water interface of the system can be used as a template to induce regioselectivity.[2] The dynamic character of these nano-reactors is one of the most important features, which has to be taken into account for a comprehensive understanding of chemical reactions carried out in these media.[3]

In recent years, attempts were made to formulate and characterize waterless/non-aqueous microemulsions, where other polar solvents like methanol, acetonitrile, glycerol, formamide, ethylene glycol etc. were exploited. The first study of non-aqueous microemulsion with ethylene glycol, lecithin and decane were reported by Friberg and Podzimek in 1984.[4] Latter, Falcone et al. studied the properties of non-aqueous reverse micelles (RMs) using six polar solvents, such as glycerol, ethylene glycol, propylene glycol, formamide, dimethyl formamide, dimethylacetamide.[5] Non-aqueous systems have distinct advantages over aqueous ones as: (i) they generally forms larger stable regions of isotropic solutions compared to the analogous aqueous systems; (ii) a large variety of different surfactants can be used to give non-aqueous microemulsions and (iii) these systems can be used as good reaction media, specifically for the reactants which react with water.[6] These pioneer studies stimulated research on the formulation of non-aqueous microemulsions containing room

temperature ionic liquids (RTILs), which also provide hydrophobic or hydrophilic nano-domains. Thus their applications can be extended to fields of reaction and separation or extraction media. Earlier report has shown that surfactant IL-based microemulsions can be used to produce polymer nanoparticles, gels, and open-cell porous materials.[7] Also, IL-in-oil microemulsions were employed to increase the solubility of a sparingly soluble drug to enhance its topical and transdermal delivery and used as template to synthesize starch nanoparticles for investigation of the drug loading and releasing properties.[8-10] ILs are considered suitable solvents for various chemical reactions and catalysis due to their characteristic properties like negligible vapour pressure and tunability in structure by modifying cation and anion moieties.[11, 12] In addition, ILs exhibit excellent chemical and thermal stability, wide polarity and are recyclable.[13, 14] Despite their great potential, reports on the performance of organic reaction in non-aqueous IL microemulsions are still very scarce. In our previous work, we reported Heck reaction in w/o non-ionic microemulsion system in the absence and the presence of an IL (1-Ethyl-3-Propylbenzimidazolium bromide), where the reaction ended with the highest yield (75%) in presence of solute amount of IL, wherein the microemulsion forms spontaneously with the highest stability.[15]

The nitration of phenol is a fundamental unit process of great industrial importance generating commercially valuable intermediates and there is a great need for regioselective pollution free processes. In earlier work on nitration of phenol in microemulsion, it was claimed that in an AOT [sodium bis(2-ethylhexyl)sulfosuccinate]-based microemulsion, ortho nitration was favoured.[16] This was explained as being due to the phenol orienting at the interface with the aromatic ring extending into the organic domain and the hydroxyl group protruding into the aqueous domain. This orientation would make the ortho positions more accessible than the para position to the approaching nitronium ion. However, we have not been able to reproduce these results. A survey of literature shows nitration of phenol lacks positional selectivity for para isomer with majority of processes giving rise to o-isomer as the major product along with minor amounts of p-isomer. Among several nitrating agents employed which include mixed acid, super acids, acyl nitrates and a variety of metal nitrates under different conditions, ferric nitrate in particular either alone or supported on solid matrices such as clays has enjoyed considerable importance.[17, 18] Herein, we formulated the non-aqueous microemulsions using cetyltrimethylammonium bromide (CTAB) as cationic surfactant and n-octanol as cosurfactant in *n*-decane with 1-ethyl-3-propylbenzimidazolium bromide ([EPbim][Br]) as a water-substitute and finally, utilized as reaction media for

regioselective nitration of substituted phenol using nontoxic and inexpensive ferric nitrate. The current studies can help to understand the microstructure of IL microemulsions and thus establish a better way of using them as a new reaction medium.

IV.B.Results and discussions

IV.B.1.Distribution of 1-octanol for the formation of stable and spontaneous IL-in-oil microemulsion

CTAB requires the presence of a cosurfactant, typically a medium chain alcohol, in order to form a stable microemulsion.[22] In IL/O microemulsion system, CTAB are considered to populate at the oil/water interface in partial association with the cosurfactant (1-octanol). On the other hand, 1-octanol further distributes between the interface and the bulk oil, because of the negligible solubility of higher chain length cosurfactant in water.[23] Thus, at a fixed [surfactant(s)], a critical concentration of 1-octanol is required for the stabilization of the IL-based microemulsions. To estimate how much amount of (in moles) 1-octanol is distributed in the interface and oil phase for formation of a stable microemulsion, we perform a simple titrimetric technique (known as the dilution method).[24] The method of dilution is a very simple but informative technique which can derive many useful parameters for the formation of IL-in-oil microemulsions.[25] In this method, by the alternate stabilization and destabilization with the successive addition of cosurfactant and oil, one can obtain the partition coefficient of 1-octanol between oil and IL interface. By suitably analyzing the distribution constant in the form of different standard thermodynamic equations, the corresponding thermodynamic parameters for the formation process can easily be evaluated.[26, 27] However, similar studies involving ILs as polar component instead of water are not common in literature. Thus the dilution studies involving the evaluation of interfacial behaviour, thermodynamic and structural parameters of IL-in-oil microemulsion are considered to be significant. The basic mathematical formalism to determine the thermodynamics of microemulsion formation and evaluation of structural parameters for the presently studied IL -in-oil microemulsion systems can be found in earlier reports.[26-28]

In the present report, this method is used for the estimation of different parameters concerning to the formation of IL-in-oil microemulsion at 358 K with varying molar ratio of IL to surfactant, R (= 1→5). The following equations are helpful to rationalize the

distribution vis-à-vis transfer process of 1-octanol from the continuous oil phase to the interfacial region:

$$k_o = \frac{n_a^o}{n_o} \tag{2}$$

$$\frac{n_a}{n_s} = \frac{n_a^i}{n_s} + k_o \frac{n_o}{n_s} \tag{3}$$

$$K_d = \frac{X_a^i}{X_a^o} = \frac{\frac{n_a^i}{n_a^i + n_s}}{\frac{n_a^o}{n_a^o + n_o}} = \frac{n_a^i (n_a^o + n_o)}{n_a^o (n_a^i + n_s)} \tag{4}$$

$$\Delta G_t^0 = -RT ln K_d = -RT ln \frac{X_a^i}{X_a^o} = -RT ln \frac{I(1+S)}{S(1+I)} \tag{5}$$

Where, n_a, n_a^i and Gibbs free energy of transfer of cosurfactant from oil to interface ($-\Delta G^0_t$), n_a^o, n_o, n_s denote the total number of moles of cosurfactant, its number at the interface, in the oil phase, the total number of moles of oil and the total number of moles of surfactant, respectively. A plot of n_a/n_s against n_o/n_s at different R (Fig. 1A) according to equation (3) yields the values of the slope (*S*) and the intercept (*I*). Slope (*S*) is actually k_o and n_a^o can be determined from equation (2). On the other hand, n_a^i can be calculated from the intercept (*I*), which is equal to n_a^i/n_s. The partition of cosurfactant between the continuous oil phase and the interface of the droplet can be expressed in terms of the distribution constant, which is represented by K_d. The values of X_a^i and X_a^o are the mole fraction of cosurfactant in the interfacial layer and in the oil, respectively. It is evident from Fig. 1B that n_a^i or n_a^i/n_s values increase with increase in R for all these systems. This indicates that with the increase in IL content, more n_a^i are required for the formation of stable IL-in-oil microemulsion systems at constant temperature. With increasing IL content, in turn, the interfacial areas are extended (which has been calculated in subsequent section with the help of droplet diameter measured by DLS), and the requirement of cosurfactant at the interface to stabilize the droplets is gradually increased. In other words, hydrophilic property of the system is strengthened as R increases. Therefore, more cosurfactant is needed to adjust the hydrophile-lipophile balance of the microemulsion, resulting in the increase in n_a^i values.[29] Similar behaviour was reported for [bmim][BF_4]/Brij-35/1-butanol/toluene[30] and [bmim][BF_4]/[C_{12}mim]Br/pentan-1-ol/octane microemulsions.[29]

The ΔG^0_t values for all studied compositions are negative, and hence, spontaneous formation of IL-in-oil microemulsion is suggested at 358 K. It is also evident from Fig. 1B that the values of $-\Delta G^0_t$, which is indicative of spontaneity of the cosurfactant transfer process (1-octanol$_{oil}$→1-octanol$_{int}$), decrease with increasing R (= 1→5) for the studied systems. In other

words, association between surfactant and cosurfactant molecules at the interface becomes less favorable with increase in ω. This type of variation was reported by Hait et al., [27] Zheng et al.[24] and Paul et al.[28] for water-in-oil microemuslion. From comparative study, the $-\Delta G^0_t$ values obtained for the present system are comparable with those reported for [bmim][BF_4]/[C_{12}mim]Br/pentan-1-ol/octane IL-in-oil microemulsions;[29] however, are higher than [bmim][BF_4]/Brij-35/1-butanol/toluene,[30] [bmim][BF_4]/CTAB/alkanol (ethanol, 1-propanol, 1-butanol)/toluene[31] and [bmim]methanesulfonate±water/(Tween-20+n-pentanol)/n-heptane microemulsion systems.[20] Thus, the present system possesses a relatively better thermodynamic stability at higher temperature.

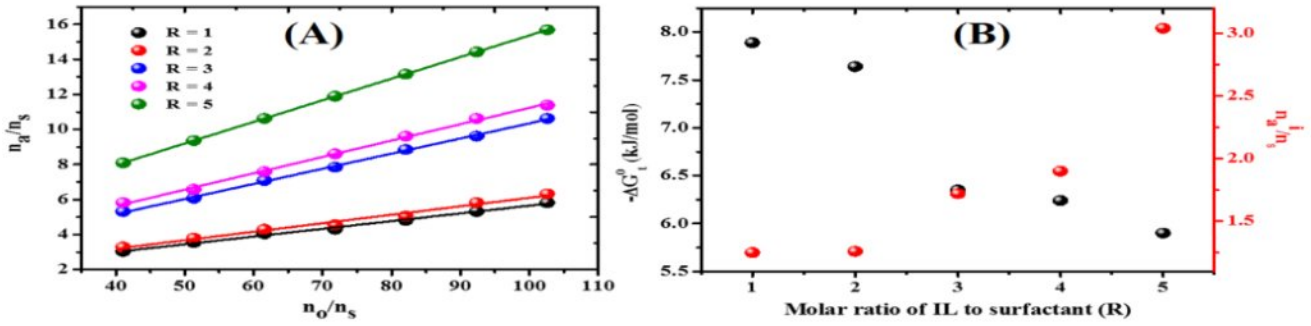

Figure-IV.1. (A) Plot of n_a/n_s vs. n_o/n_s at varied molar ratio of IL to surfactant (R); **(B)** Plots of ΔG^0_t and interfacial composition (n_a^i/n_s) as a function of R for IL/CTAB/1-octanol/decane microemulsion system at fixed temperature of 358K.

IV.B.2.Energetic parameters for IL/O microemulsion reveals organized oil/water interface along with temperature-independent formulation at a critical R

The thermodynamic studies on the formation behaviour of IL-in-oil (IL/O) microemulsions and the energetics of the interaction of the components are comparatively rare. Extensive knowledge on formation of IL/O microemulsions and their internal structures and particle aggregation, are of very much significant for their preparation, application, and use. However, the knowledge of their internal arrangement, structure, and interaction needs augmentation through thermodynamic studies. The complex nature of microemulsions has

restricted rapid growth of the thermodynamic viewpoint, which has not been sufficiently explored.[32] In this section, analysis of energetic parameters of the transfer of 1-octanol from decane to the IL-oil interface of CTAB microemulsion at higher temperature range (358→370 K) is presented in detail, which is not reported earlier. However, such reports for IL/O microemulsions at the temperature range of 293 K to 323 K are available in literature, which were recently reviewed by our group.[33]

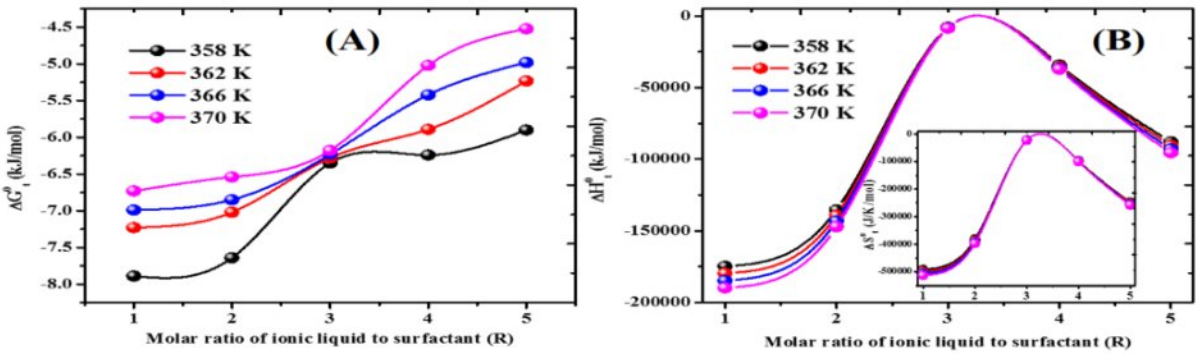

Figure-IV.2. (A) Plots of ΔG^0_t and (B) ΔH^0_t (inset: ΔS^0_t) as a function of molar ratio of IL to surfactant for IL/CTAB/1-octanol/decane microemulsion system at four different temperatures (358→370 K).

The following equations are helpful to rationalize the temperature dependent energetic parameters transfer process of cosurfactant (herein, 1-octanol) from the continuous oil phase to the interfacial region for stabilization of IL-droplets: the ΔH^0_t (standard enthalpy change of transfer process) can be evaluated by the van't Hoff equation. Thus,

$$\left[\frac{\partial\left(\frac{\Delta G^0_t}{T}\right)}{\partial\left(\frac{1}{T}\right)}\right]_p = \Delta H^0_t \qquad (6)$$

Since the dependencies of $(\Delta G^0_t/T)$ on $(1/T)$ are nonlinear for all these systems (plots are shown for brevity), a two-degree polynomial equation of following form is used.

$$\left(\frac{\Delta G^0_t}{T}\right) = A + B_1\left(\frac{1}{T}\right) + B_2\left(\frac{1}{T}\right)^2 \qquad (7)$$

The differential form of the relation helps to evaluate ΔH^0_t. Thus,

$$\left[\frac{\partial\left(\frac{\Delta G_t^0}{T}\right)}{\partial\left(\frac{1}{T}\right)}\right]_p = B_1 + 2B_2\left(\frac{1}{T}\right) = \Delta H_t^0 \quad (8)$$

Where, A, B_1 and B_2 are the polynomial coefficients. Then the Gibbs-Helmholtz equation is used to evaluate ΔS^0_t (standard entropy change of transfer process),

$$\Delta S_t^0 = \frac{\left(\Delta H_t^0 - \Delta G_t^0\right)}{T} \quad (9)$$

The standard state herein considered is the hypothetical ideal state of the unit mole fraction. The dependence of ΔG^0_t along with ΔH^0_t and ΔS^0_t as a function of IL content (R) at four different temperatures are illustrated in Figure-IV.2A and 2B. The negative ΔG^0_t value at all elevated temperatures implies that the successful formulation of "high-temperature stable IL/O microemulsions" due to spontaneous transfer of 1-octanol from the oil phase to the interfacial region. For all systems, the absolute values of ΔG^0_t decrease with increase in temperature. Hence, the formation of microemulsion was less favorable with increase in temperature, which indicates a weaker interaction between surfactant and cosurfactant at the interface at higher temperature, which corroborated well with the degree of spontaneity of the transfer process. The reduced spontaneity at elevated temperature was earlier reported for microemulsions with the oil isopropylmyristate (IPM), stabilized by trihexyl (tetradecyl) phosphonium bis 2,4,4-(trimethylpentyl)phosphinate (surfactant) + isopropanol (IP as a co-surfactant) like the triisobutyl (methyl)phosphonium tosylate/IPM/(IL-2+IP) system.[34] Further, overall transfer process is found to be exothermic in nature at all experimental temperatures along with negative entropy change with progressive addition of IL. So, 1-octanol causes release of heat during the cosurfactant transfer process. Consequently, the negative entropy change is due to more organization of the interface and its surroundings inside the IL/O droplets. Dissolution of IL into amphiphile-Dc medium can be modelled as consisting of four major processes: (i) endothermic dispersion of IL, (ii) endothermic penetration of IL in the interior of IL/O microemulsions (aggregates), (iii) exothermic reorganization of the amphiphiles at the oil /IL interface, and (iv) exothermic organization of the penetrated IL. The total heat shows exothermicity, which means that the sum of the contributions of processes one and two are, therefore, lower than those of three and four. Such negative standard enthalpy and entropy changes for w/o microemulsions stabilized by cationic cetyltrimethylammonium-based surfactant and 1-octanol were also reported in

literatures.[35,36] However from comparative study, it can be concluded that 1-octanol/cetyltrimethylammonium-based w/o systems showed much lower free energy of formation than currently studied IL/O systems even at much higher temperatures.[35]

An interesting feature reveals from Fig. 3B and its inset that both ΔH^0_t and ΔS^0_t values decrease with increase in temperature for all these systems. In other words, the transfer process (1-octanol$_{oil}$→1-octanol$_{int}$) changes from less exothermic to more exothermic with increase in temperature. It can be argued that the degree of hydrogen bonding of water around the surfactant molecules decreases with increase in temperature, and therefore, the energy required to break it diminishes i.e., ΔH^0_t decreases with increase in temperature.[37] Subsequently, variation of ΔS^0_t values with increase in temperature can be rationalized as follows: as temperature increases, the extensive hydrogen bonding in ion pair of IL molecules gradually breaks down; affecting the importance of the entropic term due to decrease in IL-hydration around the head group of surfactant.[37] It is also interesting to note that both $-\Delta H^0_t$ and $-\Delta S^0_t$ values increase with increase in IL content (R) before reaching a maximum at R = 3 and after that they gradually decrease at higher IL content. Most importantly, the enthalpic processes are quantitatively identical at the maximum, i.e., at R = 3; which indicates that the transfer events of cosurfactant from oil to the interface are physicochemically same and isenthalpic at R = 3. The mixing fraction at the interface is not greatly changed in ionic surfactant-cosurfactant systems with increasing temperature. However, the monomeric solubility of cosurfactant in oil increases monotonically in the ionic surfactant systems. In order to attain a temperature-insensitive microemulsion, the monomeric solubility of cosurfactant in oil has to be reduced by using an appropriate cosurfactant.[38] Earlier, Maiti et al. reported a couple of isenthalpic formulations for cationic w/o microemulsion composed of octadecyltrimethylammonium bromide (C_{18}TAB), n-butanol, and n-heptane.[39]

IV.B.3. Determination of extent single phase microemulsion region

From the application point of view, construction of the phase diagram is a primary task towards a microemulsion formulation. Herein, Figure-IV.3 illustrates the pseudoternary phase diagram of 1-ethyl-3-propylbenzimidazolium bromide ([EPbim][Br])-(CTAB + 1-octanol)-*n*-decane systems at fixed surfactant-cosurfactant ratios (1:4, w/w). The shaded areas under the curves represent the two-phase turbid region, where the stable microemulsions are not formed. The unshaded portions correspond to the microemulsion zone. In the currently

studied systems, oil-rich (IL-in-oil microemulsion), IL-rich (oil-in-IL microemulsion) as well as bicontinuous states are observed. However, for simplicity, all these three different regions are represented as a single phase (microemulsion zone; the unshaded portion in the pseudoternary phase diagram). All further experiments are carried out using the oil-rich (i.e., IL-in-oil) microemulsion systems. The areas under the microemulsion region (unshaded portion) and the turbid regions are calculated by simply weighing the individual areas. Similar type of phase characteristic is also reported by Zech et al. for dodecane/ ([C_{16}mim][Cl]/decanol at 1:4, w/w)/ethylammonium nitrate (EAN) microemulsion.[40]

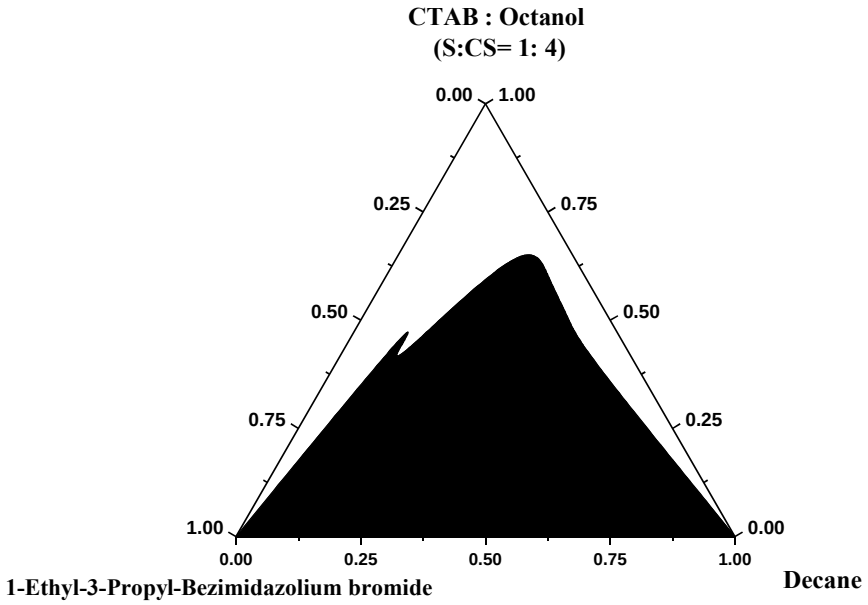

Figure-IV.3. The pseudoternary phase diagram of IL/CTAB/1-octanol/decane microemulsion system at fixed surfactant-cosurfactant ratio (1:4, w/w) and temperature (358K).

IV.B.4.Anomalous behaviour of aggregated droplet size as a function of IL content (R)

DLS is used to assess whether the ILs are encapsulated by the surfactant to create microemulsions media, because it is a powerful technique to evaluate the formation of these new organized systems. To identify and characterize the [EPbim][Br]/oil microemulsions formed by CTAB/1-octanol (1:4,w/w), the size of the aggregates formed is investigated as a function of [EPbim][Br] content (i.e., molar ratio of IL to surfactant, R) using DLS technique. Variation in the diameter of IL-in-oil microemulsion with the volume fraction of the IL (R) at

360 K is presented in Figure-IV.5. Droplets are fairly monodispersed as exemplified from the size distribution plots, which are not shown here for brevity. Earlier reports exhibit how hydrodynamic diameter of IL based reverse micelles stabilized by ionic surfactant increases as R increases. [40-44] However in the present study, it is observed from Figure-IV.5 that the size of microemulsions decreases almost linearly as R increases. Now the question arises why hydrodynamic diameter of CTAB surfactants are decreasing with increasing R? This can be envisaged considering two effects. First, the lowering of size with increasing R can primarily be resulted by poor encapsulation of [EPbim][Br] over the microemulsions. Secondly, lowering of the values of hydrodynamic diameter is a characteristic feature for formation of microemulsions in highly immiscible non-aqueous solvents. [45] For these systems, the polar solvent predominantly stays in microemulsion core instead of locating near the interfacial region of microemulsion. Here, [EPbim][Br] and *n*-decane are immiscible. So, with increasing [EPbim][Br] concentration, more and more [EPbim][Br] molecules are solubilized in microemulsion core instead of staying near the micellar interface. Increasing concentration of [EPbim][Br] leads to more favourable H-bond interaction with polar head group [$N(CH_3)_3^+$] of surfactant, CTAB. So, favourable and strong H-bonding interaction with [EPbim][Br] helps to hold the polar head groups much near to the micellar core. This fact is manifested by the lowering of hydrodynamic diameter of the microemulsions.[45] Earlier, Ghosh noticed similar behaviour for non-aqueous reverse micelles of Brij surfactants prepared in benzene and EAN.[46]

IV.B.5. Geometrical model for the determination of aggregation number and surfactant interfacial molecular area

The efficient use of newly formulated microemulsions requires a sound knowledge of the basic physicochemical properties of the specific system. For example, in order to model the distribution of various chemical species within the system, parameters such as droplet size, aggregation number, and surfactant molecular interfacial area must be known.[47] Recent work of Lemyre and coworkers confirmed that hydrodynamic diameter of reverse micelles is in direct proportion with aggregation number.[47] According to them, the relationship between hydrodynamic diameter (D_h) and aggregation number (N_{agg}) for IL-in-oil microemulsions can be expressed using the following equation,

$$\frac{D_h}{2} = \left[\frac{3N_{agg}}{4\pi}\left(\frac{V_{IL,total}}{n_{surf,in\,MEs}} + V_S\right)\right]^{\frac{1}{3}} \qquad (6)$$

Where, $V_{IL,total}$, $n_{surf,\ in\ MEs}$, and V_s are the total volume of water, number of surfactant molecules in microemulsions (MEs) and molecular volumes of surfactant(s), respectively. This equation is based on a model assuming the micelles as a compact sphere and neglects presence of any polar solvent molecules between the surfactant hydrophobic tails which would be the ideal case if two perfectly immiscible solvents are used. Molecular volume of CTAB (V_{CTAB}) can be calculated as,

$$V_{CTAB} = (V_{tail} + V_{head}) \quad (7)$$

Where, V_{tail} and V_{head} are the molecular volume of hydrocarbon chain and polar head of CTAB. V_{head} of CTAB has been determined from head group area of CTAB,[27] whereas V_{tail} can be expressed as,

$$V_{tail} = V_{CH3} - (16 - 1)V_{CH2} \quad (8)$$

Group molar volumes (i.e. V_{CH3}, and V_{CH2}) used for the estimation of molecular volume of CTAB are taken from Preu et al.[48] A representative plot of N_{agg} as a function of R (i.e., [IL]/[CTAB]) for these systems is depicted in inset of Fig. 4A. Therefore, as hydrodynamic diameter decreases with increasing R, aggregation number also decreases. Since surfactant concentration is fixed, a decrease in aggregation number with R is indicative of an increase in the number of IL droplets which provides additional support to the decreased droplet size as evidenced from DLS measurements.

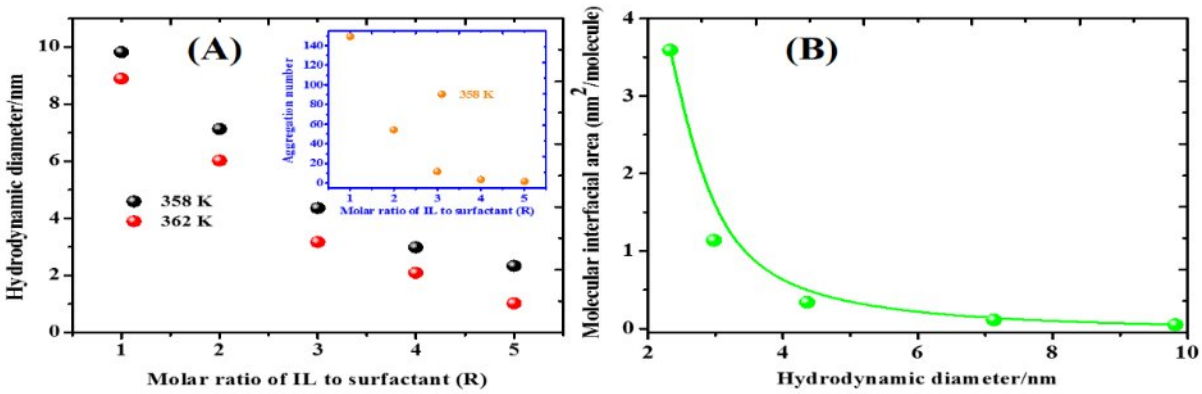

Figure-IV.4. (A) Variation in the hydrodynamic diameter with the molar ratio of IL to surfactant (R) at two different temperatures (358 and 362 K), and (B) Variation of molecular interfacial area of the surfactant as a function of hydrodynamic diameter for IL/CTAB/1-octanol/decane microemulsion system.

Once the micellar composition has been established, equation (9) can be used to determine the molecular interfacial area of the surfactant if the volume occupied by the hydrophilic part of a surfactant molecule ($V_{surf,\ hydrophilic}$ or V_{head}) and the effective length of the hydrophobic chain of the surfactant ($l_{hydrophobe}$) are known. This leads to following equation; [47]

$$\frac{D_h}{2} = \frac{3}{\sigma}\left(\frac{V_{IL,total}}{n_{surf,\in MEs}} + V_{surf,hydrophilic}\right) + l_{hydrophobe} \qquad (9)$$

Where, σ is the surfactant molecular interfacial area and $l_{hydrophobe}$ can be estimated from Tanford's formula [49] for the maximum extension of the alkyl chain of surfactant. The molecular interfacial area of the surfactant is plotted in Figure-4.B as a function of droplet size. It is clearly evident that, the interfacial area is not constant. A limiting value is reached for droplet size larger than 5 nm, but the interfacial area increases sharply with increasing IL content (R) and decreasing droplet size. The primary reason for the variation of the molecular interfacial area is the dependence of the conformation of the anchored surfactant chains on the radius of curvature.[47] The variation of these parameters with droplet size of microemulsion indicates that the decrease in thermodynamic stability (as evidenced from dilution method) with decreasing size can be attributed to the steric confinement of the hydrophilic quaternary ammonium chain of CTAB and 1-ethyl-3-propylbenzimidazolium cation ($[EPbim]^+$) of IL.

IV.B.6.Nitration of aromatic compounds in IL/O microemulsion offers regioselectivity

A nitration reaction was performed in the cationic surfactant-based IL/O microemulsion system with three different aromatic compounds and the ortho-to-para ratio was examined. The results are summarized in Table-IV.1. The corresponding conversion observed for the nitration of phenol at the end of 15 min was 81% for the para isomer and 19% for the ortho isomer.

Scheme-IV.1. Pictorial representation of the nitration reaction in IL/CTAB/1-octanol/decane microemulsion system.

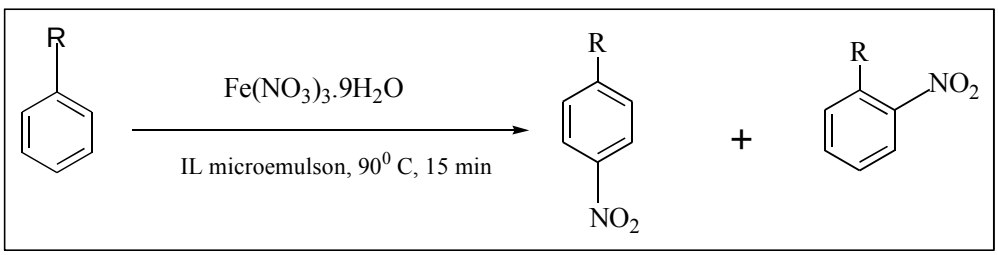

Table-IV.1. Regioselectivity in product obtained from nitration reaction in IL/CTAB/1-octanol/decane microemulsion system.

Entry	Reactant	Reaction Yield (%)	
		Ortho	Para
1.	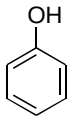 [Phenol]	19	81
2.	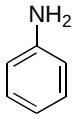 [Aniline]	23	77
3.	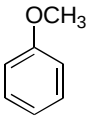 [Anisole]	30	70

Mechanistically, we proposed that in situ formation of nitronium ions is a major factor for effective nitration of aromatic compounds with ferric nitrate.[50] An efficient electrophilic substitution reaction of aromatic compounds, specially phenols, anilines and anisole with ferric nitrate as the nitrating agent in reverse micelle has been developed. As can be seen from Table-IV.1, the cationic surfactant-based microemulsion favours para substitution, i.e., regioselectivity. The para-directing effect is stronger for the phenols than for the others. It is supposed that the para-directing effect is due to an attractive interaction between the aromatic ring and the cationic headgroup of the surfactant.[18] The positively charged surfactant headgroup interacts with the electron-rich face of the aromatic ring. Because of the electronegative side of the substance, the electron cloud of the aromatic ring is pulled towards these groups. In order to obtain optimal matching of the charges, the ring will be positioned so that the cationic surfactant headgroup is closer to the ortho positions than to the para position. This will make the approach by the positively charged attacking species, the nitronium ion, more favourable at the para position than at the ortho position. The reactions went to completion in around 15 min. It is noteworthy that the reactions proceeded fast in the microemulsions despite the fact that the surfactant used carried the same charge as the

reacting nitronium ion. Evidently, the positive effect of the large oil–IL interface dominates over the charge repulsion between the surfactant head groups and the attacking nitronium ion.

IV.C. Materials and Methods

IV.C.1. Materials Cetyltrimethylammonium bromide, CTAB (≥ 99%, CAS No. 57-09-0, *Sigma*), 1-octanol (anhydrous, ≥99%, CAS No. 111-87-5, *Sigma-Aldrich*) and decane (anhydrous, ≥ 99%, CAS No. 124-18-5, *Sigma-Aldrich*) were used without further purification.

IV.C.2. Methods

IV.C.2.1. Synthesis of ILs The IL, 1-ethyl-3-propylbenzimidazolium bromide ([EPbim][Br]), is synthesized in accordance with our reported method.[19] It is important to note that the synthesized pure IL ([EPbim][Br]) is white solid at room temperature[19] and it melts around 359 K. In order to make non-aqueous IL based microheterogeneous system, all the studies are carried out at the high temperature. Nevertheless, the solubility of CTAB in the *n*-decane/1-octanol mixture is improved drastically by increasing the temperature to 360 K. This is also the reason for the necessity of tempering the system for getting optically clear solutions of IL based non-aqueous microemulsion. However, these effects can principally not be assigned to electrostatic interactions, which are most of all temperature independent in ionic surfactant-based microemulsions in contrast to non-ionic-based ones.

IV.C.2.2.Construction of phase diagram of ternary surfactant, oil and IL system The pseudoternary phase diagram comprising oil (*n*-decane/Dc), benzimidazolium IL (1-ethyl-3-propylbenzimidazolium bromide, [EPbim][Br]), cationic surfactant (CTAB), and cosurfactant (1-octanol/1-On) has been constructed by the method of titration and direct observation. In a typical experiment, mixtures of oil and surfactant (including the cosurfactant) with varying mass ratios of 4:1 are prepared in a series of stoppered test tubes. To construct the pseudoternary phase diagrams for the IL based "water-free" microemulsions, the samples are placed in a thermostatic water bath at (360 ± 0.5) K for 10 min, and then the mixture is titrated by IL under moderate agitation. The IL volumes causing the solutions to turn to turbid from clear transparent are noted to determine the phase boundaries. In each plotted phase diagram, the upper part of the phase boundary represents a single-phase region (microemulsion, 1ϕ), and the lower part is a multiphase region (2ϕ). The compositions in the phase diagrams are represented in weight fractions. The same procedure was repeated for 2 to

3 times for each mixture, and an average of these results was taken for the construction of phase diagrams.

IV.C.2.3.Dilution method study for estimation of interfacial composition and spontaneity of formation of microemulsion

In the dilution experiments, 0.00025 mole of surfactant (CTAB) is placed in a dry test tube, followed by addition of fixed 2 ml of *n*-decane and different amount of [EPbim][Br] (at different molar ratio of [EPbim][Br] to surfactant R = 1→5), respectively. The sample is placed in a thermostated water bath, stirred constantly with a magnetic stirrer, and kept covered to prevent loss due to evaporation. The cosurfactant (1-octanol) is then added slowly from an auto pipette to the initially viscous and turbid mixture until the solution becomes clear, which is indicative of the formation of the single phase. Sufficient time is given for equilibrium and then the volume of cosurfactant is noted at that point. A known but small volume of oil is again added to the system to destabilize it. A cloudy sample is made just clear by the addition of cosurfactant. The quantity of cosurfactant is recorded. The experiment is monitored at fixed temperature of 360 K. The entire experiment is then repeated for a second time to ensure accuracy, and the average values obtained are used for data processing and analysis. In order to estimate various thermodynamic parameters for the formation of IL-in-oil microemulsion, the above-mentioned experiment is carried out at three other temperatures, such as 365, 370 and 375 K.

IV.C.2.4. Dynamic light scattering (DLS) studies DLS measurements are carried out using a Zetasizer Nano ZS90 (ZEN3690, Malvern Instruments Ltd, U.K.). A 2.5 mmol of CTAB mixed with appropriate amount of 1-octanol dissolved in 2ml of *n*-decane is used for such studies. The same set of CTAB/1-octanol ratio (w/w), as used for the construction of phase diagram is employed for droplet size analysis at 360 K. Samples are filtered thrice before each measurement using Milipore^{TM} hydrophobic membrane filter of 0.25 μm pore size to remove possible dust particles. A He–Ne laser operating at a wavelength of 632.8 nm was used and the data were collected at a 90^0 angle. Temperature is controlled to within ±0.05 K using a built-in Peltier heating-cooling device. Hydrodynamic diameter (D_h) of the microemulsion solutions is estimated from the intensity autocorrelation function of the time-dependent fluctuation in intensity. According to Stokes-Einstein equation, D_h is defined as [20, 21]:

$$D = {kT}/{3\pi\eta D_h} \quad (1)$$

Where, k, T, D and η indicate the Boltzmann constant, temperature, diffusion coefficient and viscosity of the solvent (herein *n*-decane) respectively. To check the reproducibility of the results at least 6 measurements are performed.

IV.C.2.5. General procedure for nitration reaction

Fe $(NO_3)_3.9H_2O$ (0.5 mmol) and the substrate (1 mmol) were placed in a 10 mL round bottom flask containing the IL-in-Oil microemulsion (3 ml). The mixture was placed on a magnetic stirrer at 90^0 C and stirring continued for 15 min. Then the reaction mixture was diluted with water and extracted with dichloromethane (3 x 10 mL). The combined organic layer was dried over anhydrous Na_2SO_4 and concentrated under reduced pressure. The crude residue was purified by silica gel column chromatography using the mixture of petroleum ether and ethyl acetate as eluent.

IV.D. Summary

Present study is focused on the formulation and characterization of a high-temperature stable quaternary IL-in-oil microemulsions comprising of IL ([EpBzim]Br), CTAB, 1-On and Dc with a detailed description of the interfacial composition and energetic parameters for the transfer of 1-On from bulk oil phase to the interface as a function of system composition and temperatures. Additionally, nitration reaction of some aromatic compound has been performed in the IL/O microemulsion. The reaction ends up with the highest regioselectivity of para isomer. The confinement of IL imparts the regioselectivity on the nitrated product.

IV.E. References

References are given in BIBLIOGRAPHY under Chapter IV (pp. 111-113).

CHAPTER-V

Synergistic Interaction of Surfactant Blends in Aqueous Medium Reciprocates in Non-polar Medium with Improved Efficacy as Nanoreactor

V.A. Introduction

In recent years, the study of the physicochemical properties of mixed surfactant systems turns out to be a topic of interest in the area of self-assembly molecular systems.[1] Organized assemblies *viz.* micelles and microemulsions,[2] based on mixed surfactants offers substantial alteration in solubilization behaviour, enzyme kinetics, nanoparticle synthesis and chemical activity.[3-7] The interaction between surfactants in mixtures produces marked interfacial effects due to changes in adsorption as well as in the charge density of the surface.[8-12] In most cases different types of surfactants are mixed for synergistic performance and it is utilized to reduce the total amount of surfactant used in particular applications for reduction of cost and environment impact.[13,14] However, a proper justification of such modified mixing behaviour is still demands and needs a more generalized approach to optimize the mixing stoichiometry in order to yield the maximum effect. Research to date includes numerous attempts to explore combined physicochemical studies of micro-heterogeneous assemblies with interest not only in elemental aspects but also in their wide applications.[15]

The Heck reaction,[16,17] now-a-days, receives much interest in recent years as it offers a versatile process for the generation of new carbon-carbon bonds,[18] and holds much more promise in many industrial processes, especially in the synthesis of fine chemicals and active pharmaceutical intermediates.[19] In view of current economic and environmental fate, continuous efforts are now being made to develop new templates for carrying out the Heck reaction. One approach is to consider inexpensive amphiphiles as potential additives that upon self-assembly into micelles, accommodate otherwise insoluble organic substrates and catalysts within the lipophilic cores.[20] Further, microemulsions might be another, much cheaper with more potentially universal approach to this problem, based on the well-known solubilization phenomena.[21] Very recently, Heck reaction has been successfully performed in water/cetyltrimethylammonium bromide (CTAB)/1-propanol/1-dodecane based oil-in-water (o/w) microemulsion and two phase region as well at 353K.[22]

These findings driven us to extend the use of micelle as well as water-in-oil (w/o) microemulsion based on mixed cationic/non-ionic surfactants as a chemical reaction media for the Heck reaction at ambient temperature. To fulfill this objective, a comprehensive behaviour of the formation and physicochemical properties of micellization and microemulsion blends of CTAB and polyoxyethylene (20) cetyl ether ($C_{16}E_{20}$) including individual constituent is carried out. The structural features of these systems are investigated via interfacial and bulk routes by employing tensiometry, conductometry and also, by zeta potential, viscosity, dynamic light scattering (DLS), fluorescence lifetime, Fourier transform infrared spectroscopy (FTIR), and field emission scanning electron microscopy (FESEM) measurements. The choice of surfactants in this study is not arbitrary. Although the literature is dominated by studies of microemulsions formed with anionic, sodium bis(2-ethylhexyl) sulfosuccinate (AOT), there is interest in microemulsions formed with other surfactants, particularly cationic CTAB. CTAB is of increasing interest because the head group is a good model for the lipid, phosphatidylcholine.[23] Further, commercially available non-ionic surfactants such as Brijs are extensively used in pharmaceutical formulations as solubilizers and emulsifiers to improve dissolution and absorption of poorly soluble drugs.[24] Heptane (Hp) and decane (Dc) were used as oil and 1-pentanol (Pn) was used as cosurfactant. After careful evaluation of various physicochemical and thermodynamic parameters, a model C-C cross coupling reaction (Heck reaction) is performed between n-butylacrylate and 4-iodo-toluene in presence of palladium acetate and triethylamine, TEA (base) in mixed surfactant based micellar and w/o microemulsion media. To provide proper explanation of this study, we also perform the Heck reaction in media of individual constituents, which are used for the formation of these organized systems. An attempt is also made to rationalize the yield of the Heck products from the viewpoints of physicochemical and thermodynamic parameters of their formation during the course of the reaction. It is believed that the findings of this study are expected to improve the basic understanding of the formation, characterization and application of mixed micelles and w/o microemulsions.

V.B. Results and Discussion

Before going to discuss about the outcome of Heck reaction in micellar or microemulsion medium, first we emphasize on the formation of single and mixed micellar and microemulsion systems from the thermodynamic point of view and their microstructural, microenvironmental and morphological characteristics and also, interaction between the

constituents. In view of this, we divide this section in four parts; where first part of this section contains summary of formation and characterization of micellar systems in single and mixed surfactants both by experimentally and theoretically. In the second part, reaction site and yields of the Heck reaction are rationalized in terms of the interaction parameter, and Gibbs free energy of micellization. Further, the formation and microstructural characteristics of mixed microemulsions along with yields and possible location of reaction at oil/water interface are discussed in last two parts. Finally, a comparative result of reaction yield has been provided between mixed micellar and microemulsion systems along with individual constituents.

V.B.1. Formation and Characterization of Single and Mixed Micelles

The amphiphilic behaviour in terms of critical micellar concentration (CMC) of pure CTAB, $C_{16}E_{20}$ and their mixture at equimolar composition (1:1) in water is determined from the sharp inflection point in the surface tension (γ) against log [surfactant] and specific conductivity against [surfactant] plots at 303 K as shown in Figure-V.1A and B.

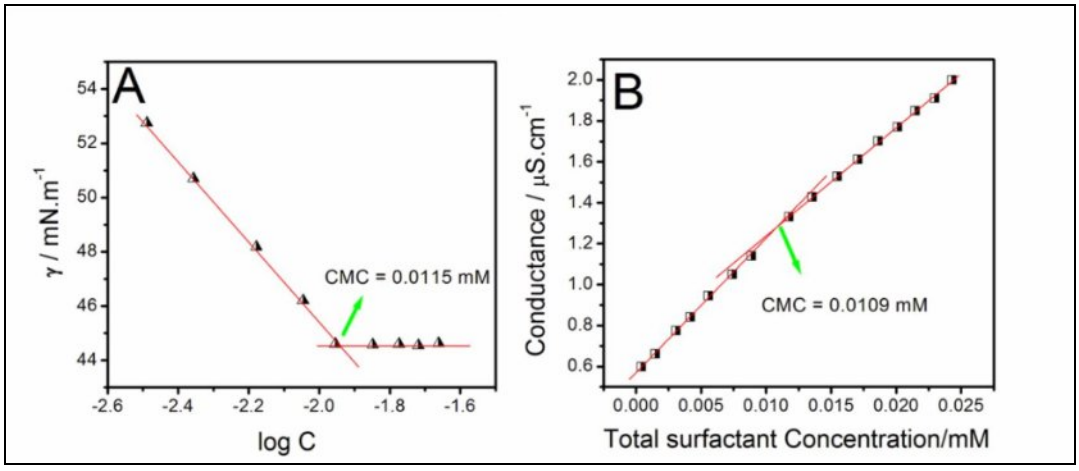

Figure-V.1. Tensiometric **(A)** and Conductometric **(B)** determination of CMC of mixed aqueous CTAB/$C_{16}E_{20}$ systems at equimolar composition at 303K.

Further, a representative illustration of CMC for aqueous $C_{16}E_{20}$ system is presented in Figure-D.S1(Appendix D). The CMC values of these systems are also presented in Table-D.S1 (Appendix D). Lower CMC for CTAB/$C_{16}E_{20}$ mixtures compared to pure CTAB attributes to the formation of a pseudo-double chain complex arising from the strong electrostatic interaction between the quaternary ammonium cationic segment (CTA^+) and the POE of $C_{16}E_{20}$. In addition, there also exists an enhanced hydrophobic interaction between

the hydrocarbon chains, which favours formation of the mixed micelle and decreases the CMC.[27]

For ideal mixing of cationic-non-ionic surfactant systems, CMC values have been calculated using the Clint equation,[28]

$$^{1}/_{CMC_{ideal}} = {}^{\alpha_1}/_{CMC_1} + {}^{\alpha_2}/_{CMC_2} \quad (2)$$

Where, α_1 and α_2 are the stoichiometric mole fractions of CTAB and $C_{16}E_{20}$, respectively. For the mixed systems, lower experimental CMC values (CMC_{12}) than those expected from Clint's equation are obtained (Table-D. S1). This observation indicates non-ideal behaviour of aqueous solution and also, demonstrates favourable synergism between the constituent surfactants in mixed micelles.

The nature and strength of interactions between the CTAB and $C_{16}E_{20}$ molecules in the mixed micelles are evaluated from the interaction parameter by employing Rubingh's approach, based on regular solution theory,[29]

$$\frac{[(X_1^m)^2 \ln(CMC_{12}\alpha_1/CMC_1X_1^m)]}{(1-X_1^m)^2 \ln[CMC_{12}(1-\alpha_1)/CMC_2(1-X_1^m)]} = 1 \quad (3)$$

Where, X_1^m is the micellar mole fraction of the CTAB incorporated in the mixed micelle. The interaction parameter, β^m is an indicator of the degree of interaction between two surfactants in mixed micelles and accounts for deviation from ideality, which is given by;[29]

$$\beta^m = [\ln(CMC_{12}\alpha_1/CMC_1X_1^m)]/(1-X_1^m)^2 \quad (4)$$

For binary system (1:1), β^m values are found to be negative (Table-V.1), which also indicates a synergistic interaction between the component surfactants. According to Rubingh model, the activity coefficient, f_i^m of individual surfactants within the mixed micelles is related to the interaction parameter through the following equations,[29,30]

$$f_1^m = exp[\beta^m(1-X_1^m)^2] \quad (5)$$

$$f_2^m = exp[\beta^m(X_1^m)^2] \quad (6)$$

Where, $f_i^m = 1$ indicates an ideal mixed system.[30] The significance of other terms is discussed earlier. It is seen from Table 1 that both the values of f_1^m and f_2^m are lower than unity, which

indicates the formation of mixed micelles and reflects the non-ideality of a multicomponent mixed system. Further, the maximum surface excess concentration at the air-water interface (Γ_{max}) and the minimum area per surfactant head group adsorbed at the interface (A_{min}) are calculated from the surface tension data by fitting the Gibbs adsorption isotherm,[31]

$$\Gamma_{max} = -\frac{1}{2.303nRT}\left(d\gamma/_{dlogC}\right) \quad (7)$$

$$A_{min} = 10^{18}/\Gamma_{max}N_a \quad (8)$$

Herein, dγ/dlogC is the slope of the plot of γ versus log C (where C represents the concentration of the surfactant). Here, for mixed micelles of cationic/non-ionic surfactants, the value of n (the number of species produced by an amphiphile and whose concentration at the interface varies with the surfactant concentration in the solution) is 3. The values of Γ_{max} and A_{min} are presented in Table 1 and followed the order; $C_{16}E_{20}$ > CTAB > CTAB/$C_{16}E_{20}$ and $C_{16}E_{20}$ < CTAB < CTAB/$C_{16}E_{20}$, respectively. At equimolar composition of mixed CTAB/$C_{16}E_{20}$, minimum Γ_{max} (and thus maximum A_{min}) values are obtained due to the intercalation of POE of $C_{16}E_{20}$ within the positively charged CTAB surfactant molecules which also reduces the repulsion among them.[32] The steric hindrance due to long POE chains of $C_{16}E_{20}$ also causes higher A_{min} values for CTAB/$C_{16}E_{20}$ combinations.[32]

Another parameter that directly proves the effectiveness of surface tension reduction is the surface pressure at the CMC i.e., Π_{CMC}. It indicates the maximum reduction of surface tension caused by the dissolution of the amphiphilic molecules and is usually defined as;

$$\Pi_{CMC} = \gamma_{sol} - \gamma_{CMC} \quad (9)$$

Where γ_{sol} and γ_{cmc} represent surface tensions of pure water, and surfactant solution at CMC, respectively. As per Table 1, the aqueous CTAB-$C_{16}E_{20}$ mixtures display higher values of Π_{CMC} than their individual counterparts in accordance with their higher surface activity as mentioned earlier, although their efficiency to bring about a reduction in the surface tension of water varies only slightly with the mixture composition.[33]

Table-V.1. Interfacial, Thermodynamic and Interaction Parameters of Single and Mixed Surfactants.

(A) Interfacial and Thermodynamic[a] parameters					
System	**T/K**	**$\Pi_{cmc}*10^3$/ N.m^{-1}**	**$10^6\Gamma_{max}$/ mol.m^{-2}**	**A_{min} / nm^2.molecule^{-1}**	**$-\Delta G_m^0$/ kJ.mol^{-1}**	**ΔG_{ads}^0/ kJ.mol^{-1}**
CTAB	303	32.0[b]	1.31[b]	1.27[b]	40.5[b]	64.9[b]
CTAB/$C_{16}E_{20}$	303	34.7	0.86	1.93	71.03	99.74
$C_{16}E_{20}$	303	27.64	2.25	0.7379	39.5	51.78
(B) Interaction[c] parameters for CTAB/$C_{16}E_{20}$ (1:1)					
CMC	**CMC**	**CMC (Avg.)**	**α and g**	**β**	**f_1**	**f_2**
0.0109	0.0115	0.0112	0.829 and 0.171	-4.58[d]	0.0114[c]	0.89[c]

[a] *The average errors in ΔG_m^0 and ΔG_{ads}^0 are ±3%;* [b] Ref;[28] *For interaction parameters;* [c] *CTAB = 1 & $C_{16}E_{20}$ = 2 and* [d] *$C_{16}E_{20}$ = 1 & CTAB = 2.*

The standard free energy of micelle formation per mole monomer unit (ΔG^0_m) for these systems is evaluated from the relation;[34]

$$\Delta G_m^0 = (1+g)RT \ln X_{cmc} \quad (10)$$

where, X_{cmc} and g are the CMC expressed in mole fraction unit and the fraction of counter ions bound to the micelle, respectively. The fraction of counter-ion binding is related to;[34]

$$g = \left(1 - {}^{S_{mic}}/_{S_{mn}}\right) \quad (11)$$

The lower values of g in mixed CTAB/$C_{16}E_{20}$ (i.e., 0.171) compared to pure CTAB micelle (i.e., 0.47) signify lowering of effective surface charge density in the mixed micelles.[35] The

standard free energy of interfacial adsorption (ΔG^0_{ads}) at the air/water interface of micelle is also evaluated from the relation;[36]

$$\Delta G^0_{ad} = \Delta G^0_m - \left(\Pi_{cmc} / \Gamma_{max} \right) \quad (12)$$

The values of ΔG^0_m and ΔG^0_{ads} are represented in Table-V.1. Both ΔG^0_m and ΔG^0_{ads} values are found to be more negative in binary mixture compared to pure micelle, which indicate that the micellization as well as adsorption processes are more favourable compared to the individual surfactant. Further, more negative ΔG^0_{ads} values compared to ΔG^0_m values suggests that the adsorption process is more spontaneous than micelle formation. Micelle formation in the bulk is a secondary process and less spontaneous than interfacial adsorption.[35,37] In order to get more insight on the surface charge and structural characteristics of pure and mixed micelles, we perform zeta potential, DLS, and FESEM measurements, which are dealt in subsequent paragraphs.

It is already established that zeta potential (ζ) is a very good indicator for the interaction and stability of colloidal systems.[38] In view of this, the effect of concentration of the amphiphile(s) on the surface charge of aqueous CTAB, $C_{16}E_{20}$ and CTAB/$C_{16}E_{20}$ systems is investigated by measuring the ζ parameter, which is presented in Figure-V.2(A). The positive ζ value for cationic CTAB increases with increasing concentration of CTAB. However, non-ionic $C_{16}E_{20}$ shows a negative potential, possibly due to the large number of oxygen atoms in POE groups.[39] Interestingly, the ζ values for CTAB/$C_{16}E_{20}$ mixtures are found to be higher than that of single CTAB, which also proves the synergistic interaction between them.[40]

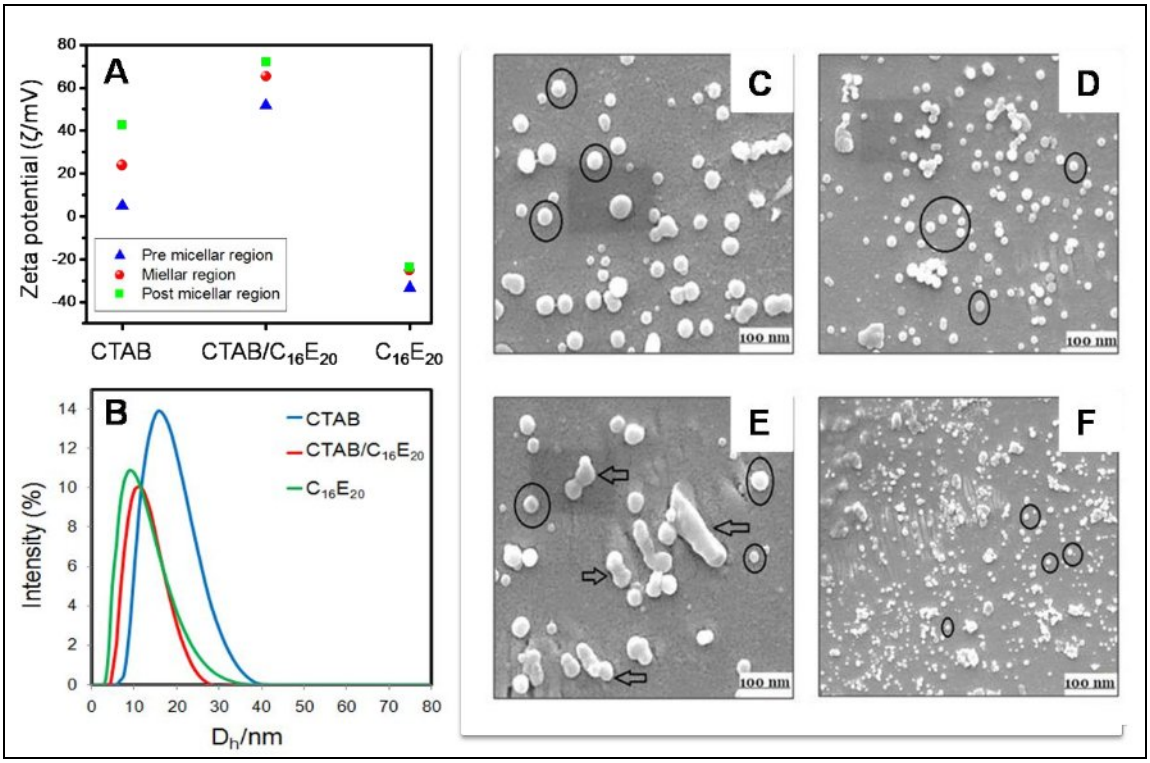

Figure-V.2. (A) Measurement of zeta potential of single and binary (equimolar) surfactants in aqueous medium at 303K. **(B)** Hydrodynamic diameter (D_h) of micellar systems at 303 K. FESEM images of **(C)** CTAB/water and **(D)** CTAB/$C_{16}E_{20}$/water at micellar region, **(E)** CTAB/$C_{16}E_{20}$/water at post-micellar region, and **(F)** $C_{16}E_{20}$/water at micellar region.

The DLS technique is employed to determine the size of the aggregates of CTAB, $C_{16}E_{20}$, and CTAB/$C_{16}E_{20}$ binary system at their corresponding CMCs at 303K and is depicted in Figure-V.2(B). DLS data shows a monomodal size distribution with hydrodynamic diameter (D_h) ranging from ~10-15 nm for all systems. The micellar size is observed to follow the trend; $C_{16}E_{20}$ < CTAB/$C_{16}E_{20}$ < CTAB. The smaller size of $C_{16}E_{20}$ micelles originates from the relatively weaker interactions of $C_{16}E_{20}$ with water in comparison to CTAB.[5,41] Further, the morphology of the four micellar systems is investigated by FESEM technique and illustrated in Figure-V.2C-2F. Uniformly distributed spherical shaped structure is observed for all these systems at micellar region (Figure-V.2C, 2D and 2F), which is indicated by circles in respective figures. Further, Figure-V.2E represents some agglomerated structures (shown by hollow arrows), which consist of two or three single spherical micro-droplets for binary CTAB/$C_{16}E_{20}$ systems at post-micellar region.

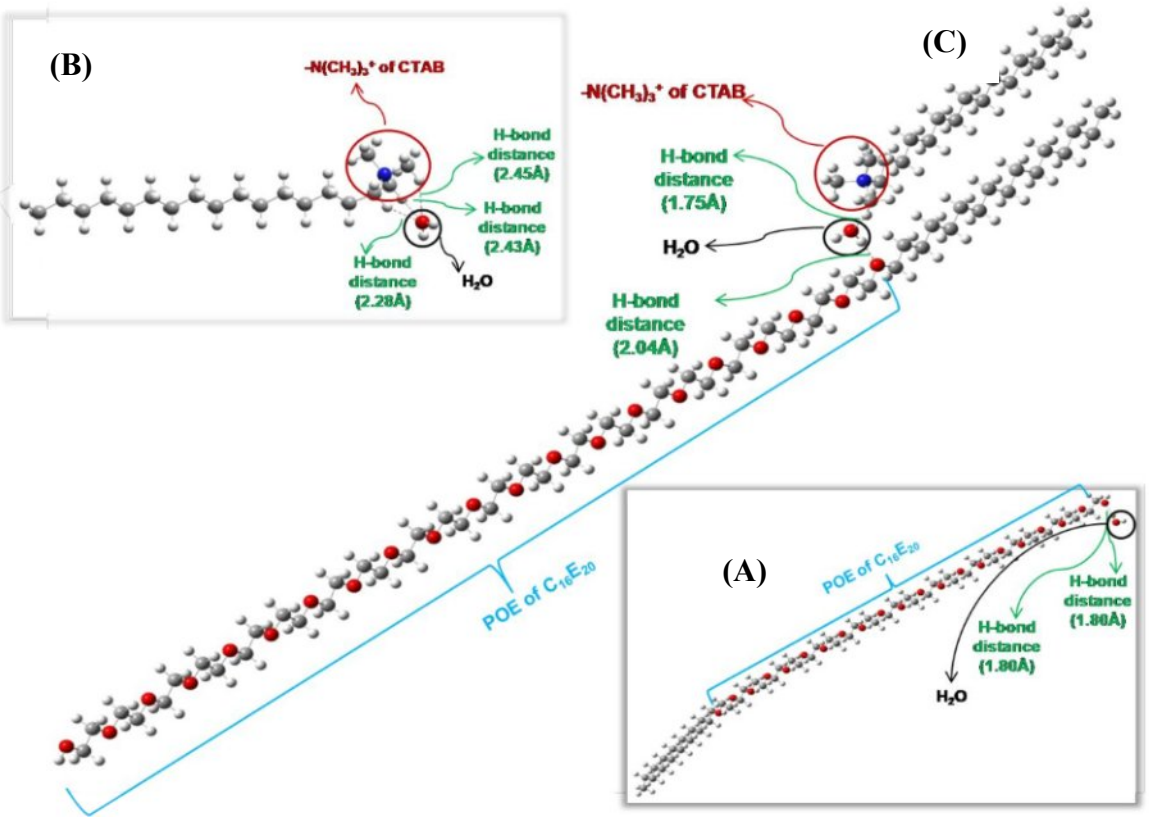

Figure-V.3. Optimized geometries at the B3LYP/6-31G level: **(A)** $C_{16}E_{20}/H_2O$ complex, **(B)** CTAB/H_2O complex, and **(C)** CTAB/$C_{16}E_{20}/H_2O$ complex. Colour code for atoms: blue, nitrogen; red, oxygen; dark gray, carbon; and light gray, hydrogen.

In order to understand the interaction of surfactant molecules with solvent qualitatively, we perform quantum chemical DFT calculation. We execute model calculations by using B3LYP functional with the basis set, 6-31G for understanding of the interactions of CTAB, $C_{16}E_{20}$ with H_2O at single and binary (1:1) compositions using Gaussian 09 program. Frequency calculations are also performed to verify that all the optimized geometries correspond to a local minimum which has no imaginary frequency. At the outset, we optimize the structures of the isolated CTAB, $C_{16}E_{20}$ and H_2O, binary complex (1:1) of CTAB and $C_{16}E_{20}$ with H_2O, and ternary complex (1:1:1) of CTAB, $C_{16}E_{20}$ and H_2O. The most stable optimized structures of binary (1:1) and ternary (1:1:1) complexes are presented in Figure-V.3, and their interaction energies (calculated from the difference of stabilization energy between complexes and monomers) are also shown in respective figure. Also, the optimized structures of isolated CTAB, $C_{16}E_{20}$ and CTAB/$C_{16}E_{20}$ are illustrated in Appendix D (Figure-D.S2). DFT calculation indicates a highly stable ternary complex, CTAB/$C_{16}E_{20}/H_2O$ with the stabilization energy of -102.09 kJ/mol. The stability of the proposed complexes follows the

order; CTAB/$C_{16}E_{20}$/H_2O > $C_{16}E_{20}$/H_2O (-59.09 kJ/mol) > CTAB/H_2O (-41.93 kJ/mol). This result suggests that the stabilization of the CTAB/$C_{16}E_{20}$/H_2O complex corroborates well the synergism in β parameter, ΔG^0_m and ΔG^0_{ads} values (Table-V.1). Similar observation was also reported earlier.[42,43]

V.B.1.2. C-C cross coupling Heck Reaction in Single and Mixed Micellar Media

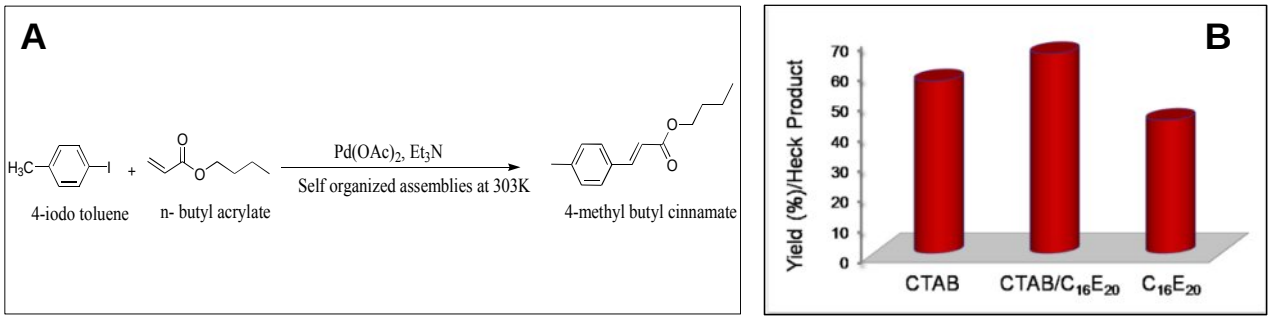

Figure-V.4. (A) Pictorial representation of Heck Reaction in self-organized media; and **(B)** Yield of Heck reaction in single (CTAB and $C_{16}E_{20}$) and mixed micelles (CTAB/$C_{16}E_{20}$, 1:1) at 303K.

Micellar media actually demonstrate that compartmentalization of these systems lead to the formation of the nanoreactor environment in the periphery of the micelle/water pseudo-phase and provide a better sustainability for synthetic organic chemistry.[44] In this report, repeated trials with a model substrate in characterized single and mixed micelles are explored to articulate the effect of restricted or confined reactor systems in the shed of their physicochemical and thermodynamic properties to rationalize the yield of the Heck reaction product at ambient temperature (303K) (Figure-V.4A). More precisely, it is expected to underline the variation in degree of performance of the Heck reaction from the viewpoints of distinctive features of micellar structure. The results are presented in Figure-V.4 and Table-D.S2 (Appendix D). Various combinations (for example, water, single and mixed micelles of CTAB and $C_{16}E_{20}$) of the nanoreactor systems (entries 1-4) are explored in order to standardize the best reaction environment from the yield of the desired product of Heck reaction (Table-D.S2). It is clearly evident that yield is very poor in water (7.0%) compares to microheterogeneous systems such as, single CTAB (57%), and $C_{16}E_{20}$ (44%) or mixed micelle (66.0%). Hence, these results clearly warrant that the envisioned need of a confined environment of aggregated systems which play a significant role in performing the Heck

reaction.[45] It can be seen from Figure-V.4 and Table-D.S2 that an equimolar composition of mixed micelle exhibits a synergism in yield of the Heck reaction product and consequently, reveals a better reactor than its constituent surfactants. More precisely, mixed micelle possesses some intrinsic properties in its formation that lead to its special characteristics toward performance of the Heck reaction. This is justified from higher negative values of interaction parameter (β^m) and free energy of mixed micelle formation (ΔG^0_m) than individual surfactants (Table-V.1). This suggests formation of the mixed micelle to be most spontaneous as well as functionally operative. Further, it is noted that cationic CTAB-mediated micelle shows higher yield than non-ionic $C_{16}E_{20}$ which corroborates well with spontaneity of formation of respective micelle as designated through the corresponding negative values of both ΔG^0_m and ΔG^0_{ads} (Table-V.1).[46] Surfactant-mediated self-assemblies or micelles are reported to be compatible with the aryl halogens.[45] Other substrates (excluding Pd^{2+} catalyst, which might be present in the continuous aqueous phase) are expected to be confined in micellar core. Hence, the probable location of micelle-mediated Heck reaction is the micelle/water pseudo-phase whereas the catalysis is likely to be operative.

So far we conclude that due to synergistic interaction between CTAB and $C_{16}E_{20}$ and spontaneous micellization, mixed surfactant based micelle produces an efficient media for performing Heck reaction. Also, the experimentally observed synergistic interaction corroborates well with the quantum chemical DFT calculation. Now, the questions arise that how the synergistic interaction between aforesaid surfactants stimulates in non-polar or non-aqueous medium and also, whether the Heck reaction occurs favorably in this mixed microemulsion system or not? To answer these questions, formation and characterization of mixed microemulsion system at different physicochemical conditions and correlation of the estimated parameters with the reaction mechanism of Heck coupled products are warranted.

V.B.2.Formation and characterization of w/o mixed microemulsions

CTAB requires the presence of a cosurfactant, typically a medium chain alcohol, in order to form a stable microemulsion.[47] In this study, Pn and Hp (or Dc) are used as cosurfactant and oil, respectively. In w/o microemulsion system, CTAB and $C_{16}E_{20}$ at equimolar composition are considered to populate at the oil/water interface in partial association with the cosurfactant (Pn). On the other hand, Pn further distributes between the interface and the bulk oil, because of its negligible solubility in water.[26] Thus, at a fixed [surfactant(s)], a critical concentration of Pn is required for the stabilization of the mixed microemulsions. To estimate

how much amount of (in moles) Pn is distributed in the interface and oil phase for formation of a stable microemulsion, we employ a simple titrimetric technique (known as the dilution method).[48] The distribution vis-à-vis transfer process of Pn from the continuous oil phase to the interfacial region is discussed in detail in Appendix D, with the help of Figure-D.S3. This method is used for the estimation of various parameters concerning to the formation of CTAB/$C_{16}E_{20}$ mixed microemulsion systems (with X_{CTAB} orX_{C16E20} = 0.5) in Hp and Dc at 303K and at different molar ratio of water to surfactant (ω = 10, 20, 30, 40 and 50). The estimated parameters, such as number of moles of Pn at the interface (n_a^i), in the oil phase (n_a^o), compositional variations of surfactants and Pn (n_a^i/n_s) at the interface, the distribution constant of Pn between the continuous oil phase and the interface of the droplet (K_d), and standard Gibbs free energy change of transfer of Pn from oil to the interface (ΔG^0_t) are presented in Table-D.S3, Appendix D. It is evident from Figure-V.5A that n_a^i or n_a^i/n_s values decrease with increase in ω for all these systems. Similar trend was reported earlier by Paul et al.[49] for water/Brij-35/Pn/Dc or Dd and Kundu et al.[50] for SDS/Brij-58 or Brij-78/Pn/Hp or Dc microemulsions. At a very low ω, the concentration of Pn at the interface is virtually constant, because long POE chain of $C_{16}E_{20}$ probably resides at the interface with twisted form due to a strong ion-dipole interaction between compact quaternary ammonium group in CTAB and EO groups in $C_{16}E_{20}$. With increase in the droplet size by the addition of more water, helically twisted POE-chains unfold and consequently, occupy larger surface area of the droplet.[51] Therefore, unoccupied surface area at the interface reduces to a greater extent and hence, n_a^i is gradually decreases with increase in ω. However, spontaneity of the transfer process further decrease with increase in ω which indicates the trend of Pn transferring from oil to the interface is weakened.[50] Hp stabilized systems also show higher spontaneity of Pn transfer process than Dc, which is also justified from the higher Pn population at the interface (n_a^i) in former system. Similar observations were reported by Kundu et al.,[50] Zheng et al.,[52] and Digout et al.[53] for w/o microemulsion systems stabilized by single as well as mixed surfactants. After successful formation of stable mixed microemulsion in conjunction with Pn in Hp or Dc at different ω, it is necessary to understand the microstructural and microenvironmental properties of these systems to reveal the nature of droplet-droplet interaction within these aggregates.

In view of these, size and size distributions of w/o microemulsion droplets are measured by DLS technique. Figure-V.5B depicts variation of the droplet size for mixed microemulsions in both oils as a function of water content (ω = 10-50) at a fixed composition ($X_{C16E20 \text{ or } CTAB}$

= 0.5), surfactant-cosurfactant mass ratio (= 1:2) and at 303K. The droplet size increases with increase in ω for both oils, keeping other parameters constant, which clearly indicates the swelling behaviour of w/o microemulsions with the addition of water.[54] The linear variation of droplet size at lower range of ω indicates that the droplets do not interact each other and are probably spherical. The deviation from linearity at higher ω value is due to several factors. Of these, the most relevant ones being enhanced droplet-droplet interaction and shape of the microemulsions. Further, Hp-based systems produce smaller droplet compared to Dc-based systems. It is probable due to the shorter chain of Hp compared to Dc, which easily penetrates to the interface to make it rigid. It can be concluded that with increase in ω, interdroplet interaction increases which is higher for Dc-based system compared to Hp. Both conductance and viscosity measurements in these systems also support the observation from DLS study (Figure-D.S4A and B and inset). The morphology of mixed microemulsions in both oils (Hp and Dc) is also investigated at a fixed X_{C16E20} = 0.5, ω = 10 and 303 K by employing FESEM and illustrated in Figure-V.5C-D. The micrographs for Hp based microemulsion (Figure-V.5C) reveal smaller particles arranged in rice grain-like patterns, which produce dispersed spheres of nearly homogeneous type morphology. On the other hand, Dc based microemulsion (Figure-V.5D) produces disintegrated isolated bodies of large globular and near globular particles forming spherical entities. All types of spherical morphology (*viz*. small as well as large) are marked by circles in both figures. For Dc based microemulsion, severe aggregation is occurred and single droplet cannot be discerned distinctly.

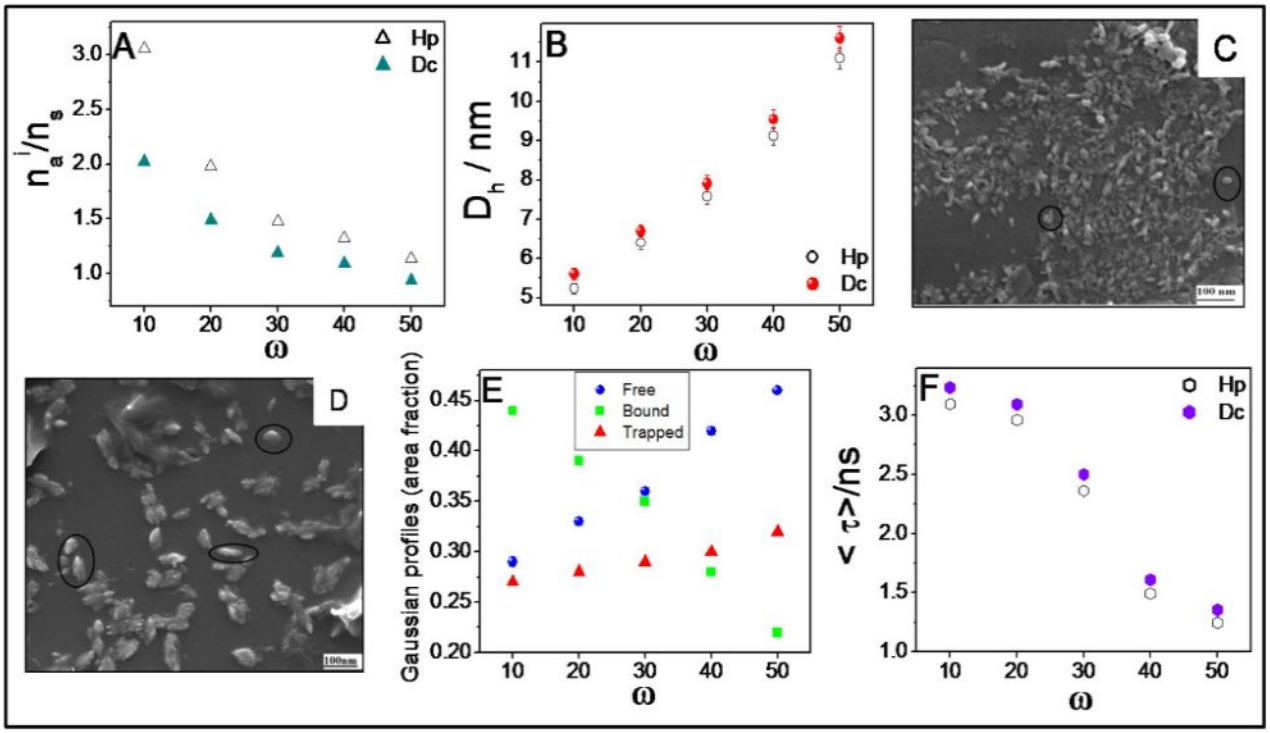

Figure-V.5. (A) Plot of n_a^i/n_s vs. water content (ω) for mixed CTAB/$C_{16}E_{20}$ microemulsions at equimolar composition comprising 0.5 mmol of mixed surfactant and 14.0 mmol of Hp or Dc stabilized by Pn. **(B)** Hydrodynamic diameter (D_h) as a function of ω for above mentioned systems. FESEM images of similar systems at a fixed X_{C16E20} = 0.5, ω = 10 and 303 K, where **(C)** Hp and **(D)** Dc oils. **(E)** The variation of Gaussian profiles (area fraction) of the normalized spectra of different water species; and **(F)** Fluorescence lifetime of HCM <τ> (λ_{ex}= 310 nm) as function of ω in CTAB/$C_{16}E_{20}$ (1:1)/Pn/ Hp/water microemulsions at 303K.

To understand the dynamics and nature of encapsulated water, we measure mid infrared region (MIR) FTIR spectra of encapsulated water in CTAB/$C_{16}E_{20}$ (1:1)/Pn/Hp/water microemulsions under varied ω (10→50). We focus our attention in the 3000-3800 cm^{-1} frequency windows as this is a fingerprint region for symmetric and asymmetric vibrational stretch of O-H bonds in water.[55,56] It is to be noted that a small amount of Pn is used as structure forming cosurfactant in the present study. Hence, the spectra of Pn (at the same concentration) is subtracted from the spectral intensity of O-H stretching band at the corresponding ω in order to eliminate the supplementary IR intensity due to O-H stretching vibration of Pn molecules, and the differential spectra are analysed.[57,58] Water usually coexists in three 'states' or 'layers' in the w/o microemulsion.[58-62] In view of this, the peaks observed for water O-H are fitted as a sum of Gaussian with the help of Gaussian curve

fitting program, and the vibrational characteristics, particularly the peak area corresponding to each peak, is analyzed using three-state models to unravel the nature of water inside the nanopool and the change in water properties as a function of ω. According to three states model, the solubilized water in microemulsions is identified as free, bound and trapped water molecules and a representative result of deconvolution is depicted in Appendix D, Figure-D.S5. The free water molecules, occupying the core of surfactant aggregates, form strong hydrogen bonds among themselves, that is, possess similar properties to that of bulk water, which shifts the O-H stretching band to lower frequency at about 3250 cm^{-1} (vide. Figure-D.S5).[58-62] The bound water i.e. the surfactant head group bound water molecules resonates in the mid frequency region and the IR peak appears at about 3450 cm^{-1} (vide. Figure-D.S5).[58-62] Apart from these two types of water species, the water molecules dispersing among long hydrocarbon chains of surfactant molecules are termed as trapped water molecules.[58-62] As the trapped water molecules are matrix-isolated dimers or monomeric in nature, they generally absorb in the high frequency region at about 3550 cm^{-1}. The relative abundance [Gaussian profiles (area fraction)] of different water species in these systems as a function of ω is presented in Figure-V.5E. It reveals that the relative abundance of free water increases from 29% to 46% and that of bound water decreases from 44% to 22% with increasing water content (ω = 10→50) vis-à-vis corresponding increase in droplet size (D_h) from 5.24 nm to 11.10 nm in same ω range. Actually, once water is added to a microemulsion forming system, a portion of the water goes to the interface and hydrates the head groups of surfactants till they become fully hydrated at a certain ω. Further addition of water goes primarily to the inner core, leading to a continuous increase in the fraction of unbounded free water with increase in ω.[61] In addition, the population corresponding to the trapped water molecules (monomers/dimmers) shows an overall weak increasing tendency with the hike of 27% to 32% with increasing ω (= 10→50). It is inferred from this investigation that a few water molecules are displaced from the structured water pool shell to the interfacial region with increasing ω.[63]

Fluorescence lifetime study of HCM (fluorophore) in mixed surfactant microemulsions is also employed to obtain information about the configuration of the altered interfacial region of mixed amphiphiles interface upon hydration (ω = 10→50). The choice of the fluorophore (HCM) is based on the fact that the probes residing at the interface and/or facing the polar core upon excitation (λ_{ex}= 310 nm).[64,65] In the present context, Figure-V.5F depicts that the fluorescence lifetime $\langle\tau\rangle$ of HCM (10^{-5} M) is found to be influenced by the variation of

water content in mixed microemulsions. A regular decreasing trend for $\langle\tau\rangle$ of fluorophore (HCM) is observed for both Hp (3.13 to 1.41 ns) and Dc (3.23 to 1.51 ns) derived systems with increasing ω (= 10→50). Larger droplet size of the microemulsion at ω = 50 compared to ω = 10 results in an increase in the curvature of the surfactant film. Hence a greater fraction of water interacts with the interface; leading to a relatively faster relaxation.[66] This result is also consistent with findings from FTIR measurements where increase in ω leads to increase in free-water population, which is responsible for observed faster life-time for CTAB/$C_{16}E_{20}$ (1:1)/Pn/Hp or Dc/water microemulsions at higher water content.[67]

V.B.2.1. C-C cross coupling Heck Reaction in Mixed Microemulsion

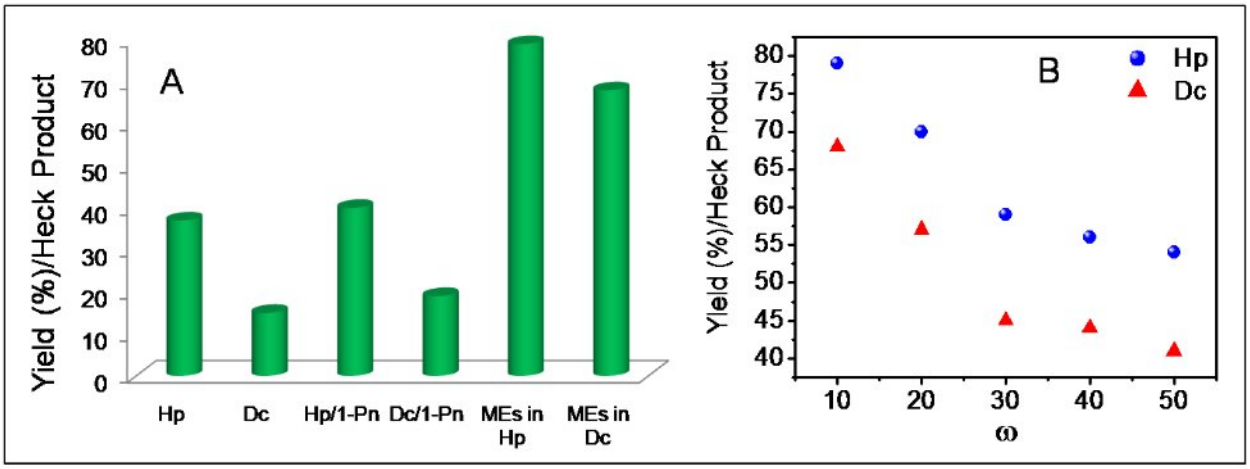

Figure-V.6. Yield of Heck product **(A)** in individual constituents as well as in w/o mixed microemulsions (MEs), CTAB/$C_{16}E_{20}$ (1:1)/Pn/Hp or Dc/water at ω = 10; and **(B)** variation of yield as a function of ω (= 10→50) in aforementioned MEs at 303K.

In view of the distinctive role of the mixed micelle at equimolar composition for carrying out the Heck reaction, another set of compartmentalized/microheterogeneous systems, water/oil (Hp or Dc) mixed surfactant microemulsions (MEs) stabilized by equimolar (1:1) composition of CTAB/$C_{16}E_{20}$ and Pn (S: CS = 1:2 wt%), are exploited as a function of ω (= 10→50) (entries 9-18, Table-D.S2 and Figure-V.6). In addition, the yields of the Heck product are also measured in the constituents of these formulations as media (entries 5-8, Table-D.S2). Both oils (Hp and Dc) and oil/Pn mixtures at 1:2 weight ratios (Hp/Pn, and Dc/Pn) show low yield compared to mixed microemulsions, while Hp derived systems show much higher yield than Dc (Figure-V.6A). A profound effect on the overall yield of the Heck product is distinctly validated by changing the template from micelle → mixed micelle (1:1)

→ mixed microemulsions (1:1) in Hp and Dc (Table-D.S2). Though, equimolar (1:1) surfactant composition (similar to that of mixed micelle) is fixed in all formulations, yields are found to be dependent on water content (ω), oil type and availability of Pn (as cosurfactant) at the oil/water interface for their stabilization (Figure-V.6B). The highest yield of the desired Heck product is achieved at ω = 10 in Hp and Dc derived microemulsions. Thereafter, a sharp decrease in yield is observed with increasing ω (up to 30) and subsequently, a mild or sluggish decrease achieve still attainment of ω = 50. It is worthy to mention that yield is much higher at lower ω = 10 (ME_{Hp}, 79% and ME_{Dc}, 68%) and 20 (ME_{Hp}, 70% only) than that of mixed micelle (66%), whereas yields are less than that of mixed micelle at rest of the ω's. However, overall results are rationalized as follows. It is inferred from the yields of the Heck product in microemulsions [ω ranges from 10 → 50 in both oils (ME_{Hp}, 79%→54% and ME_{Dc}, 68%→41%)] in conjugation with the yields in constituent elements *viz.* water (07%), oils (Hp, 37% and Dc, 15%), oil/Pn mixtures (Hp/Pn, 40% and Dc/Pn, 19%) (Figure-V.6A and Table-D.S2) that Heck reaction occurs neither in water nor in oil domain, evidently in the palisade layer of the oil/water interface of the microemulsions. This is well corroborated with previous report, where authors claim that the most plausible reaction location/site was the interfacial region or within the surfactant palisade layer of the w/o microemulsion.[68,69] In this context, the interaction between two constituents [such as, Pn (cosurfactant) and TEA] of these multicomponent systems plays a decisive role in performance of the Heck reaction leading to formation of the final product. It is worthy to mention that TEA, is an essential reactant of the Heck reaction, which requires a stoichiometric amount of base to neutralize the acid (herein, HI) ensuing from the exchange of a hydrogen atom with a aryl group.[16,17] In addition, requirement of Pn depends upon composition of the microemulsions, size of polar head group and charge type of surfactant, water content, degree of oil penetration, droplet size/microstructure, etc. and renders overall stability towards multicomponent systems from physicochemical and thermodynamic points of view.[26,49-53] More precisely, it is deciphered from the viewpoints mentioned above that predominance of the dipole-dipole interaction between Pn and TEA in confined environment enhances the availability of TEA in the vicinity of the interfacial region as well as in confined water with special reference to the bound water. Consequently, formation of OH^- base surrounding the interface proceeds in the following way;[68,70]

$$(C_2H_5)_3N + H_2O \leftrightarrow (C_2H_5)_3N.H_2O \leftrightarrow (C_2H_5)_3NH^+ + OH^-$$

Hence, the penetration of OH^- in the palisade layer of microemulsion cannot be ruled out, and subsequently, a basic environment in the vicinity of the interface is likely to be formed, which is essentially required for the Heck reaction.[68,69] Therefore, most satisfactory yield of the product is achieved at lower ω of 10 or 20 (Figure-V.6 and Table-D.S2), where predominance of Pn in this range of ω is evidenced from characterization of these microemulsions from the dilution method.[68] It reveals from Figure-V.5A and Table-D.S3 that the interfacial Pn population (n_a^i) and Gibbs free energy of Pn transfer process ($-\Delta G^0_t$) (which is an indicator for spontaneity of microemulsion formation) sharply decrease initially and thereafter mildly with increase in ω. Interestingly, it is worthy to mention that decreasing trends reflected in Figure-V.5A and Figure-V.6B resemblance to each other, which is a strong evidence for decreasing yield with increase in ω. Further, Hp based systems exhibit higher yield than Dc. It can be argued that higher values of n_a^i and $-\Delta G^0_t$ in Hp continuum than Dc continuum (Figure-V.5A and Table-D.S3) are responsible for variation in yield in these two set of systems. Herein, we report a mixed microemulsion mediated Heck coupling reaction which provides comparatively better results than single or mixed micelle validating the spontaneous nature of the reactor framework with a concomitant rapid Pn transfer process ($Pn_{oil} \rightarrow Pn_{interface}$) obtained from the dilution experiments under varied physicochemical environments. In conclusion, CTAB and $C_{16}E_{20}$ mediated micelles and microemulsions (in single and mixed state) Heck coupling procedure (through generation of new C-C bonds) is developed using ligand-free catalysts, and could be prospective in many industrial processes, especially in the synthesis of fine chemicals and active pharmaceutical intermediates.[19,71]

Currently, investigations of C-C coupling reactions catalysed by Pd(II) acetate and TEA as base in w/o microemulsions comprising different charge types of surfactants (both in single or mixed state) at different physicochemical conditions (for example, variations in composition of the system, concentration of both base and catalyst, water content, temperature etc.) are underway in our laboratory to probe the reaction mechanism of the Heck reaction in these complex microheterogeneous systems as media.

V.C. Overall Comprehension

In aqueous medium, equimolar composition of CTAB and $C_{16}E_{20}$ produces several advantages compared to individual surfactant in terms of lower CMC, more attractive

interaction between them and spontaneous micellization (*i.e.*, more negative free energy of micellization) as well as adsorption process at air/water interface. Interestingly, quantum chemical DFT calculation reveals larger interaction energy of equimolar CTAB and $C_{16}E_{20}$ with water compared to any other combinations. Zeta potential (ζ) values for CTAB/$C_{16}E_{20}$ mixtures also prove the synergistic interaction between them. Micellar aggregates produce spherical droplets with size ranges from 10 to 15 nm. To understand the distinctive features of micellar structures as chemical nanoreactors, Heck reaction is performed between 4-iodotoluene and *n*-butylacrylate. The reaction yield of Heck coupled product is found to be higher in mixed CTAB/$C_{16}E_{20}$ micellar solution compared to single CTAB or $C_{16}E_{20}$ micelle. However, a very poor yield is obtained in pure water. This result certainly proves that strong confinement effect of these assemblies. Also, the higher yield at mixed composition is correlated with spontaneous micellization and adsorption processes. It now stands interesting to further study the behaviour of these surfactants in non-polar solvents. Population of Pn at the oil/water interface of formulated w/o microemulsions vis-à-vis spontaneity of the transfer process is found to be decreased with increase in ω for both oils. Although these parameters are obtained through a straightforward macroscopic measurement, the Gibbs free energies of transfer of Pn from bulk oil to the interface are a sensitive probe of the micro-environment around various solute moieties, and are amenable for the investigation of relatively complex molecular structures. Morphology and size of mixed microemulsion droplets vary with water content as well as oil chain length. The present study also reveals that the relative abundance of free water increases and that of bound water decreases with increasing water content in mixed microemulsions and is well-corroborated with corresponding increase in droplet size under identical ω range. To search for further synergistic performance in non-polar medium in comparison to aqueous, the Heck reaction is carried out in mixed microemulsion media with aforesaid surfactants including individual constituent comprising microemulsion (*viz.* Pn, Hp or Dc). The reaction yields are found to be much higher in microemulsion systems compared to individual constituents. The yield in microemulsion is influenced by population of Pn at the oil/water interface, and chain length of oil. With increase in ω, yield of the Heck product decreases and it is lower for Dc medium compared to Hp. Both of these observations are correlated with spontaneity of Pn transfer process from oil to the interface obtained from the dilution experiment. The reaction in micellar and w/o microemulsion media has been found to be dependent on various physical parameters (such as water content, chain length of oil, composition of surfactants etc.) of these organized media.

V.D. Materials and methods

V.D.1. Materials CTAB (> 99%), $C_{16}E_{20}$ (> 98.5%) were the products of Sigma Aldrich, USA and Fluka, Switzerland, respectively. The cosurfactant [1-pentanol (Pn, > 98%)] and oils [Hp, (> 98%) and Dc(> 98%)] were products of Fluka, Switzerland, Lancaster, England and E. Merck, Germany, respectively. The dye, 7-hydroxycoumarin (HCM, > 99%) was the product of Chem. Service, West Chester, USA. Palladium acetate [$Pd(OAc)_2$, ≥ 99.98%] and 4-iodo-toluene ($CH_3C_6H_4I$, ≥ 99%) were purchased from Sigma Aldrich, USA. (TEA (≥ 99.5%) and n-butyl acrylate were purchased from Merck, Germany. All these chemicals were used without further purification. Doubly distilled water of conductivity less than 3 μS cm^{-1} was used in the experiments.

V.D.2. Methods

V.D.2.1. Tensiometry Surface tension was measured with a K9 tenisometer (Kruss, Germany) by the platinum ring detachment method. A concentrated surfactant solution was added to a known amount of water, and the surface tension values were measured after thorough mixing and temperature equilibration with an accuracy of ±0.1 mN m^{-1}.

V.D.2.2. Conductance measurements Conductivity measurements were made using an automatic temperature-compensated conductivity meter, Mettler Toledo (Switzerland) Conductivity Bridge, with cell constant of 1.0 cm^{-1}. The instrument was calibrated with a standard KCl solution. A constant temperature (303 ± 0.1 K) was maintained by circulating water through the outer jacket from a thermostatically controlled water bath. The reproducibility of the conductance measurement was found to be within ± 1%.

V.D.2.3. Dynamic light scattering (DLS) and zeta potential measurements Hydrodynamic diameter (D_h) and zeta potential (ξ/mV) measurements of the aggregated systems (single and mixed micelles and w/o mixed microemulsions) were performed using Nano ZS-90 (Malvern, U.K.) dynamic light scattering spectrometer at 303K. The solutions were equilibrated for 2-3 hours before measurement. Solutions were filtered carefully through a 0.22μm Millipore™ membrane filter loaded to a glass round aperture (PCS8501, Malvern, U.K.) cell of 1.0 cm optical path length for measurement. A He–Ne laser of 632.8 nm was used as the light source, while the scattering angle was set at 90^0. Temperature was controlled by in built Peltier heating-cooling device (± 0.1 K). D_h of the aggregated system was

estimated from the intensity autocorrelation function of the time-dependent fluctuation in intensity and can be defined as.[25]

$$D_h = {}^{k_B T}/_{3\pi\eta D} \quad (1)$$

Where, k_B, T, η and D indicate the Boltzmann constant, temperature, viscosity and diffusion coefficient of the solution, respectively. Zeta potential were measured using a folded capillary cell (DTS1060, Malvern, U.K.) made of polycarbonate with gold plated beryllium-copper electrodes. One cell was used for a single measurement. To check the reproducibility of the results at least 6 measurements were done.

V.D.2.4. Field Emission Scanning Electron Microscopy (FESEM) measurements A field emission scanning electron microscope (FESEM, HITACHI S-4800) was used to study the morphology of single and mixed micelles and w/o mixed microemulsions. High vacuum (~10^{-7} Torr) field emission setup was applied to deposit the thin film of micelle and microemulsion solution on the glass plates.

V.D.2.5. Formation of microemulsion The formation of microemulsion was accomplished by adding oil (Hp or Dc) at a constant water and surfactant level to destabilize an otherwise stable w/o microemulsion and then restabilizing it by adding a requisite amount of cosurfactant (Pn) with constant composition of interface and continuous phase. The procedure of this experiment with theoretical backgrounds was reported elsewhere.[26]

V.D.2.6. Viscosity measurements Viscosity measurements were performed using a LVDV-II+PCP cone and plate type rotoviscometer (Brookfield Eng. Lab, USA). The temperature was kept constant (303 K) for viscosity measurement within ± 0.1 K by circulating thermostated water, through a jacketed vessel containing the solution. The reproducibility of the viscosity measurement was found to be within ± 1%.

V.D.2.7. Fluorescence lifetime measurements The fluorescence lifetime measurements of w/o mixed microemulsions were performed at 303K using a bench-top spectrofluorimeter from Photon Technology International (PTI), USA (Model: Quantamaster-40). The present PTI lifetime instrument employs Stroboscopic Technique (Strobe) for time-resolved fluorescence measurements. In the present experiment, two curves are considered at the measured wavelength (at 450 nm using 310 nano LED as the light source) viz. the instrument response function (IRF) and the decay curve of probe molecules, 7-hydroxycoumarin (10^{-5}

mol dm^{-3}). IRF is acquired from a non-fluorescing scattered solution (Herein, Ludox AM-30 colloidal silica, 30 wt.% suspension in water) held in a 1 cm path length quartz cell. The lifetime values of probe molecules are then obtained by convoluting the IRF with a model function and then comparing the result with the experimental decay. Analysis has been made by Felix GX (version 2.0) software. A value of χ^2 in between 0.99-1.22 and a symmetrical distribution of residuals are considered as a good fit.

V.D.2.8. Fourier transform infrared spectroscopy (FTIR) studies FTIR spectra of w/o mixed microemulsions were performed at 303K in the 3000-3800 cm^{-1} window (mid infrared region) were recorded on a Perkin Elmer Spectrum RXI spectrometer (USA) (Absorbance mode) using a CaF_2-IR crystal window (Sigma-Aldrich) equipped with a Presslock holder with 100 number scans and spectral resolution of 4 cm^{-1} at 303K. Deconvolution of spectra has been made with the help of Gaussian curve fitting program (Origin software).

V.D.2.9. C-C cross coupling (Heck) reaction in micelles and microemulsions 3 ml of micellar or w/o microemulsion solution and 4.48 mg (0.02 mmol, 4 mol %) $Pd(OAc)_2$ were taken in a 25 ml round bottom flask and the mixture was placed in a preheated oil bath at 303 K for 30 minutes with constant stirring. Thereafter, 109 mg (0.5 mmol) of 4-iodotoluene, 76.8 mg (0.6 mmol) of *n*-butylacrylate and 101.12 mg (1 mmol) of TEA were introduced into it, and the resulting mixture was further stirred for 60 minutes at 303K. The resulting multicomponent solution (in each case) shows excellent stability towards reagents or otherwise. More precisely, similar experiments were performed in single (CTAB and $C_{16}E_{20}$) and mixed micelles (at equimolar composition), and mixed microemulsions (at equimolar composition) at different molar ratio of water to surfactant (ω) and also, in other constituents (viz. water, Hp, Dc, Hp/Pn, Dc/Pn) of the microemulsions. Progress of the reaction was monitored by silica gel thin layer chromatography (TLC). After completion, the reaction was quenched with water and the organic part was extracted thrice with diethyl ether. The combined ether layer was dried over anhydrous sodium sulphate and concentrated under vacuum. The yield of the Heck coupled product was determined by HPLC (Agilent Technologies, 1260 Infinity). Further, the product was purified by column chromatography using silica gel where a mixture of petroleum ether and ethyl acetate was used as eluent. Finally, the product was characterized by ^{1}H-NMR and ^{13}C-NMR (Bruker, 300 MHz), which were provided in Appendix D.

V.E. Summary

The present report focuses on the microstructure and properties of micelles and w/o microemulsion systems using similar set of surfactants (CTAB and $C_{16}E_{20}$) at single and mixed states and also, employment of these organized assemblies as chemical nanoreactor for performing the C-C cross coupling Heck reaction. Equimolar composition of CTAB and $C_{16}E_{20}$ shows non-ideal solution behaviour in aqueous medium with synergistic interaction between them, which further correlates with gas phase quantum chemical calculation. Understanding the microscopic origins of these mixing properties might facilitate more informed and designed use of such mixed systems in a range of novel formulations from hydrogels to surface coatings.[72,73] Mixed micellar composition provides efficient medium for carrying out Heck reaction compared to individual micellar and bulk water medium. So far, an operationally simple procedure is developed for carrying out traditional Heck couplings at ambient temperatures in mixed micelle, without resorting to sonication, electrochemistry, or water-soluble phosphine.[74] Use of inexpensive ionic and non-ionic amphiphiles, allows cross-couplings to take place especially under mild and environmentally attractive conditions. To realize whether the key features responsible for favorable micellization via synergistic interaction reciprocate the interfacial architecture of microemulsions, a multitechnique approach is applied to fully characterize mixed microemulsion systems at different hydration level. The estimation of Pn distribution at oil/water interface and bulk oil phase from dilution method complements more detailed information obtained from more labour-intensive small-angle neutron scattering (SANS) studies of w/o microemulsions.[75] Further, the droplet size and relaxation dynamics of fluoroprobe inside the confined environment correlates well with variation of different states of water. Knowledge of the such state of solubilized water in w/o microemulsion is important because this bears on the applications of these species, for example, in solubilization, catalysis of chemical reactions,[76] and in size and polydispersity of nanoparticles synthesized in the microemulsionmedia.[77] In order to understand the mechanism of Heck reaction in non-polar medium instead of aqueous medium, the formulated w/o microemulsion at different compositions along with individual constituents further used as templates for aforementioned reaction. A profound effect on the overall yield of the Heck product is distinctly validated by changing the template from micelle → mixed micelle (1:1) → mixed microemulsions (1:1), which indicates influence of the nature of the surfactant-solvent interactions, and thus affects the reaction yield.[78] Herein, it is proposed that the Heck reaction occurs neither in water nor in oil domain, and more precisely, at the

micelle/water pseudo-phase and palisade layer of the oil/water interface of microemulsions. In summary, each amphiphilic nano reactor is analogous to the traditional chemist's flask, with the added advantages of reduced reagent consumption, rapid mixing, automated handling, and continuous processing. Building on advances in continuous flow chemistry,[79] our study thus provides a new route to regulate and even to enhance the reaction yields in micellar and w/o microemulsion media according to the purpose and could be found useful for future applications in various domains such as enzyme activity, and/or organic synthesis.[80,81]

V.F. References

References are given in BIBLIOGRAPHY under Chapter V (pp. 113-118).

BIBLIOGRAPHY

Chapter-I

[1] U. M. Lindström (Ed.), *Organic Reactions in Water: Principles, Strategies and Applications*, Blackwell, Oxford, **2007**

[2] S. Narayan, J. Muldoon, M. G. Finn, V. V. Fokin, H. C. Kolb, K. B. Sharpless, *Angew. Chem. Int. Ed.* **2005**, *44*, 3275– 3279

[3] X. Wu, J. Liu, X. Li, A. Zanotti-Gerosa, F. Hancock, D. Vinci, J. Ruan, J. Xiao, *Angew. Chem. Int. Ed.* **2006**, *45*, 6718–6722

[4] Y. Jung, R. A. Marcus, *J. Am. Chem. Soc.* **2007**, *129*, 5492–5502.

[5] B. Cornils, *Angew. Chem. Int. Ed.* **2003**, *42*, 2704–2705

[6] C. M. Starks, C. I. Liotta, M. Halpern, *Phase Transfer Catalysis: Fundamentals, Applications and Industrial Perspectives*, Chapman and Hall, New York, **1994**

[7] B. D. Anderson, K. P. Flora in *The Practice of Medicinal Chemistry* (Ed.: C. G. Wermuth) Academic Press, London, **1996**

[8] C. L. Liotta, J. P. Hallett, P. Pollet, C. A. Eckert in *Organic Reactions in Water: Principles, Strategies and Applications* (Ed.: V. M. Lindström) Blackwell, Oxford, **2007**, pp. 256–300.

[9] N. E. Leadbeater, M. Marco, *Org. Lett.* **2002**, *4*, 2973–2976

[10] K. Holmberg, Eur. J. Org. Chem. **2007**, 731–742

[11] T.P. Hoar, J.H. Schulman, *Nature* **1943**, *152*, 102–103.

[12] J.H. Schulman, D.P. Riley, *J. Colloid Sci*. **1948**, *3*, 383–405.

[13] J.E. Bowcott, J.H. Schulman, *Z. Electrochem*. **1955,** *59,* 283– 290.

[14] J.H. Schulman, J.A. Friend, *J. Colloid Sci*. **1949**, *4*, 497–509.

[15] J.H. Schulman, W. Stoeckenius, L.M. Prince, *J. Phys. Chem*. **1959**, *63*, 1677–1680.

[16] R. Leung, M. J. Hou, C. Manohar, D. O. Shah, P. W. Chun, D. O. Shah, *ACS Symp. Ser*. **1985**, *272*, 325

[17] S. P. Moulik, B. K. Paul, *Adv. Colloid Interface Sci.,* **1998**, *78*, 99.

[18] Y. Sottmann, R. Strey, S. H. Chen, *J. Chem. Phys.,* **1997**, *106*, 6483.

[19] W. K. Kegel, H. N. W. Lekkerkerker, *Colloids Surf. A* **1993**, *761*, 241.

[20] R. C. Nelson, In: D. O. Shah, Eds., *Surface Phenomena in Enhance Oil Recovery,* Plenum Press, New York, 1981.

[21] B. K. Paul, S. P. Moulik, *Current. Science*, **2001**, *80*, 990.

[22] C. Solans, H. Kunieda, Eds., *Industrial Applications of Microemulsions*, Marcel Dekker Inc., New York, 1997.

[23] P. Kumar and K. L. Mittal, Eds., *Microemulsions in Science and Technology*, Marcel Dekker Inc., New York, 1999.

[24] D. Attwood, In: J. Kreutr, Eds., *Colloid Drug Delivery Systems*, Marcel Dekker Inc., New York, 1994.

[25] C.J. O'Coner, E.J. Fendler, J.H. Fendler, *J. Am. Chem. Soc.* **1973**, *95*, 600 – 602

[26] F.M. Menger, J.A. Donohue, R.F. Williams, *J. Am. Chem. Soc.* **1973**, *95*, 286 – 288

[27] A. Sanchez-Ferrer, F. Garcia-Carmona, *Enzyme Microb. Technol.* **1994**, *15*, 409

[28] K. Holmberg, *Adv. Colloid Interface Sci*. **1994**, *51*, 137

[29] H. Kunieda, K. Nakamura,D. F. Evans, *J. Am. Chem. Soc.* **1991**,*113*, 1051

[30] P. Ghosh, B. Kar, S. Bardhan, K. Kundu, S. K. Saha, B. K. Paul**,** S. Das, *J. Surface Sci. Technol.* **2016**, *32,* 8–16.

[31] R.K. Mitra, B.K. Paul, S.P. Moulik, *J. Colloid Interface Sci.* **2006**, *300*, 755

[32] I. Mukherjee, S. Mukherjee, B. Naskar, S. Ghosh, S.P. Moulik, *J. Colloid Interface Sci.* **2013**, *395*, 135

[33] M. Zhou, R.D. Rhue, *J. Colloid Interface Sci.* **2000**, *228*,18.

[34] E. Caponetti, A. Lizzio, R. Triolo, *Langmuir* **1990**, *6,* 1628

[35] E. Caponetti, A. Lizzio, R. Triolo, W.L. Griffin, J.S. Johnson, *Langmuir* **1992**, *8*, 1554

[36] S.R. Bisal, P.K. Bhattacharya, S.P. Moulik, J. Phys. Chem. **1990**, *94*, 350

[37] W.K. Kegal, G.A. van Aken, M.N. Bouts, H.N.W. Lekkerkerker, J. Th.G. Overbeek, P.L. de Bruyn, *Langmuir* **1993***, 9*, 252.

[38] R.K. Mitra, S.S. Sinha, P.K. Verma, S.K. Pal, *J. Phys. Chem. B* **2008**, *112*, 12946.

[39] S.K. Mehta, G. Kaur, R. Mutneja, K.K. Bhasin, *J. Colloid Interface Sci.* **2009**, *338*, 542

[40] M.M. Moohareb, R.M. Palepu, S.P. Moulik, *J. Disp. Sci. Technol.* **2006**, *27*, 1209

[41] B.K. Paul, D. Nandy, *J. Colloid Interface Sci.* **2007**, *316*, 751

[42] M. De, S.C. Bhattacharya, S.P. Moulik, A.K. Panda, *J. Surfact. Deterg.* **2010,** *13*, 475

[43] K. Maiti, I. Chakraborty, S.C. Bhattacharya, A.K. Panda, S.P. Moulik, *J. Phys. Chem. B* **2007**, *111*, 14175

[44] D. P. Acharya, P. G. Hartley, *Current Opinion in Colloid & Interface Science* **2012**,*17* 274–280

[45] H.F. Eicke, M. Borkovec, B. Dasgupta, *J. Phys. Chem.* **1989**, *93*, 314.

[46] N. Kallay, A. Chittofrati, *J. Phys. Chem.* **1990**, *94*, 4755

[47] H.T. Davis, J.F. Bodet, L.E. Scriven, W.G. Miller, *Physica A* **1989**, *157*, 470

[48] R. Ganguly, J.N. Sharma, N. Choudhury, *J. Colloid Interface Sci.* **2011**, *355*, 458

[49]M.A. Michaels, S. Sherwood, M. Kidwell, M.J. Allsbrook, S.A. Morrison, S.C. Rutan, E.E. Carpenter, J. Colloid Interface Sci. **2007**, *311*, 70

[50] X. Wang, X. Chen, S. Efrina, *J. Phys. Chem. B* **1999**, *103*, 7238

[51] X. Li, G. He, W. Zheng, G. Xiao, *Colloids Surf. A* **2010**, *360,* 150

[52] X. Zhang, Y. Chen, J. Liu, C. Zhao, H. Zhang, *J. Phys. Chem. B* **2012**,*116*, 3723

[53] C. M. L. Carvalho, M. R. Aires-Barros, J. M. S. Cabral, *Langmuir* **2000**, *16*, 3082

[54] G. Kaur, L. Chiappisi, S. Prevost, R. Schweins, M. Gradzielski, S.K. Mehta, *Langmuir* **2012**, *28*, 10640

[55] K.J. Mutch, J.S. Duijneveldt, J. Eastoe, I. Grillo, R.K. Heenan, *Langmuir* **2008,** *24*, 3053

[56] D.G. Hayes, M.H. Alkhatib, J.G. del Rio, V.S. Urban, *Colloids Surf. A* **2013**, *417*, 99

[57] M.A. Bolzinger, M.A. Thevenin, J.L. Grossiord, M.C. Poelman, *Langmuir* **1999**, *15,* 2307

[58] T.N. Zemb, I.S. Barnes, P.J. Derian, B.W. Ninham, *Prog. Colloid Polym. Sci.* **1990**, *81*, 20

[59] A. Kljajic, M.B. Rogac, S. Trost, R. Zupet, S. Pejovnik, *Colloids Surf. A* **2011**, *385*, 249

[60] S. Sharifi, M. Amirkhani, J.M. Asla, M.R. Mohammadi, O. Marti, *Soft Nanoscience Lett.* **2012**, 2, 8

[61] R. Hilfiker, H.F. Eicke, W. Sager, U. Hofmeier, R. Gehrke, *Ber. Bunsenges Phys. Chem.* **1990**, *94*, 677

[62] R. Saha , S. Rakshit , R.K. Mitra , S.K. Pal *Langmuir* **2012**, *28*, 8309

[63] R. Pramanik, S. Sarkar, C. Ghatak, V.G. Rao, N. Sarkar, *Chem Phys Lett.* **2011**, *512,* 217

[64] D. Seth , A. Chakraborty , P. Setua , N. Sarkar, *J Phys Chem B* **2007,** *111*, 4781.

[65] J. R. Lakowicz, Principles of Fluorescence Spectroscopy; Plenum Press: New York, **1983**

[66] E. Haustein, P. Schwille, *Annu Rev Biophys Biomol Struct*. **2007**, 36, 151

[67] G.R. Burnett, G.D. Rees, D.C. Steytler, B.H. Robinson, *Colloids Surf A Physicochem Eng Asp.* **2004,** *250*, 171

[68] N. Zhou, Q. Li, J. Wu, J. Chen, S. Wang, G. Xu, *Langmuir* **2001**,*17*, 4505

[69] Q. Li, T. Li, J. Wu, N. Zhou, *J. Colloid Interface Sci.* **2000**, *229*, 298.

[70] J.J. Silber, A. Biasutti, E. Abuin, E. Lissi, *Adv. Colloid Interface Sci.* **1999**, *82*, 189.

[71] A. Das, A. Patra, R.K. Mitra, *J. Phys. Chem. B* **2013,** *117*, 3593

[72] R. Strey, *Colloid Polym. Sci.* **1994**, *272*, 1005

[73] Bellare, J.R., Haridas, M.M., Li, X.J; Characterization of microemulsions using Fast Freeze – Fracture and Cryo-Electron Microscopy In Handbook of Microemulsion, Science and Technology; Ed : Kumar, P., Mittal, K.L.; Marcel Dekker, Inc., New York, **1999**; 411-523

[74] Jonsson, B. Lindman, K. Holmberg, B. Kronberg, *Surfactants and Polymers in Aqueous Solution*, Wiley, Chichester, **1998**.

[75] M.A. Lopez-Quintela, C. Tojo, M.C. Blanco, L. Garcia Rio, J.R. Leis, *Current Opinion in Colloid & Interface Science* **2004,** *9*, 264–278

[76] L. G.-Río, A. Godoy, P. R.-Dafonte, *Eur. J. Org. Chem.* **2006**, 3364–3371

[77] B. K. Mishra, B. S. Valandikar, J. J. Kunjappu and C. J. Manohar, *Colloid Interface Sci*., **1989**, *127*, 373

[78] K. Holmberg*, Curr. Opin. Colloid and Interface Science,* **2003**, *8*, 187

[79] Structure and Reactivity in Reversed Micelles, Ed. M.P. Pileni, Elsevier, Amsterdam, **1989**.

[80] H.-C. Hung, T.-M. Huang, G.-G. Chang, *J. Chem. Soc., Perkin Trans*. **1997**, *2*, 2757

[81] L. Mukherjee, N. Mitra, P. K. Bhattacharya, S. P. Moulik, *Langmuir,* **1995**, *11*, 2866

[82] C. Izquierdo, J. Casado, A. Rodriguez and M. L.Moya, *Int. J. Chem. Kinet*., **1922**, *19*, 24.

[83] M. L. Moya, C. Izquierdo, J. J. Casado, *Phys. Chem.* **1991**, *95*, 6001

[84] V. Vashchenko, A. Krivoshey, I. Knyazeva, A. Petrenko, J. W. Goodby, *Tetrahedron Letters* **2008**, *49*, 1445–1449

[85] J.-Z. Jiang, C. Cai, *Journal of Dispersion Science and Technology* **2008**, *29*, 453–456.

[86] R. F. Heck, J. P. Nolley, *J. Org. Chem.* **1972**, *37*, 2320–2322

[87] J.-Z. Jiang, C. Cai, *Journal of Colloid and Interface Science* **2006**, *299*, 938–943

[88] G. Zhang, H. Zhou, J. Hu, M. Liu*,* Y. Kuang, *Green Chem.* **2009**, *11*, 1428–1432

[89] F. Gayet, C. E. Kalamouni, P. Lavedan, J.-D. Marty, A. Brulet, N. L.-de Viguerie, *Langmuir* **2009**, *25*, 9741–9750.

[90] J-Z. Jiang, C. Cai, *Colloids and Surfaces A: Physicochem. Eng. Aspects* **2006**, *287*, 212–216

[91] J.-Z. Jiang, Y.-A. Wei, C. Cai, *Journal of Colloid and Interface Science* **2007**, *312*, 439–443

[92] J. M-Brusco, S. Prevost, D. Lugo, M. Gradzielski, R. Schomacker, New J. Chem. **2009**, *33*, 1726–1735

[93] J. B. F. N. Engberts, E. Fernandez, L. Garcıa-Rıo, J. R. Leis *J. Org. Chem.* **2006**, *71*, 4111-4117

[94] J. B. F. N. Engberts, E. Fernandez, L. Garcia-Rio, and J. R. Leis *J. Org. Chem.* **2006**, *71*, 6118-6123

[95] Huihong Lü, Xueqin An, Jianguo Yu, Xingfu Song, *J. Phys. Org. Chem.* **2012**, *25* 1210–1216

[96] P. Blach, Z. Bostrom, S. F.-Messant, A. Lattes, E. Perez , I. Rico-Lattes, *Tetrahedron* **2010**, *66,* 7124-7128

[97] L. García-Río, J. C. Mejuto, M. Pérez-Lorenzo, *J. Phys. Chem. B* 2006, **110**, 812.

[98] L. García-Río, J. R. Leis, J. C. Mejuto, M. P-Lorenzo, Pure Appl. Chem. **2007**, 79(6), 1111–1123.

[99] J. J. Shrikhandea, P.A. Hassanb, R.V. Jayaram, *Colloids and Surfaces A: Physicochem. Eng. Aspects* **2010**, *370*, 64–71

[100] P. R. Arivalagan, Y. Zhao, *Org. Biomol. Chem.* **2015**, *13*, 770–775

[101] M. Hojo , R. Kato, A. Narutaki, T. Maeda, Y. U. Hojo , R. Kato, A. Narutaki, T. Maeda, Y. Uji-yie, *Journal of Molecular Liquids* **2011**, *163*, 161–169

[102] J. Jiang , L. Dai , Z. Cui , L. Lu, Z. Cui, *Journal of Dispersion Science and Technology* **2014**, *35*, 524–527.

[103] S. K. Mehta, K. Kaur, E. Arora, K. K. Bhasin. *J. Phys. Chem. B* **2009**, *113,* 10686–10692

[104] **V.** Uskoković, M. Drofenik, *Advances in Colloid and Interface Science* **2007**, *133*, 23–34

[105] R. McIntosh, D. Nicastro, D. Mastronarde, *Trends Cell Biol.* **2005**, *15*, 43–51.

[106] T. Maruyama, T. Hosogi, M. Goto, *Chem. Commun*. **2007**, 4450–4452

[107] S. Pramanik, S. Nagatoishia, N. Sugimoto, *Chem. Commun.* **2012**, *48*, 4815

[108] A. Singh, K. Misra, International journal of hydrogen energy **2008**, *33*, 6100 – 6108.

Chapter-II

[1] C. Patrascu, F. Gauffre, F. Nallet, R. Bordes, J. Oberdisse, N. de Lauth-Viguerie, C. Mingotaud, *Chem. Phys. Chem.* **2006**, *7***,** 99-101.

[2] F. Zhou, Y. Liang, W. Liu, *Chemical Society Reviews* **2009**, ***38,*** 2590-2599.

[3] H. Tokuda, K. Hayamizu, K. Ishii, Md. A. B. H. Susan, M. Watanable, *J. Phys. Chem. B* **2005**, *109*, 6103–6110.

[4] S. Gupta, A. Chatterjee, S. Das, B. Basu, B. Das, *J. Chem. Eng. Data* **2013**, *58*, 1−6.

[5] Y. Özkay, Y. Tunalı, H. Karaca, İ. Işıkdağ, *European J. Medicinal Chem*. **2010**, *45*, 3293-3298.

[6] W. Kunz, T. Zemb, A. Harrar, *Curr. Opin. Colloid Interface Sci.* **2012**, *17,* 205-211.

[7] M. Andújar-Matalobos, L. García-Río, S. López-García, P. Rodríguez-Dafonte, *J. Colloid Interface Sci.* **2011**, *363*, 261-267.

[8] H. Lu, X. An, J. Yu, X. Song, *J. Phys. Org. Chem.* **2012**, *25***,** 1210-1216.

[9] F. Gayet, C. E. Kalamouni, P. Lavedan, J-D. Marty, A. Brûlet, N. L-d. Viguerie, *Langmuir* **2009**, *25,* 9741-9750.

[10]Microemulsion-background, New Concepts, Applications, Perspectives, C. Stubenrauch (Eds.), *Blackwell*, Oxford, **2009**.

[11] K. Kundu, G. Guin, B. K. Paul, *J. Colloid Interface Sci.* **2012**, *385*, 96-110.

[12] S. Bardhan, K. Kundu, S. K. Saha, B. K. Paul, *J. Colloid Interface Sci.* **2013**, *402*, 180-189.

[13] S. Bardhan, K. Kundu, B. K. Paul, S. K. Saha, *Colloid Surfaces A* **2013**, *433*, 219-229.

[14] F. Wang, Z. Zhang, D. Li, J. Yang, C. Chu, L. Xu, *J. Chem. Eng. Data,* **2011**, *56*, 3328–3335.

[15] X-F. Wu, P. Anbarasan, H. Neumann, M. Beller, *Angew. Chem. Int. Ed.* **2010**, *49*, 9047 – 9050.

[16] G. Zhang, H. Zhou, J. Hu, M. Liu, Y. Kuang, *Green Chem.* **2009**, *11*, 1428-1432.

[17] S. Paul, A. K. Panda, *Colloids and Surfaces A: Physicochem. Eng. Aspects* **2013***, 419*, 113–124.

[18] Z. Zhang, F. Wang, D. Li, J. Yang, *J. Disp. Sci. Technol.* **2012**, *33*, 141-146.

[19] I. Mukherjee, S. Mukherjee, B. Naskar, S. Ghosh, S. P. Moulik, *J. Colloid Interface Sci.* **2013,** *395,* 135-144.

[20] R. Zhang, L. Zhang, P. Somasundaran, *J. Colloid Interface Sci.* **2004**, *278,* 453-460.

[21] R.H Petrucci, F.G. Herring, J.D. Madura, C. Bissonnette, General Chemistry: Principles and Modern Applications, 9th Eddition, Upper Saddle River, N.J.: Pearson/Prentice Hall, **2007**

[22] B.J. Shiau, D.A. Sabatini, J.H. Harwell, D.Q. Vu, *Env. Sci. Technol.* **1995**, *30*, 97-103

[23] J.L. Salager, E. Vasquez, J.C. Morgan, R.S. Schechter, W.H. Wade, *Soc. Pet. Eng. J.* **1979**, *19*, 107-115

[24] P.M. Holland, D.N. Rubingh, *J. Phys. Chem.* **1983**, *87*, 1984-1990

[25] J.F. Rathman, J.F. Scamehorn, *Langmuir* **1987**, *3*, 372-377

[26] K. Kawakami, T. Yoshikawa, Y. Moroto, E. Kanaoka, K. Takahashi, Y. Nishihara, K. Masuda, *J. Controlled Release* **2002**, *81*, 65-74

[27] T. Inoue, K. Kawashima, Y. Miyagawa, *J. Colloid Interface Sci.* **2011**, *363*, 295-300

[28] T. Inoue, Y. Iwasaki, *J. Colloid Interface Sci.* **2010**, *348,* 522-528

[29] M. De, S. C. Bhattacharya, A. K. Panda, S.P. Moulik, *J. Disp. Sci. Technol.* **2009**, *30*, 1262-1272.

[30] J. Łuczak, C. Jungnickel, M. Joskowska, J. Thöming, J. Hupka, *J. Colloid Interface Sci.* **2009**, *336*, 111-116.

[31] S. Ray, S.P. Moulik, *J. Colloid Interface Sci.* **1995**, *173*, 28-33.

[32] S. Ghosh, A.D. Burman, G.C. De, A.R. Das, *J. Phys. Chem. B* **2012**, *115*, 11098-11112.

[33] K. Khougaz, Z. Gao, A. Eisenberg, *Langmuir* **1997**, *13***,** 623-631.

[34] B. Šarac, M. Bešter-Rogač, *J. Colloid Interface Sci.* **2009**, *338*, 216-221.

[35] J. L. López-Fontán, A. González-Pérez, J. Costa, J. M. Ruso, G. Prieto, P. C. Schulz, F. Sarmiento, *J. Colloid Interface Sci.* **2006**, *297,* 10-21.

[36] G. Liu, D. Gu, H. Liu, W. Ding, Z. Li, *J. Colloid Interface Sci.* **2011**, *358*, 521-526.

[37] M. Tomsic, A. Jamnik, in Microemulsions: Properties and Applications, M. Fanun (Eds.), *Taylor and Francis*, CRC Press, USA, **2009**, 143-181.

[38] S. Bardhan, K. Kundu, B. K Paul, S.K. Saha, *J. Colloid Interface Sci.* **2013**, *411*, 152-161.

[39] S. K. Mehta, S. Chadhary, K. K. Bhasin, *J. Colloid Interface Sci.* **2008**, *321***,** 426-433.

[40] S. Perez-Casas, R. Castillo, M. Costas, *J. Phys. Chem. B* **1997**, *101*, 7043-7054.

[41] P. Bauduin, D. Touraud, W. Kunz, *Langmuir* **2005**, *21*, 8138-8145.

[42] Y. A. Gao, N. Li, L. Q. Zheng, X. T. Bai, L. Yu, X. Y. Zhao, J. Zhang, M. W. Zhao, Z. Li, *J. Phys. Chem. B* **2007,** *111*, 2506-2513.

[43] L. Liu, P. Bauduin, T. Zemb, J. Eastoe, J. Hao, *Langmuir* **2009**, *25*, 2055-2059.

[44] R. Leung, D. O. Shah, *J. Colloid Interface Sci.* **1987**, *120,* 330-334.

[45] C-L. Chang, H. S. Fogler, *Langmuir* **1997**, *13***,** 3295-3307.

[46] D. Liu, J. Ma, H. Cheng, Z. Zhao, *Colloids Surf. A* **1998**, *135,* 157-164.

[47] J.-B. Brubach, A. Mermet, A. Filabozzi, A. Gerschel, D. Lairez, M. P. Krafft, P. Roy, *J. Phys. Chem. B* **2001**, *105*, 430-435.

[48] R. K. Mitra, S. S. Sinha, P. K. Verma, S. K. Pal, *J. Phys. Chem. B*, **2008**, *112*, 12946-12953.

[49] S.S. Narayanan, S. S. Sinha, R. Sarkar, S.K. Pal, *Chemical Physics Lett.* **2008**, *452*, 99–104.

[50] I. R. Piletic, D. E. Moilanen, D. B. Spry, N. E. Levinger, M. D. Fayer, *J. Phys. Chem. A* **2006**, *110,* 4985-4999.

[51] J. Vicente, A. Arcas, *Coordination Chemistry Reviews* **2005**, *249*, 1135-1154.

[52] S. Gupta, B. Basu, S. Das, *Tetrahedron* **2013**, *69*, 122-128

[53] S-J. Sung, K-Y. Cho, H. Hah, J. Lee, H-K. Shim, J-K. Park, *Polymer* **2006**, *47*, 2314–2321.

[54] N. Li, Q. Cao, Y. Gao, J. Zhang, L. Zheng, X. Bai, B. Dong, Z. Li, M. Zhao, L. Yu, *Chem. Phys. Chem.* **2007**, *8*, 2211 – 2217.

[55] E. Abuin, E. Lissi, K. Olivares, *J. Colloid Interface Sci*. **2004**, *276*, 208-211.

Chapter-III

[1] D. A. Horton, G. T. Bourne, M. L. Smythe, *Chem. Rev.* **2003**, *103*, 893-930.

[2] K. J. Jr. Henry, J. Wasicak, A. S. Tasker, J. Cohen, P. Ewing, M. Mitten, J. J. Larsen, D. M. Kalvin, R. Swenson, S. C. Ng, B. Saeed, S. Cherian, H. Sham, S. H. Rosenberg, *J. Med. Chem.* **1999**, *42*, 4844-4852.

[3] D. J. Augeri, D. Janowick, D. M. Kalvin, G. Sullivan, J. J. Larsen, D. Dickman, H. Ding, J. Cohen, J. Lee, R. Warner, P. Kovar, S. Cherian, B. Saeed, H. Zhang, S. Tahir, S. C. Ng, H. Sham, S. H. Rosenberg, *Bioorg. Med. Chem. Lett.* **1999**, *9*, 1069-1074.

[4] C. Amatore, C. Cammoun, A. Jutand, *Eur. J. Org. Chem*. **2008,** 4567-4570.

[5]A. Prastaro, P. Ceci, E. Chiancone, A. Boffi, G. Fabrizi, S. Cacchi, *Tetrahedron. Lett.* **2010**, *51*, 2550-2552.

[6] H. Firouzabadi, N. Iranpoor, F. Kazemi, *J. Mol. Cat. A: Chem* **2011**, *348*, 94-99.

[7] Z. Zhoua, M. Liua, X. Wua, H. Yub, G. Xua, Y. Xiea, *Appl. Organometal. Chem.* **2013**, *27*, 562-569.

[8] S. Gupta, B. Basu, S. Das, *Tetrahedron* **2013**, *69*, 122-128.

[9] S. Gupta, P. Ghosh, S. Dwivedi, S. Das, *RSC Adv.* **2014**, *4*, 6254-6260.

[10] S. Dwivedi, S. Bardhan, P. Ghosh, S.Das, *RSC Adv*. **2014**, *4*, 41045-41050.

[11] S. Gupta, B. Ganguly, S. Das, *RSC Adv.* **2014**, *4*, 41148-41151.

[12] S. Carrettin, J. Guzman, A. Corma, *Angew.Chem. Int. Ed.* **2005**, *44* 2242-2245.

[13]L. Wang, W. Zhang, D.S. Su, X. Meng, F-S. Xiao, *Chem. commun.* **2012**, *48*, 5476-5478.

[14] N. Kirai, Y. Yamamoto, *Eur. J. Org. Chem.* **2009**, 1864-1867.

[15] B. Kaboudin, R. Mostafalua, T. Yokomatsub, *Green Chem.* **2013**, *15*, 2266-2274.

[16] S. Pramanik, S. Nagatoishia, N. Sugimoto, *Chem. Commun.* **2012**, *48*, 4815-4817.

[17] K. Bhattacharyya, B. Bagchi, *J. Phys. Chem. A.* **2000**, *104*, 10603-10613.

[18] R. Biswas, S. K. Pal, *Chem. Phys. Lett.* **2004**, *387*, 221-226.

[19] K. Holmberg, *Eur. J. Org. Chem.* **2007**, 731–742.

[20] K. Holmberg, *Curr. Opin. Colloid Interface Sci.* **2003**, *8*, 187–196.

[21] M. Hager, F. Currie, K. Holmberg, Top Curr. Chem. **2003**, *227*, 53–74.

[22] B. Kar, S. Bardhan, K. Kundu, S. K. Saha, B. K. Paul, S. Das, *RSC Adv.* **2014**, *4*, 21000-21009.

[23] X. Zhang, Y. Chen, J. Liu, C. Zhao, H. Zhang, *J. Phys. Chem. B.* **2012**, *116*, 3723−3734.

[24] H.-F. Eicke, M. Borkovec, B. Das-Gupta, J. Phys. Chem. **1989**, *93*, 314-317.

[25] N. Kallay, A. Chittofrati, *J. Phys. Chem.* **1990**, *94*, 4755-4756.

[26] Q. Li, T. Li, J. Wu, *J. Phys. Chem. B.* **2000**, *104,* 9011-9016.

[27] Q. Li, T. Li, J. Wu, *J. Colloid. Interface. Sci.* **2001**, *239,* 522–527.

[28] P. Hanarp, D. S. Sutherland, J. Gold, B. Kasemo, *Colloids Surf. A.* **1999**, *160*, 23–36.

[29] M. Dubois, Th. Zemb, *Langmuir* **1991**, *7*, 1352-1360

[30] T.K. De, A. N. Maitra, *Adv. Colloid Interface Sci.* **1995**, *59*, 95-193.

[31] A. Das, R. K. Mitra, *Colloid. Polym. Sci.* **2014,** *292*, 635–644.

[32] K. M. Goncalves, I. I. Junior, V. Papadimitriou, M. Zoumpanioti, I. C. R. Leal, R. O. M. A. De Souza, Y. Cordeiro, A. Xenakis, *Langmuir* **2016**, *32*, 6746−6756.

[33] S. Bardhan, K. Kundu, B. K. Paul, S. K. Saha, *Colloid Surf. A.* **2013**, *433*, 219-229.

[34] S. Bardhan, K. Kundu, S. Saha, B.K. Paul, *J.Colloids.Interface.Sci.* **2013**, *411*, 152-161.

[35] D. J. Mitchell, B.W. Ninham, *J. Chem. Soc. Faraday Trans. 2*, **1981**,*77*, 601.

[36] D. F. Evans, B. W. Ninham, *J. Phys. Chem.* **1986**, *90*, 225-226.

[37] M. Schick. J. Nonionic surfactants: Physical chemistry, Dekker, New York, **1987**, vol. 23.

[38] D. Liu, J. Ma, H. Cheng, Z. Zhao, *Colloids Surf. A.* **1998**, *135*, 157-167.

[39] S. Ghosh, C. Banerjee, S. Mandal, V. G. Rao, N. Sarkar, *J. Phys. Chem. B.* **2013,** *117*, 5886−5897.

[40] S. Bardhan, K. Kund, S. Das, M. Poddar, S. K. Saha, B. K. Paul, *J.Colloids.Interface.Sci.* **2014**, *430*, 129-139.

[41] T. K. Jain, M. Varshney, A. Maitra, J. Phys. Chem. **1989,** *93*, 7409-7416.

[42] Y. Gao, N. Li, L. Zheng, X. Bai, L. Yu, X. Zhao, J. Zhang, M. Zhao, Z. Li, *J. Phys. Chem. B.* **2007**, *111*, 2506-2513.

[43] Y. Gao, L. Hilfert, A. Voigt, K. Sundmacher, *J. Phys. Chem. B.* **2008**, *112*, 3711-3719.

[44] A. J. Lock, H. J. Bakker, *J. Chem. Phys.* **2002**, *117*, 1708−1713.

[45] S. A. Corcelli, J. L. Skinner, *J. Phys. Chem. A.* **2005**, *109*, 6154−6165.

[46] A. Das. A. Patra, R. K. Mitra, *J. Phys. Chem. B.* **2013**, *117*, 3593−3602.

[47] S. Bardhan, K. Kundu, S. Saha, B. K. Paul, *Colloids. Surf. A.* **2014**, *450*, 130-140.

[48] R. K. Mitra, S. S. Sinha, P. K. Verma, S.K. Pal, *J. Phys. Chem. B.* **2008**, *112*, 12946-12953.

[49] D. E. Moilanen, E. E. Fenn, D. Wong, M. D. Fayer, *J. Am. Chem. Soc.* **2009***,131,* 8318–8328.

[50] S. Bardhan, K. Kundu, B. Kar, G.Chakraborty, D. Ghosh, D. Sarkar, S. Das. S. Senapati, S. Saha, B.K. Paul, *RSC. Adv.* **2016**, *6*, 55104–55116.

[51] I.S. Barnes, S. T. Hyde, B. W. Ninham, P. J. Derian, M. Drifford, Th. Zemb, *J. Phys. Chem.* **1988**, *92*, 2286-2293.

[52] J. Eastoe, K. J. Hetherington, J.S. Dalton, D. Sharpe, J. R. Liu, R. K. Heenan, *J.Colloids.Interface.Sci.* **1997**, *190*, 449-455.

[53] S.P. Moulik, K. Mukherjee, *Proc. Indian Natl. Sci. Acad.* **1996**, *62(3)*, 215-222.

[54] D. Das, D. N. Nath, *J. Phys. Chem. B*. **2007**, *111*, 11009-11015.

[55] C. Kumar, D. Balasubramanian, *J. Phys. Chem.* **1980**, *84*, 1895-1899.

[56] J. Vicente, A. Arcas, *Coord. Chem. Rev.* **2005**, *249*, 1135–1154.

[57] L. Mukhopadhyay, P. Bhattacharya, S. P. Moulik, Colloids Surf. 50 (1990) 295-308.

[58] M. Tomsic, A. Jamnik, (Eds.: M. Fanun.), Taylor and Francis, CRC Press, USA. (**2009**) 143-181.

[59] P. Bauduin, D. Touraud, W. Kunz, *Langmuir* **2005**, *21*, 8138-8145.

[60] I. R. Piletic, D. E. Moilanen, D. B. Spry, N. E. Levinger, M. D. Fayer, *J. Phys. Chem. A.* **2006**, *111*, 4985-4999.

[61] S. K. Mehta, K. Kaur, E. Arora, K. K. Bhasin, *J. Phys. Chem. B.* **2009**, *113*, 10686–10692.

[62] J. S. Chen, K. K. Jespersen, J. G. Khinast, *J. Mol. Cat. A: Chem.* **2008**, *285*, 14–19.

[63] I. D. Kostas, F. J. Andreadaki, D. Kovala-Demertzi, C. Prentjas, M. A. Demertzis, *Tet. Lett.* **2005**, *46*, 1967–1970.

[64] X. Xu, D. Cheng, V. Pei, *J. Org. Chem.* **2006**, *71*, 6637-6639.

[65] P. Puthiaraj, P. Suresha, K. Pitchumani, *Green Chem.* **2014**, *16*, 2865–2875.

[66] T. Sone, Y. Abe, *Bull. Chem. Soc. Jpn.* **1973**, *48*, 3603-3605.

[67] A. Kar, N. Mangu, H. M. Kaiser, M. Beller, M. K. Tse, *Chem. Commun.* **2008**, 386-388**.**

[68] K. Lee, P. H. Lee, *Tet. Lett.* **2008**, *49*, 4302–4305.

[69] V. Pandarus, G. Gingras, F. Beland, R. Ciriminna, M. Pagliaro, *Org. Process Res. Dev*. **2012,** *16*, 117–122.

[70] L. Xu, B. Yin, H. Huang, M. C. Liu, *Tetrahedron* **2016**, *72*, 2065-2071.

[71] S. Shi, Y. J. Zhang, *Org. Chem.* **2007**, *72*, 5927-5930.

[72] A. Schmidt, A. Rahimi, *Chem. Commun.* **2010**, *46,* 2995-2997.

[73] T. Mahamo, M. M. Mogorosi, J. R. Moss, S. F. Mapolie, J. Slootweg, K. Lammertsma, G. S. Smith, *J. Organomet. Chem.* **2012**, *703*, 34-42.

Chapter-IV

[1] D. Langevin, *Annu. Rev. Phys. Chem.* **1992**, *43*, 341-369.

[2] K. Holmberg, *Eur. J. Org. Chem.* **2007**, 731–742.

[3] M.A. Lopez-Quintela, C. Tojo, M.C. Blanco, L. Garcia Rio, J.R. Leis, *Current Opinion in Colloid & Interface Science* **2004**, *9*, 264-278.

[4] S. E. Friberg, M. Podzimek,*Colloid Polym. Sci.* **1984**, *262*, 252-253.

[5] R. Dario Falcone, N. Mariano Correa, M. Alicia Biasutti, Juana J. Silber, *Langmuir* **2000**, *16* (7), 3070-3076.

[6] K. P. Das, A. Ceglie, B. Lindman, *J. Phys. Chem.* **1987**, *91* (11), 2938-2946.

[7] F. Yan, J. Texter, *Chem. Commun.* **2006**, 2696-2698.

[8] M. Moniruzzaman, N. Kamiya, M. Goto, *Journal of Colloid and Interface Science* **2010**, *352*, 136-142.

[9] M. Moniruzzaman, M. Tamura, Y. Tahara, N. Kamiya, M. Goto, *International Journal of Pharmaceutics* **2010**, *400*, 243-250.

[10] X. Wang, J. Cheng, G. Ji, X. Peng, Z. Luo, *RSC Adv.* **2016**, *6*, 4751-4757.

[11] T. Welton, Chem. Rev. **1999**, *99 (8)*, 2071-2083.

[12] J. P. Hallett, T. Welton, *Chem. Rev.* **2011**, *111 (5)*, 3508-3576.

[13] T. Welton, *Coord. Chem. Rev.* **2004**, *248*, 2459-2477.

[14] T. Welton, *Green Chem.* **2011**, *13* (2), 225.

[15] B. Kar, S. Bardhan, K. Kundu, S. K. Saha, B. K. Paul, S. Das, *RSC Adv.* **2014**, *4*, 21000-21009.

[16] A.S. Chhatre, R.A. Joshi, B.D. Kulkarni, *J. Colloid Interface Sci.* **1993**, *158*, 183-187.

[17] M. Hojo, R. Kato, A. Narutaki, T. Maeda, Y. Uji-yie, *Journal of Molecular Liquids.* **2011**, *163*, 161-169.

[18] F. Currie, K. Holmberg, G. Westman, *Colloids and Surfaces A*: *Physicochem. Eng. Aspects*. 2001, *182*, 321-327.

[19] S. Gupta, A. Chatterjee, S. Das, B. Basu, *J. Chem. Eng. Data.* **2013**, *58*, 1-6.

[20] S. Paul, A. K. Panda, *Colloids Surf. A.* **2013**, *419*, 113-124.

[21] S. Paul, A. K. Panda, *RSC Adv.* **2014**, *4*, 32383-32390.

[22] G. Palazzo, L. Carbone, G. Colafemmina, R. Angelico, A. Ceglie, M. Giustini, *Phys. Chem. Chem. Phys*. **2004**, *6*, 1423-1429.

[23] S. P. Moulik, L. G. Digout, W. M. Aylward, R. Palepu, *Langmuir*. **2000**, *16*, 3101-3106.

[24] O. Zheng, J-X. Zhao, X-M. Fu, *Langmuir.* **2006,** *22*, 3528-3532.

[25] C. Petit, A. S. Bommarius, M-P. Pileni, T. A. Hatton, *J. Phys. Chem.* **1992**, *96*, 4653-4658.

[26] K. Maiti, D. Mitra, R. N. Mitra, A. K. Panda, P. K. Das, A. K. Rakshit, S. P. Moulik, *J. Phys. Chem. B*. **2010**, *114*, 7499-7508.

[27] S. K. Hait, S. P. Moulik, *Langmuir.* **2002**, *18*, 6736-6744.

[28] B. K. Paul, D. Nandy, *J. Colloid Interface Sci.* **2007**, *316*, 751-761.

[29] J. Chai, L. Xu, W. Liu, M. Zhu, *J. Chem. Eng. Data.* **2012**, *57*, 2394-2400.

[30] F. Wang, Z. Zhang, D. Li, J. Yang, C. Chu, L. Xu, *J. Chem. Eng. Data.* **2011**, *56*, 3328-3335.

[31] Z. Zhang, F. Wang , D. Li, J. Yang, *J. Dispersion Science and Technology.* **2012**, *33*, 141–146.

[32] S. Ray, S. R. Bisal, S. P. Moulik, *Langmuir.* **1994***, 10*, 2507-2510.

[33] S. Bardhan, K. Kundu, G. Chakraborty, S. K. Saha, B. K. Paul, *J. Surfact. Deterg.* **2015**, *18,* 547-567.

[34] I. Mukherjee, S. Mukherjee, B. Naskar, S. Ghosh, S. P. Moulik, *Journal of Colloid and Interface Science.* **2013**, *395*, 135-144.

[35] F. Wang, B. Fang, Z. Zhang, L. Qiao, Y. Chen, *J. Chem. Eng. Data.* **2008**, *53*, 1256-1261.

[36] F. Wang, B. Fang, Z. Zhang, S. Zhang, Y. Chen, *Fuel.* **2008**, *87*, 2517-2522.

[37] K. Kundu, S. Bardhan, S. Banerjee, G. Chakraborty, S. K. Saha, B. K. Paul, *Colloids and Surfaces A.* **2015**, *469*, 117-131.

[38] M. A. Pes, K. Aramaki, N. Nakamura, H. Kunieda, *Journal of Colloid and Interface Science.* **1996**, *178*, 666-672.

[39] K. Maiti, I. Chakraborty, S. C. Bhattacharya, A. K. Panda, S. P. Moulik, *J. Phys. Chem. B.* **2007**, *111*, 14175-14185.

[40] O. Zech, S. Thomaier, P. Bauduin, T. Ruck, D. Touraud, W. Kunz, *J. Phys. Chem. B.* **2009**, *113*, 465–473.

[41] D. Blach, J. J. Silber, N. M. Correa, R. D. Falcone, *Phys. Chem. Chem. Phys.* **2013**, *15*, 16746-16757.

[42] D. D. Ferreyra, N. M. Correa, J. J. Silber, R. D. Falcone, *Phys. Chem. Chem. Phys*. **2012**, *14,* 3460–3470.

[43] C. Rabe, J. Koetz, *Colloids and Surfaces A.* **2010**, *354*, 261–267.

[44] O. Rojas, B. Tiersch, S. Frasca, U. Wollenberger, J. Koetz, *Colloids and Surfaces A.* **2010**, *369*, 82–87.

[45] R. E. Riter, J. R. Kimmel, E. P. Undiks, N. E. Levinger, *J. Phys. Chem. B.* **1997**, *101*, 8292-8297.

[46] S. Ghosh, *J. Colloid Interface Sci.* **2011**, *360*, 672–680.

[47] J-L. Lemyre, S. Lamarre, A. Beaupre, A. M. Ritcey, *Langmuir* **2010**, *26(13)*, 10524-10531.

[48] H. Preu, A. Zradba, S. Rast, W. Kunz, E. H. Hardy**,** M. D. Zeidler**,** *Phys. Chem. Chem. Phys.***1999**, *1*, 3321-3329.

[49] C. Tanford, *J. Phys. Chem.* **1972**, *76*, 3020-3024.

[50] N. Haghnazari, C. Karami, K. Ghodrati, F. MalekiInt, *Nano Lett.* **2011**, *1*, 30-33.

Chapter-V

[1] P.M. Holland, D.N. Rubingh, Mixed Surfactant Systems: An Overview, *Vol. 501***,** Ch. 1, *ACS Symposium Series;* American Chemical Society: Washington, DC, **1992**, pp 2-30.

[2] R. Zana, Dynamics of Surfactant Self-Assemblies: Micelles, Microemulsions, Vesicles and Lyotropic Phases, CRC Press, Taylor & Francis Group, Boca Raton, **2005**.

[3] D.N. Rubingh, M. Bauer, Lipase Catalysis of Reactions in Mixed Micelles, *ACS Symposium Series*, American Chemical Society: Washington, DC, **1992**, *Vol. 501*, Ch. 12, pp 210–226.

[4] A. Shome, S. Roy, P. Das, *Langmuir* **2007**, *23*, 4130-4136.

[5] A. Das, R. K. Mitra, *J. Phys. Chem. B* **2014**, *118***,** 5488-5498.

[6] J. Zhang, B. Han, J. Liu, X. Zhang, J. He, Z. Liu, T. Jiang, G. Yang, *Chem.-Eur. J.* **2002**, *8*, 3879-3883.

[7] J. Hao, Self-Assembled Structures: Properties and Applications in Solution and on Surfaces, CRC Press, Taylor & Francis Group, Boca Raton, **2010**.

[8] N. Azum, M.A. Rub, A.M. Asiri, *J. Mol. Liq.* **2016**, *216*, 94-98.

[9] N. Azum, M.A. Rub, A.M. Asiri, H.M. Marwani, *J. Mol. Liq.* **2014**, *197*, 339-345.

[10] N. Azum, M.A. Rub, A.M. Asiri, *Colloids Surf. B* **2014**, *121*, 158-164.

[11] M.A. Rub, F. Khan, N. Azum, A.M. Asiri, H.M. Marwani, *J. Taiwan Ins. Chem. Eng.* **2016**, *60*, 32-43.

[12] N. Azum, M.A. Rub, A.M. Asiri, K.A. Alamry, H.M. Marwani, *J. Disp. Sci. Techn.* **2014**, *35*, 358-363.

[13] K. Ogino, M. Abe (Eds.), Mixed Surfactant Systems, Surfactant Science Series, *vol. 46*, Marcel Dekker, New York, **1993**.

[14] D. Blankschtein, A. Shiloach, *Langmuir* **1998**, *14***,** 1618-1636.

[15] F. D. Souza, B. S. Souza, D. W. Tondo, E. C. Leopoldino, H. D. Fiedler, F. Nome, *Langmuir* **2015**, *31***,** 3587-3595.

[16] R. F. Heck, *J. Am. Chem. Soc.* **1968**, *90,* 5526-5531.

[17] R. F. Heck, *J. Am. Chem. Soc.* **1968**, *90*, 5546-5548.

[18] X.-F. Wu, P. Anbarasan, H. Neumann, M. Beller, *Angew. Chem. Int. Ed.,* **2010**, *49***,** 9047-9050.

[19] J. G. deVries, A. H. M. de Vries, *Eur. J. Org.Chem.* **2003**, *2003***,** 799-811.

[20] T. Dwars, E. Paetzold, G. Oehme, *Angew. Chem. Int. Ed.,* **2005**, *44***,** 7174-7199.

[21] J.-Z. Jiang, C.Cai, *J. Colloid Interface Sci.* **2006**, *299***,** 938-943.

[22] Y. Kasaka, B. Bibouche, I. Volovych, M. Schwarze, R. Schomäcker, *Colloids and Surfaces A,* **2016**, *494,* 49-58.

[23] D. C. Crans, S. Schoeberl, E. Gaidamauskas, B. Baruah, D. A. Roess, *J. Biol. Inorg. Chem*. **2011**, *16***,** 961-972.

[24] J. Tang , Y. Wang , D. Wang, Y. Wang, Z. Xu, K. Racette, F. Liu, *Biomacromolecules* **2013,** *14*, 424-430.

[25] Arkady L. Kholodenko, Jack F. Douglas, *Phys. Rev. E* **1995**, *51*, 1081-1090.

[26] S.P. Moulik, L. Digout, W. Aylward, R. Palepu, *Langmuir* **2000**, *16*, 3101–3106.

[27] R. K. Mahajan, R. Sharma, *J. Colloid Interface Sci.* **2011**, *363,* 275-283.

[28] J. H. Clint, *J. Chem. Soc., Faraday Trans. 1* **1975**, *71***,** 1327–1334.

[29] D. N. Rubingh, in Solution Chemistry of Surfactants, (Ed.), K. L. Mittal, Plenum Press, New York, **1979**, *vol. 1***,** pp. 337.

[30] M.J. Rosen, X.Y. Hua, J. Colloid Interface Sci. **1982**, *86,* 164-172.

[31] M.J. Rosen, Surfactants and Interfacial Phenomena, 2nd ed.; Wiley-Interscience: New York, **1989**; pp 65-68.

[32] W.H. Ansari, N. Fatma, M. Panda, K. Ud-Din, *Soft Matter*, **2013**, *9***,** 1478-1487

[33] R. Sanan, R. Kaur, R. K. Mahajan, *RSC Adv.* **2014**, *4***,** 64877–64889.

[34] C.C. Ruiz, *Colloid Polym. Sci.* **1999**, *277*, 701-707.

[35] T. Chakraborty, S. Ghosh, S.P. Moulik*, J. Phys. Chem. B* **2005**, *109***,** 14813-14823.

[36] M.J. Rosen, S. Aronson, *Coll. Surf.* **1981**, *3*, 201–208.

[37] A. B. Pereiro, J.M.M. Araujo, F. S. Teixeira, I. M. Marrucho, M. M. Pineiro, L.P.N. Rebelo, *Langmuir* **2015**, *31***,** 1283-1295.

[38] A. V. Delgado, F. Gonzalez-Caballero, R. J. Hunter, L. K. Koopal, J. Lyklema, *Pure Appl. Chem.* **2005**, *77***,** 1753-1805.

[39] P.K. Misra, P. Somasundaran, *J. Surfact. Deterg.* **2004**, *7,* 373-378.

[40] S.K. Mehta, S. Chaudhary, *Colloids Surf. B* **2011**, *83***,** 139-147.

[41] E. Odella, R. D. Falcone, J. J. Silber, N. M. Correa, *Phys. Chem. Chem. Phys.* **2014**, *16***,** 15457-15468.

[42] A. Pan, S.S. Mati, B. Naskar, S.C. Bhattacharya, S. P. Moulik, *J. Phys. Chem. B* **2013**, *117***,** 7578-7592.

[43] N. Cheng, P. Yu, T. Wang, X. Sheng, Y. Bi, Y. Gong, L.Yu, *J. Phys. Chem. B* **2014**, *118***,** 2758-2768.

[44] S. Khamarui, D. Sarkar, P. Pandit, D. K. Maiti, *Chem. Commun.,* **2011**, *47***,** 12667-12669.

[45] M. M. Shinde, S. S. Bhagwat, *J. Dispersion Sci. Tech.* **2012**, *33***,** 117-122.

[46] S. Bhattacharya, A. Srivastava, S. Sengupta, *Tetrahedron Letts*. **2005**, *46***,** 3557-3560.

[47] E. Palazzo, L. Carbone, G. Colafemmina, R. Angelico, A. Ceglieb, M. Giustini, *Phys. Chem. Chem. Phys*. **2004**, *6,* 1423-1429.

[48] J.E. Bowcott, J.H. Schulman, *Z. Elektrochem.* **1955**, *59*, 283-290.

[49] B. K. Paul, D. Nandy, *J. Colloid Interface Sci.* **2007**, *316,* 751-761.

[50] K. Kundu, B. K. Paul, *Colloid Polym. Sci.* **2013**, *291***,** 613-632.

[51] H. Preu, A. Zradba, S. Rast, W. Kunz, E. H. Hardy, M. D. Zeidler, *Phys. Chem. Chem. Phys.* **1999**, *1***,** 3321-3329.

[52] O. Zheng, J-X.Zhao, X.-M. Fu, *Langmuir* **2006,** *22,* 3528-3532.

[53] L. Digout, K. Bren, R. Palepu, S. P. Moulik, *Colloid Polym. Sci.* **2001**, *279***,** 655-663.

[54] C. C. Villa, J. J. Silber, N. M. Correa, R. D. Falcone, *Chem. Phys. Chem.* **2014**, *15,* 3097-3109.

[55] S.A. Corcelli, J.L. Skinner, *J. Phys. Chem. A* **2005**, *109*, 6154−6165.

[56] H. Graener, G. Seifert, *J. Chem. Phys.* **1993**, *98*, 36−45.

[57] Z.S. Nickolov, V. Paruchi, D.O. Shah, J.D. Miller, *Colloids Surf. A* **2004**, *232*, 93-99.

[58] S.K. Mehta, G. Kaur, R. Mutneja, K.K. Bhasin, *J. Colloid Interface Sci.* **2009**, *338*, 542-549.

[59] J.-B. Brubach, A. Mermet, A. Filabozzi, A. Gerschel, D. Lairez, M.P. Krafft, P. Roy, *J. Phys. Chem. B* **2001**, *105*, 430-435.

[60] A. Das, A. Patra, R. K. Mitra, *J. Phys. Chem. B* **2013**, *117***,** 3593-3602.

[61] Q. Zhong, D.A. Steinhurst, E.E. Carpenter, J.C. Owrutsky, *Langmuir* **2002**, *18*, 7401-7408

[62] S. Bardhan, K. Kundu, S. Das, M. Poddar, S.K. Saha, B.K. Paul, *J. Colloid Interface Sci*. **2014**, *430***,** 129-139.

[63] C. G.-Blanco, L.J. Rodriguez, M.M. Velazquez, *J. Colloid Interface Sci*. **1999**, *211***,** 380-386.

[64] S. Biswas, S.C. Bhattacharya, B.B. Bhowmik, S.P. Moulik, *J. Colloid Interface Sci.* **2001**, *244*, 145-153.

[65] S. Chatterjee, R.K. Mitra, B.K. Paul, S.C. Bhattacharya, *J. Colloid Interface Sci.* **2006**, *298,* 935–941.

[66] D. M. Willard, N. E. Levinger, *J. Phys. Chem. B* **2000**, *104***,** 11075-11080.

[67] P. Setua, C. Ghatak, V.G. Rao, S.K. Das, N. Sarkar, *J. Phys. Chem. B* **2012**, *116***,** 3704-3712.

[68] B. Kar, S. Bardhan, K. Kundu, S. K. Saha, B. K. Paul, S. Das, *RSC Adv.* **2014**, *4***,** 21000-21009.

[69] M. Hager, U. Olsson, K. Holmberg, *Langmuir* **2004**, *20,* 6107-6115.

[70] N. Li, Q. Cao, Y. Gao, J. Zhang, L. Zheng, X. Bai, B. Dong, Z. Li, M. Zhao, L. Yu, *Chem. Phys. Chem.* **2007**, *8,* 2211-2217

[71] H.U. Blaser, A. Indolese, A. Schnyder, H. Steiner, M. Studer, *J. Mole. Catal. A* **2001**, *173***,** 3–18.

[72] M.A. Haque, T. Kurokawa, J.P. Gong, *Soft Matter* **2012**, *8,* 8008

[73] A.M. Alkilany, P.K. Nagaria, M.D. Wyatt, C.J. Murphy, *Langmuir* **2010**, *26***,** 9328.

[74] B. H. Lipshutz, B. R. Taft, *Org. Lett.* **2008**, *10***,** 1329-1332.

[75] A. L. Compere, W. L. Griffith, and J. S. Johnson, Jr., E. Caponetti, D. Chillura-Martino, and R. Triolo, *J. Phys. Chem. B* **1997**, *101***,** 7139-7146.

[76] P. López-Cornejo, P. Pérez, F. García, R. De la Vega, F. Sánchez, *J. Am. Chem. Soc.* **2002**, *124***,** 5154-5164.

[77] W. Zhang, X. Qiao, J. Chen, *Colloid Surface A.* **2007**, *299***,** 22-28.

[78] G. N. Smitha, P. Browna, C. James, S. E. Rogers, J. Eastoe, *Colloids and Surfaces A* **2016**, *494***,** 194-200.

[79] D. T. McQuade, P. H. Seeberger, *J. Org. Chem.* **2013**, *78***,** 6384−6389.

[80] F. Lopez, G. Cinelli, L. Ambrosone, G. Colafemmina, A. Ceglie, G. Palazzo, Colloids Surf. A **2004**, *237*, 49-59.

[81] K. Holmberg, *Eur. J. Org. Chem.* **2007**, 731–742.

INDEX

REPRINT OF PAPERS

RSC Advances

PAPER

Cite this: *RSC Adv.*, 2014, **4**, 21000

Physicochemical studies of water-in-oil nonionic microemulsion in presence of benzimidazole-based ionic liquid and probing of microenvironment using model C–C cross coupling (Heck) reaction†

Barnali Kar,[a] Soumik Bardhan,[a] Kaushik Kundu,[b] Swapan Kumar Saha,[a] Bidyut K. Paul[b] and Sajal Das*[a]

Received 13th November 2013
Accepted 1st April 2014

DOI: 10.1039/c3ra46632a

www.rsc.org/advances

The present report focuses on the evaluation of the interfacial composition and the thermodynamics of the transfer of 1-pentanol (Pn) from a continuous oil phase to the interface of w/o nonionic microemulsion [Tween-20/Pn/cyclohexane(Cy)/water] in the absence and the presence of an ionic liquid (IL) (1-butyl-3-propylbenzimidazolium bromide) under different physicochemical conditions [*viz.* variation in concentrations of IL (0.0 → 0.20 mol dm^{-3}) and temperature (293 → 323 K] at a fixed molar ratio of water to surfactant (ω) by the Schulman's method of cosurfactant titration at the oil/water interface. The overall transfer process has been found to be spontaneous, exothermic and organized in the absence or the presence of IL, but shown to be influenced by [IL]. The microstructure and state of water organization inside a pool of these systems have been characterized by different experimental techniques, *e.g.*, conductivity, DLS and FTIR in the absence or the presence of IL. In addition, a C–C cross coupling reaction (Heck reaction) has been employed to explore the properties of IL (additive) in the confined environment of the microemulsion *vis-à-vis* its interaction with the constituents of the interface. The reaction progress has been monitored using the above techniques. The reaction ended with the highest yield (75%) in the presence of 0.05 mol dm^{-3} of IL, wherein the microemulsion forms spontaneously with the highest stability.

Introduction

Ionic liquids (ILs) are organic salts/solvents constituted of distinct cations and anions and have low vapor pressure and high thermal and chemical stability. They are non-inflammable and have good catalytic and solvation power.[1] The importance and the application of ILs are reflected by the contribution of different researchers.[2] A number of physicochemical investigations of imidazole-based ILs are available in literature,[3] whereas the study of benzimidazole-based ILs is relatively new and rare.[4] Benzimidazole is an important motif found in both naturally occurring and biologically active compounds. It is an important pharmacophore as well.[5]

In the field of colloid and interface science, the investigation of surfactant molecular assemblies in a room temperature ionic liquid (RTIL) is of great interest because the former systems can solubilize substances that are essentially insoluble in the latter, and thus, the solubilizing power of surfactant assemblies may widen the application of RTILs. From this point of view, the elucidation of the self-assembling phenomena of surfactant molecules in ILs and their applications have become an interesting area of research.[6] Furthermore, IL based microemulsions are used as reaction media in various organic transformations, *viz.* aminolysis of esters,[7] Diels–Alder reaction,[8] and Matsuda–Heck reaction.[9] Water-in-oil (w/o) microemulsions or reverse micelles (RMs) are macroscopically homogeneous mixtures of oil, water, surfactant and/or cosurfactant, whereas at the microscopic level, they consist of individual domains of oil and water separated by a monolayer of the surfactant and/or the cosurfactant. The stability, flexibility and microheterogeneity of microemulsions make them convenient for biological and technological applications.[10] The microstructure of microemulsions critically depends on the system composition, temperature, and additives.[10] Very recently, we have reported the characteristic roles of the surfactant(s), the cosurfactant and

[a]*Department of Chemistry, University of North Bengal, Darjeeling 734 013, India. E-mail: sajal.das@hotmail.com; Fax: +91-0353-2699-001; Tel: +91-0353-2776-381*

[b]*Surface and Colloid Science Laboratory, Geological Studies Unit, Indian Statistical Institute, Kolkata 700 108, India. E-mail: bidyut.isical@gmail.com*

† Electronic supplementary information (ESI) available: Basics of the dilution method, interfacial composition, thermodynamic parameters, plots of conductivity and hydrodynamic diameter. FTIR spectra of O–H band with deconvoluted curves, mechanism of Heck reaction, UV-visible spectra, ^{1}H-NMR and ^{13}C-NMR analysis. See DOI: 10.1039/c3ra46632a

oils for the formation and stabilization of w/o microemulsions in the absence or presence of an additive by employing Schulman's method of cosurfactant titration of the oil/water interface (or, the dilution method).[11–13] Wang *et al.*[14] employed the dilution method for the first time to investigate the physicochemical parameters of [bmim][BF_4]/Brij-35/1-butanol/toluene-based IL/O microemulsion.

In view of these studies, we have undertaken the study of the formation of a water-in-oil (w/o) nonionic surfactant microemulsion, water/Tween-20/Pn/Cy, with special reference to its characteristic features of the oil/water interface under different physicochemical conditions in the absence or presence of IL, 1-butyl-3-propylbenzimidazolium bromide ([bpBzim]Br), as an additive. Thermodynamics of formation, microstructure, transport properties and dynamics of H-bonding of this system, water–IL/Tween-20/Pn/Cy w/o microemulsion, have been investigated by employing the dilution method, conductivity, DLS, and FTIR. Further, an in-depth characterization of the microenvironment of the system in the absence or presence of IL has been made by performing a model C–C cross coupling reaction (Heck reaction). The famous reaction, Heck, is one of the finely studied responses in the meadow of organic synthesis.[15] A report on the study of the Heck reaction in IL-microemulsion is available in literature.[16] The yield of the Heck coupled product depends on the type of surfactant used as well as the nature of confinement of these systems.[9,16] An attempt has been made to monitor the effective physicochemical changes in the microemulsion, leading to microenvironmental changes during the course of reaction. Finally, a correlation of the results in terms of the evaluated physicochemical parameters *vis-à-vis* microstructural features during the Heck reaction has been drawn and provides a new horizon to understand the most plausible location/site as well as to determine the actual reaction parameter required for an effective reaction in the studied micro-heterogeneous system. To the best of our knowledge, such a comprehensive study on w/o microemulsion in the presence of benzimidazole-based IL has not been reported earlier.

Results and discussions

Schulman's cosurfactant titration at the oil/water interface (the dilution method)

In order to underline the influence of IL and its content on the interfacial composition of Tween-20-based w/o microemulsion stabilized in Pn and Cy under various physicochemical conditions (*i.e.*, at different temperatures and a fixed molar ratio of water to the surfactant, ω), n_a^i/n_s values [*i.e.* compositional variations of amphiphiles (both Tween-20 and Pn) at the interface] are plotted against [IL] (0.0 → 0.20 mol dm^{-3}) and the respective plots are depicted in Fig. 1 (inset A). The mathematical evaluation and the results of interfacial composition have been discussed elaborately indicating all possible interactions among the constituents in the microenvironment of this compartmentalized system (depicted in Scheme 1) and are presented in ESI (Sec. A and B) and Fig. S1.†

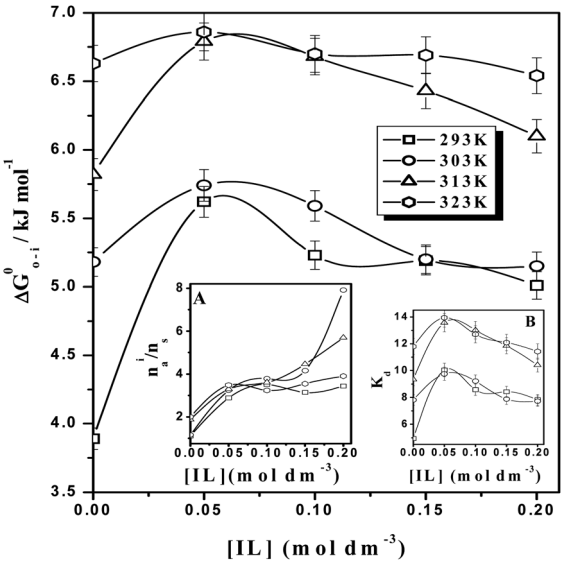

Fig. 1 Plots of $\Delta G^0_{0\rightarrow i}$ as a function of [IL] for water/Tween-20/Pn/Cy microemulsion system at ω (= 30) with varying temperatures. Inset A: plots of interfacial composition (n_a^i/n_s) as a function of [IL] for water/Tween-20/Pn/Cy microemulsion system at ω (= 30) with varying temperatures. Inset B: same plots for K_d.

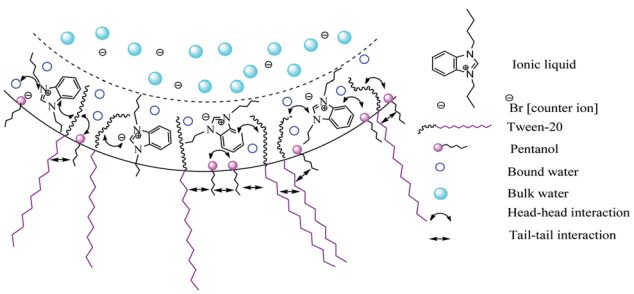

Scheme 1

Thermodynamics of transfer of Pn (oil → interface) (in absence or presence of IL)

In this section, an analysis of the transfer of Pn from the oil phase to the interface (Pn_{oil} → $Pn_{interface}$) of the water (IL)/Tween-20/Pn/Cy microemulsion system by employing the dilution method is presented from a thermodynamic point of view, which is rarely reported.[14,17] The details of the estimation have been given in ESI (Sec. A, eqn (S1)–(S16)).†

Effect of [IL] and temperature on $\Delta G^0_{0\rightarrow i}$

$\Delta G^0_{0\rightarrow i}$ values are negative in the absence or presence of IL, and hence, spontaneous formation of w/o microemulsions is suggested. Both similar and dissimilar values of this energetic parameter under comparable physicochemical conditions are reported.[14,17–19] Both K_d and $\Delta G^0_{0\rightarrow i}$ show maxima in the presence of 0.05 mol dm^{-3} of IL at each temperature (Fig. 1 and inset B).

Although the variations of K_d and $\Delta G^0_{0\rightarrow i}$ values between 0.05 mol dm^{-3} and 0.10 mol dm^{-3} may be small at higher temperatures (*viz.* 313 and 323 K), both the values are still higher at 0.05 mol dm^{-3} as compared to the other concentrations of IL (Fig. 1 and inset B, Table S1†). This indicates that the transfer process of Pn from the oil phase to the interface is much favoured at 0.05 mol dm^{-3} of IL irrespective of the temperature. Further, a low line secondary maximum in K_d or $\Delta G^0_{0\rightarrow i}$ values appears at 0.15 mol dm^{-3} of [IL] (Fig. 1, including the error bars). A plausible explanation for this type of trend can be explained from the view of the physicochemical (molecular) interactions among the constituents involved in the transfer process of Pn (oil → interface).[11,12,14,17] In this system, the interaction between the nonionic surfactant (Tween-20) and the alkanol (Pn) is of the dipole–dipole or dipole-induced dipole or London dispersion type, because of the presence of uncharged or neutral hydroxyl groups and POE chains (Tween-20); in contrast, the interaction between [bpBzim]$^+$ and Pn is possibly of the ion–dipole type. An ion–dipole interaction is much stronger than dipole–dipole or dipole-induced dipole or London dispersion interactions.[20] Therefore, the association between Pn and Tween-20 becomes more favorable in the presence of 0.05 mol dm^{-3} of [bpBzim][Br]. Consequently, the transfer process of Pn from the oil phase to the interface is much favoured at 0.05 mol dm^{-3} of [IL] irrespective of the temperature. However, at a higher IL concentration (*i.e.*, 0.10 → 0.20 mol dm^{-3}), the addition of IL diminishes the interfacial area per polar head group of surfactant molecules by screening the steric repulsion between nonionic surfactants (herein, Tween-20), and this makes the interfacial layer more rigid and favors a greater curvature of the interface.[14,17] As a result, the attractive interaction among the droplets decreases, and subsequently, the transfer process of Pn (oil → interface) is diminished. However, the appearance of a low line secondary maximum at [IL] that is equal to 0.15 mol dm^{-3} is likely to be originated from the non-ideality of the systems. Usually, different types of forces (*viz.* London dispersion forces, dipole–dipole forces, and dipole–dipole induced forces) act on real mixtures, making it difficult to predict the properties of such solutions. Non-ideal mixtures are identified by determining the strength and types (specifics) of intermolecular forces (*viz.* intermolecular forces between similar molecules and intermolecular forces between dissimilar molecules) in that particular system.[21] However, non-ideal behavior is not uncommon in multicomponent derived microemulsion systems.[22–26]

Further, it has been observed that K_d or $\Delta G^0_{0\rightarrow i}$ gradually increases with an increase in temperature (Fig. 1 and inset B); this suggests that the transfer of Pn (oil → interface) is much favored at higher temperatures. The higher absolute values of $\Delta G^0_{0\rightarrow i}$ at higher temperatures indicate a comparatively stronger interaction between Tween-20 and Pn at the interface, which corroborates well with the interfacial composition (Fig. 1, inset A). This trend corroborates well with the reports of Zhang *et al.*[18] and Wang *et al.*[14] for [bmim][BF_4]/CTAB/alkanol/toluene and [bmim][BF_4]/Brij-35/1-butanol/toluene w/o microemulsion systems, respectively. However, the overall scenario indicates a tendency towards the formation of a more spontaneous w/o microemulsion accompanied with 0.05 mol dm^{-3} of IL, as evident from K_d and $\Delta G^0_{0\rightarrow i}$ values at each temperature (Table S1,† Fig. 1 and inset B).

Further, a significant difference in the K_d or $\Delta G^0_{0\rightarrow i}$ values has been observed for 303 K and 313 K (Fig. 1 and inset B). This may be due to the influence of temperature on the constituents (particularly, on Tween-20 consisting of POE chains as polar head groups and IL as an organic electrolyte, [bpBzim][Br]), and hence, two different mechanisms might be operative for the formation of microemulsions in the lower temperature region (*i.e.*, 293 and 303 K) as well as in the higher temperature region (*i.e.*, 313 and 323 K). The ordered structure formed from IL molecules around the hydrophilic moiety (POE chains) of Tween-20, produced by an ionic interaction instead of a hydrogen bonding interaction, is considered to be an origin for the surfactant self-assembly[27] as represented in Scheme 1. It is obvious that Tween-20 molecules assemble to form reverse micelles in order to avoid the entropy loss due to the ordered arrangement of IL molecules in the low temperature region. On the other hand, in the higher temperature region, the IL molecules participating in the ionic interaction with POE chains of Tween-20 may be less ordered (more disordered) due to their enhanced dehydration.[27,28] Hence, it is imperative that the enthalpy loss for the release of solvated IL molecules be overcome by the enthalpy gain for the contact of POE chains in the higher temperature region. The reversal of entropy and enthalpy parameters might occur during the transition from the low temperature region (293 and 303 K) to the high temperature region (313 and 323 K). This is why, a significant difference in $\Delta G^0_{0\rightarrow i}$ values has been observed for two sets of temperatures.

Effect of [IL] and temperature on $\Delta H^0_{0\rightarrow i}$ and $\Delta S^0_{0\rightarrow i}$

Due to the nonlinear dependence of $(\Delta G^0_{0\rightarrow i}/T)$ on $(1/T)$ (the result fits a two degree polynomial equation (Fig. S2†)), at each composition of the surfactant (at [IL] = 0.0 → 0.20 mol dm^{-3}), four values of the standard enthalpy change, $\Delta H^0_{0\rightarrow i}$ and the standard entropy change ($\Delta S^0_{0\rightarrow i}$) of the Pn transfer process (oil → interface) at four different temperatures have been evaluated according to eqn (S12) and (S15)† and are presented in Table S1† and Fig. 2. For a pure Tween-20 system (*i.e.*, in the absence of IL), the overall transfer process is exothermic at all experimental temperatures with a negative entropy change (more ordered) in Cy (Table S1† and Fig. 2). Therefore, Pn causes heat release during the transfer process. Consequently, the negative entropy change may be due to more organization of the interface and its surroundings. Therefore, it may be argued that in the presence of Pn and Tween-20, the interface to some extent becomes ordered. A similar observation was also reported by Bardhan *et al.*[12] for water/Brij-35/Pn/IPM microemulsion systems. However, De *et al.*[29] and Kundu *et al.*[11] reported an opposite behavior (*i.e.*, positive enthalpy and entropy changes) for Tween-20/Bu or Pn/Hp/water and Brij-58 or Brij-78/Pn/Hp or Dc/water microemulsion systems, respectively. Hence, the difference in the trends of $\Delta H^0_{0\rightarrow i}$ and $\Delta S^0_{0\rightarrow i}$ may be attributed to the differences in the hydrophobic configuration and/or the

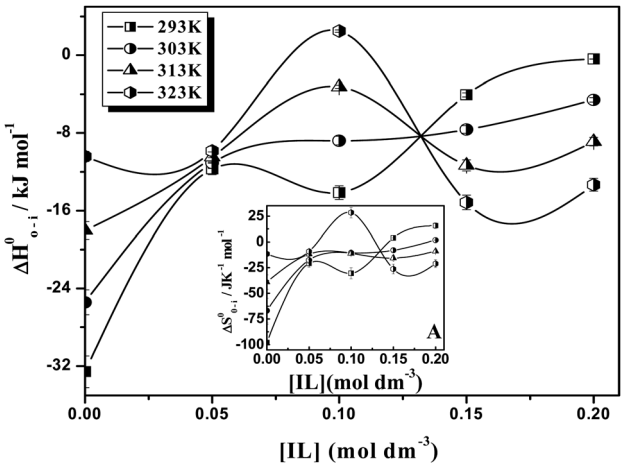

Fig. 2 Plots of $\Delta H^0_{0\rightarrow i}$ as a function of [IL] for water/Tween-20/Pn/Cy microemulsion system at ω (= 30) and varying temperatures. Inset A: same plot for $\Delta S^0_{0\rightarrow i}$.

size of the polar head group of the nonionic surfactants *vis-à-vis* the type of oil.

Further, it can be observed from Table S1† and Fig. 2 that, the overall transfer process is exothermic at all the experimental temperatures with negative entropy change (order) in Tween-20/Pn system in the presence of IL ([IL] = 0.05 → 0.20 mol dm^{-3}). Such a negative enthalpy or entropy change was observed by Mukherjee *et al.*[19] for triisobutyl (methyl) phosphoniumtosylate/IPM/trihexyl (tetradecyl) phosphoniumbis 2,4,4-(trimethylpentyl) phosphinate–isopropanol or butanol systems. It is quite likely that the negative contribution towards $\Delta H^0_{0\rightarrow i}$ is identified with the transfer of the surfactant tail from water to liquid hydrocarbon state in the interfacial layer and for restoring the hydrogen bonding structure of the water around the surfactant head group.[30] Further, it can be argued for negative entropy, $\Delta S^0_{0\rightarrow i}$ as follows: during formation of nano-droplets in w/o microemulsions, the penetration of water into the oil (Cy)/Tween-20/Pn (amphiphiles) continuum forming cavity and subsequently, organization of the amphiphiles at the droplet interface results in an increase in overall order with negative entropy of the multicomponent system.[31] Further, – $\Delta S^0_{0\rightarrow i}$ suggests that both entropy as well as enthalpy are involved in the transfer process.[32] Consequently, IL dependent microemulsion compositions with larger – $\Delta H^0_{0\rightarrow i}$ values (more exothermic) results in larger – $\Delta S^0_{0\rightarrow i}$ values (ordered) *i.e.*, greater interaction between the constituents at the interface, leading to more ordered interface due to transfer of Pn (oil → interface).[33]

The variation of $\Delta H^0_{0\rightarrow i}$ and $\Delta S^0_{0\rightarrow i}$ values with temperatures from Table S1† and Fig. 2 indicates that the presence of IL influences the degree of exothermicity with orderliness of the transfer process (oil → interface). Interestingly, the transfer process approaches towards less exothermic as well as less ordered with increase in temperature up to 0.10 mol dm^{-3} of IL, and thereafter, the degree of exothermicity and orderliness reverses in the vicinity of 0.136 mol dm^{-3}. Subsequently, the process is more exothermic as well as more ordered with increase in temperature at [IL] equals to 0.15 and 0.20 mol dm^{-3} (Fig. 2). This trend can be explained in the following way: the addition of IL to Tween-20 based microemulsions might have at least two effects. First, the partial reduction of the hydration of water around the polar head group of the non-associated surfactant molecule occurs with increase in temperature. As a result, a decrease in the energy needed for breaking down this structure during the process of microemulsion formation and also for a decrease in the exothermic contribution *i.e.*, decrease in the value of $\Delta H^0_{0\rightarrow i}$. The second consequence of the presence of higher IL concentrations appears to be related to the influence of counter ion binding on the structure of the microemulsions.[34] The reduction in disorder may be attributed to the effect of the liberation of surfactant hydration water molecules on microemulsification to be less important than the loss of freedom when monomers join each other to form reverse micelles.[35]

Also, $\Delta S^0_{0\rightarrow i}$ values have been found to increase up to 0.10 mol dm^{-3} of IL with temperature, and thereafter, a reversal of trend has been observed in the vicinity of 0.136 mol dm^{-3}, as in the case of $\Delta H^0_{0\rightarrow i}$ (Fig. 2, inset A). This result is indeed interesting. It is quite likely that molecular interactions, arising from the tendency of the water molecules to regain their normal tetrahedral structure, and the attractive dispersion forces between hydrocarbon chains act cooperatively to remove the hydrocarbon chains from the water cages, leading to the disorder of water, and subsequently, increase in the entropy values.[36,37] On the other hand, the decrease in entropy may be due to the breakdown of the normal hydrogen-bonded structure of water accompanied by the formation of water with different structures.[36,37] The presence of a higher concentration of hydrophilic species (herein, IL) promotes an ordering of water molecules in the vicinity of the hydrophilic head group of Tween-20.[36] However, no significant change in both thermodynamic parameters (*i.e.*, $\Delta H^0_{0\rightarrow i}$ and $\Delta S^0_{0\rightarrow i}$) with temperature has been observed at certain IL concentrations (*i.e.*, at 0.05 and ~0.136 mol dm^{-3}), leading to the formation of isoenthalpic and isoentropic microemulsion systems (Fig. 2 and inset A). A similar observation was also reported earlier for mixed surfactant microemulsion systems consisting of cationic or anionic–nonionic structures.[11,12,38]

Effect of [IL] on $(\Delta C^0_p)_{0\rightarrow i}$

Since $\Delta H^0_{0\rightarrow i}$ is a function of temperature, the $(\Delta C^0_p)_{0\rightarrow i}$ values have been evaluated for these systems (in the absence or presence of IL) from the slope (= $\delta\Delta H^0_{0\rightarrow i}/\delta T$) of the plots of $\Delta H^0_{0\rightarrow i}$ *vs.* T (not illustrated) according to eqn (S11†).[12] All these values are presented in Table S1.† It can be observed from Table S1† that, at [IL] = 0.0 → 0.10 mol dm^{-3}, $(\Delta C^0_p)_{0\rightarrow i} > 0$; whereas, $(\Delta C^0_p)_{0\rightarrow i} < 0$ at [IL] = 0.15 and 0.20 mol dm^{-3}. Negative values are usually observed for the self-association of amphiphiles and can be attributed to the removal of large areas of non-polar surface from contact with water on the formation of reverse micelles.[39] However, $(\Delta C^0_p)_{0\rightarrow i}$ tends to almost zero at [IL] = 0.05 and ~0.136 mol dm^{-3}, which corroborates well with the profile of $\Delta H^0_{0\rightarrow i}$ *vs.* [IL] at different temperatures (Fig. 2). This

indicates the formation of temperature-insensitive microemulsions at [IL] of 0.05 and ~0.136 mol dm^{-3}. Similar observation [*i.e.*, reversal of trend of $(\Delta C_p^0)_{0\rightarrow i}$ with concentration of methanol] was reported earlier by Perez-Casas *et al.*[40] for water/AOT/methanol/decane reverse micelles. Kunz *et al.*[41] reported that the formation of temperature-insensitive microemulsions is important for some practical purposes (*e.g.* for formulation of a product).

Electrical conductivity and dynamic light scattering measurement

The electrical conductivity, size and size distribution of w/o microemulsion systems have been measured by conductometric and DLS, respectively, for a water/Tween-20/Pn/Cy microemulsion system with the variation of [IL] (= 0.0 → 0.20 mol dm^{-3}) at a constant ω (= 30) and fixed temperature (303 K). The results are depicted in Fig. S3.† It can be observed from Fig. S3† that the electrical conductivity gradually increases with an increase in [IL] in the microemulsion. This trend may be attributed to the high conducting nature of IL, as the blank experiment (similar concentration of IL in water) shows an identical trend with the variation of [IL] (Fig. S3,† inset A). It can be observed that the conductance values in the water–IL media range from 0.0016 to 8.2 mS cm^1, whereas low values (17.84–231.0 μS cm^1) are obtained for IL in microemulsions at similar concentrations. The low value in the microemulsion system can be justified as follows: in the present system, the electrostatic interaction between the imidazolium cation of IL and the electronegative oxygen atoms of the POE units of Tween-20 is quite likely to occur along with the water–IL hydrogen bonding interaction (Scheme 1). However, the latter part, *i.e.*, a water–IL hydrogen bonding interaction is present in the bulk IL or water–IL media. The electrostatic interaction makes the palisade layer comprising Tween-20/Pn/IL more rigid[42] and subsequently, decreases the conductance values. Hence, it can be concluded that the physicochemical properties of water molecules localized in the interior of the microemulsions are different from those of the water–IL media.

Further, the hydrodynamic diameter (D_h) of a microemulsion droplet decreases from 3.90 nm to 2.31 nm with an increase in [IL] (0.0 → 0.20 mol dm^{-3}) wherein about a 3 fold increase of the droplet count rate has been observed under the prevailing condition (Fig. S3,† inset B and C). The droplet count rate is directly proportional to the droplet number of the microemulsion system. Hence, the addition of IL shrinks the droplet size and thereby, increases the droplet number. It was reported earlier that the curvature of the oil/water interface of a microemulsion can be adjusted by adding IL (a class of organic electrolyte)[43] or NaCl (inorganic electrolyte)[44] at different concentrations. The addition of electrolyte gives rise to a decrease in the repulsive interaction between the head groups of the nonionic surfactant, Tween-20, which further increases the packing parameter of the surfactant molecules ($P = v/al$, where 'v' and 'l' are the volume and the length of a hydrophobic chain, respectively, and 'a' is the area of the polar head group of the surfactant) and decreases the droplet diameter. In addition, the presence of IL within the water pool weakens the hydrogen-bonding between water and the POE chains of Tween-20, thereby reducing the hydration of POE chains, which results in the formation of smaller droplets due to a decrease in the swelling of the POE chains.[45] In other words, when IL is solubilized in microemulsions, it decreases the average area occupied by each head group of surfactant (Tween-20) and subsequently enhances the packing density and rigidity of the surfactant monolayer of the droplet, which may reduce the size of the droplets.[46] Typical values of the polydispersity index (PDI) obtained here are in the range between 0.1–0.2, which indicates the monodispersity of the sample.[12,13,38]

FTIR spectroscopy

Reports on the properties of the encapsulated water in the range of the size and type of w/o microemulsions by studying the states of water organization using an FTIR measurement, are available in literature.[13,37,41,47] The characteristics of the water molecules in a confined environment of w/o microemulsion depend strongly on the water content or the droplet size and the nature of the interface as well.[47,48] As discussed in the previous section, the values of the hydrodynamic diameter of a droplet (D_h) varies from 3.90 nm to 2.31 nm as a function of [IL] (0.0 → 0.20 mol dm^{-3}) at fixed ω (= 30) and temperature (= 303 K) from DLS measurements. Further, the values of the hydrodynamic diameter of a droplet (D_h) are well comparable with those of microemulsion systems, wherein the existence of different types/states of water species is reported in a confined environment by using an FTIR measurement.[47,49] However, the influence of Pn (cosurfactant) on the O–H stretching vibration of the confined water needs to be underlined for the present system. To eliminate the effect of Pn on the O–H vibration of water, the spectra of Pn at the same concentration are subtracted from the spectral intensity of the O–H stretching band, and the differential spectra have been analyzed. Different types of hydrogen bonded water molecules exist in reverse micelles, which can be broadly classified into two major classes, namely, bound and bulk-like water molecules.[13,37,41,50] The differential spectra obtained in the present study have been deconvoluted into two peaks at ~3500 and ~3300 cm^1, corresponding to the O–H stretching frequency of the bound and bulk-like water molecules, respectively (Fig. S4†), and a representative result of deconvolution (relative abundance of different water species) is depicted in Fig. S5.† It is observed from Fig. S5† that the bound water proportion is the least in the absence of IL. In contrast, the proportion of bound water increases with an increase in [IL] in the microemulsion. These results indicate the significant role of IL in determining the proportion of different water species (bound and bulk) in the confined environment of w/o microemulsion. However, this result is not very surprising if one considers the possibility of interaction between IL and water molecules. With an increase in the IL content, more bulk water molecules hydrate IL molecules and subsequently, increase the proportion of bound water molecules in the microemulsion core.[42] Further, it is evident from the DLS measurements that the droplet size decreases with an increase in the IL content. It

is reported that as the droplet size decreases, the bound water proportion increases in the microemulsion and *vice versa*.[47,50] Hence, DLS and FTIR results corroborate each other.

Study of C–C cross coupling (Heck) reaction in microemulsion

A model Heck reaction (Scheme 2) has been performed in the well characterized system (presented herein), to explore the properties of IL (additive) within the restricted geometry provided by microemulsions and the nature of interaction of the IL with the constituents of the interface and the subsequent changes in the microenvironment during the reaction and the detection of the most probable reaction site and yield of the Heck reaction. The reaction progress was monitored by employing various instrumental techniques such as, conductance, FTIR, and UV-visible spectroscopy.

Standardization of Heck coupling reaction

The reaction has been performed in the presence of different bases (inorganic and organic) to optimize the reaction at 323 K. It has been found that water soluble bases (potassium carbonate and tetramethyl ethelene diamine) produce an almost comparable yield (30% and 40%, respectively) of the desired product, whereas the highest yield (75%) has been achieved using a sparingly water soluble base, *viz.*, triethyl amine (TEA) (Table S2†). Hence, a subsequent study on the Heck reaction in microemulsion media at varying [IL] (0.0 → 0.2 mol dm^{-3}) was performed in the presence of TEA as the base, and the standard mechanism of the Heck coupling reaction is presented in Scheme S1.†

In order to underline the effect of encapsulation or compartmentalization (provided with microemulsion), the Heck reaction has also been performed in bulk IL (water–IL media) containing [IL] similar to that available in microemulsions, and the results are presented in Table 1. The study showed (Table 1) that the yield of the desired product in water–IL media was very low in comparison with that in the microemulsion systems. The strong effect of the confined environment of the microemulsion, therefore, seems to play a vital role in studying this reaction.[9] However, the yield of the final product in the microemulsion is not a direct function of the IL concentration (Table 1). The reaction has also been critically monitored in the case of two different temperature-insensitive formulations at [IL] = 0.05 and 0.136 mol dm^{-3} (discussed in the previous section, "Effect of [IL] on $(\Delta C_p^0)_{0\rightarrow i}$", Fig. 2). The yield of the final product has been found to be the highest in the lower range of [IL] (*i.e.*, at 0.05 mol dm^{-3}), at which the highest spontaneity of the Pn transfer process and temperature-insensitivity were exhibited (Fig. 1 and 2). However, in the higher range of [IL] (*i.e.*, at ~0.136 mol dm^{-3}), the yield is the least, where another temperature-insensitive formulation is obtained. Hence, it can be suggested that the temperature insensitive composition is not the sole factor affecting the product yield; rather, the highest spontaneity of the Pn transfer (oil → interface) leads to the highest yield of the product.

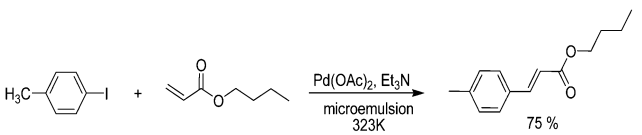

Scheme 2

Table 1 Heck coupling reaction in both water and microemulsion media (water/Tween-20/Pn/Cy) as a function of [IL] in the presence of TEA at a fixed ω (= 30) and 323 K

Ionic liquid (mol dm^{-3})	Yield (%) in water–IL	Yield (%) in microemulsion
0.00	07.0	17
0.05	04.5	75
0.10	06.8	25
0.136	08.3	13
0.15	10.0	59
0.20	12.0	22

Conductance study

Electrical conductance of the w/o microemulsion system has been measured at regular intervals during the course of reaction both in the absence and in the presence of IL, and the results are displayed in Fig. 3. In both cases, the trend of the conductance curve is almost identical with smaller values in the absence of IL. In the absence of IL, the addition of palladium acetate [$Pd(OAc)_2$] results in a small increase in conductance due to the presence of a charge carrier (*viz.* $Pd(OAc)_2$) and is followed by a decrease in conductivity, which may be due to the formation of the aqua palladium complex in the mixture.[51]

On the contrary, in the presence of IL, the addition of $Pd(OAc)_2$ decreases the conductivity indicating the formation of a palladium complex (Pd–NHC) with IL, the precursor of N-heterocyclic carbene (NHC).[52] However, the process of Pd–NHC complexation is much faster in comparison with the palladium–aqua complexation which subsides the conducting properties of $Pd(OAc)_2$. However, a sharp increase in conductivity has been

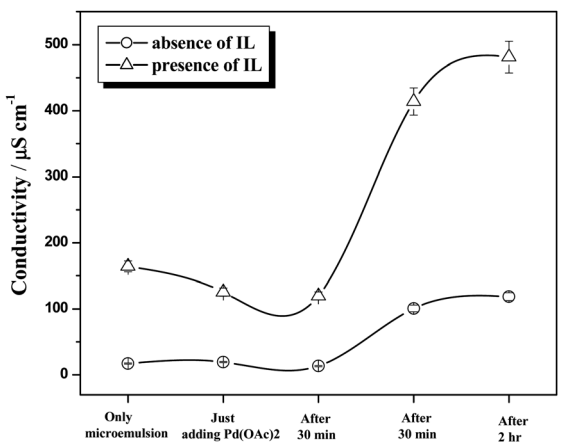

Fig. 3 The conductivity of microemulsion in absence and presence of IL (= 0.05 mol dm^{-3}) at regular intervals during Heck reaction at 323 K.

observed in both cases after the addition of reagents (4-iodotoluene, triethylamine and butylacrylate), implying the progress of the Heck reaction.

FTIR measurement

The FTIR observation studies during the reaction (Fig. 4) are very supportive of the conductivity experiment. The addition of palladium acetate reduces the amount of bound water and indicates the formation of a Pd–NHC complex which decreases the interaction with water molecules. Further, the optimal decrease of bound water implies the end point of complexation. Thereafter, a regular enhancement of the amount of bound water has been observed with the addition of reagents (4-iodotoluene, triethylamine and butylacrylate), indicating the formation of the Heck product and the other possible side products (such as halogen acid and the corresponding amine salt). This trend continues until the completion of reaction.

UV-visible spectroscopy

Comparing the UV-visible spectra of individual components and the spectra recorded during the course of reaction at regular intervals of time, a single absorption peak at 271 nm has been observed after 10 minutes of the reaction (Fig. S6†). The λ_{max} value of the product is reported to be 274 nm.[53] The little decrease in λ_{max} of the product from that of the literature value may be due to the H-bonding between the ester group of the product and the reaction medium. The absorption became more intense after 40 minutes of reaction. The intensity of the spectral band increases with the progress of the reaction, indicating an increase in the concentration of the product with the progress of time.

Comprehension of the results

The Heck reaction was carried out in the w/o microemulsion with a varying amount of IL (0.0 → 0.20 mol dm^{-3}), and the corresponding results are presented in Table 1. The optimal concentration of IL required for an effective Heck reaction is 0.05 mol dm^{-3} in the present system. Further, it is evident from the dilution method that the spontaneity of formation with maximization in the stability of the microemulsion system can be achieved with 0.05 mol dm^{-3} of IL (Table S1† and Fig. 1). It is obvious that 0.05 mol dm^{-3} of IL facilitates the Pn transfer process (oil → interface) due to the favorable organization of the constituents at the interface and thereby, results in achieving more stability, which leads to better performance of the Heck reaction in a microemulsion medium. The decrease in the conductance with the addition of palladium acetate [Pd(OAc)$_2$] indicates the formation of a palladium complex (Pd–NHC) with IL (Fig. 3). The FTIR study also supported the formation of the Pd–NHC complex which reduces the number of IL molecules inside the water pool and thereby decreases the amount of bound water (Fig. 4). The ratio between the amounts of bound and bulk water indicates that no interaction persists between water and the newly formed Pd–NHC complex. However, it can be concluded that the availability of the Pd–NHC complex inside the water pool is the least. In bulk IL, *i.e.*, water–IL media, the possibility of the Pd–NHC complex formation is negligible because of the instability of N-heterocyclic carbene in water; this subsequently reduces the rate of the forward reaction. It can be inferred from the low yield of the desired product in the water–IL media indicates that the formation of the stable Pd–NHC complex during the performance of Heck reaction in compartmentalized systems plays a pivotal role, which leads to higher yields as compared to the corresponding bulk [IL] (Table 1). In addition, the use of water soluble bases (*viz.*, K_2CO_3 and TMEDA) which are quite likely to be located in the water pool of microemulsion, results in a low yield of the desired product. In contrast, TEA is preferentially soluble in Pn, as revealed by the solubility analysis, and ends up with the best results (75% yield of the product) (entry 2, Table S2†). A plausible explanation emerges from the increase in the population of Pn at the interfacial region *vis-à-vis* its interaction with TEA, which rationalizes the availability of all constituents involved in this reaction. It can be inferred that apart from the molecular interactions of the constituents involved in the formation of the microemulsion as a template (discussed in ESI (Sec. B†)), two types of interactions are likely to occur at the oil/water interface or in the palisade layer of the microemulsion. For example, (i) the dipole–dipole interaction between Pn and TEA, which enhances the availability of TEA in the interfacial region with an increasing population of Pn at the interface, and (ii) water binding to TEA to form a surrounding OH^- base in the following fashion [eqn (1)]:[54]

$$(C_2H_5)_3N + H_2O \leftrightarrow (C_2H_5)_3N\cdot H_2O \leftrightarrow (C_2H_5)_3NH^+ + OH^- \quad (1)$$

Hence, small amounts of OH^- are likely to have entered the palisade layer of the microemulsion, and subsequently, a basic environment develops in the peripheral region of the interface, which is essentially required for the Heck reaction (Scheme 2 and S1†) and a good yield of the product is achieved. However, the correlation between [IL] and the reaction yield is not straightforward. After getting the utmost yield of 75% at [IL] (= 0.05 mol dm^{-3}), the reaction yield decreases to 25% at

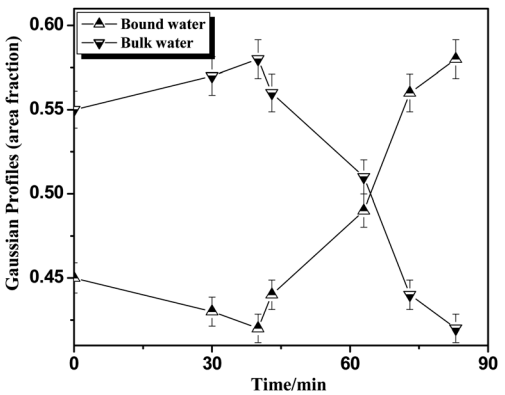

Fig. 4 The variation of Gaussian profiles (area fraction) of the normalized spectra of different water species (bound water and bulk water) of IL containing a (0.05 mol dm^{-3}) w/o microemulsion system with the reaction time.

[IL] (= 0.10 mol dm^{-3}) and shows a further increase (59%) at [IL] (= 0.15 mol dm^{-3}). As stated earlier, a low line secondary maxima in K_d and $\Delta G^0_{0\rightarrow i}$ values appear at 0.15 mol dm^{-3} of [IL] after achieving the highest values at 0.05 mol dm^{-3} of [IL] (Fig. 1) and the second highest yield of the Heck product has been found at the same IL concentration (= 0.15 mol dm^{-3}) (Table 1). K_d and $\Delta G^0_{0\rightarrow i}$ values actually signify the spontaneity of the Pn transfer process from the bulk to the interface. Hence, it is probable that the accumulation of Pn at the interface governs the availability of TEA and OH in the vicinity of the interface as well as tunes the interfacial characteristics to different degrees by an interaction with IL (of different contents), which influences the yield of the desired Heck product. Gayet *et al.*[9] reported that the IL content affects the yields of the Matsuda–Heck reaction in reverse microemulsions. All these observations together imply that the most plausible location or site of the Heck reaction in the studied microheterogeneous system is the interfacial region. However, the present report is not comprehensive from the viewpoint of the direct correlation between the IL content and the reaction yield (herein, the Heck couple product). However, this is trivial as a maximum in both K_d and $\Delta G^0_{0\rightarrow i}$ values was obtained at 0.05 mol dm^{-3} and we compare the maximum values of physicochemical parameters (K_d and $\Delta G^0_{0\rightarrow i}$) with those of the highest yield of the Heck product at the same concentration of [IL]. Several factors, such as changes in molecular interactions between the constituents at the interface, microstructure, and polarity due to the presence of phenyl group in IL with the variation in [IL], might be responsible for the overall yield of the final product. Further studies in this direction by employing SANS, ^{1}H-NMR along with two-dimensional rotating frame Nuclear Overhauser Effect (NOE) experiments (ROESY) are warranted.

Experimental

Materials and methods

Polyoxyethylenesorbitanmonolaurate (Tween-20, ≥99%), palladium acetate [$Pd(OAc)_2$, ≥99.98%] and 4-iodo-toluene ($CH_3C_6H_4I$, ≥99%) were purchased from Sigma Aldrich, USA. 1-Pentanol (Pn, ≥99%) and cyclohexane (Cy, ≥98%) were the products of Fluka, Switzerland. Triethyl amine (TEA, ≥99.5%) and *n*-butyl acrylate were purchased from Merck, Germany. All these chemicals were used without further purification. The IL, 1-butyl-3-propylbenzimidazolium bromide ([bpBzim]Br), was synthesized in accordance with our reported method.[4] Doubly distilled water of conductivity less than 3 μS cm^{-1} was used in the experiments.

The dilution experiment was performed to investigate the interfacial composition of the Tween-20 based microemulsion under different physicochemical conditions, as described earlier[11–14,17] by using the spectrophotometric technique[55] to measure the change in the sample turbidity produced by Pn addition (Fig. S7†). The details of the spectrophotometric technique are provided in our previous report.[12] Basics of the dilution method and thermodynamics of the transfer of the cosurfactant from oil to the interface have been dealt in ESI (Sec. A†).

Conductivity measurements were performed using Mettler Toledo (Switzerland) Conductivity Bridge. The instrument was calibrated with a standard KCl solution. The uncertainty in the conductance measurement was within ±1%.

DLS measurements were carried out using Zetasizer Nano ZS90 (ZEN3690, Malvern Instruments Ltd, U.K.). He–Ne laser having a wavelength of 632.8 nm was used, and the measurements were made at a scattering angle of 90°. Details of the measurement have been provided in our previous report.[12,13]

FTIR absorption spectra were recorded in the range of 400–4000 cm^1 with a Shimadzu 83000 spectrometer (Japan) by using a CaF_2-IR crystal window (Sigma-Aldrich) equipped with a press lock holder with 100 number scans and a spectral resolution of 4 cm^1. The deconvolution of spectra was performed using the Origin software.

Three milliliters of microemulsion (water/Tween-20/Pn/Cy) containing IL (0–0.20 mol dm^{-3}) at ω (= 30) and 4.48 mg (0.02 mmol, 4 mol%) $Pd(OAc)_2$ were taken in a 25 ml round bottom flask and the mixture was placed in a preheated oil bath at 323 K for 30 minutes with constant stirring. Thereafter, 109 mg (0.5 mmol) of 4-iodotoluene, 76.8 mg (0.6 mmol) of *n*-butylacrylate and 101.12 mg (1 mmol) of triethylamine (TEA) were introduced into it, and the resulting mixture was heated at 323 K for 45 minutes. The resulting multicomponent solution shows no instability towards temperature or otherwise. The progress of the reaction was monitored by silica gel thin layer chromatography (TLC). In addition, conductance, FTIR, and UV-Vis spectroscopy were employed to characterize the microenvironment of the microemulsion with the progress of the reaction. The yield of the Heck coupled product was determined by HPLC. Finally, the product was characterized by ^{1}H-NMR and ^{13}C-NMR (ESI, Sec. C†). A similar experiment was performed in the water–IL media (bulk IL) at the corresponding [IL] as used in the microemulsion system.

Conclusions

The present study is focused on the characterization of a quaternary water-in-oil microemulsion comprising of Tween-20, Pn and Cy in the absence and presence of IL, 1-butyl-3-propylbenzimidazolium bromide ([bpBzim]Br), with a detailed description of the interfacial composition as a function of the transfer of Pn from a bulk oil phase to the interface on the system composition. Synergism in the distribution constant (K_d) and $-\Delta G^0_{0\rightarrow i}$ has been observed in the vicinity of 0.05 mol dm^{-3} of IL at each temperature (293, 303, 313 and 323 K). This indicates that the transfer process of Pn from the oil phase to the interface is more favoured at 0.05 mol dm^{-3} of IL irrespective of the temperature. The standard enthalpy change ($\Delta H^0_{0\rightarrow i}$) and the standard entropy change ($\Delta S^0_{0\rightarrow i}$) of the transfer process have been found to be negative [*i.e.*, exothermic process with less disorder (organized)] in the absence or presence of IL at all the experimental temperatures. Further, a temperature-insensitive microemulsion has been formed at [IL] of 0.05 and ~0.136 mol dm^{-3}. FTIR study reveals an increase in

the proportion of bound water molecules with increasing [IL]. This shows the significant role of IL in determining the states of different water species (bound and bulk) in the confined environment of the w/o microemulsion.

Additionally, an in-depth characterization of the microenvironment of the w/o microemulsion in the presence of IL has been made during the performance of the model C–C cross coupling (Heck) reaction. The reaction ends up with the highest yield in the presence of 0.05 mol dm^{-3} of IL, wherein the Pn transfer process is reported to be the most spontaneous as evident from the physicochemical and thermodynamic parameters obtained by the dilution method. All findings of the present investigation, starting from the simple titrimetric method to sophisticated instrumentations, lead to the conclusion that the most plausible reaction location/site is the interfacial region of the w/o microemulsion, where the population of all the active ingredients of both the template and the Heck reaction impart stability to the system. The confinement of IL (as additive) improved the reactivity of the Heck reaction, which can be used in various domains, such as biocatalysts or nanomaterial synthesis.[9] The understanding of physicochemical parameters and interactions during the progress of the organic reaction in the w/o microemulsion has implications for the design of suitable reaction media for organic synthesis.

Acknowledgements

We thank the Council of Scientific & Industrial Research, New Delhi for financial support (02(0022)/11/EMR-II). BK and SB are thankful to UGC for their fellowship. The financial support in the form of an operating research grant to BKP and Senior Research Fellowship to KK from the authority of Indian Statistical Institute, Kolkata, India are thankfully acknowledged.

Notes and references

1 C. Patrascu, F. Gauffre, F. Nallet, R. Bordes, J. Oberdisse, N. de Lauth-Viguerie and C. Mingotaud, *ChemPhysChem*, 2006, **7**, 99–101.
2 F. Zhou, Y. Liang and W. Liu, *Chem. Soc. Rev.*, 2009, **38**, 2590–2599.
3 H. Tokuda, K. Hayamizu, K. Ishii, Md. A. B. H. Susan and M. Watanable, *J. Phys. Chem. B*, 2005, **109**, 6103–6110.
4 S. Gupta, A. Chatterjee, S. Das, B. Basu and B. Das, *J. Chem. Eng. Data*, 2013, **58**, 1–6.
5 Y. Özkay, Y. Tunalı, H. Karaca and İ. Işıkdağ, *Eur. J. Med. Chem.*, 2010, **45**, 3293–3298.
6 W. Kunz, T. Zemb and A. Harrar, *Curr. Opin. Colloid Interface Sci.*, 2012, **17**, 205–211.
7 M. Andújar-Matalobos, L. García-Río, S. López-García and P. Rodríguez-Dafonte, *J. Colloid Interface Sci.*, 2011, **363**, 261–267.
8 H. Lu, X. An, J. Yu and X. Song, *J. Phys. Org. Chem.*, 2012, **25**, 1210–1216.
9 F. Gayet, C. E. Kalamouni, P. Lavedan, J.-D. Marty, A. Brûlet and N. L.-d. Viguerie, *Langmuir*, 2009, **25**, 9741–9750.
10 *Microemulsion-background, New Concepts, Applications, Perspectives*, ed. C. Stubenrauch, Blackwell, Oxford, 2009.
11 K. Kundu, G. Guin and B. K. Paul, *J. Colloid Interface Sci.*, 2012, **385**, 96–110.
12 S. Bardhan, K. Kundu, S. K. Saha and B. K. Paul, *J. Colloid Interface Sci.*, 2013, **402**, 180–189.
13 S. Bardhan, K. Kundu, B. K. Paul and S. K. Saha, *Colloids Surf., A*, 2013, **433**, 219–229.
14 F. Wang, Z. Zhang, D. Li, J. Yang, C. Chu and L. Xu, *J. Chem. Eng. Data*, 2011, **56**, 3328–3335.
15 X.-F. Wu, P. Anbarasan, H. Neumann and M. Beller, *Angew. Chem., Int. Ed.*, 2010, **49**, 9047–9050.
16 G. Zhang, H. Zhou, J. Hu, M. Liu and Y. Kuang, *Green Chem.*, 2009, **11**, 1428–1432.
17 S. Paul and A. K. Panda, *Colloids Surf., A*, 2013, **419**, 113–124.
18 Z. Zhang, F. Wang, D. Li and J. Yang, *J. Dispersion Sci. Technol.*, 2012, **33**, 141–146.
19 I. Mukherjee, S. Mukherjee, B. Naskar, S. Ghosh and S. P. Moulik, *J. Colloid Interface Sci.*, 2013, **395**, 135–144.
20 R. Zhang, L. Zhang and P. Somasundaran, *J. Colloid Interface Sci.*, 2004, **278**, 453–460.
21 R. H Petrucci, F. G. Herring, J. D. Madura and C. Bissonnette, *General Chemistry: Principles and Modern Applications*, Pearson/Prentice Hall, Upper Saddle River, N.J., 9th edn, 2007.
22 B. J. Shiau, D. A. Sabatini, J. H. Harwell and D. Q. Vu, *Environ. Sci. Technol.*, 1995, **30**, 97–103.
23 J. L. Salager, E. Vasquez, J. C. Morgan, R. S. Schechter and W. H. Wade, *Soc. Pet. Eng. J.*, 1979, **19**, 107–115.
24 P. M. Holland and D. N. Rubingh, *J. Phys. Chem.*, 1983, **87**, 1984–1990.
25 J. F. Rathman and J. F. Scamehorn, *Langmuir*, 1987, **3**, 372–377.
26 K. Kawakami, T. Yoshikawa, Y. Moroto, E. Kanaoka, K. Takahashi, Y. Nishihara and K. Masuda, *J. Controlled Release*, 2002, **81**, 65–74.
27 T. Inoue, K. Kawashima and Y. Miyagawa, *J. Colloid Interface Sci.*, 2011, **363**, 295–300.
28 T. Inoue and Y. Iwasaki, *J. Colloid Interface Sci.*, 2010, **348**, 522–528.
29 M. De, S. C. Bhattacharya, A. K. Panda and S. P. Moulik, *J. Dispersion Sci. Technol.*, 2009, **30**, 1262–1272.
30 J. Łuczak, C. Jungnickel, M. Joskowska, J. Thöming and J. Hupka, *J. Colloid Interface Sci.*, 2009, **336**, 111–116.
31 S. Ray and S. P. Moulik, *J. Colloid Interface Sci.*, 1995, **173**, 28–33.
32 S. Ghosh, A. D. Burman, G. C. De and A. R. Das, *J. Phys. Chem. B*, 2012, **115**, 11098–11112.
33 K. Khougaz, Z. Gao and A. Eisenberg, *Langmuir*, 1997, **13**, 623–631.
34 B. Šarac and M. Bešter-Rogač, *J. Colloid Interface Sci.*, 2009, **338**, 216–221.
35 J. L. López-Fontán, A. González-Pérez, J. Costa, J. M. Ruso, G. Prieto, P. C. Schulz and F. Sarmiento, *J. Colloid Interface Sci.*, 2006, **297**, 10–21.
36 G. Liu, D. Gu, H. Liu, W. Ding and Z. Li, *J. Colloid Interface Sci.*, 2011, **358**, 521–526.

37 M. Tomsic and A. Jamnik, in *Microemulsions: Properties and Applications*, ed. M. Fanun, Taylor and Francis, CRC Press, USA, 2009, pp. 143–181.
38 S. Bardhan, K. Kundu, B. K Paul and S. K. Saha, *J. Colloid Interface Sci.*, 2013, **411**, 152–161.
39 S. K. Mehta, S. Chadhary and K. K. Bhasin, *J. Colloid Interface Sci.*, 2008, **321**, 426–433.
40 S. Perez-Casas, R. Castillo and M. Costas, *J. Phys. Chem. B*, 1997, **101**, 7043–7054.
41 P. Bauduin, D. Touraud and W. Kunz, *Langmuir*, 2005, **21**, 8138–8145.
42 Y. A. Gao, N. Li, L. Q. Zheng, X. T. Bai, L. Yu, X. Y. Zhao, J. Zhang, M. W. Zhao and Z. Li, *J. Phys. Chem. B*, 2007, **111**, 2506–2513.
43 L. Liu, P. Bauduin, T. Zemb, J. Eastoe and J. Hao, *Langmuir*, 2009, **25**, 2055–2059.
44 R. Leung and D. O. Shah, *J. Colloid Interface Sci.*, 1987, **120**, 330–334.
45 C.-L. Chang and H. S. Fogler, *Langmuir*, 1997, **13**, 3295–3307.
46 D. Liu, J. Ma, H. Cheng and Z. Zhao, *Colloids Surf., A*, 1998, **135**, 157–164.
47 J.-B. Brubach, A. Mermet, A. Filabozzi, A. Gerschel, D. Lairez, M. P. Krafft and P. Roy, *J. Phys. Chem. B*, 2001, **105**, 430–435.
48 R. K. Mitra, S. S. Sinha, P. K. Verma and S. K. Pal, *J. Phys. Chem. B*, 2008, **112**, 12946–12953.
49 S. S. Narayanan, S. S. Sinha, R. Sarkar and S. K. Pal, *Chem. Phys. Lett.*, 2008, **452**, 99–104.
50 I. R. Piletic, D. E. Moilanen, D. B. Spry, N. E. Levinger and M. D. Fayer, *J. Phys. Chem. A*, 2006, **110**, 4985–4999.
51 J. Vicente and A. Arcas, *Coord. Chem. Rev.*, 2005, **249**, 1135–1154.
52 (*a*) S. Gupta, B. Basu and S. Das, *Tetrahedron*, 2013, **69**, 122–128; (*b*) S. Gupta, P. Ghosh, S. Dwivedi and S. Das, *RSC Advances*, 2014, **4**, 6254.
53 S.-J. Sung, K.-Y. Cho, H. Hah, J. Lee, H.-K. Shim and J.-K. Park, *Polymer*, 2006, **47**, 2314–2321.
54 N. Li, Q. Cao, Y. Gao, J. Zhang, L. Zheng, X. Bai, B. Dong, Z. Li, M. Zhao and L. Yu, *ChemPhysChem*, 2007, **8**, 2211–2217.
55 E. Abuin, E. Lissi and K. Olivares, *J. Colloid Interface Sci.*, 2004, **276**, 208–211.

ChemPubSoc Europe

DOI: 10.1002/slct.201601986

Chemistry SELECT Full Papers

Organic & Supramolecular Chemistry

A Fast and Additive Free C–C Homo/Cross-Coupling Reaction in Reverse Micelle: An Understanding of Role of Surfactant, Water Content and Base on the Product Yield and Reaction Site

Barnali Kar,[a] Soumik Bardhan,[a] Prasanjit Ghosh,[a] Bhaskar Ganguly,[a] Kaushik Kundu,[b, c] Sonali Sarkar,[a] Bidyut Kumar Paul,[b] and Sajal Das*[a]

A fresh modus operandi was designed for additive and ligand free transition metal-catalyzed C–C homo/cross-coupling reactions of arylboronic acid in reverse micellar (RMs) templates. Three RMs based on different charge types of polar head groups and length of hydrophobic moieties of surfactants [e.g., anionic (AOT), cationic (DDAB), and non-ionic (TX 100)] in cyclohexane were chosen herein. The reaction proceeded rapidly in these RMs and completed within 10 minutes at ambient condition. Performance of reaction in terms of yield of the desired product in RMs, was correlated with various physicochemical parameters of these systems as obtained from conductance, DLS and FTIR techniques. The results revealed that AOT is best suited for further studies. The progress of the reaction with time was monitored in AOT RMs as supplementary study by using above mentioned methods. It was emphasized that types of base and catalyst, water content influenced the product yield and plausible reaction location. Finally, the development of a series of symmetrical and unsymmetrical biaryl *via* above reaction in AOT RM was explored successfully.

INTRODUCTION

Biaryls are important structural motifs, available in various natural products, ligands, drug molecules and functional materials. Various distinct classes of therapeutic molecules are containing biaryl framework.[1] Biaryls are also known to have potential as antitumor,[2] and antihypertensive agents.[3] Several synthetic methods have been developed so far for the construction of biaryl skeletons through C–C coupling reactions. The field of C–C homo/cross coupling reactions is dominated by palladium catalyst.[4–11] Use of additive is very common in palladium catalyzed homocoupling reaction of arylboronic acid. In addition to the palladium (Pd) catalysis, some gold (Au)[12,13] copper (Cu)[14] and manganese [Mn(III)][15] catalyzed homocoupling reactions of arylboronic acids have also been reported. But the common problems associated with these methods are high temperature and long reaction time.[12] In view of these, searching a suitable medium for studying these types of reactions is warranted.

Reverse micelles (RMs) can execute as an excellent biomimetic model since it provide local hydrophilic moiety in an organic phase resembling to biological membranes of the amphiphilic phospholipids. The water pool of the RM provides a compartmentalized environment with properties considered to be similar to those found at polar/non-polar interfaces in vivo.[16] In the confined region, free movement of water molecules is restricted and the three-dimensional hydrogen-bonded network is disrupted.[17] The dynamics of confined water in the vicinity of biomacromolecules are believed to be responsible for many biological functions, such as molecular recognition and enzymatic catalysis.[18] In view of these, RMs are reported to be used as microreactors to study a variety of organic reactions[19–22] and yield of the product(s) depend on the type of surfactant used, also on the nature of confinement in RMs.[19–21] Thus, the task specific RMs can, therefore, be formulated by judicious selection of the ingredients. Very recently, we have reported the Pd-NHC catalyzed Heck reaction in ionic liquid based w/o non-ionic microemulsions/RMs.[22] Highest yield of the coupled product was obtained where microemulsion formed spontaneously with maximum stability. Sometimes, surfactant monolayer also plays vital role in controlling the reaction dynamics in confined environment by attracting reagents at the interfacial region which was considered as the reaction site.[19–22] Hence, a wide scope prevails to study organic reactions in RMs comprising surfactants with different charge types [*viz.* anionic, AOT, (sodium 1,4-bis(2-ethylhexyl)sulfosuccinate, Na(DEHSS)), cationic, DDAB (didodecyldimethylammonium bromide) and non-ionic TX-100 (t-octylphenoxypolyethoxy ethanol)] with variation in configura-

[a] *B. Kar, Dr. S. Bardhan, P. Ghosh, B. Ganguly, S. Sarkar, Dr. S. Das*
Department of Chemistry, University of North Bengal, Darjeeling 734 013, India;
E-mail: sajal.das@hotmail.com
[b] *Dr. K. Kundu, Prof. B. K. Paul*
Surface and Colloid Science Laboratory, Geological Studies Unit, Indian Statistical Institute, Kolkata 700 108, India
[c] *Dr. K. Kundu*
Department Inorganic and Physical Chemistry, Indian Institute of Science, Bangalore-560012, India

Supporting information for this article is available on the WWW under http://dx.doi.org/10.1002/slct.201601986

tion of polar head groups and hydrophobic moieties (Scheme 1,) under varied physicochemical conditions. the variation in electron withdrawing groups in arylhalides (Cl^-, Br^- and I^-) and bond strength between C-halides.

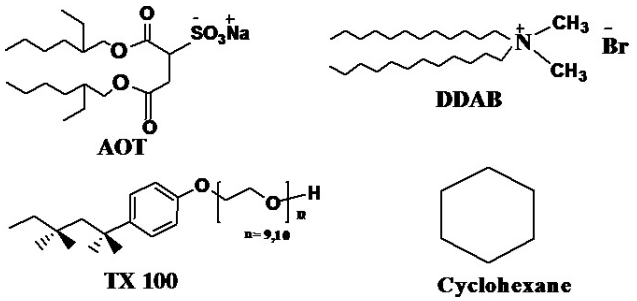

Scheme 1. Molecular structures of AOT, DDAB, TX-100 and cyclohexane.

RESULTS AND DISCUSSION

Before going to discuss about the construction of C–C bond and design of different organic motif through the transition metal catalyzed additive free C–C homo/cross-coupling reaction in reverse micellar media at ambient condition, first we emphasize on the microstructural and microenvironmental characteristics of the templates viz. anionic, cationic and non-ionic surfactant based reverse micelles (RMs).

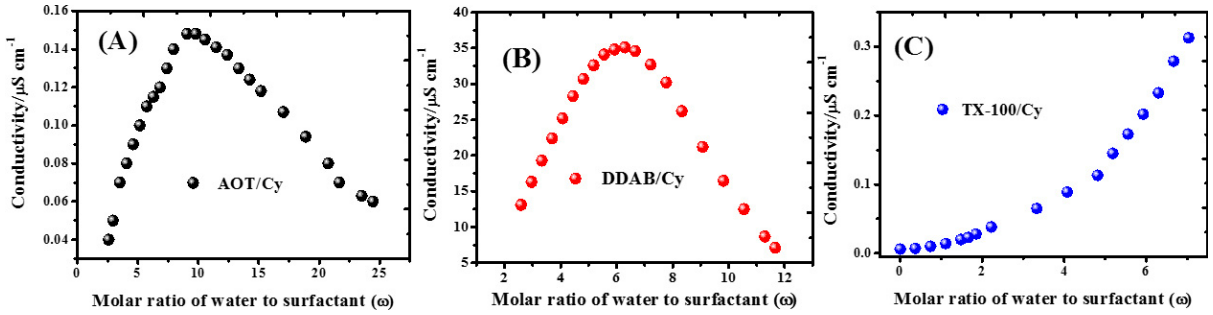

Figure 1. The variation of electrical conductivity as a function of water content (ω) for AOT (A), DDAB (B) and TX-100 (C) RMs, respectively in cyclohexane (Cy) at 303 K..

Cyclohexane (Cy) has been chosen as bulk phase for convenient extraction of the final products.

This report has been emphasized on the construction of C–C bond with special reference to the transition metal catalyzed additive free C–C homo/cross-coupling reaction of arylboronic acid (herein, phenylboronic acid was selected as a model compound) in these reverse micellar gallows at ambient condition. At the outset, all these RMs (stabilized by surfactants of different molecular structures and physicochemical properties etc. mentioned earlier) have been characterized by employing conductance, DLS and FTIR techniques in order to provide an outline on the performance of the reaction as well as a comparative output of the final product in terms of the yield. Further, a series of studies were undertaken to perform above mentioned reaction in the medium which produces highest yield (herein, AOT/Cy RM) to find out a more suitable base (which is essential for this type of reaction) and also, variation of the yield as a function of water content (ω) under optimized conditions. A rationale on the progress of the reaction(s) in constrained environment of AOT RM and the possible reaction site, have also been assessed by employing conductance, DLS and FTIR techniques. Finally, it was contemplated to explore the construction of unsymmetrical biaryl *via* Suzuki-Miyaura cross-coupling reaction of aryl halides with phenylboronic acid (28 different entries) in AOT RM using the same protocol. The yield of the coupled products has been discussed in view of

Formation and Characterization of anionic, cationic and non–ionic RMs

The anionic AOT, cationic DDAB and nonionic TX-100 surfactants are well-known emulsifiers and envisioned for the formulation of RMs in cyclohexane by exploiting the same.[7–12] All the measurements were performed at a fixed surfactant concentration, [S_T] of 0.5 mol dm^{-3} at 303 K.

Conductivity measurement

Electrical conductivity is a structure sensitive property of water-in-oil (w/o) microemulsions/RMs. The existence of microstructural regimes, namely spherical droplets and aggregated clusters, can be predicted from the nature of the plots[23] Figure 1. (A, B and C) shows the variation of electrical conductivity as a function of water content (ω) for AOT/Cy, DDAB/Cy and TX-100/Cy RMs, respectively at 303 K.

It can be seen from the Figure 1. A that the conductivity of AOT/Cy RM increases upon increasing ω at the initial stage. After reaching a maximum (at $\omega = 10$), it decreases until phase separation. The low-conductance behavior and also, a maximum in conductivity in this medium can be explained as follows:[24,25] At low water content, the solubilized water

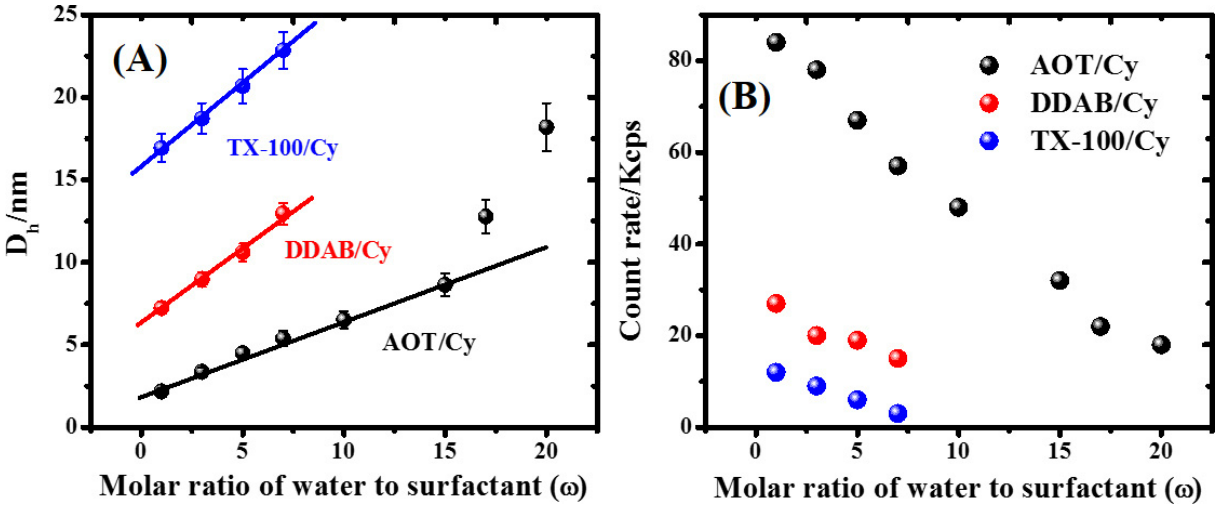

Figure 2. The variation of droplet size (A) and droplet count rate (B) for AOT, DDAB and TX-100-Cy blended RMs as a function of water content (ω) at a fixed temperature (303 K). .

molecules, which are mainly encapsulated in nanosized domains, are preferably involved in ion hydration and associate to Na^+ and head groups tightly. Some of these Na^+ ions bind to the surfactant reside in close proximity of the oil/water interface or palisade layer and hence, they are immobilized, which makes the aqueous environment quite rigid. The surfactant aggregates approach and fuse to form a short-lived dimer and subsequently, they separate to form two new isolated droplets. During this process, the counter ions randomly redistribute and give rise to separately charged droplets, which migrate in the oil-rich medium under an electrical field and result in the low conductance.[26,27] The appearance of maximum in conductivity is an outcome of several antagonistic effects that influence the conductance behaviors of the system. The added water tends to form water pools in the cores of nanodroplets as the water content exceeds the demand for hydrating surfactant headgroups and counter ions. With increase in water solubilization, the hydrated counter ions exchange and redistribute readily during the process of droplet collision and transient fusion, which contributes to the increase in conductivity.[27] An analogous variation in conductance i.e. appearance of bell-shaped curve with a maximum in conductivity (at $\omega = 6$), has been observed for DDAB/Cy RM as a function of ω, as shown in Figure 1B and can be attributed to charge fluctuation.[28] The conductivity of DDAB RMs show higher values than that of AOT based RM and the maxima in conductance occur at lower water content (ω) (Fig 1A and B). Different types of (i) polar head groups and counter ions of AOT ($DEHSS^-/Na^+$) and DDAB (DDA^+/Br^-), (ii) size of polar head groups (55 A^{02} for AOT/ 68 A^{02} for DDAB) and (iii) penetration of their polar head groups inside the water pool and constitution of the interface *vis-a-vis* its flexibility or rigidity might be effective for above variation in conductance.[29,30] However, TX-100/Cy RM shows gradual increase in conductivity with increase in ω. However, no maximum in conductivity was observed even at high water content (in the presence of 0.9% NaCl) till phase separation, [31] as illustrated in Figure 1C. This reflects a regular buildup of an infinite network containing connected or fused droplets in TX-100 RMs.

Dynamic light scattering measurement

A DLS experiment allows the droplet size determination of the RMs, and is also, competent to identify populations with distinct size distributions, and therefore, reveals the presence/formation of aggregates.[32] In view of this, the size and size distributions of RM droplets are measured by DLS technique. Figure 2 (A, B) depicts the variation of droplet size and droplet count rate for AOT, DDAB and TX-100 based RMs in cyclohexane as a function of water content (ω) at a fixed temperature (303 K). The hydrodynamic diameter (D_h) of RM droplet increases with increase in water content (ω) for all the RMs whereas decrease of the droplet count rate has been observed under the prevailing condition, keeping other parameters constant [Figure 2 (A, B)]. Bardhan et al. reported that the droplet count rate is directly proportional to the droplet number of the RMs.[33,34] Hence, it clearly indicates the swelling behaviour of RMs and aggregation of smaller droplets into large one and thereby, increases the droplet size and decreases the droplet number with the addition of water. Further, the results clearly indicated that D_h follows the order: $RM_{AOT} < RM_{DDAB} < RM_{TX\text{-}100}$ at comparable ω (up to 7.0) whilst droplet count rate shows reverse trend [Figure 2A and B)].

The droplet size of RMs depends, among many other variables, on the surfactant packing parameter (P).[23] Such phenomena could be attributed to the variation in an effective packing parameter of surfactant, v/al_c, in which v and l_c are the volume and the length of the hydrocarbon chain, respectively, and a is the head group area of surfactant.[27,35,36] It is noteworthy that the polar head group area (a) of the nonionic surfactant (herein, TX-100) is larger than that of cationic (DDAB) and/or anionic (AOT) surfactant as nonionic surfactant pos-

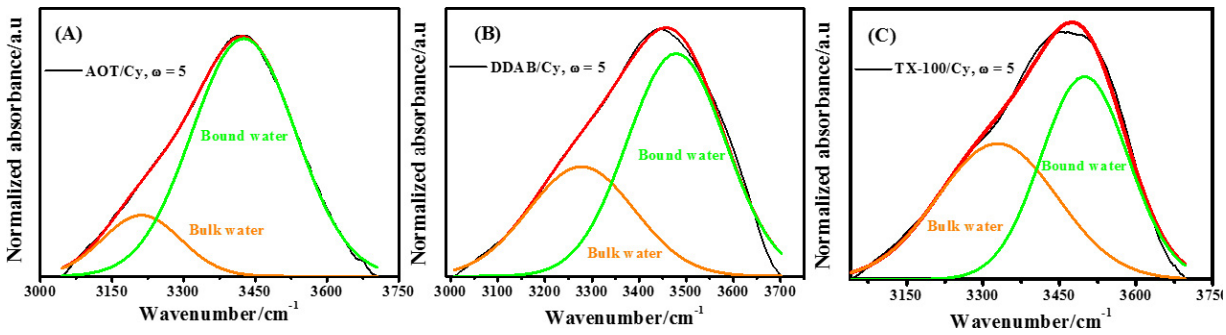

Figure 3. Representative normalized (normalized to intensity of 1.0) FTIR spectra of O–H band for AOT (A), DDAB (B) and TX-100 (C) - Cy blended RMs at a fixed water content ($\omega = 5$) and temperature (303 K). Specification: Experimental spectra (black curve), overall fitted line (red) and deconvoluted curves (bulk water (orange), bound water (green)..

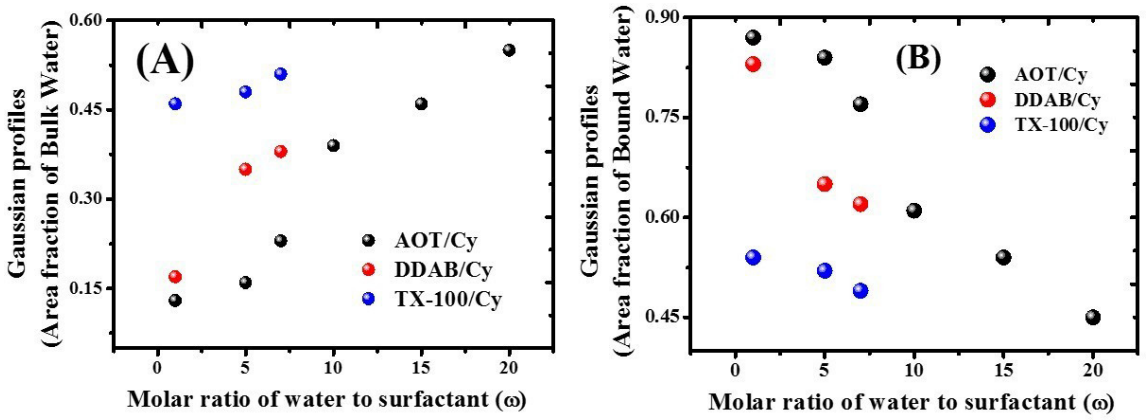

Figure 4. The relative abundance [Gaussian profiles (area fraction)] of different water species [bulk (A) and bound (B)] in AOT, DDAB and TX-100/Cy blended RMs as a function of ω.

sesses long polyoxyethylene chain (9/10-POE chains) as polar head thereby decrease the value of effective packing parameter (P).[37,38] It gives rise to an increase in radius of the droplets in nonionic RMs (herein, TX-100).[27,33] It can be inferred that variation in D_h of these RMs depends on type and size of polar head groups and hydrophobic moieties of surfactant (AOT, DDAB and TX-100), which influence the formation of reverse aggregates (Figure 2 A). Moreover, the linear variation of droplet size as function of ω indicates that the droplets do not interact each other and are probably spherical. The deviation from linearity as evident for AOT RMs at higher ω value (> 10) is due to several factors. Of these, the most relevant one being enhanced droplet-droplet interaction and shape of the RMs.[39]

FTIR spectroscopy

Reports on the properties of the encapsulated water in a range of size and charge type of RMs by studying the states of water organization using FTIR measurement, are available in literature.[22,34,40–43] We have measured mid infrared region (MIR) FTIR spectra for different RMs in cyclohexane as a function of water content (ω) and the temperature (303 K). We focus our attention to the 3000–3800 cm^{-1} frequency window as this is a fingerprint region for the symmetric and asymmetric vibrational stretch of O – H bonds in water.[44–46] It is well known that the nanoscopic confinement and droplet size have a strong impact on water hydrogen bond network dynamics regardless of the nature of the interface in RMs. Different types of hydrogen bonded water molecules exist in RMs which can broadly be classified into two major classes, namely, bound and bulk-like water molecules.[40–43] Hence, FTIR spectra of O–H band of water for AOT, DDAB and TX-100 derived RMs have been analyzed and deconvoluted into two peaks at ~3450 and ~3250 cm^{-1}, corresponding to the O–H stretching frequency of the bound and bulk-like water molecules, respectively. A representative result of deconvolution (relative abundance of different water species) is depicted in Figure.3 A, B and C.[40–43]

The relative abundance [Gaussian profiles (area fraction)] of different water species in these systems as a function of ω is presented in Figure 4. It reveals that the relative abundance of bulk water increases and that of bound water decreases with increasing water content vis-à-vis droplet size (D_h) for all the RMs. Actually, once water is added to a RM forming system, a portion of the water goes to the interface and hydrates the head groups of surfactants till they become fully hydrated at a certain ω. Further addition of water goes primarily to the inner

core, leading to a continuous increase in the fraction of unbounded free bulk like water with increase in ω.[47] Interestingly, it reveals from Figure 3 and 4 that the bound water proportion is the least in TX-100 formed RMs. Whereas, the proportion of bound water increases in presence ionic surfactant (AOT or DDAB) derived RMs and follows the order: $RM_{TX\text{-}100} < RM_{DDAB} < RM_{AOT}$. These results indicate a significant role of surfactant charged types and polar head group in determining the proportion of different water species (bound and bulk) in the confined environment of RMs. Uncharged head group nonionic surfactant (herein, POE chain of TX-100) interacts less strongly with the water molecules as does the ionic surfactant head groups (DDAB and AOT), thereby decreasing the population of bound type water molecules in TX-100 formed RMs.[48] Further, the surface area per AOT head group is larger, leading to its interactions with more water molecules and increased water penetration at the interface of AOT RMs leading to water-ester interactions by intermolecular H-bonding vis-à-vis highest bound water population.[49] It is noteworthy that lowest D_h of AOT RMs also subsidizes the highest bound water population as decreasing droplet size increases the bound water proportion in RMs and vice versa.[22,33,34]

Standardization of Homocoupling reaction

In preceding paragraphs, AOT, DDAB and TX-100 RMs in cyclohexane show considerable difference in physicochemical characteristics which depend on the charge types, configuration of polar head groups and hydrophobic moieties of surfactant under varied conditions, as evident from conductivity, DLS and FTIR measurements. In view of all these aspects an attempt has been made to compare the effect of different types of RMs on the reaction yield and also, to find out the best combination of RM medium and the base required for effective C–C homocoupling reaction of arylboronic acid which is albeit a major part of presentation of this section. Herein, phenylboronic acid was selected as a model compound for homocoupling reaction.

Triton X-100 RMs in cyclohexane can solubilize maximum amount of water only up to ω (molar ratio of water to surfactant) equals to 7 at a fixed surfactant concentration, $[S_T]$ of 0.5 mol dm^{-3}. Hence, identical hydration level and $[S_T]$ of other two surfactants (viz. AOT and DDAB) has been chosen to underline the comparative efficacy and the corresponding results are summarized in Table 1.

Both nonionic TX 100 and cationic DDAB based RMs responded well and resulted in good yield (64% and 75%, respectively) of desired homo-coupled product (Table 1; entry 3, 4). However, highest yield (81%) was obtained in presence of anionic AOT under identical condition. In addition, the yields of the product are also measured in the constituents of these formulations as media (Table 1; entries 1, 2). Both water and cyclohexane results in low yield compared to RM, Hence, it may be concluded that AOT, DDAB and TX-100 surfactants are quite competent to tune the architecture of RMs starting from the interfacial film to the confined environment (water pool) in a different way due to their inherent characteristics and subsequently, effect the reaction yield at comparable physicochemical condition.[34,50]

Table 1. Optimization of reaction condition for homocoupling reaction in RMs.[a]

Entry	Solvent	ω	Base	Yield(%)d
1	Cy[b]		K_2CO_3	50
2	H_2O[b]		K_2CO_3	62
3	Water/TX-100/Cy[c]	7	K_2CO_3	64
4	Water/DDAB/Cy[c]	7	K_2CO_3	75
5	Water/AOT/Cy[c]	7	K_2CO_3	81
6	Water/AOT/Cy[c]	5	K_2CO_3	73
7	Water/AOT/Cy[c]	10	K_2CO_3	88
8	Water//AOTCy[c]	15	K_2CO_3	91
9	Water/AOT/Cy[c]	20	K_2CO_3	82
10	Water/AOT/Cy[c]	15	Na_2CO_3	86
11	Water/AOT/Cy[c]	15	Cs_2CO_3	96
12	Water/AOT/Cy[c]	15	K_3PO_4	93
13	Water/AOT/Cy[c]	15		86
14[e]	Water/AOT/Cy[c]	15	Cs_2CO_3	<10

[a]Reaction Condition: Phenylboronic acid (1 mmol), base (2 mmol), $Pd(OAc)_2$ (2 mol%), solvent (3 ml), reaction was carried out at 303 K for 10 minutes; [b]Reaction was continued for overnight; [c]Water/surfactant/oil RM contains 1 mmol surfactant and 2 ml oil in each case; [d]Isolated Yield; [e]$Cu(OTf)_2$ was used as catalyst.

For example, DDAB is essentially insoluble in pure oil, and the small amount water required to form reverse micelle is believed to solvate the head groups and counterion, and beyond which phase separation occurs. Further, because of its poor solubility in water and oil too, it is reported that DDAB molecules are predominantly adsorbed at the oil/water interface and results in less flexible (rigid) so that penetration of the bulkier headgroups (cationic, DDA^+) into the water pool makes difficult (Scheme 1).[51,52] On the other hand, AOT has received much larger attention to form RM due to its ability to solubilize large amounts of water in a variety of nonpolar solvents over a wide range of concentrations. Its special structural characteristics (Scheme 1) reveal formation of a more flexible interface so that a comparable less dimension of polar headgroups (anionic, $DEHSS^-$) can protrude towards water pool more easily.[53] Whereas, TX 100 contains polyoxyethylene (POE) group as a hydrophobic part (polar head group), which may be larger than the hydrophobic part of the molecule. Because of the presence of long POE group, polar interior of reverse micellar aggregates thus formed, has shown much different nature from formed with ionic surfactants.[54,55] Interestingly, the

results reveal that AOT is best suited for present study. The low conductivity, small droplet size and high population of bound water species of AOT RMs might be operational for the hike in reaction yield therein. In addition, a plausible explanation in view of the foregoing discussions on difference in characteristic features of microenvironment of the water pool of three RMs can be drawn that stronger electrostatic interaction between catalyst [$Pd(OAc)_2$] and anionic head group of AOT prevails inside the pool, which corroborates stronger catalytic support to enhance the yield. Whereas, DDAB and TX 100 do not subscribe any additional support due to difference in micro-environments and microstructures of these RMs emerges from bulkier cationic polar head group (DDA^+) and bulkier POE group (as dipole).

Henceforth, the optimization with respect to other reaction parameters (viz. droplet size, base etc.) has been resolved using AOT based RMs in subsequent sections. The schematic diagram for the homocoupling reaction in AOT based RMs is depicted in Scheme 2, which reveals compartmentalization of hydrophilic

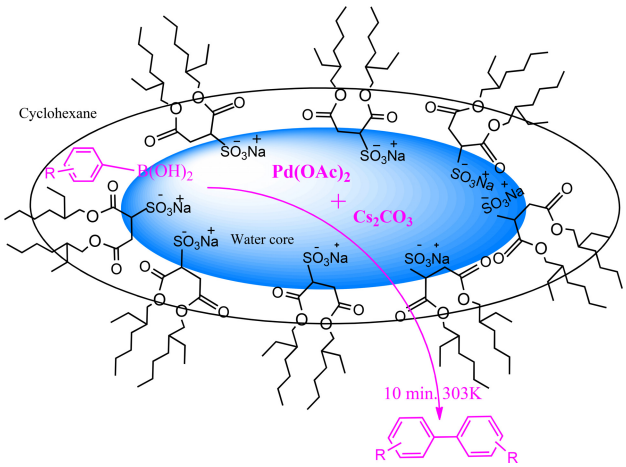

Scheme 2. Homocoupling of arylboronic acid in RMs.

and lipophilic reactants in water pool and palisade layer of surfactant, respectively separated by the oil/water interface. Size of the aggregated droplets, characterized by ω, affects the local aqueous environments of RMs.[16] Changes in the droplet size of RMs are another proposition to tune the population of amphiphiles at the droplet surface under identical [S_T]. In order to compare the effect of encapsulation or compartmentalization of the constituents/reactants in the present reaction with variation of ω (= 5→20) vis-à-vis droplet size (D_h = 4.49→18.20), we have performed model reaction in water/AOT/cyclohexane RMs and the results are presented in Table 1 (Entry-6,7,8,9). It is evident from Table 1 that the yield of the desired product increases with ω up to 15 and thereafter, it decreases. More precisely, the highest yield of the desired product (91%) has been observed at ω = 15 indicating the finest level of size (D_h = 8.64) which facilitates the coupling reaction therein. Hence, it reveals that the different degrees of confinement as a function of ω in water pool can enable to control the reactivity in RMs.[19]

Among the different bases as enlisted in Table 1, highest yield (96%) of the product (Table1; entry-8) was obtained in the presence of Cs_2CO_3 and its superiority to all bases validated under the reaction condition. After optimizing all parameter, we have tested one reaction in presence of $Cu(OTf)_2$, and corresponding result is given in Table 1, entry 14. It is cleared from the results that $Pd(OAc)_2$ is better catalyst in comparison to the $Cu(OTf)_2$ for the homocoupling reaction of arylboronic acids.

Growth of reaction in RMs gallows and plausible reaction site therein

From preceding sections, it reveals that AOT/Cy RM has been found to be an effective reaction medium for C–C coupling reactions. The model homocoupling reaction has been performed in this medium and followed by evaluation of different physicochemical properties during proceedings of the reaction to monitor the growth of reaction and accordingly, most plausible reaction location in AOT RM has been deciphered in the following sections.

Conductivity measurement

Electrical conductivity of RM has been measured at regular interval during progress of the reaction under optimized condition and the results are presented in Figure 5A and Table S1. At onset, increase in conductivity upon addition of catalyst $Pd(OAc)_2$ is obvious but subsequent decrease in conductivity reflecting the formation of non-conducting aqua-palladium complex.[22,56] A sharp increase in conductivity has observed after addition of other reagents and this trend is continued until the completion of reaction. In homocoupling reaction, the product biaryls are formed along with highly conducting side-products [$B(OH)_4^-Cs^+$, $CsHCO_3$] which are responsible for hike in conductivity during reaction.[57] Hence, it can be reasonable to assume that the reaction probably occurring within the droplets of AOT RM.

Dynamic light scattering (DLS) measurement

Results of DLS measurement of droplet sizes (D_h) of AOT RMs during course of reaction are presented in Figure 5B. A sudden increase in D_h (from 8.64 to 13.35 nm) has been observed after addition of reagents, and this trend continues until it reaches to optimal label which actually indicates the end point of reaction. Water soluble reagents [*viz.* catalyst, base mentioned in Table 1] get easily solubilized inside the water pool whereas phenylboronic acid, being a sparingly water soluble reagent which possess both hydrophilic and hydrophobic components is expected to be located at the vicinity of oil/water interface of RMs. As a consequence, hydrophilic part of the molecule extends towards water pool due to hydrogen bonding and hydrophobic part obviously incorporates into hydrocarbon domain in the vicinity of the interface/palisade layer.[20,22]

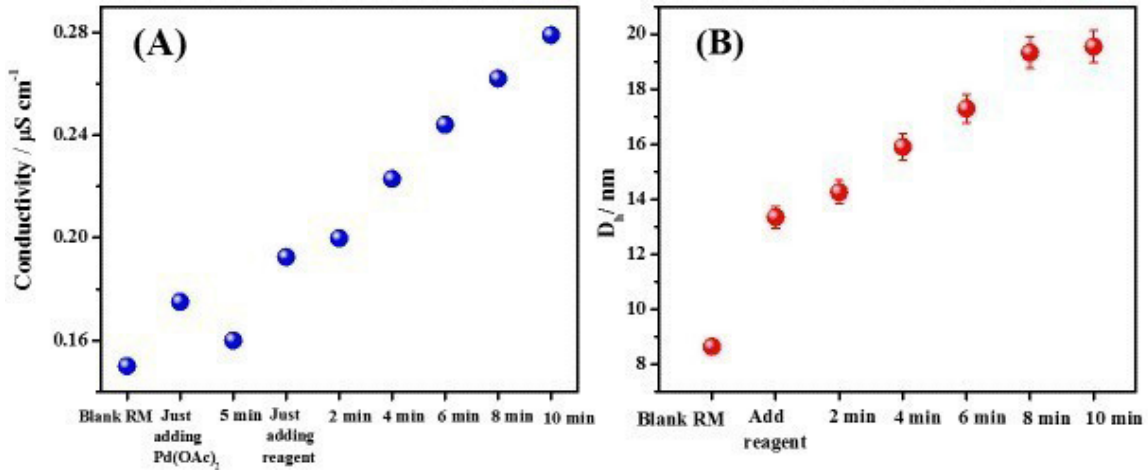

Figure 5. (A) The conductivity and (B) the hydrodynamic diameter (D_h) of RMs during course of the reaction.

Nevertheless, accumulation of reagents inside water droplets and the presence of phenylboronic acid in the palisade layer of RMs together are responsible for enlargement of droplet size. The regular increase in droplet size during reaction might be due to the formation of the products (both desired and side) and optimal droplet size reflecting the end of reaction. All these observations together sensing that the reaction takes place inside the water droplets.

FTIR measurement

As discussed earlier, the different types of hydrogen bonded water molecules exist in RMs, can broadly be classified into two major classes, namely, bound and bulk-like water molecules[34,40–43,58–61] with a characteristic O–H stretching frequency in IR spectroscopy at ~3450 and ~3250 cm^{-1}, respectively (Figure 6 and Inset A). Interestingly, the progress of the reaction monitored by FTIR reveals that the addition of palladium acetate initially reduces the population of bound water due to the formation of aqua-palladium complex, which decreases the interaction of bound water with polar head groups of AOT. Subsequently, the addition of phenylboronic acid initially enhances the population of bound water as it form H-bond with confined water molecules. Hence, it can be inferred that the molecules of phenylboronic acid essentially reside in the vicinity of the oil/water interface. Thereafter, the bound water population regularly decreases till the completion of reaction. This observation indicated by the formation of biaryls results in decrease in population of phenylboronic acid at the oil/water interface. Further, the decrease in bound water population may be due to the effect of limiting the interaction between the polar head groups ($DEHSS^-$) of AOT and water.[61] Hence, it can be concluded from overall observations that the reaction takes place in droplets of RMs with special reference to the bound layer of water molecules.

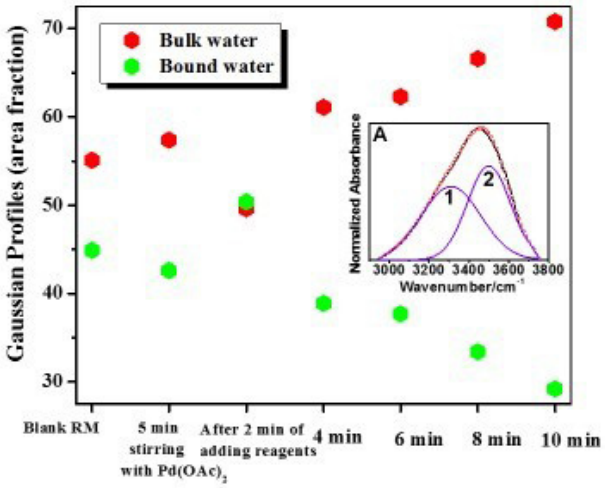

Figure 6. The Gaussian profiles of FTIR study of AOT RMs at regular interval during homocoupling reaction at fixed ω (= 15) and 303 K. **Inset A.** Representative normalized (normalized to intensity of 1.0) FTIR spectra of O–H band for blank AOT RMs at constant ω (= 15) and 303 K. Specification: Experimental spectra (black curve), overall fitted points (red) and deconvoluted curves (1: bulk water; 2: bound water).

Generalization of AOT RM as reaction media

With this optimized condition presented, an attempt has been made further to establish the versatility of our present protocol. A variety of arylboronic acids were examined under the optimal reaction condition in AOT RMs and the corresponding results/products are summarized in Table 2. The reaction progressed smoothly and functional groups were well tolerated under the reaction condition. It is clear from the results that arylboronic acids bearing electron withdrawing groups, (e.g., -Br, -Cl, -F, -CN and $-NO_2$), participate in reactions smoothly and results in good yield of the desired homo-coupled products (Table 2; 2b,2c,2g–2i). Arylboronic acids bearing electron-donating groups, (e.g.,–Me and –OMe) furnished the desired products with high yields

Table 2. Homocoupling of different arylboronic acids[a]

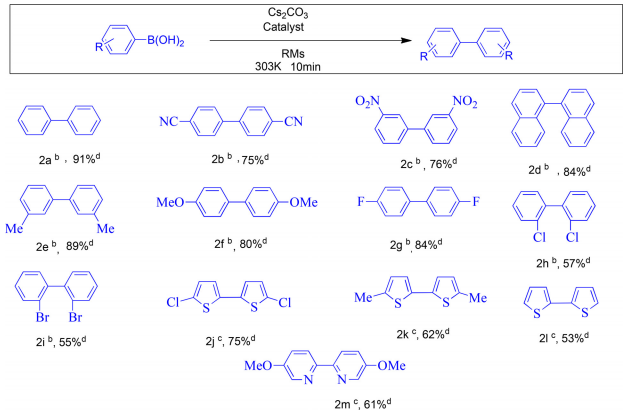

[a]Reaction condition: Arylboronic acid (1mmol); base (2 mmol); catalyst (2 mol%); RMs (3 ml); [b]$Pd(OAc)_2$ used as catalyst; [c]$Cu(OTf)_2$ used as catalyst; [d]Isolated yield after column chromatography.

of 89% and 80%, respectively (Table 2; 2e,2f) upon isolation. Para and meta substituted arylboronic acids afforded good yields whereas, the dimerisation of ortho substituted phenylboronic acids produced the corresponding product with low yields (Table 2; 2 h,2i), which may be attributed to the steric effect of the substituents present in ortho position. Under the same reaction condition, 84% of binaphthyl product was isolated from the naphthylboronic acid (Table 2; 2d).

After successful completion of homo-coupling reaction of arylboronic acid, we turned to apply same protocol in case of heteroarylboronic acids. Homo-coupling of heteroarylboronic acid under optimized condition persistently resulted in low yield of the desired product. It might be due to the strong affinity of hetero atom to palladium and accordingly, poisons of the catalyst.[62] We then, modified our protocol and introduced $Cu(OTf)_2$ as catalyst instead of $Pd(OAc)_2$. Under this modified condition, heteroarylboronic acid proficiently responded in homo-coupling reaction and resulted in good yield of the desired product (Table 2; 2j–2m).

Suzuki cross coupling reaction of aryl halides with phenylboronic acid

In this section, scope of the protocol under investigation was further explored for the construction of unsymmetrical biaryl *via* Suzuki-Miyaura cross-coupling reaction. Accordingly, we have performed a few cross-coupling reactions and results are presented in Table 3. Interestingly, the cross-coupling reaction under optimized condition facilitated over homo-coupling reaction and resulted in unsymmetrical biaryl in good to moderate yield. Aryl iodides are ended up with the good yield of cross-coupled product in comparison to arylbromides (Table 3). Whereas arylchlorides are not responding in reaction under the optimized condition even after 24 hrs (3 l, 3 m).

A slight decrease in product yield for aryl bromides has been observed, and may be due to the higher bond strength of C–Br in comparison with C–I.[63] The presence of electron

Table 3. Suzuki-Miyaura cross coupling of different Aryl halides with Phenylboronic acid.[a]

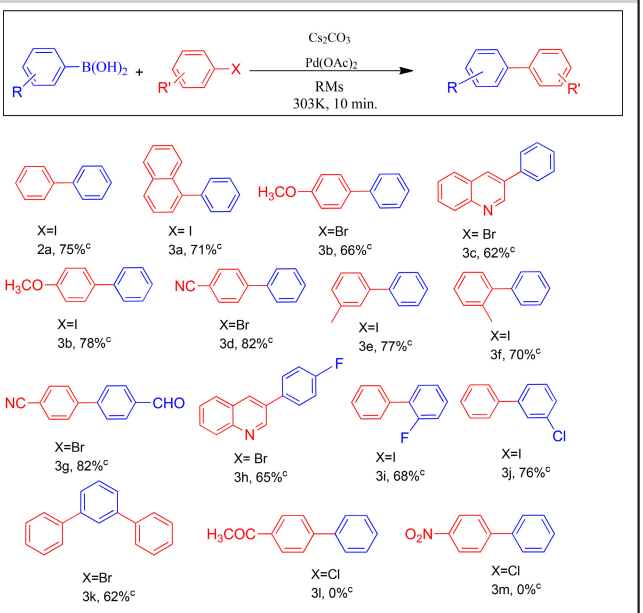

[a] Reaction condition: Arylboronic acid (1mmol); aryl halide (1mmol); base (2 mmol); catalyst (2 mol%); RMs (3 ml); [c]Isolated yield after column chromatography.

withdrawing group in arylhalide (Table 3, entry 3d, 3 g) enhances the yield of the coupled product. The cross-coupled product 1-(3-chlorophenyl)benzene (3j) has been isolated in good yield upon reaction between 1-chloro-3-iodobenzene and phenylboronic acid on selective basis. When 1,3-dibromobenzne treated with phenylboronic acid (2 equivalent) under optimized condition, a decent yield (62%) of 1,3-diphenylbenzene (3k) has been observed.

CONCLUSION

This report summarizes anionic, water/AOT/Cy RM as an efficient reaction medium for additive and ligand-free transition metal catalysed C–C homo/cross coupling reactions with a broad range of substrates compares to cationic (DDAB) and non-ionic (TX 100) RMs in cyclohexane under comparable physicochemical conditions. The reaction proceeds rapidly and completes within 10 mins at ambient condition. Performance of the reaction has been correlated with different physicochemical parameters of these self-organized media using conductance, DLS and FTIR techniques. A plausible explanation is suggested in favor of AOT/Cy RM to be an effective reaction medium in terms of yield of the final product. Subsequently, a series of studies were undertaken to find out a most suitable base and the influence of water content (ω) of this medium under optimized condition for effective C–C homocoupling reaction of arylboronic acid (herein, phenylboronic acid was selected as a model compound) which constitute a major part of this report. K_2CO_3 (91%) and Cs_2CO_3 (96%) have been found to be least and most effective base, respectively in terms of

yield. Droplet size [in other words (ω)] influences the yield in studied ω range (= 5→20) and shows a maximum at ω equals to 5. The progress of the reaction in constrained environment of RM and the possible reaction site have also been assessed by employing conductance, DLS and FTIR techniques. The droplet core in nano-cage of RM, especially the bound water layer of RM gallows has been emphasized as the probable reaction site. Finally, it was explored for the construction of symmetrical and unsymmetrical biaryl *via* C–C bond forming homo/cross-coupling reaction (28 different entries) in AOT RM using same protocol. The yield of coupled products have been discussed in view of variation in electron withdrawing group in arylhalides (Cl^-, Br^- and I^-) and bond strength between C-halide. Investigations of other organic reactions in such promising micellar and RM media comprising single and mixed surfactant(s) are currently underway in our laboratory.

Supporting Information Summary

The supporting information contains details experimental procedure, basic data of electrical conductivity and DLS measurements during progress of reactions, ^{1}H and ^{13}C NMR data of all products along with ^{1}H and ^{13}C NMR spectra.

Acknowledgements

We are thankful to the CSIR, New Delhi for financial support [02 (0022)/11/EMR-II].

Conflict of Interest

The authors declare no conflict of interest.

Keywords: Homo/Cross Coupling Reaction · Palladium/Copper Catalyst · Reaction Mechanism · Reverse Micelle · Surfactant.

[1] D. A. Horton, G. T. Bourne, M. L. Smythe, *Chem. Rev.* **2003**, *103*, 893–930.
[2] K. J. Jr. Henry, J. Wasicak, A. S. Tasker, J. Cohen, P. Ewing, M. Mitten, J. J. Larsen, D. M. Kalvin, R. Swenson, S. C. Ng, B. Saeed, S. Cherian, H. Sham, S. H. Rosenberg, *J. Med. Chem.* **1999**, *42*, 4844–4852.
[3] D. J. Augeri, D. Janowick, D. M. Kalvin, G. Sullivan, J. J. Larsen, D. Dickman, H. Ding, J. Cohen, J. Lee, R. Warner, P. Kovar, S. Cherian, B. Saeed, H. Zhang, S. Tahir, S. C. Ng, H. Sham, S. H. Rosenberg, *Bioorg. Med. Chem. Lett.* **1999**, *9*,1069-1074.
[4] C. Amatore, C. Cammoun, A. Jutand, *Eur. J. Org. Chem.* **2008**, 4567–4570.
[5] A. Prastaro, P. Ceci, E. Chiancone, A. Boffi, G. Fabrizi, S. Cacchi, *Tetrahedron Lett.* **2010**, *51*, 2550–2552.
[6] H. Firouzabadi, N. Iranpoor, F. Kazemi, *J. Mol. Cat. A: Chem.* **2011**, *348*, 94–99.
[7] Z. Zhoua, M. Liua, X. Wua, ; H. Yub, G. Xua, ; Y. Xiea, *Appl. Organometal. Chem.* **2013**, *27*, 562–569.
[8] S. Gupta, B. Basu, S. Das, *Tetrahedron* **2013**, *69*, 122–128.
[9] S. Gupta, P. Ghosh, S. Dwivedi, S. Das, *RSC Adv.* **2014**, *4*, 6254–6260.
[10] S. Dwivedi, S. Bardhan, P. Ghosh, S. Das, *RSC Adv.* **2014**, *4,* 41045–41050.
[11] S. Gupta, B. Ganguly, S. Das, *RSC Adv.* **2014**, *4*, 41148–41151.
[12] S. Carrettin, J. Guzman, A. Corma, *Angew. Chem.* **2005**, *117*, 2282–2285; *Angew. Chem. Int. Ed.* **2005**, *44*, 2242–2245.
[13] L. Wang, W. Zhang, D. S. Su, X. Meng, F–S. Xiao, *Chem. Commun.* **2012**, *48,* 5476–5478.
[14] N. Kirai, Y. Yamamoto, *Eur. J. Org. Chem.* **2009**, 1864–1867.
[15] B. Kaboudin, R. Mostafalua, T. Yokomatsub, *Green Chem.* **2013**, *15*, 2266–2274.
[16] S. Pramanik, S. Nagatoishia, N. Sugimoto, *Chem. Commun.* **2012**, *48*, 4815–4817.
[17] K. Bhattacharyya, B. Bagchi, *J. Phys. Chem. A.* **2000**, *104*, 10603–10613.
[18] R. Biswas, S. K. Pal, *Chem. Phys. Lett.* **2004**, *387*, 221–226.
[19] K. Holmberg, *Eur. J. Org. Chem.* **2007**, 731–742.
[20] K. Holmberg, *Curr. Opin. Colloid Interface Sci.* **2003**, *8*, 187–196.
[21] M. Hager, F. Currie, K. Holmberg, *Top Curr. Chem.* **2003**, *227*, 53–74.
[22] B. Kar, S. Bardhan, K. Kundu, S. K. Saha, B. K. Paul, S. Das, *RSC Adv.* **2014**, *4*, 21000–21009.
[23] X. Zhang, Y. Chen, J. Liu, C. Zhao, H. Zhang, *J. Phys. Chem. B* **2012**, *116*, 3723 – 3734.
[24] H.-F. Eicke, M. Borkovec, B. Das-Gupta, *J. Phys. Chem.* **1989**, *93*, 314–317.
[25] N. Kallay, A. Chittofrati, *J. Phys. Chem.* **1990**, *94*, 4755–4756.
[26] Q. Li, T. Li, J. Wu, *J. Phys. Chem. B* **2000**, *104*, 9011–9016.
[27] Q. Li, T. Li, J. Wu, *J. Colloid. Interface. Sci.* **2001**, *239*, 522–527.
[28] P. Hanarp, D. S. Sutherland, J. Gold, B. Kasemo, *Colloids Surf. A* **1999**, *160*, 23–36.
[29] M. Dubois, Th. Zemb, *Langmuir* **1991**, *7*, 1352–1360
[30] T. K. De, A. N. Maitra, *Adv. Colloid Interface Sci.* **1995**, *59*, 95–193.
[31] A. Das, R. K. Mitra, *Colloid. Polym. Sci.* **2014**, *292*, 635–644.
[32] K. M. Goncalves, I. I. Junior, V. Papadimitriou, M. Zoumpanioti, I. C. R. Leal, R. O. M. A. De Souza, Y. Cordeiro, A. Xenakis, *Langmuir* **2016**, *32*, 6746 – 6756.
[33] S. Bardhan, K. Kundu, B. K. Paul, S. K. Saha, *Colloid Surf. A* **2013**, *433*, 219–229.
[34] S. Bardhan, K. Kundu, S. Saha, B. K. Paul, *J. Colloids. Interface. Sci.* **2013**, *411*, 152–161.
[35] D. J. Mitchell, B. W. Ninham, *J. Chem. Soc. Faraday Trans. 2* **1981**, *77*, 601.
[36] D. F. Evans, B. W. Ninham, *J. Phys. Chem.* **1986**, *90*, 225–226.
[37] M. Schick. J. Nonionic surfactants: Physical chemistry, Dekker, New York, Vol. 23, **1987**.
[38] D. Liu, J. Ma, H. Cheng, Z. Zhao, *Colloids Surf. A* **1998**, *135*, 157–167.
[39] S. Ghosh, C. Banerjee, S. Mandal, V. G. Rao, N. Sarkar, *J. Phys. Chem. B* **2013**, *117,* 5886 – 5897.
[40] a) S. Bardhan, K. Kundu, S. Das, M. Poddar, S. K. Saha, B. K. Paul, *J. Colloids Interface. Sci.* **2014**, *430*, 129–139; b) L. P. Novaki, N. M. Correa, J. J. Silber, O. A. El Seoud, *Langmuir* **2000**, *16*, 5573–5578; c) Q. Li, S. Weng, J. Wu, N. Zhou, *J. Phys. Chem. B* **1998**, *102*, 3168–3174; d) N. Zhou, Q. Li, J. Wu, J. Chen, S. Weng, G. Xu, *Langmuir* **2001**, *17*, 4505–4509; e) J.-B. Brubach, A. Mermet, A. Filabozzi, A. Gerschel, D. Lairez, M. P. Krafft, P. Roy, *J. Phys. Chem. B* **2001**, *105*, 430–435.
[41] T. K. Jain, M. Varshney, A. Maitra, *J. Phys. Chem.* **1989**, *93*, 7409–7416.
[42] Y. Gao, N. Li, L. Zheng, X. Bai, L. Yu, X. Zhao, J. Zhang, M. Zhao, Z. Li, *J. Phys. Chem. B* **2007**, *111*, 2506–2513.
[43] Y. Gao, L. Hilfert, A. Voigt, K. Sundmacher, *J. Phys. Chem. B* **2008**, *112*, 3711–3719.
[44] A. J. Lock, H. J. Bakker, *J. Chem. Phys.* **2002**, *117*, 1708 – 1713.
[45] S. A. Corcelli, J. L. Skinner, *J. Phys. Chem. A* **2005**, *109*, 6154 – 6165.
[46] A. Das. A. Patra, R. K. Mitra, *J. Phys. Chem. B* **2013**, *117*, 3593 – 3602.
[47] S. Bardhan, K. Kundu, S. Saha, B. K. Paul, *Colloids. Surf. A* **2014**, *450*, 130–140.
[48] R. K. Mitra, S. S. Sinha, P. K. Verma, S. K. Pal, *J. Phys. Chem. B* **2008**, *112*, 12946- 12953.
[49] D. E. Moilanen, E. E. Fenn, D. Wong, M. D. Fayer, *J. Am. Chem. Soc.* **2009**, *131*, 8318–8328.
[50] S. Bardhan, K. Kundu, B. Kar, G. Chakraborty, D. Ghosh, D. Sarkar, S. Das. S. Senapati, S. Saha, B. K. Paul, *RSC. Adv.* **2016**, *6,* 55104–55116.
[51] I. S. Barnes, S. T. Hyde, B. W. Ninham, P. J. Derian, M. Drifford, Th. Zemb, *J. Phys. Chem.* **1988**, *92,* 2286–2293.
[52] J. Eastoe, K. J. Hetherington, J. S. Dalton, D. Sharpe, J. R. Liu, R. K. Heenan, *J. Colloids Interface. Sci.* **1997**, *190*, 449–455.
[53] S. P. Moulik, K. Mukherjee, *Proc. Indian Natl. Sci. Acad.* **1996**, *62,* 215–222.
[54] D. Das, D. N. Nath, J. *Phys. Chem. B.* **2007**, *111,* 11009–11015.
[55] C. Kumar, D. Balasubramanian, *J. Phys. Chem.* **1980**, *84,* 1895–1899.
[56] J. Vicente, A. Arcas, *Chem. Rev.* **2005**, *249*, 1135–1154.
[57] L. Mukhopadhyay, P. Bhattacharya, S. P. Moulik, *Colloids Surf.* **1990**, *50*, 295–308.
[58] M. Tomsic, A. Jamnik, (Eds.: M. Fanun.), Taylor and Francis, CRC Press, USA, **2009**, 143–181.

[59] P. Bauduin, D. Touraud, W. Kunz, *Langmuir* **2005**, *21*, 8138–8145.
[60] I. R. Piletic, D. E. Moilanen, D. B. Spry, N. E. Levinger, M. D. Fayer, *J. Phys. Chem. A* **2006**, *111*, 4985–4999.
[61] S. K. Mehta, K. Kaur, E. Arora, K. K. Bhasin, *J. Phys. Chem. B* **2009**, *113*, 10686–10692.
[62] J. S. Chen, K. K. Jespersen, J. G. Khinast, *J. Mol. Cat. A: Chem.* **2008**, *285*, 14–19.
[63] I. D. Kostas, F. J. Andreadaki, D. Kovala-Demertzi, C. Prentjas, M. A. Demertzis, *Tetrahedron Lett.* **2005**, *46*, 1967–1970.

Submitted: December 16, 2016
Accepted: January 13, 2017

RSC Advances

PAPER

Cite this: *RSC Adv.*, 2016, **6**, 55104

Synergistic interactions of surfactant blends in aqueous medium are reciprocated in non-polar medium with improved efficacy as a nanoreactor†

Soumik Bardhan,‡§[a] Kaushik Kundu,§[bc] Barnali Kar,[a] Gulmi Chakraborty,[a] Dibbendu Ghosh,[c] Debayan Sarkar,[d] Sajal Das,[a] Sanjib Senapati,[c] Swapan K. Saha*[a] and Bidyut K. Paul*[b]

Organized assemblies in aqueous and non-aqueous media based on mixed surfactants are one of the desired areas for experimental studies and carrying out chemical reactions due to synergistic performance and efficient solvents for various substrates. In this report, a model C–C cross coupling Heck reaction between *n*-butyl acrylate and 4-iodo-toluene is performed both in micelles and water/oil microemulsion systems as reaction media using a similar set of surfactants, [cetyltrimethylammonium bromide (CTAB) and polyoxyethylene (20) cetyl ether ($C_{16}E_{20}$)], in their single and mixed states for the first time. In order to explain the possible location and mechanism of reaction in these media, multitechnique approaches are employed to understand the mutual interactions between surfactant(s) and other constituents in pure and mixed states at air–water as well as oil–water interfaces. A synergistic interaction is evidenced experimentally for a mixed CTAB/$C_{16}E_{20}$ micellar system, which is also supported by theoretical calculations using density functional theory (DFT). The yield of Heck product in different media follows the order water < pure micelle < mixed micelle, which indicates a significant role of the confined environment of the aggregated systems. Further, mixed microemulsions including constituents of the formulations 1-pentanol and *n*-heptane or *n*-decane are explored as nanoreactors for carrying out such a reaction. Reaction yield in mixed water-in-oil (w/o) systems as a function of different hydration levels has been correlated with formation and microstructural characteristics of these systems. Further, mixed microemulsions at lower hydration levels produce synergistic performance compared to micelles and individual constituents in terms of reaction yield. These results reveal that the reaction occurs in neither the water nor oil domain, evidently in the micelle/water pseudo-phase and at the palisade layer of the oil/water interface of microemulsions. Moreover, reaction yields in the studied media are rationalized in terms of interaction parameters, spontaneity of micellization, interfacial population of 1-pentanol, and spontaneity of formation of w/o microemulsions.

Received 14th March 2016
Accepted 23rd May 2016

DOI: 10.1039/c6ra06776j

www.rsc.org/advances

1. Introduction

In recent years, the study of the physicochemical properties of mixed surfactant solutions has become a topic of interest in the area of self-assembly of molecular systems.[1] Organized assemblies *viz.* micelles and microemulsions,[2] based on mixed surfactants offer substantial modification in solubilisation behaviour, enzyme kinetics, nanoparticle synthesis and chemical activity.[3–7] The interaction between surfactants in mixtures produces marked interfacial effects due to changes in adsorption as well as in the charge density of the surface.[8] Earlier, Azum and his co-workers explored various binary and ternary mixtures of amphiphiles in aqueous media, which were found to exhibit different surface and colloidal properties from those of the pure individual components.[9–12] In most cases different types of surfactants are purposely mixed for synergistic performance and this is utilized to reduce the total amount of surfactant used in particular applications in order to reduce cost and environmental impact.[13,14] However, a proper rationale of such modified mixing behaviour is still required and needs a more generalized approach to optimize mixing stoichiometry in order to obtain a maximum effect. Research to date includes

[a]*Department of Chemistry, University of North Bengal, Darjeeling-734 013, India. E-mail: ssahanbu@hotmail.com; Fax: +91-0353-2699001; Tel: +91-0353-2776381*

[b]*Surface and Colloid Science Laboratory, Geological Studies Unit, Indian Statistical Institute, 203, B.T. Road, Kolkata-700 108, India. E-mail: bidyut.isical@gmail.com; Fax: +91-33-25773026; Tel: +91-33-25753164*

[c]*Department of Biotechnology, Bhupat and Jyoti Mehta School of Biosciences, Indian Institute of Technology Madras, Chennai 600036, India*

[d]*Department of Chemistry, National Institute of Technology, Rourkela, Odisha-769 008, India*

† Electronic supplementary information (ESI) available. See DOI: 10.1039/c6ra06776j

‡ Present address: Department of Biotechnology, Bhupat and Jyoti Mehta School of Biosciences, Indian Institute of Technology Madras, Chennai 600036, India.

§ S. B. and K. K. have contributed equally to this work.

numerous attempts to explore combined physicochemical studies of micro-heterogeneous assemblies with attention paid not only to their fundamental aspects but also their wider applications.[15]

The Heck reaction[16,17] has received much attention in recent years as it offers a versatile method for the generation of new carbon–carbon bonds,[18] and holds much promise in many industrial processes, especially in the synthesis of fine chemicals and active pharmaceutical intermediates.[19] In the view of current economic and environmental concerns, continuous efforts are now being made to develop new templates for carrying out the Heck reaction. One approach is to consider inexpensive amphiphiles as potential additives that upon self-assembly into micelles accommodate otherwise insoluble organic substrates and catalysts within lipophilic cores.[20] Further, microemulsions might be another, much cheaper and potentially more universal approach to this problem, based on well-known solubilisation phenomena.[21] Very recently, the Heck reaction has been successfully performed in water/cetyltrimethylammonium bromide (CTAB)/1-propanol/1-dodecene based oil-in-water (o/w) microemulsion and two phase region as well at 353 K.[22]

These findings prompted us to extend the use of micelle as well as water-in-oil (w/o) microemulsion based on mixed cationic/non-ionic surfactants as a chemical reaction media for the Heck reaction at ambient temperature. To fulfil this goal, a comprehensive study of the formation behaviour and physicochemical properties of micellization and microemulsion using blends of CTAB and polyoxyethylene (20) cetyl ether ($C_{16}E_{20}$) including individual constituent is carried out. The structural features of these systems are investigated *via* interfacial and bulk routes by employing tensiometry, conductometry, and also zeta potential, viscosity, dynamic light scattering (DLS), fluorescence lifetime, Fourier transform infrared spectroscopy (FTIR) and field emission scanning electron microscopy (FESEM) measurements. The choice of surfactants in this study is not arbitrary. Although the literature is dominated by studies of microemulsions formed with anionic sodium bis(2-ethylhexyl) sulfosuccinate (AOT), there is interest in microemulsions formed with other surfactants, particularly cationic CTAB. CTAB is of increasing interest because the head group is a good model for the lipid phosphatidylcholine.[23] Further, commercially available non-ionic surfactants such as Brijs are extensively used in pharmaceutical formulations as solubilizers and emulsifiers to improve the dissolution and absorption of poorly soluble drugs.[24] Heptane (Hp) and decane (Dc) were used as oil and 1-pentanol (Pn) was used as cosurfactant. After careful evaluation of various physicochemical and thermodynamic parameters, a model C–C cross coupling reaction (Heck reaction) was performed between *n*-butylacrylate and 4-iodo-toluene in the presence of palladium acetate and triethylamine, TEA (base), in mixed surfactant based micellar and w/o microemulsion media. To provide a proper justification for this study, we also performed the Heck reaction in media of individual constituents, which are used for the formation of these organized systems. An attempt is also made to rationalize the yields of the Heck products from the viewpoint of the physicochemical and thermodynamic parameters of their formation during the course of the reaction. It is expected that the findings of this study would improve the basic understanding of the formation, characterization and application of mixed micelles and w/o microemulsions.

2. Materials and methods

2.1. Materials

CTAB (>99%) and $C_{16}E_{20}$ (>98.5%) were obtained from Sigma Aldrich, USA and Fluka, Switzerland, respectively. The cosurfactant [1-pentanol (Pn, >98%)] and oils [Hp (>98%), and Dc (>98%)] were obtained from Fluka, Switzerland, Lancaster, England and E. Merck, Germany, respectively. The dye, 7-hydroxycoumarin (HCM, >99%) was obtained from Chem. Service, West Chester, USA. Palladium acetate [$Pd(OAc)_2$, ≥99.98%] and 4-iodo-toluene ($CH_3C_6H_4I$, ≥99%) were purchased from Sigma Aldrich, USA. TEA (≥99.5%) and *n*-butyl acrylate were purchased from Merck, Germany. All these chemicals were used without further purification. Doubly distilled water with a conductivity of less than 3 μS cm^{-1} was used in the experiments.

2.2. Methods

2.2.1. Tensiometry. Surface tension was measured using a K9 tenisometer (Kruss, Germany) by a platinum ring detachment method. A concentrated surfactant solution was added to a known amount of water, and the surface tension values were measured after thorough mixing and temperature equilibration with an accuracy of ±0.1 mN m^{-1}.

2.2.2. Conductance measurements. Conductivity measurements were made using an automatic temperature-compensated conductivity meter, Mettler Toledo (Switzerland) Conductivity Bridge, with a cell constant of 1.0 cm^{-1}. The instrument was calibrated with a standard KCl solution. A constant temperature (303 ± 0.1 K) was maintained by circulating water through the outer jacket from a thermostatically controlled water bath. The reproducibility of the conductance measurements was found to be within ±1%.

2.2.3. Dynamic light scattering (DLS) and zeta potential measurements. Hydrodynamic diameter (D_h) and zeta potential (ξ/mV) measurements of the self-assembled systems (single and mixed micelles and w/o mixed microemulsions) were performed using a Nano ZS-90 (Malvern, U.K.) dynamic light scattering spectrometer at 303 K. The solutions were equilibrated for 2–3 hours before measurement. Solutions were filtered carefully through a 0.22 μm Millipore™ membrane filter loaded to a glass round aperture (PCS8501, Malvern, U.K.) cell with a 1.0 cm optical path length for measurements. A He–Ne laser of 632.8 nm was used as the light source, while the scattering angle was set at 90°. Temperature was controlled by an inbuilt Peltier heating–cooling device (±0.1 K). D_h of each sample was estimated from the intensity autocorrelation function of the time-dependent fluctuation in intensity and can be defined as.[25]

$$D_h = k_B T/3\pi\eta D \quad (1)$$

where, k_B, T, η and D indicate the Boltzmann constant, temperature, viscosity and diffusion coefficient of the solution, respectively. Zeta potentials were measured using a folded capillary cell (DTS1060, Malvern, U.K.) made of polycarbonate with gold plated beryllium-copper electrodes. One cell was used for a single measurement. To check the reproducibility of the results at least 6 measurements were performed.

2.2.4. Field emission scanning electron microscopy (FESEM) measurements. A field emission scanning electron microscope (FESEM, HITACHI S-4800) was used to study the morphology of single and mixed micelles and w/o mixed microemulsions. A high vacuum ($\sim 10^{-7}$ Torr) field emission setup was applied to deposit a thin film of micelle and microemulsion solutions on glass plates.

2.2.5. Formation of microemulsion. Microemulsion formation was accomplished by adding oil (Hp or Dc) at a constant water and surfactant level to destabilize an otherwise stable w/o microemulsion and then restabilizing it by adding a requisite amount of co-surfactant (Pn) with a constant composition of interface and continuous phase. The experimental procedure with theoretical backgrounds has been reported elsewhere.[26]

2.2.6. Viscosity measurements. Viscosity measurements were performed using a LVDV-II + PCP cone and plate type Rotoviscometer (Brookfield Eng. Lab, USA). The temperature was kept constant (303 K) for viscosity measurements within ± 0.1 K by circulating thermostated water, through a jacketed vessel containing the solution. The reproducibility of the viscosity measurements was found to be within $\pm 1\%$.

2.2.7. Fluorescence lifetime measurements. The fluorescence lifetime measurements of w/o mixed microemulsions were performed at 303 K using a bench-top spectrofluorimeter from Photon Technology International (PTI), USA (Model: Quantamaster-40). The present PTI lifetime instrument employs the stroboscopic technique (Strobe) for time-resolved fluorescence measurements. In the present experiments, two curves were considered at the measured wavelength (450 nm using a 310 nano LED as a light source) *viz.* the instrument response function (IRF) and the decay curve of the probe molecule, 7-hydroxycoumarin (10^{-5} mol dm^{-3}). The IRF was acquired from a non-fluorescing scattering solution (herein, Ludox AM-30 colloidal silica, 30 wt% suspension in water) held in a quartz cell of 1 cm path length. The lifetime values of probe molecules were then obtained by convoluting the IRF with a model function and then comparing the results with experimental decay. Analysis was performed using Felix GX (version 2.0) software. A value of χ^2 in between 0.99 and 1.22 and a symmetrical distribution of residuals are considered as a good fit.

2.2.8. Fourier transform infrared spectroscopy (FTIR) studies. FTIR spectra of w/o mixed microemulsions were recorded using a Perkin Elmer Spectrum RXI spectrometer (USA) (absorbance mode) using a CaF_2-IR crystal window (Sigma Aldrich) equipped with a Presslock holder with a scan number of 100 and a spectral resolution of 4 cm^{-1} at 303 K. We focused our attention on the 3000–3800 cm^{-1} window (mid-infrared region). Deconvolution of spectra was done with the help of a Gaussian curve fitting program (Origin software).

2.2.9. C–C cross coupling (Heck) reaction in micelles and microemulsions. 3 ml of micellar or w/o microemulsion solution and 4.48 mg (0.02 mmol, 4 mol%) of $Pd(OAc)_2$ were taken in a 25 ml round bottom flask and the mixture placed in a pre-heated oil bath at 303 K for 30 minutes with constant stirring. Thereafter, 109 mg (0.5 mmol) of 4-iodotoluene, 76.8 mg (0.6 mmol) of *n*-butylacrylate and 101.12 mg (1 mmol) of TEA were introduced into it, and the resulting mixture was further stirred for 60 minutes. The resulting multicomponent solution (in each case) showed excellent stability towards the reagents. More precisely, similar experiments were performed in single (CTAB and $C_{16}E_{20}$) and mixed micelles (at equimolar composition), and mixed microemulsions (at equimolar composition) at a different molar ratio of water to surfactant (ω) and also, in microemulsions of other constituents (*viz.* water, Hp, Dc, Hp/Pn, Dc/Pn). Progress of the reaction was monitored by silica gel thin layer chromatography (TLC). After completion, the reaction was quenched with water and the organic part was extracted thrice with diethyl ether. The combined ethereal layer was dried over anhydrous sodium sulphate and concentrated under vacuum. The yield of the Heck coupled product was determined by HPLC (Agilent Technologies, 1260 Infinity). Further, the product was purified by column chromatography using silica gel where a mixture of petroleum ether and ethyl acetate was used as an eluent. Finally, the product was characterized using ^{1}H-NMR and ^{13}C-NMR (Bruker, 300 MHz), which are provided in the ESI.†

3. Results and discussion

Before discussing the outcome of the Heck reaction in a micellar or microemulsion medium, first we focus on the formation of single and mixed micellar and microemulsion systems from a thermodynamic point of view. In order to understand the interactions between individual constituents, we discuss the microstructural, microenvironmental and morphological characteristics of the formulated systems. In view of this, we divide this section into four parts; where the first part of this section contains a summary of the formation and characterization of micellar systems in single and mixed surfactants both experimentally and theoretically. In the second part, reaction site and yields of the Heck reaction are rationalized in terms of the interaction parameters and Gibbs free energy of micellization. Further, the formation and microstructural characteristics of the mixed microemulsions along with the yields and possible locations of the reaction at the oil/water interface are discussed in the last two parts. Finally, a comparison of reaction yields is provided between mixed micellar and microemulsion systems along with individual constituents.

3.1. Formation and characterization of single and mixed micelles

The amphiphilic behaviour in terms of the critical micellar concentration (CMC) of pure CTAB, $C_{16}E_{20}$ and their mixture at

an equimolar composition (1 : 1) in water is determined from the sharp inflection point in the surface tension (γ) against log [surfactant] and specific conductivity against [surfactant] plots at 303 K, as shown in Fig. 1A and B.

Further, a representative illustration of CMC for aqueous $C_{16}E_{20}$ system is presented in Fig. S1 (ESI†). The CMC values of these systems are also presented in Table S1 (ESI†). The lower CMC for CTAB/$C_{16}E_{20}$ mixtures compared to pure CTAB is attributed to the formation of a pseudo-double chain complex arising from the strong electrostatic interaction between the quaternary ammonium cationic segment (CTA^+) and the POE of $C_{16}E_{20}$. In addition, there also exists an enhanced hydrophobic interaction between the hydrocarbon chains, which favours mixed micelle formation and decreases the CMC.[27]

For ideal mixing of cationic/non-ionic surfactant systems, CMC values have been calculated using the Clint equation,[28]

$$1/\mathrm{CMC}_{\mathrm{ideal}} = \alpha_1/\mathrm{CMC}_1 + \alpha_2/\mathrm{CMC}_2 \quad (2)$$

where, α_1 and α_2 are the stoichiometric molar fractions of CTAB and $C_{16}E_{20}$, respectively. For the mixed systems, lower experimental CMC values (CMC_{12}) are obtained than those expected from the Clint equation (Table S1†). This observation indicates non-ideal behaviour in aqueous solution and also, demonstrates favourable synergism between the constituent surfactants in mixed micelles.

The nature and strength of interactions between the CTAB and $C_{16}E_{20}$ molecules in the mixed micelles are evaluated from the interaction parameter by employing Rubingh's approach, based on regular solution theory,[29]

$$\frac{\left[(X_1^{\mathrm{m}})^2 \ln(\mathrm{CMC}_{12}\alpha_1/\mathrm{CMC}_1 X_1^{\mathrm{m}})\right]}{(1-X_1^{\mathrm{m}})^2 \ln[\mathrm{CMC}_{12}(1-\alpha_1)/\mathrm{CMC}_2(1-X_1^{\mathrm{m}})]} = 1 \quad (3)$$

where, X_1^{m} is the micellar molar fraction of the CTAB incorporated in the mixed micelle. The interaction parameter, β^{m}, is an indicator of the degree of interaction between two surfactants in mixed micelles and accounts for the deviation from ideality, which is given by;[29]

$$\beta^{\mathrm{m}} = [\ln(\mathrm{CMC}_{12}\alpha_1/\mathrm{CMC}_1 X_1^{\mathrm{m}})]/(1-X_1^{\mathrm{m}})^2 \quad (4)$$

For a binary system (1 : 1), β^{m} values are found to be negative (Table 1), which also indicates a synergistic interaction between the component surfactants. According to Rubingh's model, the activity coefficient, f_i^{m}, of individual surfactants within the mixed micelles is related to the interaction parameter through the following equations,[29,30]

$$f_1^{\mathrm{m}} = \exp[\beta^{\mathrm{m}}(1-X_1^{\mathrm{m}})^2] \quad (5)$$

$$f_2^{\mathrm{m}} = \exp[\beta^{\mathrm{m}}(X_1^{\mathrm{m}})^2] \quad (6)$$

where, $f_i^{\mathrm{m}} = 1$ indicates an ideal mixed system.[30] The significance of the other terms was discussed earlier. It is seen from Table 1 that both the values of f_1^{m} and f_2^{m} are lower than unity, which indicates the formation of mixed micelles and reflects the non-ideality of a multicomponent mixed system. Further, the maximum surface excess concentration at the air–water interface ($\Gamma_{\max}$) and the minimum area per surfactant head group adsorbed at the interface ($A_{\min}$) are calculated from the surface tension data by fitting the Gibbs adsorption isotherm,[31]

$$\Gamma_{\max} = -\frac{1}{2.303nRT}(\mathrm{d}\gamma/\mathrm{dlog}\ C) \quad (7)$$

$$A_{\min} = 10^{18}/\Gamma_{\max}N_{\mathrm{a}} \quad (8)$$

Herein, $\mathrm{d}\gamma/\mathrm{dlog}\ C$ is the slope of the plot of γ *versus* log C (where C represents the concentration of the surfactant). Here, for mixed micelles of cationic/non-ionic surfactants, the value of n (the number of species produced by an amphiphile and whose concentration at the interface varies with surfactant concentration in the solution) is 3. The values of $\Gamma_{\max}$ and $A_{\min}$ are presented in Table 1 and follow the order $C_{16}E_{20}$ > CTAB > CTAB/$C_{16}E_{20}$ and $C_{16}E_{20}$ < CTAB < CTAB/$C_{16}E_{20}$, respectively. At an equimolar composition of mixed CTAB/$C_{16}E_{20}$, minimum $\Gamma_{\max}$ (and thus maximum $A_{\min}$) values are obtained due to the

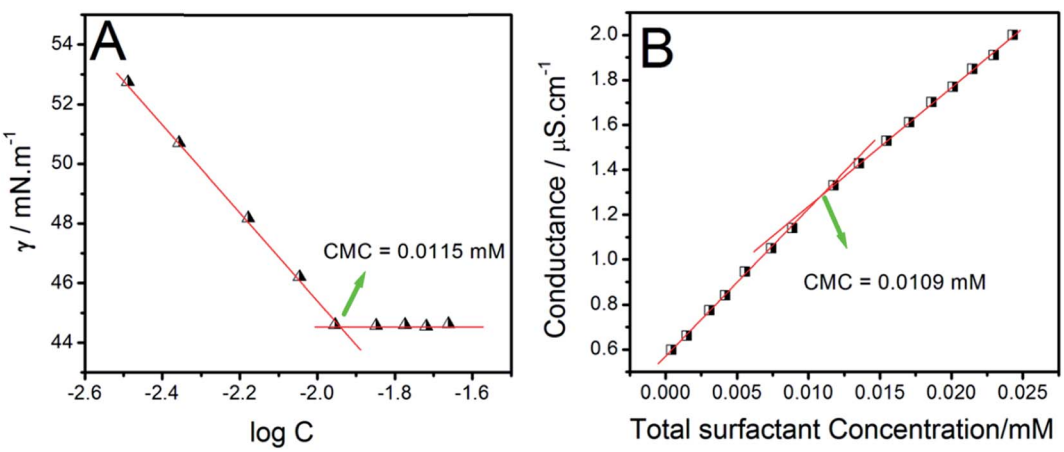

Fig. 1 Tensiometric (A) and conductometric (B) determination of the CMC of mixed aqueous CTAB/$C_{16}E_{20}$ systems at an equimolar composition at 303 K.

Table 1 Interfacial, thermodynamic and interaction parameters of single and mixed surfactants

(A) Interfacial and thermodynamic[a] parameters

System	T/K	Π_{CMC} $\times 10^3$/N m^{-1}	10^6 $\times \Gamma_{max}$/mol m^{-2}	A_{min}/nm^2 per molecule	$-\Delta G^0_m$/kJ mol^{-1}	$-\Delta G^0_{ads}$/kJ mol^{-1}
CTAB	303	32.0[b]	1.31[b]	1.27[b]	40.5[b]	64.9[b]
CTAB/$C_{16}E_{20}$	303	34.7	0.86	1.93	71.03	99.74
$C_{16}E_{20}$	303	27.64	2.25	0.7379	39.5	51.78

(B) Interaction[c] parameters for CTAB/$C_{16}E_{20}$ (1 : 1)

CMC (Cond.)	CMC (ST)	CMC (Avg.)	α and g	β	f_1	f_2
0.0109	0.0115	0.0112	0.829 and 0.171	−4.58[c] −4.47[d]	0.0114[c] 0.2465[d]	0.89[c] 0.0461[d]

[a] The average errors in ΔG^0_m and ΔG^0_{ads} are ±3%. [b] Ref. 27. [c] For interaction parameters CTAB = 1 & $C_{16}E_{20}$ = 2. [d] For interaction parameters $C_{16}E_{20}$ = 1 & CTAB = 2.

intercalation of the POE of $C_{16}E_{20}$ within the positively charged CTAB surfactant molecules which also reduces the repulsion among them.[32] The steric hindrance due to the long POE chains of $C_{16}E_{20}$ also causes higher A_{min} values for CTAB/$C_{16}E_{20}$ combinations.[32]

Another parameter that directly proves the effectiveness of surface tension reduction is the surface pressure at the CMC, *i.e.* Π_{CMC}. It indicates the maximum reduction of surface tension caused by the dissolution of the amphiphilic molecules and is usually defined as;

$$\Pi_{CMC} = \gamma_{sol} - \gamma_{CMC} \quad (9)$$

where, γ_{sol} and γ_{CMC} represent the surface tension of pure water and surfactant solution at the CMC, respectively. As per Table 1, the aqueous CTAB-$C_{16}E_{20}$ mixtures display higher values of Π_{CMC} than their individual counterparts in accordance with their higher surface activity as mentioned earlier, although their efficiency in bringing about a reduction in the surface tension of water varies only slightly with the mixture composition.[33]

The standard free energy of micelle formation per mole of monomer unit (ΔG^0_m) for these systems is evaluated from the equation;[34]

$$\Delta G^0_m = (1 + g)RT \ln X_{CMC} \quad (10)$$

where, X_{CMC} and g are the CMC expressed in mole fraction unit and the fraction of counter ions bound to the micelle, respectively. The fraction of counter-ion binding is related to;[34]

$$g = (1 - S_{mic}/S_{mn}) \quad (11)$$

The lower values of g for mixed CTAB/$C_{16}E_{20}$ (*i.e.* 0.171) compared to the pure CTAB micelle (*i.e.* 0.47) signify a lowering of effective surface charge density in the mixed micelles.[35] The standard free energy of interfacial adsorption (ΔG^0_{abs}) at the air–water interface of micelles is evaluated from the relation;[36]

$$\Delta G^0_{ads} = \Delta G^0_m - (\Pi_{CMC}/\Gamma_{max}) \quad (12)$$

The values of ΔG^0_m and ΔG^0_{ads} are represented in Table 1. Both the ΔG^0_m and ΔG^0_{ads} values are found to be more negative in the binary mixture compared to the pure micelle, which indicates that the micellization as well as adsorption processes are more favourable compared to the individual surfactant. Further, more negative ΔG^0_{ads} values compared to ΔG^0_m values suggest that the adsorption process is more spontaneous than micelle formation. Micelle formation in the bulk is a secondary process and less spontaneous than interfacial adsorption.[35,37] In order to get more insight into the surface charge and structural characteristics of pure and mixed micelles, we performed zeta potential, DLS and FESEM measurements, which are dealt with in subsequent paragraphs.

It is already established that zeta potential (ζ) is a very good indicator of the interaction and stability of colloidal systems.[38] In view of this, the effect of amphiphile(s) concentration on the surface charge of aqueous CTAB, $C_{16}E_{20}$ and CTAB/$C_{16}E_{20}$ systems was investigated by measuring the ζ parameter, which is presented in Fig. 2A. The positive ζ value for cationic CTAB increases with increasing the concentration of CTAB. However, non-ionic $C_{16}E_{20}$ shows a negative potential, possibly due to the large number of oxygen atoms in the POE groups.[39] Interestingly, the ζ values for CTAB/$C_{16}E_{20}$ mixtures are found to be higher than that of single CTAB, which also proves the synergistic interaction between them.[40]

The DLS technique is employed to determine the size of the aggregates of CTAB, $C_{16}E_{20}$, and CTAB/$C_{16}E_{20}$ binary system at their corresponding CMCs at 303 K and is depicted in Fig. 2B. DLS data shows a monomodal size distribution with a hydrodynamic diameter (D_h) ranging from ~10–15 nm for all the systems. The micellar size is observed to follow the trend $C_{16}E_{20}$ < CTAB/$C_{16}E_{20}$ < CTAB. The smaller size of $C_{16}E_{20}$ micelles originates from the relatively weaker interactions of $C_{16}E_{20}$ with water in comparison to CTAB.[5,41] Further, the morphology of the four micellar systems was investigated using an FESEM technique and is illustrated in Fig. 2C–F. A uniformly distributed spherical shaped structure is observed for all these systems at micellar region (Fig. 2C, D and F), which is indicated by circles

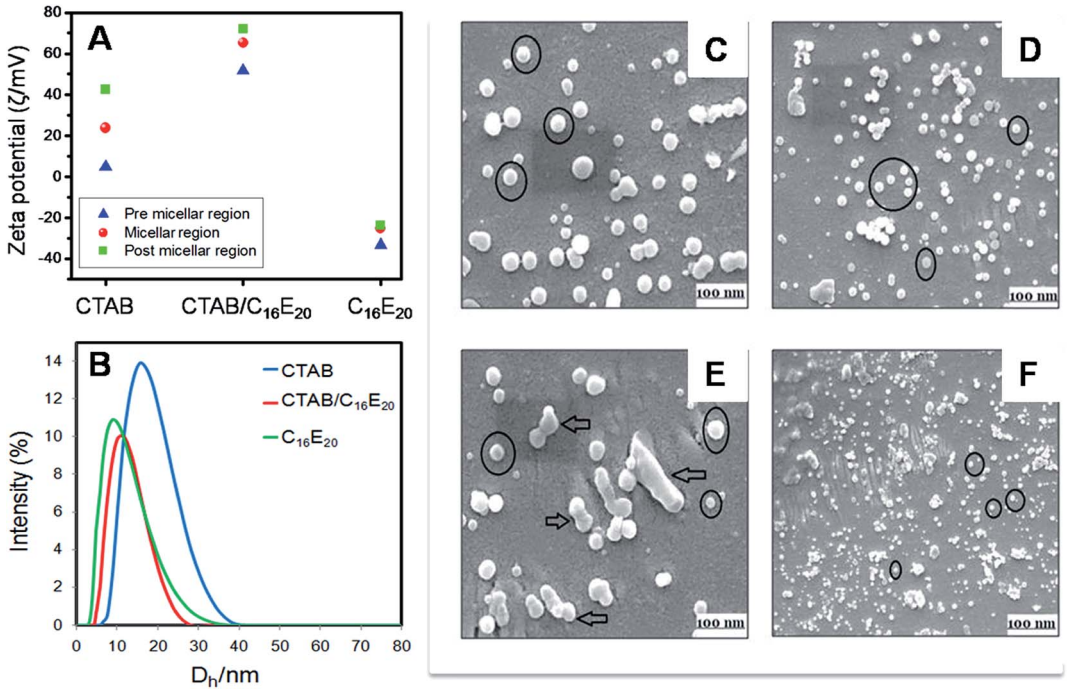

Fig. 2 (A) Measurement of the zeta potential of single and binary (equimolar) surfactants in an aqueous medium at 303 K. (B) Hydrodynamic diameter (D_h) of micellar systems at 303 K. FESEM images of (C) CTAB/water and (D) CTAB/$C_{16}E_{20}$/water at the micellar region, (E) CTAB/$C_{16}E_{20}$/water at the post-micellar region, and (F) $C_{16}E_{20}$/water at the micellar region.

in the respective figures. Further, Fig. 2E represents some agglomerated structures (shown by hollow arrows), which consist of two or three single spherical micro-droplets for binary CTAB/$C_{16}E_{20}$ systems at the post-micellar region.

In order to understand the interaction of surfactant molecules with solvent qualitatively, we performed quantum chemical DFT calculations. We executed model calculations by using the B3LYP functional with the 6-31G basis set to understanding the interactions of CTAB and $C_{16}E_{20}$ with H_2O at single and binary (1 : 1) compositions using the Gaussian 09 program. Frequency calculations were also performed to verify that all the optimized geometries correspond to a local minimum which has no imaginary frequency. At the outset, we optimized the structures of the isolated CTAB, $C_{16}E_{20}$ and H_2O, binary complex (1 : 1) of CTAB and $C_{16}E_{20}$ with H_2O, and ternary complex (1 : 1 : 1) of CTAB, $C_{16}E_{20}$ and H_2O. The most stable optimized structures of binary (1 : 1) and ternary (1 : 1 : 1) complexes are presented in Fig. 3, and their interaction energies (calculated from the difference in stabilization energy between complexes and monomers) are also shown in the respective figure. Also, the optimized structures of isolated CTAB, $C_{16}E_{20}$ and CTAB/$C_{16}E_{20}$ are illustrated in the ESI (Fig. S2†). DFT calculations indicate a highly stable ternary complex, CTAB/$C_{16}E_{20}$/H_2O, with a stabilization energy of −102.09 kJ mol^{-1}. The stability of the proposed complexes follows the order CTAB/$C_{16}E_{20}$/H_2O > $C_{16}E_{20}$/H_2O (−59.09 kJ mol^{-1}) > CTAB/H_2O (−41.93 kJ mol^{-1}). This result suggests that the stabilization of the CTAB/$C_{16}E_{20}$/H_2O complex corroborates well the synergism in the β parameter, ΔG^0_m and ΔG^0_{ads} values (Table 1). A similar observation was also reported earlier.[42,43]

3.2. C–C cross coupling Heck reaction in single and mixed micellar media

Micellar media actually demonstrate that the compartmentalization of these systems leads to the formation of a nanoreactor environment at the periphery of the micelle/water pseudo-phase and provides a more sustainable approach for synthetic organic chemistry.[44] In this report, repeated experiments with a model substrate in the characterized single and mixed micelles were performed to articulate the effect of restricted or confined reactor systems in the light of their physicochemical and thermodynamic properties to rationalize the yield of Heck reaction products at ambient temperature (303 K) (*vide.* Fig. 4A). More precisely, it is expected to underline the variation in degree of performance of the Heck reaction from the viewpoint of the distinctive features of micellar structure. The results are presented in Fig. 4 and Table S2 (ESI†). Various combinations (for example, water, single and mixed micelles of CTAB and $C_{16}E_{20}$) of the nanoreactor systems (entries 1–4) were explored in order to standardize the best reaction environment in terms of the yield of the desired product of the Heck reaction (Table S2†). It is clearly evident that the yield is very poor in water (7%) compared to microheterogeneous systems such as single CTAB (57%), $C_{16}E_{20}$ (44%) or mixed micelle (66%). Hence, these results clearly warrant the envisaged need for a confined environment of aggregated systems which plays a significant role in performing the Heck reaction.[45] It can be seen from Fig. 4 and Table S2† that an equimolar composition of mixed micelle exhibits a synergism in the yield of Heck reaction products and consequently, offers a better reactor than its constituent

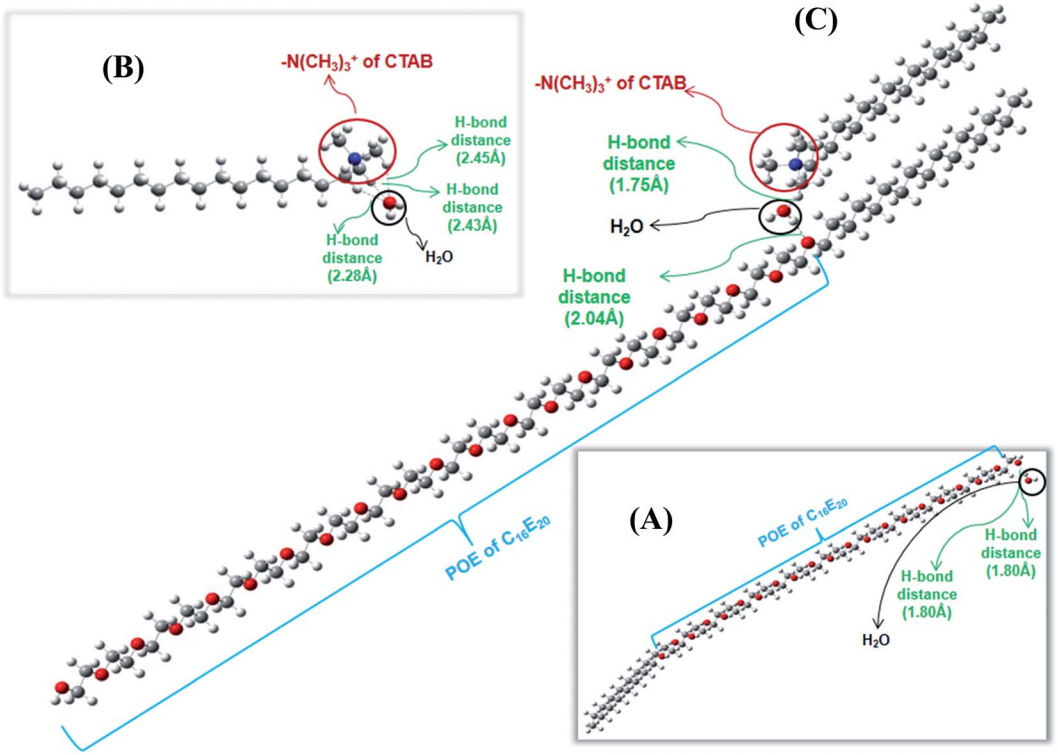

Fig. 3 Optimized geometries at the B3LYP/6-31G level: (A) $C_{16}E_{20}/H_2O$ complex, (B) CTAB/H_2O complex, and (C) CTAB/$C_{16}E_{20}/H_2O$ complex. Colour code for atoms: blue, nitrogen; red, oxygen; dark gray, carbon; and light gray, hydrogen.

surfactants. More precisely, the mixed micelle possesses some intrinsic properties of its formation that lead to its special characteristics towards Heck reaction performance. This is justified from the higher negative values of interaction parameter (β^m) and free energy of mixed micelle formation (ΔG^0_m) than individual surfactants (Table 1). This suggests that the formation of the mixed micelle is most spontaneous as well as functionally operative. Further, it is noted that the cationic CTAB-mediated micelle shows a higher yield than non-ionic $C_{16}E_{20}$ which corroborates well with the spontaneity of formation of the respective micelle as designated through the corresponding negative values of both ΔG^0_m and ΔG^0_{ads} (Table 1).[46] Surfactant-mediated self-assemblies or micelles are reported to be compatible with aryl halogens.[45] Other substrates (excluding the Pd^{2+} catalyst, which might be present in the continuous aqueous phase) are expected to be confined in the micellar core. Hence, the probable location of the micelle-mediated Heck reaction is in the micelle/water pseudo-phase whereas the catalysis is likely to be operative.

So far we conclude that due to synergistic interaction between CTAB and $C_{16}E_{20}$ along with spontaneous micellization, a mixed surfactant based micelle provides an efficient medium for performing the Heck reaction. Also, the experimentally observed synergistic interaction corroborates well with quantum chemical DFT calculations. Now, questions arise how the synergistic interaction between the aforementioned surfactants is stimulated in a non-polar or non-aqueous medium and also, whether the Heck reaction occurs

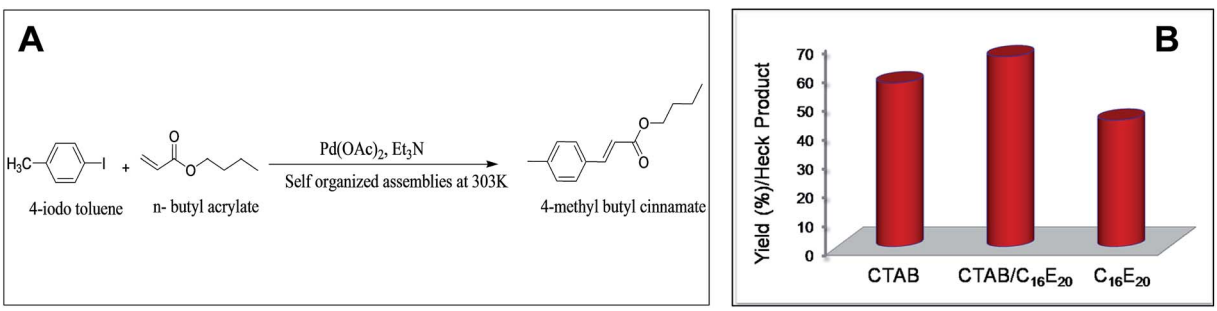

Fig. 4 (A) Pictorial representation of the Heck reaction in self-organized media, and (B) yield of Heck reaction in single (CTAB and $C_{16}E_{20}$) and mixed micelles (CTAB/$C_{16}E_{20}$, 1 : 1) at 303 K.

favourably in this mixed microemulsion system or not. To answer these questions, the formation and characterization of a mixed microemulsion system at different physicochemical conditions and correlation of the estimated parameters with the reaction mechanism of Heck coupled products is required.

3.3. Formation and characterization of w/o mixed microemulsions

CTAB requires the presence of a co-surfactant, typically a medium chain alcohol, in order to form a stable microemulsion.[47] In this study, Pn and Hp (or Dc) were used as a co-surfactant and oil, respectively. In a w/o microemulsion system, CTAB and $C_{16}E_{20}$ in an equimolar composition are considered to populate the oil/water interface in partial association with the co-surfactant (Pn). On the other hand, Pn is further distributed between the interface and the bulk oil, because of its negligible solubility in water.[26] Thus, at a fixed [surfactant(s)], a critical concentration of Pn is required for the stabilization of the mixed microemulsions. To estimate what amount of Pn (in moles) is distributed at the interface and in the oil phase for the formation of a stable microemulsion, we employed a simple titrimetric technique (known as the dilution method).[48] The distribution *vis-à-vis* the transfer process of Pn from the continuous oil phase to the interfacial region is discussed in detail in the ESI, and shown in Fig. S3.† This method is used for the estimation of various parameters concerned with the formation of CTAB/$C_{16}E_{20}$ mixed microemulsion systems (with X_{CTAB} or $X_{C_{16}E_{20}} = 0.5$) in Hp and Dc at 303 K and at different molar ratios of water to surfactant (ω = 10, 20, 30, 40 and 50). The estimated parameters, such as number of moles of Pn at the interface (n_a^i), in the oil phase (n_a^o), compositional variations of surfactants and Pn (n_a^i/n_s) at the interface, the distribution constant of Pn between the continuous oil phase and the interface of the droplet (K_d), and standard Gibbs free energy change of transfer of Pn from oil to the interface (ΔG_t^0) are presented in Table S3 in the ESI.† It is evident from Fig. 5A that n_a^i or n_a^i/n_s values decrease with an increase in ω for all these systems. A similar trend was reported earlier by Paul *et al.*[49] for water/Brij-35/Pn/Dc or Dd and Kundu *et al.*[50] for SDS/Brij-58 or Brij-78/Pn/Hp or Dc microemulsions. At a very low ω, the concentration of Pn at the interface is virtually constant, because long POE chain of $C_{16}E_{20}$ probably resides at the interface in a twisted form due to strong ion–dipole interactions between the compact quaternary ammonium group in CTAB and EO groups in $C_{16}E_{20}$. With an increase in droplet size by the addition of more water, helically twisted POE chains unfold and consequently, occupy a larger surface area of the droplet.[51] Therefore, unoccupied surface area at the interface is reduced to a greater extent and hence, n_a^i gradually decreases with an increase in ω. However, the spontaneity of the transfer process further decreases with an increase in ω which indicates that the trend of Pn transferring from the oil to the interface is weakened.[50] Hp stabilized systems also show higher spontaneity of the Pn transfer process than Dc, which is also justifiable from the higher Pn population at the interface (n_a^i) in the former system. Similar observations were reported by Kundu *et al.*,[50] Zheng *et al.*,[52] and Digout *et al.*[53] for w/o microemulsion systems stabilized by single as well as mixed surfactants. After successful formation of a stable mixed microemulsion in conjunction with Pn in Hp or Dc at different ω, it is necessary to understand the microstructural and microenvironmental properties of these systems to reveal the nature of droplet–droplet interactions within confined environments.

In view of this, size and size distributions of w/o microemulsion droplets were measured by the DLS technique. Fig. 5B depicts the variation in droplet size for the mixed microemulsions in both oils as a function of water content (ω = 10–50) at a fixed composition ($X_{C_{16}E_{20}\text{ or CTAB}} = 0.5$) and surfactant–cosurfactant mass ratio (=1 : 2) at 303 K. The droplet size increases with an increase in ω for both oils, keeping other parameters constant, which clearly indicates the swelling behaviour of w/o microemulsions with the addition of water.[54] The linear variation of droplet size at a lower range of ω values indicates that the droplets do not interact with each other and are probably spherical. The deviation from linearity at higher ω value is due to several factors, of these, the most relevant ones being enhanced droplet–droplet interaction and shape of the microemulsions. Further, Hp-based systems produce smaller droplets compared to Dc-based systems. This is probably due to the shorter chain of Hp compared to Dc, which easily penetrates the interface to make it rigid. It can be concluded that with an increase in ω, inter-droplet interaction increases which is higher for the Dc-based system compared to Hp. Both conductance and viscosity measurements in these systems also support the observations from the DLS study (Fig. S4A and B† and inset). The morphology of mixed microemulsions in both oils (Hp and Dc) was also investigated at a fixed $X_{C_{16}E_{20}} = 0.5$, ω = 10 and 303 K by employing FESEM and is illustrated in Fig. 5C–D. The micrographs for the Hp based microemulsion (Fig. 5C) reveal smaller particles arranged in rice grain-like patterns, which produce dispersed spheres of nearly homogeneous type morphology. On the other hand, the Dc based microemulsion (Fig. 5D) produces disintegrated isolated bodies of large globular and near globular particles forming spherical entities. All types of spherical morphology (*viz.* small as well as large) are marked by circles in both figures. For Dc based microemulsion, severe aggregation occurs and single droplets cannot be discerned distinctly.

To understand the dynamics and nature of encapsulated water, we recorded FTIR spectra of encapsulated water in CTAB/$C_{16}E_{20}$ (1 : 1)/Pn/Hp/water microemulsions at varied ω (10 → 50). We focus our attention on the 3000–3800 cm^{-1} frequency window as this is the fingerprint region for symmetric and asymmetric vibrational stretching of O–H bonds in water.[55,56] It is to be noted that a small amount of Pn is used as structure forming co-surfactant in the present study. Hence, the spectrum of Pn (at the same concentration) is subtracted from the spectral intensity of the O–H stretching band at the corresponding ω in order to eliminate the supplementary IR intensities due to the O–H stretching vibrations of Pn molecules, and the differential spectra are analysed.[57,58] Water usually coexists in three 'states' or 'layers' in the w/o microemulsion.[58–62] In view of this, the peaks observed for water O–H were fitted as a sum of Gaussian

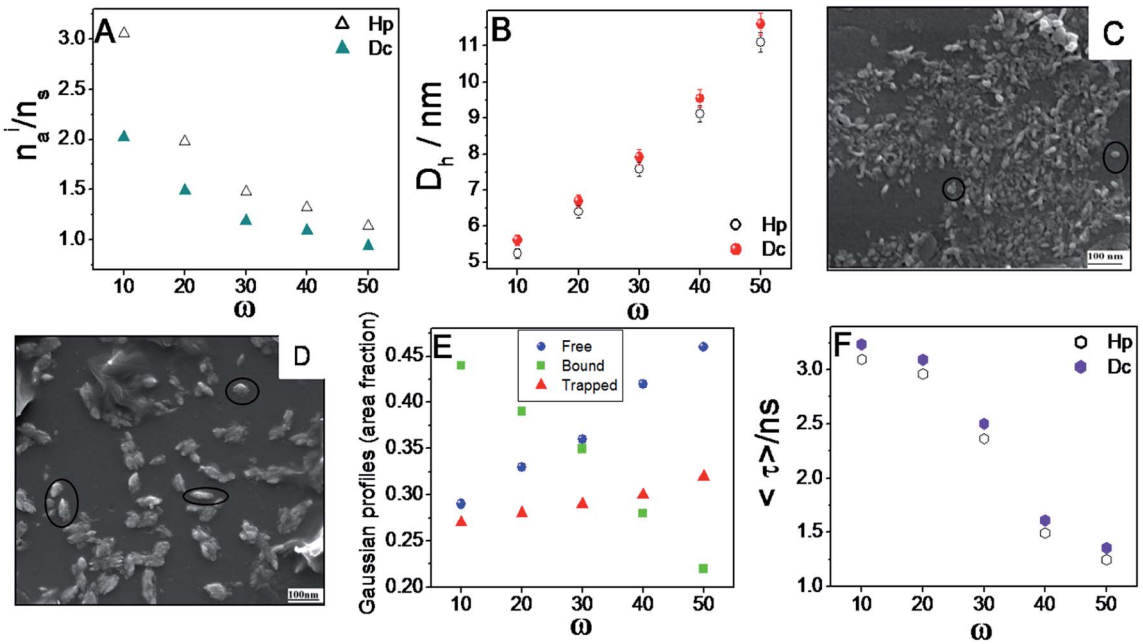

Fig. 5 (A) Plot of n_a^i/n_s *vs.* water content (ω) for mixed CTAB/$C_{16}E_{20}$ microemulsions at equimolar composition comprising 0.5 mmol of mixed surfactant and 14.0 mmol of Hp or Dc stabilized by Pn. (B) Hydrodynamic diameter (D_h) as a function of ω for the systems mentioned above. FESEM images of similar systems at a fixed $X_{C_{16}E_{20}} = 0.5$, $\omega = 10$ and 303 K, where (C) Hp and (D) Dc are the oil. (E) Variation in the Gaussian profiles (area fraction) of the normalized spectra of different water species, and (F) fluorescence lifetime ($\langle\tau\rangle$) of HCM (at $\lambda_{ex} = 310$ nm) as a function of ω in CTAB/$C_{16}E_{20}$ (1 : 1)/Pn/Hp/water microemulsions at 303 K.

functions with the help of a Gaussian curve fitting program, and the vibrational characteristics, particularly the peak area corresponding to each peak, were analyzed using a three states model to unravel the nature of water inside the nanopool and the change in water properties as a function of ω. According to the three states model, the solubilized water in microemulsions is identified as free, bound and trapped water molecules and a representative result of deconvolution is depicted in the ESI, Fig. S5.† The free water molecules, occupying the core of the surfactant aggregates, form strong hydrogen bonds among themselves, that is, they possess similar properties to those of bulk water, which shifts the O–H stretching band to a lower frequency at about 3250 cm^{-1} (*vide.* Fig. S5†).[58–62] The bound water, *i.e.* the surfactant head group bound water molecules, resonates in the mid frequency region and an IR peak appears at about 3450 cm^{-1} (*vide.* Fig. S5†).[58–62] Apart from these two types of water species, the water molecules dispersed among the long hydrocarbon chains of the surfactant molecules are termed trapped water molecules.[58–62] As the trapped water molecules are matrix-isolated dimers or monomeric in nature, they generally absorb in the high frequency region at about 3550 cm^{-1}. The relative abundance [Gaussian profiles (area fraction)] of different water species in these systems as a function of ω are presented in Fig. 5E. It reveals that the relative abundance of free water increases from 29% to 46% and that of bound water decreases from 44% to 22% with increasing water content (ω = 10 → 50) *vis-à-vis* the corresponding increase in droplet size (D_h) from 5.24 nm to 11.10 nm in the same ω range. Actually, once water is added to a microemulsion forming system, a portion of the water goes to the interface and hydrates the head groups of surfactants until they become fully hydrated at a certain ω. Further added water goes primarily to the inner core, leading to a continuous increase in the fraction of unbound free water with an increase in ω.[61] In addition, the population corresponding to the trapped water molecules (monomers/dimmers) shows an overall weak increasing tendency with a hike from 27% to 32% with increasing ω (=10 → 50). It is inferred from this investigation that a few water molecules are displaced from the structured water pool shell to the interfacial region with increasing ω.[63]

A fluorescence lifetime study of HCM (fluorophore) in mixed surfactant microemulsions was also employed to obtain information about the configuration of the altered interfacial region of mixed amphiphiles interface upon hydration (ω = 10 → 50). The choice of HCM is based on the fact that the probes reside at the interface and/or face the polar core upon excitation (at λ_{ex} = 310 nm).[64,65] In the present context, Fig. 5F depicts that the fluorescence lifetime $\langle\tau\rangle$ of HCM is found to be influenced by the variation of water content in mixed microemulsions. A regular decreasing trend in $\langle\tau\rangle$ for the fluorophore (HCM) is observed for both Hp (3.13 to 1.41 ns) and Dc (3.23 to 1.51 ns) derived systems with an increase in ω (10 → 50). The larger droplet size of the microemulsion at $\omega = 50$ compared to $\omega = 10$ results in an increase in the curvature of the surfactant film. Hence a greater fraction of water interacts with the interface, leading to a relatively faster relaxation.[66] This result is also consistent with findings from FTIR measurements where increase in ω leads to an increase in free water population,

which is responsible for the observed faster lifetime for CTAB/$C_{16}E_{20}$ (1 : 1)/Pn/Hp or Dc/water microemulsions at a higher ω.[67]

3.4. C–C cross coupling Heck reaction in mixed microemulsion

In view of the distinctive role of the mixed micelle at equimolar composition in carrying out the Heck reaction, another set of compartmentalized/microheterogeneous systems, water/oil (Hp or Dc) mixed surfactant microemulsions (MEs) stabilized by equimolar (1 : 1) composition of CTAB/$C_{16}E_{20}$ and Pn (S : CS = 1 : 2 wt%), were explored as a function of ω (=10 → 50) (entries 9–18, Table S2† and Fig. 6). In addition, the yields of Heck products are also measured in the constituents of these formulations as media (entries 5–8, Table S2†). Both oils (Hp and Dc) and oil/Pn mixtures at 1 : 2 weight ratios (Hp/Pn, and Dc/Pn) show a low yield compared to that of mixed microemulsions, while Hp-derived systems show much higher yield than Dc (Fig. 6A). A profound effect on the overall yield of Heck products is distinctly validated by changing the template from micelle → mixed micelle (1 : 1) → mixed microemulsions (1 : 1) in Hp and Dc (Table S2†). Though, equimolar (1 : 1) surfactant composition (similar to that of mixed micelle) is fixed in all formulations, yields are found to be dependent on water content (ω), oil type and availability of Pn (as co-surfactant) at the oil–water interface for their stabilization (Fig. 6B). The highest yield of the desired Heck product is achieved at $\omega = 10$ in Hp and Dc derived microemulsions. Thereafter, a sharp decrease in yield is observed with increasing ω (up to 30) and subsequently, a mild or sluggish decrease is achieved when $\omega =$ 50. It is worthy to mention that yield is much higher at lower $\omega = 10$ (ME_{Hp}, 79% and ME_{Dc}, 68%) and 20 (ME_{Hp}, 70% only) than that of mixed micelle (66%), whereas yields are less than that of mixed micelle at rest of the ω values. However, the overall results are rationalized as follows. It is inferred from the yields of the Heck products in microemulsions [ω range from 10 → 50 in both oils (ME_{Hp}, 79% → 54% and ME_{Dc}, 68% → 41%)] in conjugation with the yields in constituent elements *viz.* water (7%), oils (Hp, 37% and Dc, 15%), and oil/Pn mixtures (Hp/Pn, 40% and Dc/Pn, 19%) (Fig. 6A and Table S2†) that the Heck reaction occurs neither in the water or the oil domain; evidently it occurs in the palisade layer of the oil–water interface of the microemulsions. This is well corroborated by previous reports, in which the authors claim that the most plausible reaction location or site was the interfacial region or within the surfactant palisade layer of the w/o microemulsion.[68,69] In this context, the interaction between two constituents [such as, Pn (cosurfactant) and TEA] of these multicomponent systems plays a decisive role in the performance of the Heck reaction leading to formation of the final product. It is worthy of mentioning that TEA is an essential reactant in the Heck reaction, which requires a stoichiometric amount of base to neutralize the acid (herein, HI) ensuing from the exchange of a hydrogen atom with an aryl group.[16,17] In addition, the requirements of Pn depend upon the composition of microemulsions, size of the polar head group and charge type of surfactant, water content, degree of oil penetration, droplet size/microstructure, *etc.* and render the overall stability towards multicomponent systems from a physicochemical and thermodynamic point of view.[26,49–53] More precisely, it is revealed from the viewpoints mentioned above that the predominance of dipole–dipole interactions between Pn and TEA in a confined environment enhances the availability of TEA in the vicinity of the interfacial region as well as in confined water with special reference to bound water. Consequently, the formation of OH^- base surrounding the interface proceeds in the following way;[68,70]

$$(C_2H_5)_3N + H_2O \leftrightarrow (C_2H_5)_3N{\cdot}H_2O \leftrightarrow (C_2H_5)_3NH^+ + OH^-$$

Hence, the penetration of OH^- in the palisade layer of microemulsion cannot be ruled out, and subsequently, a basic environment in the vicinity of the interface is likely to be formed, which is essentially required for the Heck reaction.[68,69] Therefore, the most satisfactory yield of the product is achieved at a lower ω of 10 or 20 (Fig. 6 and Table S2†), where predominance of Pn in this range of ω is evidenced by characterization of these microemulsions using the dilution method.[68] It is revealed from Fig. 5A and Table S3† that the interfacial Pn population (n_a^i) and Gibbs free energy of the Pn transfer process ($-\Delta G_t^0$) (which is an indicator of the spontaneity of microemulsion formation) sharply decrease initially and thereafter mildly with an increase in ω. Interestingly, it is worthy of mentioning that decreasing trends reflected in Fig. 5A and 6B bear resemblance to each other, which is strong evidence for decreasing yield with increasing ω. Furthermore, Hp-based

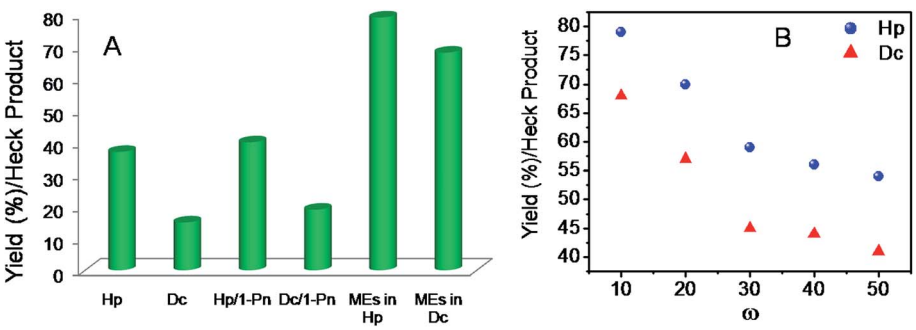

Fig. 6 Yield of Heck products (A) in individual constituents as well as in w/o mixed microemulsions (MEs), CTAB/$C_{16}E_{20}$ (1 : 1)/Pn/Hp or Dc/water at $\omega = 10$, and (B) variation in yield as a function of ω (=10 → 50) in the aforementioned MEs at 303 K.

systems exhibit higher yields than Dc-based systems. It can be argued that higher values of n_a^i and $-\Delta G_t^0$ in Hp continuum than Dc continuum (Fig. 5A and Table S3†) are responsible for the variation in yield in these two sets of systems. Herein, we report a mixed microemulsion mediated Heck coupling reaction which provides comparatively better results than single or mixed micelle, validating the spontaneous nature of the reactor framework with a concomitant rapid Pn transfer process (Pn_{oil} → $Pn_{interface}$) obtained from dilution experiments in varied physicochemical environments. In conclusion, a CTAB and $C_{16}E_{20}$ mediated micelle and microemulsion (in single and mixed states) Heck coupling procedure (through the generation of new C–C bonds) is developed using ligand-free catalysts, and could be applied in many industrial processes, especially in the synthesis of fine chemicals and active pharmaceutical intermediates.[19,71]

Currently, investigations of C–C coupling reactions catalysed by Pd(II) acetate and TEA as a base in w/o microemulsions comprising surfactants of different charge types (both in single and mixed states) under different physicochemical conditions (for example, variations in composition of the system, concentration of both base and catalyst, water content, temperature, *etc.*) are underway in our laboratory to probe the reaction mechanism of the Heck reaction in these complex microheterogeneous systems.

4. Overall comprehension

In aqueous medium, an equimolar composition of CTAB and $C_{16}E_{20}$ provides several advantages compared to the individual surfactants in terms of a lower CMC, more attractive interaction between them and spontaneous micellization (*i.e.*, more negative free energy of micellization) as well as adsorption process at the air–water interface. Interestingly, quantum chemical DFT calculations reveal the larger interaction energy of equimolar CTAB and $C_{16}E_{20}$ with water compared to any other combination. The zeta potential (ζ) value for CTAB/$C_{16}E_{20}$ mixtures also confirms the synergistic interaction between them. Micellar aggregates produce spherical droplets with size ranges from 10 to 15 nm. To understand the distinctive features of micellar structures as chemical nanoreactors, the Heck reaction is performed between 4-iodotoluene and *n*-butylacrylate. The reaction yield of the Heck coupled product is found to be higher in a mixed CTAB/$C_{16}E_{20}$ micellar solution compared to single CTAB or $C_{16}E_{20}$ micelles and even higher than bulk water. The higher yield at mixed composition correlates with spontaneous micellization and adsorption processes. It is now interesting to study the behaviour of these surfactants in non-polar solvents further. Population of Pn at the oil–water interface of the formulated w/o microemulsions *vis-à-vis* spontaneity of the transfer process is found to decrease with an increase in ω for both oils. The morphology and size of mixed microemulsion droplets vary with water content as well as oil chain length. The present study also reveals that the relative abundance of free water increases and that of bound water decreases with increasing water content in mixed microemulsions and is well corroborated with the corresponding increase in droplet size under an identical range of ω. The product yield of the Heck reaction significantly increases in mixed microemulsion systems compared to with individual constituents. With increasing water content in a microemulsion, the product yield diminishes and it is found to be lower for Dc-stabilized systems compared to Hp. The spontaneity of the Pn transfer process from oil to the interface for stabilization of the microemulsion (as obtained from dilution experiments) finely correlates with trends in product yield in these systems.

5. Summary and future outlook

The present report focuses on the microstructure and properties of micelles and w/o microemulsion systems using a similar set of surfactants (CTAB and $C_{16}E_{20}$) at single and mixed states, and also employing these organized assemblies as a chemical nanoreactor for performing the C–C cross coupling Heck reaction. An equimolar composition of CTAB and $C_{16}E_{20}$ shows non-ideal solution behaviour in aqueous medium with synergistic interaction between them, which further correlates with gas phase quantum chemical calculations. Understanding the microscopic origins of these mixing properties might facilitate a more informed and designed use of such mixed systems in a range of novel formulations from hydrogels to surface coatings.[72,73] The mixed micellar composition provides an efficient medium for carrying out the Heck reaction compared to individual micellar and bulk water media. So far, an operationally simple procedure is developed for carrying out traditional Heck couplings at ambient temperature in a mixed micelle, without resorting to sonication, electrochemistry, or using water-soluble phosphine.[74] Use of inexpensive ionic and non-ionic amphiphiles allows cross-coupling to take place especially under mild and environmentally attractive conditions. To determine whether the key features responsible for favorable micellization *via* synergistic interaction reciprocate the interfacial architecture of microemulsions, a multitechnique approach was applied to fully characterize the mixed microemulsion systems at different hydration levels. The estimation of Pn distribution at the oil–water interface and bulk oil phase along with related energetics from a dilution method complements more detailed information obtained from more labour intensive small-angle neutron scattering (SANS) studies of w/o microemulsions.[75] Although these parameters are obtained through straightforward macroscopic measurements, the Gibbs free energies of transfer of Pn from bulk oil to the interface are a sensitive probe of the microenvironment around various solute moieties, and are amenable for the investigation of relatively complex molecular structures. The droplet size and relaxation dynamics of a fluoroprobe inside the confined environment correlate well with variation in the different states of water. Knowledge of such states of solubilized water in w/o microemulsions is important because has a bearing on the applications of these species, for example, in solubilisation, catalysis of chemical reactions,[76] and also on the size and polydispersity of nanoparticles synthesized in microemulsion media.[77] In order to understand the mechanism of the Heck reaction in a non-polar medium instead of an aqueous medium, the formulated w/o

microemulsion at different compositions along with individual constituents is used as a template for the aforementioned reaction. A profound effect on the overall yield of the Heck product is distinctly validated by changing the template from micelle → mixed micelle (1 : 1) → mixed microemulsion (1 : 1), which indicates the influence of the nature of surfactant–solvent interactions, and thus affects the reaction yield.[78] Herein, it is proposed that the Heck reaction occurs in neither the water or the oil domain, and more precisely, occurs at the micelle–water pseudo-phase and palisade layer of the oil–water interface of microemulsions. In summary, each amphiphilic nanoreactor is analogous to the traditional chemist's flask, with the added advantages of reduced reagent consumption, rapid mixing, automated handling, and continuous processing. Building on advances in continuous flow chemistry,[79] our study thus provides a new route to regulate and even to enhance reaction yields in micellar and w/o microemulsion media according to the purpose and could be found useful for future applications in various domains such as enzyme activity, and/or organic synthesis.[80,81]

Acknowledgements

S. B. and K. K. thank DBT, Govt. of India for Senior Research Fellowship (SRF) and Research Associateship, respectively. G. C. thanks UGC, New Delhi, India for UGC-BSR Research Fellowship. Professor BKP would like to thank ISI, Kolkata. Professor SKS also thanks Science & Engineering Research Board (SERB), DST, Govt. of India (Sanction No. SB/S1/PC-034/2013) for financial assistance. The computer resources of Computer Centre, IIT Madras are gratefully acknowledged.

References

1 P. M. Holland and D. N. Rubingh, *Mixed Surfactant Systems: An Overview, ACS Symposium Series*, American Chemical Society, Washington, DC, 1992, vol. 501, ch. 1, pp. 2–30.
2 R. Zana, *Dynamics of Surfactant Self-Assemblies: Micelles, Microemulsions, Vesicles and Lyotropic Phases*, CRC Press, Taylor & Francis Group, Boca Raton, 2005.
3 D. N. Rubingh and M. Bauer, Lipase Catalysis of Reactions in Mixed Micelles, *ACS Symposium Series*, American Chemical Society, Washington, DC, 1992, vol. 501, ch. 12, pp. 210–226.
4 A. Shome, S. Roy and P. Das, *Langmuir*, 2007, **23**, 4130–4136.
5 A. Das and R. K. Mitra, *J. Phys. Chem. B*, 2014, **118**, 5488–5498.
6 J. Zhang, B. Han, J. Liu, X. Zhang, J. He, Z. Liu, T. Jiang and G. Yang, *Chem.–Eur. J.*, 2002, **8**, 3879–3883.
7 J. Hao, *Self-Assembled Structures: Properties and Applications in Solution and on Surfaces*, CRC Press, Taylor & Francis Group, Boca Raton, 2010.
8 N. Azum, M. A. Rub, A. M. Asiri and H. M. Marwani, *J. Mol. Liq.*, 2014, **197**, 339–345.
9 N. Azum, M. A. Rub and A. M. Asiri, *J. Mol. Liq.*, 2016, **216**, 94–98.
10 N. Azum, M. A. Rub and A. M. Asiri, *Colloids Surf., B*, 2014, **121**, 158–164.
11 M. A. Rub, F. Khan, N. Azum, A. M. Asiri and H. M. Marwani, *J. Taiwan Inst. Chem. Eng.*, 2016, **60**, 32–43.
12 N. Azum, M. A. Rub, A. M. Asiri, K. A. Alamry and H. M. Marwani, *J. Dispersion Sci. Technol.*, 2014, **35**, 358–363.
13 *Mixed Surfactant Systems, Surfactant Science Series*, ed. K. Ogino and M. Abe, Marcel Dekker, New York, 1993, vol. 46.
14 D. Blankschtein and A. Shiloach, *Langmuir*, 1998, **14**, 1618–1636.
15 F. D. Souza, B. S. Souza, D. W. Tondo, E. C. Leopoldino, H. D. Fiedler and F. Nome, *Langmuir*, 2015, **31**, 3587–3595.
16 R. F. Heck, *J. Am. Chem. Soc.*, 1968, **90**, 5526–5531.
17 R. F. Heck, *J. Am. Chem. Soc.*, 1968, **90**, 5546–5548.
18 X.-F. Wu, P. Anbarasan, H. Neumann and M. Beller, *Angew. Chem., Int. Ed.*, 2010, **49**, 9047–9050.
19 J. G. deVries and A. H. M. de Vries, *Eur. J. Org. Chem.*, 2003, **2003**, 799–811.
20 T. Dwars, E. Paetzold and G. Oehme, *Angew. Chem., Int. Ed.*, 2005, **44**, 7174–7199.
21 J.-Z. Jiang and C. Cai, *J. Colloid Interface Sci.*, 2006, **299**, 938–943.
22 Y. Kasaka, B. Bibouche, I. Volovych, M. Schwarze and R. Schomäcker, *Colloids Surf., A*, 2016, **494**, 49–58.
23 D. C. Crans, S. Schoeberl, E. Gaidamauskas, B. Baruah and D. A. Roess, *J. Biol. Inorg. Chem.*, 2011, **16**, 961–972.
24 J. Tang, Y. Wang, D. Wang, Y. Wang, Z. Xu, K. Racette and F. Liu, *Biomacromolecules*, 2013, **14**, 424–430.
25 A. L. Kholodenko and J. F. Douglas, *Phys. Rev. E: Stat. Phys., Plasmas, Fluids, Relat. Interdiscip. Top.*, 1995, **51**, 1081–1090.
26 S. P. Moulik, L. Digout, W. Aylward and R. Palepu, *Langmuir*, 2000, **16**, 3101–3106.
27 R. K. Mahajan and R. Sharma, *J. Colloid Interface Sci.*, 2011, **363**, 275–283.
28 J. H. Clint, *J. Chem. Soc., Faraday Trans. 1*, 1975, **71**, 1327–1334.
29 D. N. Rubingh, in *Solution Chemistry of Surfactants*, ed. K. L. Mittal, Plenum Press, New York, 1979, vol. 1, p. 337.
30 M. J. Rosen and X. Y. Hua, *J. Colloid Interface Sci.*, 1982, **86**, 164–172.
31 M. J. Rosen, *Surfactants and Interfacial Phenomena*, Wiley-Interscience, New York, 2nd edn, 1989, pp. 65–68.
32 W. H. Ansari, N. Fatma, M. Panda and K. Ud-Din, *Soft Matter*, 2013, **9**, 1478–1487.
33 R. Sanan, R. Kaur and R. K. Mahajan, *RSC Adv.*, 2014, **4**, 64877–64889.
34 C. C. Ruiz, *Colloid Polym. Sci.*, 1999, **277**, 701–707.
35 T. Chakraborty, S. Ghosh and S. P. Moulik, *J. Phys. Chem. B*, 2005, **109**, 14813–14823.
36 M. J. Rosen and S. Aronson, *Colloids Surf.*, 1981, **3**, 201–208.
37 A. B. Pereiro, J. M. M. Araujo, F. S. Teixeira, I. M. Marrucho, M. M. Pineiro and L. P. N. Rebelo, *Langmuir*, 2015, **31**, 1283–1295.
38 A. V. Delgado, F. Gonzalez-Caballero, R. J. Hunter, L. K. Koopal and J. Lyklema, *Pure Appl. Chem.*, 2005, **77**, 1753–1805.
39 P. K. Misra and P. Somasundaran, *J. Surfactants Deterg.*, 2004, **7**, 373–378.

40 S. K. Mehta and S. Chaudhary, *Colloids Surf., B*, 2011, **83**, 139–147.
41 E. Odella, R. D. Falcone, J. J. Silber and N. M. Correa, *Phys. Chem. Chem. Phys.*, 2014, **16**, 15457–15468.
42 A. Pan, S. S. Mati, B. Naskar, S. C. Bhattacharya and S. P. Moulik, *J. Phys. Chem. B*, 2013, **117**, 7578–7592.
43 N. Cheng, P. Yu, T. Wang, X. Sheng, Y. Bi, Y. Gong and L. Yu, *J. Phys. Chem. B*, 2014, **118**, 2758–2768.
44 S. Khamarui, D. Sarkar, P. Pandit and D. K. Maiti, *Chem. Commun.*, 2011, **47**, 12667–12669.
45 M. M. Shinde and S. S. Bhagwat, *J. Dispersion Sci. Technol.*, 2012, **33**, 117–122.
46 S. Bhattacharya, A. Srivastava and S. Sengupta, *Tetrahedron Lett.*, 2005, **46**, 3557–3560.
47 E. Palazzo, L. Carbone, G. Colafemmina, R. Angelico, A. Ceglieb and M. Giustini, *Phys. Chem. Chem. Phys.*, 2004, **6**, 1423–1429.
48 J. E. Bowcott and J. H. Schulman, *Z. Elektrochem.*, 1955, **59**, 283–290.
49 B. K. Paul and D. Nandy, *J. Colloid Interface Sci.*, 2007, **316**, 751–761.
50 K. Kundu and B. K. Paul, *Colloid Polym. Sci.*, 2013, **291**, 613–632.
51 H. Preu, A. Zradba, S. Rast, W. Kunz, E. H. Hardy and M. D. Zeidler, *Phys. Chem. Chem. Phys.*, 1999, **1**, 3321–3329.
52 O. Zheng, J.-X. Zhao and X.-M. Fu, *Langmuir*, 2006, **22**, 3528–3532.
53 L. Digout, K. Bren, R. Palepu and S. P. Moulik, *Colloid Polym. Sci.*, 2001, **279**, 655–663.
54 C. C. Villa, J. J. Silber, N. M. Correa and R. D. Falcone, *ChemPhysChem*, 2014, **15**, 3097–3109.
55 S. A. Corcelli and J. L. Skinner, *J. Phys. Chem. A*, 2005, **109**, 6154–6165.
56 H. Graener and G. Seifert, *J. Chem. Phys.*, 1993, **98**, 36–45.
57 Z. S. Nickolov, V. Paruchi, D. O. Shah and J. D. Miller, *Colloids Surf., A*, 2004, **232**, 93–99.
58 S. K. Mehta, G. Kaur, R. Mutneja and K. K. Bhasin, *J. Colloid Interface Sci.*, 2009, **338**, 542–549.
59 J.-B. Brubach, A. Mermet, A. Filabozzi, A. Gerschel, D. Lairez, M. P. Krafft and P. Roy, *J. Phys. Chem. B*, 2001, **105**, 430–435.
60 A. Das, A. Patra and R. K. Mitra, *J. Phys. Chem. B*, 2013, **117**, 3593–3602.
61 Q. Zhong, D. A. Steinhurst, E. E. Carpenter and J. C. Owrutsky, *Langmuir*, 2002, **18**, 7401–7408.
62 S. Bardhan, K. Kundu, S. Das, M. Poddar, S. K. Saha and B. K. Paul, *J. Colloid Interface Sci.*, 2014, **430**, 129–139.
63 C. G. Blanco, L. J. Rodriguez and M. M. Velazquez, *J. Colloid Interface Sci.*, 1999, **211**, 380–386.
64 S. Biswas, S. C. Bhattacharya, B. B. Bhowmik and S. P. Moulik, *J. Colloid Interface Sci.*, 2001, **244**, 145–153.
65 S. Chatterjee, R. K. Mitra, B. K. Paul and S. C. Bhattacharya, *J. Colloid Interface Sci.*, 2006, **298**, 935–941.
66 D. M. Willard and N. E. Levinger, *J. Phys. Chem. B*, 2000, **104**, 11075–11080.
67 P. Setua, C. Ghatak, V. G. Rao, S. K. Das and N. Sarkar, *J. Phys. Chem. B*, 2012, **116**, 3704–3712.
68 B. Kar, S. Bardhan, K. Kundu, S. K. Saha, B. K. Paul and S. Das, *RSC Adv.*, 2014, **4**, 21000–21009.
69 M. Hager, U. Olsson and K. Holmberg, *Langmuir*, 2004, **20**, 6107–6115.
70 N. Li, Q. Cao, Y. Gao, J. Zhang, L. Zheng, X. Bai, B. Dong, Z. Li, M. Zhao and L. Yu, *ChemPhysChem*, 2007, **8**, 2211–2217.
71 H. U. Blaser, A. Indolese, A. Schnyder, H. Steiner and M. Studer, *J. Mol. Catal. A: Chem.*, 2001, **173**, 3–18.
72 M. A. Haque, T. Kurokawa and J. P. Gong, *Soft Matter*, 2012, **8**, 8008.
73 A. M. Alkilany, P. K. Nagaria, M. D. Wyatt and C. J. Murphy, *Langmuir*, 2010, **26**, 9328.
74 B. H. Lipshutz and B. R. Taft, *Org. Lett.*, 2008, **10**, 1329–1332.
75 A. L. Compere, W. L. Griffith, J. S. Johnson Jr, E. Caponetti, D. Chillura-Martino and R. Triolo, *J. Phys. Chem. B*, 1997, **101**, 7139–7146.
76 P. López-Cornejo, P. Pérez, F. García, R. De la Vega and F. Sánchez, *J. Am. Chem. Soc.*, 2002, **124**, 5154–5164.
77 W. Zhang, X. Qiao and J. Chen, *Colloids Surf., A*, 2007, **299**, 22–28.
78 G. N. Smitha, P. Browna, C. James, S. E. Rogers and J. Eastoe, *Colloids Surf., A*, 2016, **494**, 194–200.
79 D. T. McQuade and P. H. Seeberger, *J. Org. Chem.*, 2013, **78**, 6384–6389.
80 F. Lopez, G. Cinelli, L. Ambrosone, G. Colafemmina, A. Ceglie and G. Palazzo, *Colloids Surf., A*, 2004, **237**, 49–59.
81 K. Holmberg, *Eur. J. Org. Chem.*, 2007, **2007**, 731–742.